Mendelova univerzita v Brně

Agronomická fakulta

Ústav chemie a biochemie

Izolace, separace a studium významných kov-vazných proteinů

Disertační práce

Vedoucí práce:

doc. RNDr. Pavel Kopel, Ph.D.

Vypracovala:

Ing. Sylvie Skaličková

Školitel specialista:

Mgr. Markéta Vaculovičová, Ph.D.

Brno 2016

PROHLÁŠENÍ

Prohlašuji, že jsem disertační práci na téma Izolace, separace a studium významných kov-vazných proteinů, vypracovala samostatně a použila jsem jen pramenů, které cituji a uvádím v přiloženém seznamu literatury.

Disertační práce je školním dílem a může být použita ke komerčním účelům jen se souhlasem vedoucího diplomové práce a děkana Agronomické fakulty Mendelovy univerzity v Brně.

dne .....

podpis.....

PODĚKOVÁNÍ

Na prvním místě chci poděkovat Mgr. RNDr. Ondřeji Zítkovi, Ph.D. za cené rady a čas, který mi věnoval během celého mého studia.

Mé poděkování také patří prof. Ing. Renému Kizekovi, Ph.D. za zkušenosti, které mi předal během svého působení na Mendelově univerzitě.

Děkuji Mgr. Markétě Vaculovičové, Ph.D, doc. RNDr. Pavlu Kopelovi, Ph.D. a prof. Vojtěchu Adamovi, Ph.D za podporu a vedení mé práce.

Děkuji také všem spoluautorům a kolegům z ústavu Chemie a biochemie, kteří dokázali vytvořit neopakovatelnou pracovní atmosféru a podpořili mě v mé vědecké činnosti. Hlavně Ing. Kristýně Číhalové a Ing. Lukáši Nejdlovi, Ph.D. za vytvoření skvělého pracovního týmu.

V neposlení řadě děkuji své rodině, která mi poskytla zázemí pro mé studium a byla mi velkou oporou.

„Jsou skutečnosti, které vědec přehlédne, jsou skutečnosti, kam člověk nedohlédne. Avšak svět stojí za poznání, protože lidstvo je předurčeno k objevování.“

Tato práce vznikla v rámci CEITEC - Středoevropského technologického institutu s pomocí výzkumné infrastruktury financované projektem CZ.1.05/1.1.00/02.0068 z Evropského fondu regionálního rozvoje.

EUROPEAN UNION
EUROPEAN REGIONAL DEVELOPMENT FUND
INVESTING IN YOUR FUTURE

OP Research and
Development for Innovation

ABSTRAKT

Kov-vazné proteiny jsou významnou skupinou biomolekul v živých organismech. Zastupují zde mnoho životně důležitých funkcí jako je udržení homeostázy esenciálních kovů v organismu, podílejí se na detoxifikaci těžkými kovy, pomáhají antioxidačnímu systému vyrovnat se s volnými radikály způsobujícími oxidační stres. Řada z nich patří do skupiny životně důležitých enzymů, katalyzující biochemické reakce. Mimo jiné jsou kov-vazné proteiny součástí vrozené imunity pro boj proti patogenním bakteriím a také jsou výbornými transportéry nejen pro esenciální molekuly, ale mohou být využity pro cílený transport ve velmi rozvíjející se oblasti, nanomedicíny. Existuje řada metod, jak lze tyto specifické proteiny studovat a sledovat jejich interakce s dalšími biomolekulami. Mezi základní metody patří kapalinová chromatografie, která umožňuje jejich izolaci z biologických vzorků, dále byly v této práci použity imunochemické metody, spektrofotometrické metody a elektrochemické metody, pomocí kterých lze objasnit chování a vlastnosti těchto molekul v různém prostředí. Cílem předkládané práce bylo optimalizovat metody pro separaci a studium kov-vazných proteinů.

Klíčová slova: kov-vazné proteiny, apoferrinin, laktoferrin, metalothionein, kapalinová chromatografie, spektrofotometrie, elektrochemie

ABSTRACT

The metal binding proteins are important group of biomolecules effects in living organisms. They represent series of vital important functions such as homeostasis of essential metals, they are involved in heavy metals detoxification, helps antioxidant system with free radical neutralization to prevent oxidation stress. Lot of them belongs to group of important enzymes catalyzing biochemical reactions. Last, but not least they are part of innate immunity system against pathogenes and could be utilized as a carrier cages in target drug therapy due to their unique transporter properties. A number of methods have been developed to study and observe the interactions between metalloproteins and specific biomolecules. First of all, the liquid chromatography enables isolation of required proteins from biological matrices. Further experiments utilized immunochemical, spectrophotometrical and electrochemical methods to clarify their properties and behaviour in various environments. The aim of the thesis was optimized analytical methods for separation and studying of the metal binding proteins.

Keywords: metalloproteins, apoferritin, metallothionein, lactoferrin, liquid chromatography, spectrophotometry, electrochemistry

OBSAH

1 ÚVOD 10
2 CÍLE PRÁCE 11
3 LITERÁRNÍ ČÁST 12
3.1 Význam kov-vázajících proteinů v organismu 12
3.2 Funkce kov-vazných proteinů 14
3.2.1 Transportní a zásobní kov-vazné proteiny 14
3.2.1.1 Metallothionein 15
3.2.1.2 Feritin 17
3.2.1.3 Přehledový článek I: 18
Apoferritin applications in nanomedicine 18
3.2.3 Metaloenzymy 33
3.2.4 Metaloproteiny singnální transdukce 33
3.2.5 Metaloproteiny transkripční regulace 35
3.2.6 Imunitní metaloproteiny 37
3.2.6.1 Laktoferin 39
3.3 Analytické metody pro studium významných kov-vazných proteinů 40
3.3.1 Kapalinová chromatografie 42
3.3.2 Enzymová imunoanalýza 44
3.3.3 Optické metody pro detekci proteinů 47
3.3.4 Elektrochemické metody 48
3.4.5 Hmotnostní spektrometrie 50
4 MATERIÁL A METODY 52
4.1 Chemikálie 52
4.2 Příprava CdTe Qds 52
4.3 Biologický materiál 53
4.4 Kapalinová chromatografie s UV detekcí 53
4.5 Spektrofotometrická analýza 54
4.6 ELISA 55
4.7 Injekční analýza v zastaveném toku (SFIA) 55
5 VÝSLEDKY A DISKUZE 56
5.1 Separace a detekce kov-vazných proteinů 56

5.1.1 Vědecký článek I 56
Isolation and determination of lactoferrin in human saliva 56
5.1.2 Vědecký článek II 66
Microfluidic tool coupled with electrochemical assay for detection of lactoferrin isolated by antibody-modified paramagnetic beads 66
5.2 Studium interakce proteinů s kovy 77
5.2.1 Vědecký článek III 77
Single amino acid change in metallothionein metal-binding cluster influences interaction with cisplatin 77
5.2.2 Vědecký článek IV 89
Study of interaction between metallothionein and cdte quantum dots 89
5.2.3 Vědecký článek V 100
Use of nucleic acids anchor system to reveal apoferritin modification by cadmium telluride nanoparticles 100
6 ZÁVĚR 112
7 ZDROJE INFORMACÍ 114
8 SEZNAM ZKRATEK 134
9 SEZNAM OBRÁZKŮ 135

1 ÚVOD

V současné době narůstá enormní zájem vědecké společnosti o objasnění mechanismů a principů vzniku řady civilizačních chorob jako je rakovina, kardiovaskulární onemocnění, diabetes aj, stejně tak jako vysvětlení rezistence organismu či patogenních mikroorganismů a virů na dosavadní léčiva. Ve vědě se uplatňují dva přístupy, které pomáhají objasnit příčiny a definovat důsledky civilizačních chorob; základní výzkum a aplikovaný výzkum.

Základní výzkum je motivován zvědavostí a studiem vlastností přírody. Jeho cílem je získat znalosti o základech či podstatě pozorovaných jevů, vysvětlení jejich příčin a možných dopadů při využití získaných poznatků. Jeho dílčím úkolem je otevřít nové otázky a podnítit zájem o nalezení odpovědí. Zatímco aplikovaný výzkum je více zaměřený na získání nových poznatků zaměřených na budoucí využití v praxi. Je to ta část výzkumu, jejíž výsledky se prostřednictvím vývoje využívají v nových výrobcích, technologiích a službách. Poskytuje odezvu na to, co společnost potřebuje a co společnost očekává. Oba přístupy by jeden bez druhého nemohly existovat. Jedná se o propojený celek, díky kterému se dnešní společnost posouvá ve vývoji a používá jej jako nástroj pro sebezdokonalení a pokrok lidstva.

Kov-vazné proteiny jsou chápány oběma přístupy jako důležitý předmět studia spojující anorganický „svět“ s organickým. Je mimořádně zajímavé, jak navzájem oba chemické obory spolu interagují. O to zajímavější je fakt, že tato interakce může být pro živý organismus prospěšná, ba ji ke svému životu potřebuje; anebo toxická, která jej může usmrtit.

Předkládaná disertační práce se zabývá izolací a studiem významných kov-vazných proteinů. V literárním přehledu je uveden momentální stav poznání této oblasti proteomiky a jsou popsány dostupné analytické metody pro jejich studium. Výsledková část je zaměřena na aplikovaný a základní výzkum interakce proteinů s kovy. Ačkoliv je předpokládáno, že v budoucnu bude řada výsledků překonána a nové otázky otevřeny, věřím, že získané poznatky pomohou obohatit vědění na úrovni analytické chemie a biochemie.

2 CÍLE PRÁCE

→ Literární přehled přehled týkající se kov-vazných proteinů a metod vhodných pro jejich studium

→ Optimalizace izolace a stanovení laktoferinu

→ Monitorování interakce metalothioneinu a apoferitinu s kov-obsahujícími léčivy a kovovými nanočásticemi

3 LITERÁRNÍ ČÁST

3.1 Význam kov-vázajících proteinů v organismu

Téměř jedna polovina všech proteinů v lidském organismu obsahuje iont kovu. Jedna čtvrtina až jedna třetina všech proteinů vyžadují kovové ionty pro svou správnou funkci (Thomson, A. J. and Gray, H. B. 1998). Vzhledem k důležitosti této problematiky, zájem o studium kov-vazných proteinů značně narůstá, což dokládá statistika citovanosti daného oboru podle vědecké databáze Web of Science (Obrázek 1).

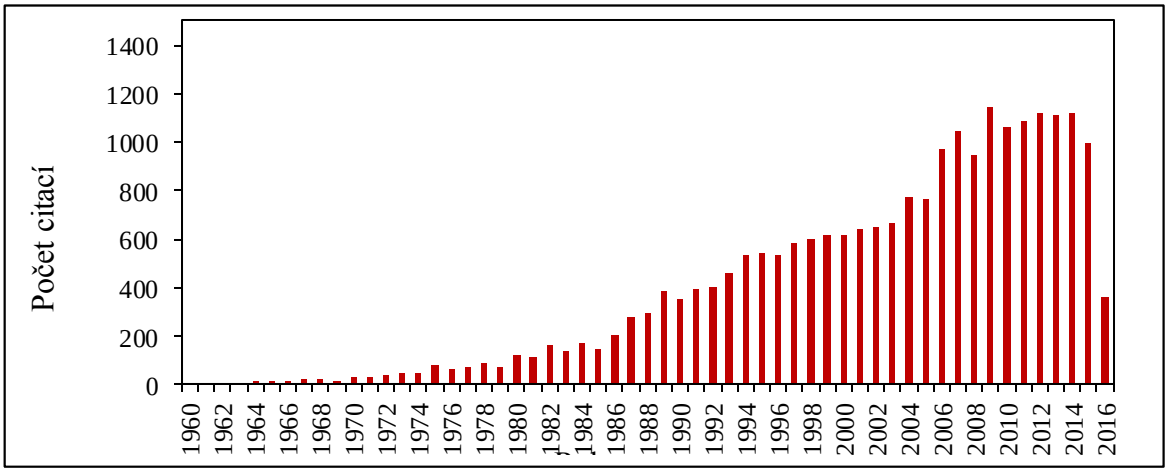

Obrázek 1: Citovanost článků obsahující klíčové slovo "metal binding proteins" od roku 1960 do roku 2016.

Kov-vazné proteiny váží ionty kovů nejčastěji mezi atomy dusíku, kyslíku nebo síry. Tyto donorové skupiny jsou často součástí proteinových postranních řetězců, imidazolových substituentů histidinových zbytků, thiolových substituentů cysteinových zbytků a karboxylátových skupin (Nara, Masayuki and Tanokura, Masaru 2008; Wang, Chu, Vernon, Robert et al. 2010; Amrein, Beat, Schmid, Maurus et al. 2012). S ohledem na rozmanitost metaloproteinů, bylo prokázáno, že v podstatě všechny zbytky aminokyselin jsou schopné vázat kovy. Peptidová kostra taktéž poskytuje donorové skupiny, které zahrnují deprotonované amidy a karbonylová kyslíková centra. Kromě

donorové skupiny mohou další organické kofaktory fungovat jako kov-vazné ligandy (Yamauchi, O., Odani, A. et al. 2002).

Různé kovy ve struktuře proteinu mohou být ve formě aktivních redoxních iontů, jako jsou Fe^{2+}, Cu^{2+}, Co^{2+} a Mn^{2+} a neaktivních redoxních iontů jako je Ca^{2+} a Zn^{2+}. Tyto prvky se uplatňují jako transkripční faktory pro řadu enzymů, které jsou zapojeny do metabolismu DNA. Aktivní redoxní kovy mohou v organismu snadno tvořit volné radikály poškozující biomolekuly, avšak jsou velmi vhodné pro funkci enzymů, které jsou součástí reakcí a přeměn aktivních složek obsahující kyslík (Harding, Marjorie M., Nowicki, Matthew W. et al. 2010). Ionty kovů hrají velmi významnou roli ve všech biologických systémech. Jejich interakce s proteiny mají význam pro regulaci proteinových struktur a pro enzymatickou aktivitu (Zitka, Ondrej, Ryvolova, Marketa et al. 2012). Na druhou stranu jsou tyto esenciální prvky při zvýšené hladině v organismu toxické. Nedostatek nebo přebytek kovových iontů může vyústit ve vznik genetických poruch, stejně tak jako vznik malnutrice může způsobit smrt nebo řadu závažných onemocnění (Fraga, Cesar G. 2005). Bylo prokázáno, že abnormální příjem železa je spojován se vznikem dědičného onemocnění hemochromatózou, anémií, aterosklerózou a neurologickými onemocněními jako jsou Parkinsonova, Alzheimerova Huntingenova choroba (Askwith, C. and Kaplan, J. 1998; Li, W., Hellsten, A. et al. 2004; Moos, T. and Morgan, E. H. 2004). Pro udržení buněčné homeostázy všech iontů kovů se v organismu uplatňují biochemické procesy pro regulaci jejich příjmu, uskladnění a sekrece. Právě faktory, které kontrolují transport kovových iontů přes buněčné membrány, intracelulární homeostázu a regulační odezvu buněk na změnu prostředí byly předmětem mnoha výzkumů v předchozích letech (Radisky, D. and Kaplan, J. 1999). Obzvláště studovanými jsou díky jejich významu v buněčném metabolismu, kde se uplatňují hlavně jako kofaktory mnoha enzymů divalentní stopové kovy jako Cu^{2+}, Mn^{2+}, Fe^{2+} a Zn^{2+}. Obvykle je jejich intracelulární koncentrace udržována na stálé fyziologické hladině. Těžké kovy jako $Cd^{2+,}$ Co^{2+} a Ni^{2+} jsou ve vysokých dávkách toxické pro mnoho savců, ale také pro rostliny (Islam, Ejaz Ul, Yang Xiao, E. et al. 2007). Vlastností těchto kovů je schopnost se navázat do proteinů na místa, která jsou určena pro vazbu jiných prvků tak, že vyvazují původní iont z jeho přirozeného

vazebného místa (Bozhkov, Anatoliy, Padalko, Vladimir et al. 2010). Výzkumy ukázaly, že vazbou těžkých kovů do struktury DNA a jaderných proteinů vzniká oxidační poškození biologických makromolekul (Schroder, H. C., Di Bella, G. et al. 2005; Zhang, Ying-Mei, Wang, Ye-Jing et al. 2006; Sebbio, Claudia, Carere, Claudio et al. 2014). Pro eliminaci toxicity kovů si buňky vyvinuly řadu strategií, z nichž nejdůležitější jsou transport nebo sekvestrace do organel či navázání na thiolové skupiny (Hediger, M. A. 1997; Eide, D. J. 1998; Nelson, N. 1999).

3.2 Funkce kov-vazných proteinů

Funkce metaloproteinů závisí na jemných interakcích mezi ionty kovů, jejich koordinaci a stabilitě proteinové konformace. V prvním případě může iont kovu dominovat a při absenci kovu je protein zcela rozvolněn (příkladem jsou zinkové prsty). V druhém případě dominuje protein, který váže iont kovu do své struktury. Tento efekt je výrazný u různých superoxidových dismutasových metaloenzymů (SOD). Například CuZn-SODs (Tainer, J. A., Getzoff, E. D. et al. 1983; Zou, Yu, Sun, Yunxiang et al. 2016) řídí svůj redoxní potenciál a rychlost katalýzy deformací proteinové geometrie kolem Cu iontu. Naproti tomu, Ni-SODs (Barondeau, D. P., Kassmann, C. J. et al. 2004) vykazuje aktivní místo na svém N konci, který je neuspořádaný v nepřítomnosti iontu kovu. Ionty kovů mají tedy významnou roli v konformaci specifických míst ve struktuře proteinu a díky této specifitě tak tyto proteiny vykazují řadu důležitých funkcí nezbytných pro život. Kov-vazné proteiny lze rozdělit na základě kovu, který daný protein váže anebo na základě jejich funkce, kterou celý komplex vykonává.

3.2.1 Transportní a zásobní kov-vazné proteiny

Transportní proteiny umožňují přenášení iontů kovů napříč organismem a jsou životně důležité pro všechny typy živočichů. Tyto proteiny se transportu mohou účastnit přímo jako tzv. přenašeče, nebo umožňují aktivní či pasivní difúzi kovů do buňky (Ruotolo, Roberta, Marchini, Gessica et al. 2008; Wille, Holger, Ehsani, Sepehr et al. 2010). Pro přehled membránových transportních proteinů byla vytvořena klasifikační databáze (TCDB z aj. Transporter Classification Database) dostupná z webové stránky

www.tcdb.org. Databáze obsahuje více než 10 000 proteinů, které prezentují všechny dosud poznané rodiny molekulárních transportních systémů všech známých organismů. Proteiny jsou v databázi organizovány do pěti úrovní hierarchického systému, kde první dvě úrovně jsou třída a podtřída, další dvě jsou rodiny a pod rodiny a poslední jsou transportní systémy (Saier, Milton H., Jr., Reddy, Vamsee S. et al. 2014).

Významným proteinem náležící do podskupiny hemoproteinů, hemoglobin, je principiálním přenašečem kyslíku v organismu. Jeho struktura obsahuje čtyři podjednotky, ve kterých jsou Fe^{2+} ionty koordinovány do planárních, makrocyklických ligandů protoporfyrinu IX a imidazolového atomu dusíku histidinových zbytků (Buergers, Anja C. and Lammert, Eckhard 2011). Šest koordinačních míst obsahuje molekuly vody nebo kyslíku (Liddington, Robert 1994; Safo, M. K. and Abraham, D. J. 2003). Na rozdíl od hemoglobinu, myoglobin, který se nachází ve svalových buňkách, má pouze jednu takovou jednotku. Jeho aktivní místo je lokalizováno v hydrofobní kapse uvnitř molekuly. Zde se odehrává ireverzibilní oxidace Fe^{2+} na Fe^{3+}. Rovnovážná konstanta pro tvorbu HbO_2 je udržována uvolněním kyslíku v závislosti na jeho parciálním tlaku v plicích a ve svalech. Čtyři podjednotky hemoglobinu vykazují kooperativní působení, které umožňuje snadný přenos kyslíku z hemoglobinu do myoglobinu (Pin, S., Valat, P. et al. 1985; Hardison, Ross C. 2012). Transfer elektronů v organismu zprostředkovává skupina proteinů označovaných jako cytochromy. Přítomnost iontů kovu umožňuje metaloenzymům vystupovat v redoxních reakcích, které nemohou být snadno zprostředkované pomocí funkčních skupin aminokyselin. Atom železa ve většině cytochromů obsahuje i hemovou skupinu. Různorodá koordinace kovu ve struktuře cytochromů rozhoduje o různém Fe^{2+} a Fe^{3+} redoxnímu potenciálu, díky čemuž jsou cytochromy zapojeny do mitochondriálního elektronového transportního řetězce (Pelletier, H. and Kraut, J. 1992; Giorgio, M., Migliaccio, E. et al. 2005; Dai, Yuejie, Zhen, Jing et al. 2015).

3.2.1.1 Metalothionein

Metalothioneiny (MTs) jsou nízkomolekulární kov-vazné proteiny, které ve své sktruktuře obsahují téměř jednu třetinu cysteinových zbytků. Lidské MTs mají celkově

11 funkčních isoforem, které mohou být rozděleny do čtyř tříd MT-1 - 4. Tyto třídy jsou kódovány osmi aktivními MT1 geny (MT1A, B, E, F, G, H, M a X) a jedinou kopií MT2 (známé také jako MT2A), MT3 a MT4. Lidský genom také obsahuje pět pseudo-MT1 genů, které jsou odvozeny od duplikací, a které mutací ztratily funkci původního prenatálního MT1 (Raudenska, Martina, Gumulec, Jaromir et al. 2014). Nejčastěji se vyskytující isoformy MT-1 a -2, které jsou široce zkoumány v souvislosti s metabolismem zinku. Bylo zjištěno, že jsou exprimovány v mnoha typech buněk různých orgánů a tkání, a také v kultivovaných buňkách. Jejich funkcí je udržování buněčné Zn homeostázy a vypořádávání se buňky s cytotoxicitou vyvolanou těžkými kovy chlelatací těchto iontů a snižováním jejich intracelulární koncentrace (Spahl, D. U., Berendji-Grun, D. et al. 2003; Barbato, John C., Catanescu, Otilia et al. 2007). Dnes již je také velmi dobře objasněn a popsán mechanismus MT vychytávání volných radikálů a redoxní cyklus zinku a metalothioneinu (Obrázek 2) (Lazo, J. S., Kondo, Y. et al. 1995), ale dosud není zcela jasné, jak se MT-1 a -2 funkčně odlišují. Oba proteiny mají podobnou aminokyselinovou sekvenci a indukovatelnost v odpovědi na zinek a různé stresové podmínky. Avšak mnoho studií nerozlišuje mezi oběma isoformami a jejich funkce je zatím zcela neobjasněná (Ruttkay-Nedecky, Branislav, Nejdl, Lukas et al. 2013).

Transkripce MT1/2 je regulována kov-responzivním elementem vazbou transkripčního faktoru 1, který reguluje odezvu genové exprese na ionty kovů (Kimura, Tomoki, Itoh, Norio et al. 2009). MTF-1 je základní faktor pro expresi genu MT1/2 vyvolanou těžkými kovy. Bylo zjištěno, že MTF-1 reguluje zinek-dependentní odezvu pro transkripci ZnT1 a ZnT2 (Langmade, S. J., Ravindra, R. et al. 2000; Guo, Liang, Lichten, Louis A. et al. 2010) a potlačuje expresi Zip10 (Lichten, Louis A., Ryu, Moon-Suhn et al. 2011), což značí roli MTF-1 v homeostáze zinku. Tumor supresorová fosfatáza a homolog tensinu modulují MTF-1 zprostředkovanou expresi ZnT1 a MT (Lin, Meng-Chieh, Liu, Ya-Chuan et al. 2012), což naznačuje vztah mezi tumorgenezí a homeostázou zinku v organismu.

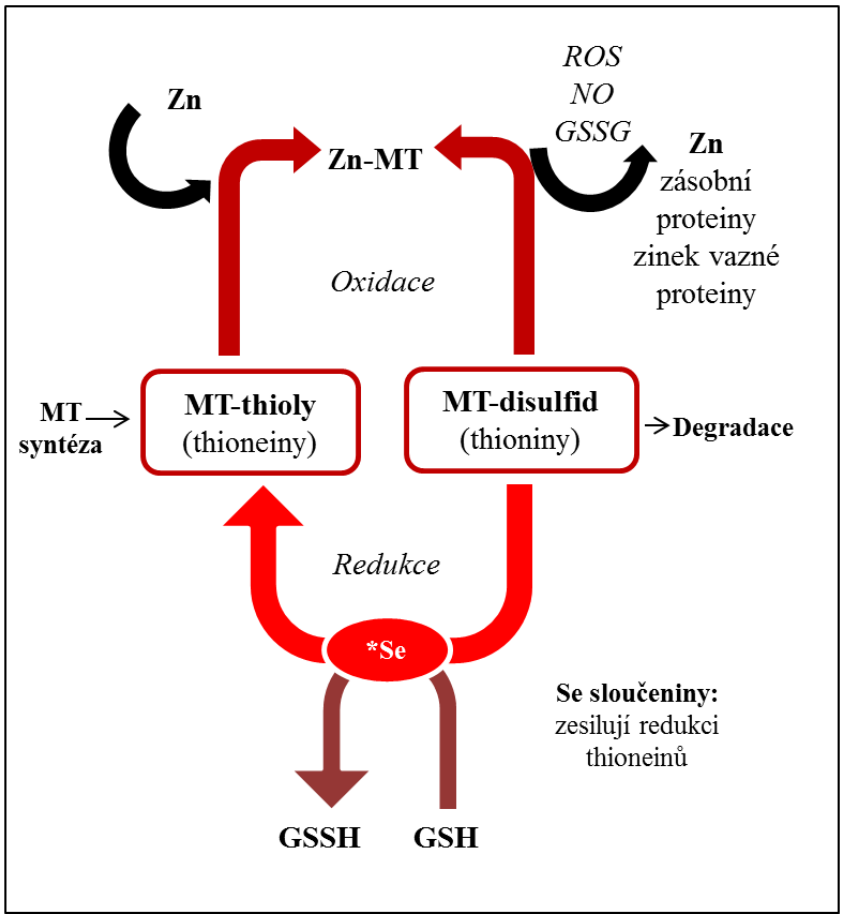

Obrázek 2: Redoxní cyklus metalothioneinu. Zinek navázaný na MT je uvolněn do zinkových zásobních a zinek vázajících proteinů pod fyziologickými oxidačními podmínkami za tvorby MT-disulfidu (thionin). Tento proces je zesílen v přítomnosti volných radikálů, jako jsou nitridy oxidu (NO), reaktivními částicemi kyslíku (ROS) a oxidovaným glutathionem (GSSG). MT-disulfid může být degradován nebo v redukčních podmínkách redukován na MT-thiol (thionein). Tato redukce je doprovázena přítomností selenokatalyzátorů. MT-thiol váže zinek a vytváří Zn-MT, který je termodynamicky stabilní. Přepracováno z (Gonzalez-Iglesias, Hector, Alvarez, Lydia et al. 2014).

3.2.1.2 Feritin

Dalším významným metaloproteinem lidského organizmu zásobní protein, který slouží jako hlavní zásobní forma železa - feritin. Skládá se z 24 proteinových podjednotek apoferitinu a v jeho struktuře je uzavřeno až 4500 iontů železa. Většina z celkového množství ferritinu je intracelulární a jen malá část se nachází v plazmě (Bradley, Justin

M., Le Brun, Nick E. et al. 2016). Feritiny se v tkáních nachází ve dvou izoformách: bazická izoforma ferritinu obsahuje ve své struktuře více kyselé H (heavy) podjednotky a slabě bazické L (light) podjednotky. Bazické izoferitiny jsou odpovědné za dlouhodobé skladování železa a nacházejí se především v játrech, slezině a kostní dřeni. Kyselé izoferitiny jsou zastoupeny především v myokardu, placentě, nádorových tkáních a v menším rozsahu v depotních orgánech (Erikson, K. M., Beard, J. L. et al. 1998).

3.2.1.3 Přehledový článek I:

Apoferritin applications in nanomedicine

Heger, Z., Skalickova, S., Zitka, O., Adam, V. and Kizek, R

Nanomedicine, 2014, 2233-2245, 1743-5889

Podíl autora Skalickova S.: 40 % textové části práce

Nanomedicína je neustále se vyvíjející vědní obor, který se snaží zavést do klinické praxe moderní nanotechnologie. Zejména se jená o nanostrukturované materiály, které sebou přináší nové možnosti v cíleném transportu léčiv a *in vivo/in vitro* zobrazování. Velký potenciál v tomto oboru je zaměřen na syntetické a biologické materiály, jako jsou fulereny, porézní křemičitanové nanočástice,nanočástice z oxidu železa, zlaté nanočástice, uhlíkové nanotrubičky, liposomy, dendrimery, proteinové klece (apoferitin) a různé nanosféry. Ačkoliv jsou tyto materiály akceptovány organismem a nespouštějí imunitní odezvu, jsou v tomto oboru uplatnitelné také proteiny, které jsou organismu vlastní, a organismus je dokáže po ukončení jejich působení zcela rozložit. Nápříklad se jedná o feritiny , které jsou přítomny v mnoha živých organismech napříč evolucí a díky jejich transportní funkci, mohou být využity v mnoha nanotechnologických aplikací.

Cílem přehledového článku bylo shrnutí dosavadních znalostí o apoferritinu, jeho struktuře, využití jako materiálu pro různé použití v medicíně a také jeho aplikace jako

platformy pro syntézu nanočástic. Řada studií demonstruje možnosti uplatnění apoferritinů jako přenašeče léčiv pro jejich cílený transport. Apoferitin chrání transportované molekuly před jejich degradací, zamezuje jejich předčasnému uvolnění a chrání necílové tkáně před účinky přenášených terapeutik. Proteinové nanoklece mají také schopnost zabránit spontánní makromolekulární agregaci. Díky těmto vlastnostem, je apoferitin využitelný v genové terapii a jako transportér uplatnitelný v léčbě různých onemocnění, včetně rakoviny.

Review

Nanomedicine

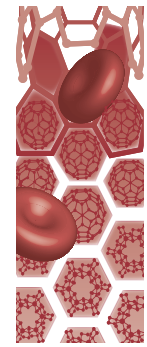

Apoferritin applications in nanomedicine

Nanomedicine as a continuously evolving discipline is still looking for a structure with perfect properties that is usable as a multifunctional transporter. Great potential is attributed to synthetic materials such as fullerenes, porous hollow silica nanoparticles and single-wall nanotubes, among others. However, materials that are natural to the human body are more acceptable by the organism, and thus become an attractive approach in this field of research. Ferritins are proteins that naturally occur in most living organisms throughout evolution and may be a possible transporter choice. Numerous applications have demonstrated the possibilities of iron-free ferritins, called apoferritins, serving as platforms for various nanomedical purposes This article summarizes the advantages and disadvantages of these proteins and discusses their practical applications and future perspectives.

Keywords: horse spleen ferritin • magnetic resonance imaging • nanoscale • nanotrasporter • photodynamic therapy • self-assembly • therapeutic agents

Zbynek Heger[1], Sylvie Skalickova[1], Ondrej Zitka[1,2], Vojtech Adam[1,2] & Rene Kizek*[,1,2]

[1]Department of Chemistry & Biochemistry, Faculty of Agronomy, Mendel University in Brno, Zemedelska 1, CZ-613 00 Brno, Czech Republic

[2]Central European Institute of Technology, Brno University of Technology, Technicka 3058/10, CZ-616 00 Brno, Czech Republic

*Author for correspondence:
Tel.: +420 5 4513 3350
Fax: +420 5 4521 2044
kizek@sci.muni.cz

Ferritins (FRTs) are the major iron storage and detoxifying oligomeric proteins in most organisms, from humans through to invertebrates, plants and microorganisms [1–3]. In such different organisms, the structure of FRTs varies only slightly [4,5]. Their main role is to prevent the harmful accumulation of iron inside the organism by collecting free iron in the form of ferrihydrite phosphate ($[FeOOH]_8[FeOPO_3H_2]$) in its core for further usage of these ions as enzymatic cofactors [6–9]. In nature, the interiors of FRTs are filled with iron, but when expressed artificially in iron-free conditions, the yielded apoferritins are hollow, comprising a cavity that can be loaded with different substances, including those of an inorganic and/or organic nature [10,11].

Based on the aforementioned properties, apoferritins have attracted great interest not only because of their nanoscale nature and ability to serve as transporters, but also because of their high stability and special structure [12]. Researchers in nanotoxicology have indicated that these pharmacological properties, as well as biodegradability, biocompatibility and nontoxicity, are crucial for transporting molecules [13–15], considering the fact that nanoscale materials have become the most rapidly developing area in the biomedical research field, particularly in the field of targeted therapy [16–18]. In this field, the apoferritins, as naturally occurring proteins, meet the requirements for targeted therapy. The aim of this article is to summarize the knowledge regarding apoferritin structure, its utilization as a material for various nanomedicine applications and, furthermore, its application as a platform for the synthesis of nanoparticles.

FRT protein superfamily

The FRT superfamily can be divided into three subfamilies: the classical FRTs; the bacterioferritins (BFRs); and the DNA-binding proteins from starved cells (DPSs). The FRT and BFR proteins are considered to be maxi-ferritins, whereas DPS proteins are considered to be mini-ferritins. These three subfamilies share the same character-

Future Medicine part of fsg

istic four-helix bundle fold [19,20]. The most significant difference between the FRT and BFR proteins is the presence of 12 heme moieties in BFRs. In addition, the DPS proteins form a smaller molecule made up of only 12 monomers with a lower iron storage capacity than the FRTs and BFRs and utilize unique ferroxidase sites [21].

Apoferritin structure

The structure of apoferritin is remarkably stable and robust, and it is able to withstand biologically extreme temperatures (up to 70°C) and a wide pH range (pH 2.0–10.0) for an appreciable period of time without significant disruption of their quaternary structure [22,23]. The native, cytosolic FRTs are proteins that are composed of two types of subunits – H-type (heavy) and L-type (light) – where we can find 53% sequence identity [24,25]. They are encoded by separate genes with nonexchanangeable functions [26,27], whereas those from plants and bacteria contain only H-type chains [28]. Twenty-four FRT subunits form a spherical cage-shaped protein shell folded in a bundle of four long parallel and antiparallel α-helices (A, B, C and D) with a fifth shorter C-terminal helix E, inclined at 60° to the major helix bundle [29]. Each subunit is formed by an individual molecule that joins its neighboring subunit through noncovalent interactions in order to form the whole molecule with a molecular mass of approximately 20 kDa occurring in octahedral (*F*432) symmetry [30,31]. The apoferritin structure has six twofold symmetry axes, four threefold symmetry axes and three fourfold symmetry axes. It is known that there are narrow hydrophilic channels along the threefold symmetry axes consisting of negatively charged amino acids (glutamic and aspartic acid) and hydrophobic channels along the fourfold symmetry axes [32,33]. Several channels transversing the shell facilitate inorganic or organic ions to enter and exit the protein cavity [34–36]. The protein shell forms an inner cavity with inner and outer diameters of 7–8 and 12–13 nm, respectively [29–30,37]. The inner cavity, with an 80-Å diameter, is capable of storing up to 4500 Fe(III) atoms [38,39].

Apoferritin self-assembly ability

The self-assembling ability of apoferritin is widely used by researchers in the field of nanomedicine because the protein cage may be reversibly disassociated in unfavorable environments and after a change in the environment, the conditions may be reconstituted backwards, retaining the therapeutic agent in its cavity. The same principles are also applied for the enclosure of contrast agents in imaging protocols. This natural ability is advantageous in many ways: the resulting nanoparticles form size-uniformed cavities, and thus encapsulation of cargo can be highly reproducible; the encapsulation protocol is simple, based only on changes to environment conditions; and the undesired release of cargo in blood vessels is eliminated due to the absence of the required conditions. The overall scheme of the encapsulation of target molecules into apoferritin cages is shown in Figure 1. The properties of the FRT assembly were first found in natural horse spleen FRTs in 1978 [40]. The protein cage can be disassociated into all 24 subunits at low pH (2.0) and the subunits can be reconstituted backwards under the influence of higher pH [41]. As was observed using synchrotron small-angle x-ray scattering in the presence of an environment with a pH below 0.8, the disassembled subunits aggregated, which is attributed to the denaturation of the stable protein structure of FRTs [42]. The overall assembly mechanism of apoferritin was first designed by Gerl and Jaenicke using data obtained by intrinsic fluorescence, far-UV circular dichroism and glutaraldehyde cross-linking experiments [43]. The apoferritin self-assembled product was formed during a series of reactions with a mixture of partially assembled subunits, including monomers, most frequently trimers, hexamers and dodecamers [43]. It was also shown that two hexamers could be used to form a dodecamer, and two dodecamers could assemble into a 24-mer. These results led to a refined model where the 24-meric cage assembles from a dimer (M2) via tetramers (M4) and hexamers (M6) [40].

Apoferritin utilization for targeted imaging

As drug or contrast agent carriers, apoferritins could protect their cargo against degradation and prereleasing, which would cause undesired side effects. As has been described previously, apoferritins may effectively carry a cargo towards different types of tissue, as shown in Figure 2. In this area, it can be mentioned that the apoferritins may be efficiently taken up from blood by their specific receptors, SCARA5 [44,45] and TfR1. Moreover, the amount of apoferritin that is taken up can be quantitatively visualized when the protein is loaded with an MRI contrast agent, such as gadolinium and/or manganese [46,47]. Manganese–apoferritin complexes were used as highly sensitive MRI contrast agents for the detection of hepatocellular carcinoma based on manganese–apoferritin complex uptake by liver SCARA5 [48]. When injected into hepatitis B virus-transgenic mice with spontaneously developed hepatocellular carcinoma, manganese–apoferritin enabled the clear distinguishing of healthy liver tissue and tumor lesions as hyperintense and hypointense T_1-weighted magnetic resonance images. The apoferritin-encapsulated gadolinium, as a possible candidate for a new MRI contrast agent, was suggested by Makino

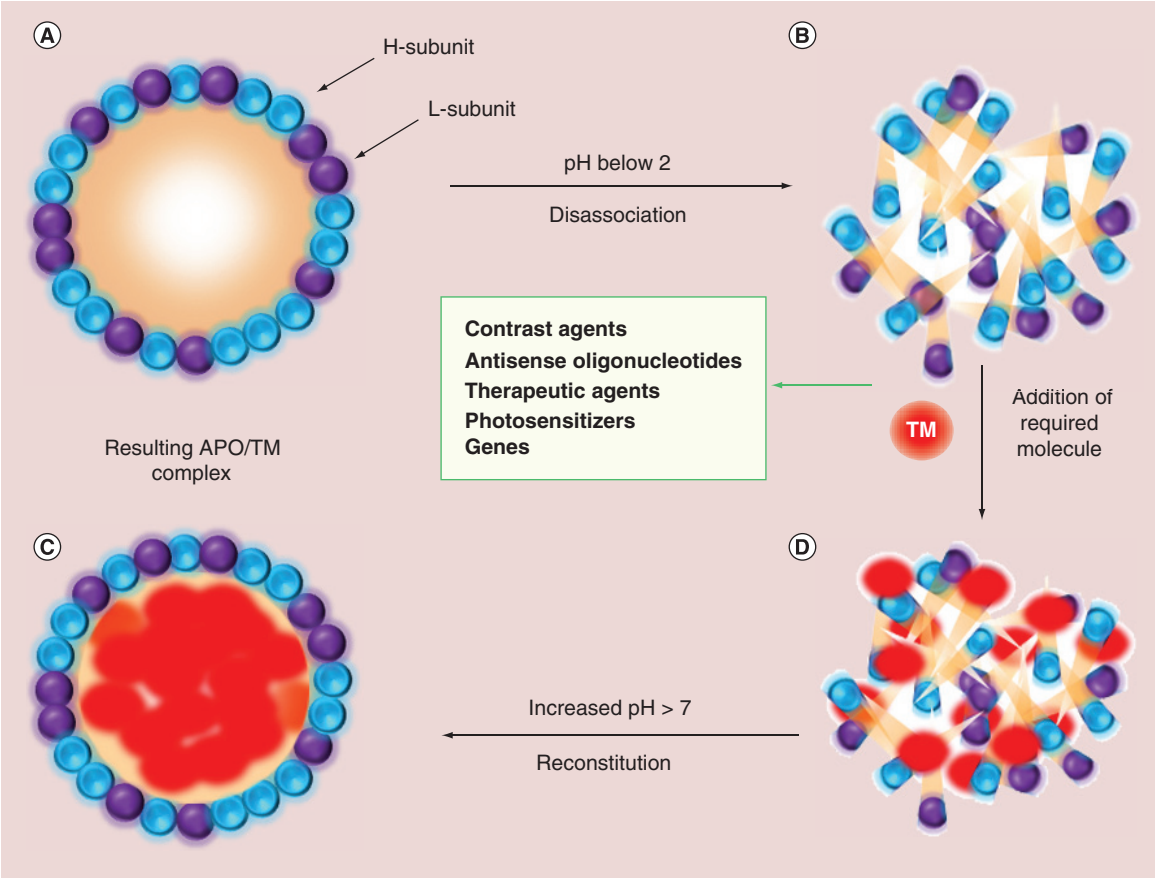

Figure 1. Overall scheme of apoferritin reversible disassociation under the influence of pH changes.
(A) Twenty-four subunits divided into H- and L-subunits form the stable apoferritin protein molecule. **(B)** Low pH (below 2.0) protein disassociates reversibly into the basic 24 subunits. **(C)** The addition of the TM required for complex formation follows. **(D)** After an increase of the pH value of solution, the protein molecule reconstitutes, thus encapsulating the target molecules in its inner cavity.
APO: Apoferritin; TM: Target molecule.

et al. [44]. Gadolinium was efficiently encapsulated into the apoferritin cavity and enhanced the T_1 relaxivity to as much as tenfold higher than the commercially used contrast agent gadolinium-DOTA. Furthermore, the *in vivo* blood clearance time of apoferritin was prolonged by its surface modification with dextran. An increased accumulation of this complex was observed mainly in the tumor region due to passive targeting via enhanced permeability and retention effect. Moreover, single-dose toxicity tests showed no serious side effects [44]. It was previously shown that the modification of apoferritin with the substrate peptides of MMP-2 and a hydrophilic polymer (PEG) may cause the aggregation of nanoparticles initiated by the action of a tumor-associated protease, MMP-2, leading to T_2 shortening on MRI [49]. Sun *et al.* demonstrated that two gold nanoclusters localized at the ferroxidase active sites of the FRT H-chain nanocomplex not only retained the intrinsic fluorescence properties of gold, but also gained enhanced intensity with a red shift and exhibited tunable emissions due to the coupling interaction between paired gold clusters bound in the H-chain of apoferritin [50]. Furthermore, this complex showed an organ-specific targeting ability due to the high expression of the FRT receptor SCARA5 in kidney cells, the high biocompatibility and the low cytotoxicity. Such agents are very promising for *in vitro* and *in vivo* imaging [50]. The importance of the possibility of apoferritin outer-shell functionalization was shown by Valero *et al.* [51]. In this case, apoferritin-enclosed nanomaghemite was modified with *N*-acetyl-D-glucosamine and D-mannose, and the carbohydrate-functionalized apomaghemite nanoparticles retained their recognition abilities, as demonstrated by the strong affinity with their corresponding carbohydrate-binding lectins. The *in vivo* MRI studies showed the efficiency in contrasting images, where the r_2 nuclear magnetic resonance relaxivities, as well as the precontrast and postcontrast T_2*-weighted images, were comparable with those obtained from the commercially used Endorem® (Guerbet, Villepinte, France).

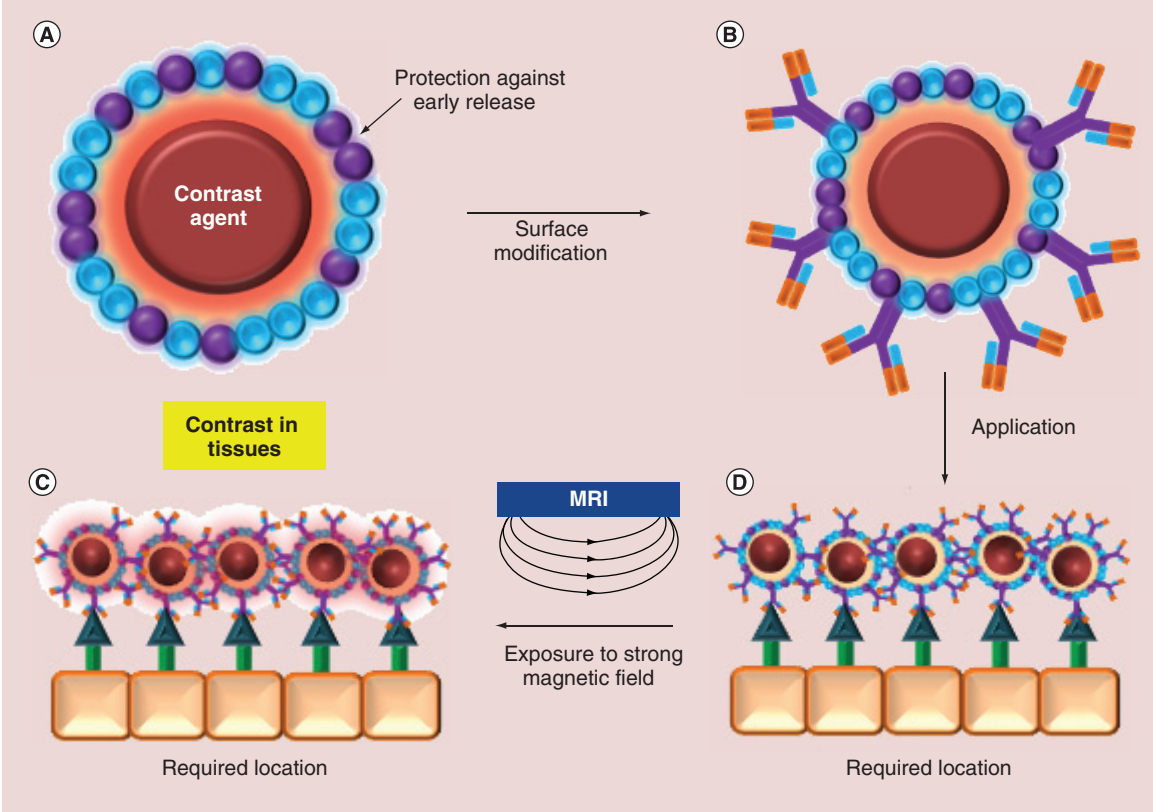

Figure 2. Apoferritin may be simply exploited as a nanotransporter, bearing various contrast agents. (A) Contrast agents may be encapsulated into the apoferritin cavity in the classical way. **(B)** After encapsulation, the surface of the apoferritin–contrast agent complex may be functionalized through antibodies or carbohydrates in order to form targeted imaging conjugates. **(C)** After application of the apoferritin–contrast agent, the complex is driven by recognition elements placed on its surface towards the required location. Moreover, the apoferritin protects the cargo against undesired degradation. **(D)** After exposure to a strong magnetic field produced by MRI, a radiofrequency signal is emitted and, subsequently, the contrast between different tissues is determined.

Apoferritins as drug nanotransporters

The first mention of the ability of FRTs to encapsulate anticancer therapeutics was published in 2005 by Simsek and Kilic in their paper entitled 'Magic ferritin: a novel chemotherapeutic encapsulation bullet' [52]. Seven years later in 2012, Kilic *et al.* formed an apoferritin complex with doxorubicin, a commonly used cytostatic drug [53]. The doxorubicin encapsulation was carried out using direct and step-wise changes of the pH of the solution from 2.5 to 7.4. It was found that up to 28 molecules of doxorubicin could be capsulated per apoferritin protein and no significant drug leakage occurred over several days' storage [53]. In the same manner, doxorubicin was encapsulated into biotinylated apoferritin whose surface was modified with streptavidin-functionalized magnetic particles [54]. This complex can be tracked by fluorescence detection and, furthermore, be applied in targeted transport using an external magnetic field. Other cytostatics, such as carboplatin, cisplatin [55,56] or daunorubicin [57], can also be encapsulated in the apoferritin cavity and the drug-loaded protein has cytotoxic effects on tumor cells (summarized in Table 1). Although apoferritin exhibits great attributes for serving as a platform for nanomedicine, the possible undesired immune response of patients still exists. The ideal nanotransporter has to go through the body undetected by immune system. Despite evidence that excessive amounts of apoferritin administered for long periods can trigger immune complex glomerulonephritis in mice [58], there is still a lack of evidence regarding immune responses in human.

In addition to its well-documented encapsulation capacity, apoferritin can also bind specifically to a variety of cell types due to the presence of FRT receptors on the surfaces of various cells [63–65]. Besides SCARA5, only one FRT receptor in human cells, TfR1, has been shown to bind both FRT (via binding with H-subunit of the protein) and transferrin [66]. The internalization of apoferritin is performed by clathrin-mediated endocytosis (also called receptor-mediated endocytosis) [67] during the acidification of endosome, thus the cargo is released gradually (Figure 3). Moreover, the functionalization of the protein surface with various

types of antibodies may offer the possibility to transport cargo towards the required site very specifically. As was shown by Cutrin *et al.*, the encapsulation of curcumin, a therapeutic with antioxidant and anti-inflammatory properties, inside the apoferritin cavity significantly increased its stability and bioavailability [47]. This complex was used to attenuate the thioacetamide-induced hepatitis, and mice pretreated with the intraperitoneal administration of apoferritin–curcumin showed significantly attenuated hepatic injury as assessed by measuring alanine aminotransferase activity [47]. In addition, the cytostatic drug 5-fluorouracil (5-FU) can be sequestered into the void space of the apoferritin modified with gold in order to produce a nanoscale hybrid apoferritin modified with gold carrying 5-FU. Gold-modified apoferritin then serves as a bionanochemosensitizer, rendering tumor cells more susceptible to 5-FU by cell-cycle regulation, therefore leading to a significant decrease in the IC_{50} value of 5-FU in a human carcinoma cell line (HepG2) from 138.3 to 9.2 μM [59]. Bradshaw *et al.* proposed a complex comprising lead(II) sulfide quantum dots enclosed in an apoferritin cage, and it was shown that after the application on colorectal carcinoma cells, they failed to recover their proliferative capacity [60]. Moreover, the generation of reactive oxygen species triggered their apoptosis. By contrast, the apoferritin–lead(II) sulfide quantum dot complex did not negatively affect non-tumor human microvessel endothelial HMEC-1 cells [60]. Genetic modification of the protein can lead to the presence of a peptide with a required sequence on the surface. Zhen and colleagues genetically modified FRT with the Cys–Asp–Cys–Arg–Gly–Asp–Cys–Phe–Cys (RGD4C) peptide, showing affinity towards tumor cells through the RGD–integrin $\alpha_v\beta_3$ interaction [10]. Doxorubicin-loaded RGD FRT nanocages exhibited longer circulation times, higher tumor uptake and tumor inhibition. In addition, these nanocages decreased cardiotoxicity compared with free doxorubicin. Apoferritin can also be fused to other proteins in order to form chimeras. With the insertion of hemagglutinin onto the interface of adjacent apoferritin subunits, the spontaneously assembly and generation of nanoparticles with immunization attributes were

Table 1. Overview of apoferritin utilization in drug delivery.

Cargo	Complex	Application	Apoferritin role	Ref.
DOX	APO–DOX	–	Encapsulation concept	[52]
DOX	APO–DOX	–	Drug leakage elimination	[53]
DOX	MPs@APO–DOX	–	Encapsulation and surface modification	[54]
Cisplatin-; carPt	APO-cisplatin-; carPt	–	Improvement of drug toxicity profiles	[55]
Cisplatin-; oxali-; carPt	APO-cisplatin; oxali-; carPt	PC12	Enhancement of platinum-based drug uptake	[56]
Daunorubicin	APO–DNR–PLAA	–	Modification to improve complex stability	[57]
Cur; Gd	APO–Cur–Gd	Mice with thioacetamide-induced hepatitis	Enhancement of Cur and Gd stability and bioavailability	[47]
5-FU	APO–AuNP–5-FU	HepG2	Chemosensitization, decrease of drug IC_{50}	[59]
PbSQDs	APO–PbSQDs	CRCs	Platform for theranostics – imaging and treatment	[60]
X	APO–BIBA–PNIPAAm–DMIAAm	–	Surface modification to provide specifity	[61]
DOX	APOfilm–DOX	–	Controllable drug delivery and release	[62]
DOX	RGD@APO–DOX	U87-MG	Increased tumor uptake and circulation time, decreased cardiotoxicity	[10]

5-FU: 5-fluorouracil; APO: Apoferritin; APOfilm: Apoferritin mesoporous film; AuNP:Gold nanoparticle; BIBA: 2-bromo-isobutyric acid; CarPt: Carboplatin; CRC: Colorectal carcinoma cell; Cur: Curcumin; DMIAAm: 2-(dimethyl maleinimido)-*N*-ethyl-acrylamide; DNR: Daunorubicin; DOX: Doxorubicin; Gd: Gadolinium; MP: Magnetic particle; Oxali-: Oxaliplatin; PbSQD: Lead(II) sulfide quantum dot; PLAA: Poly-L-aspartic acid; PNIPAAm: Poly(*N*-isopropyl acrylamide); X: No cargo defined.

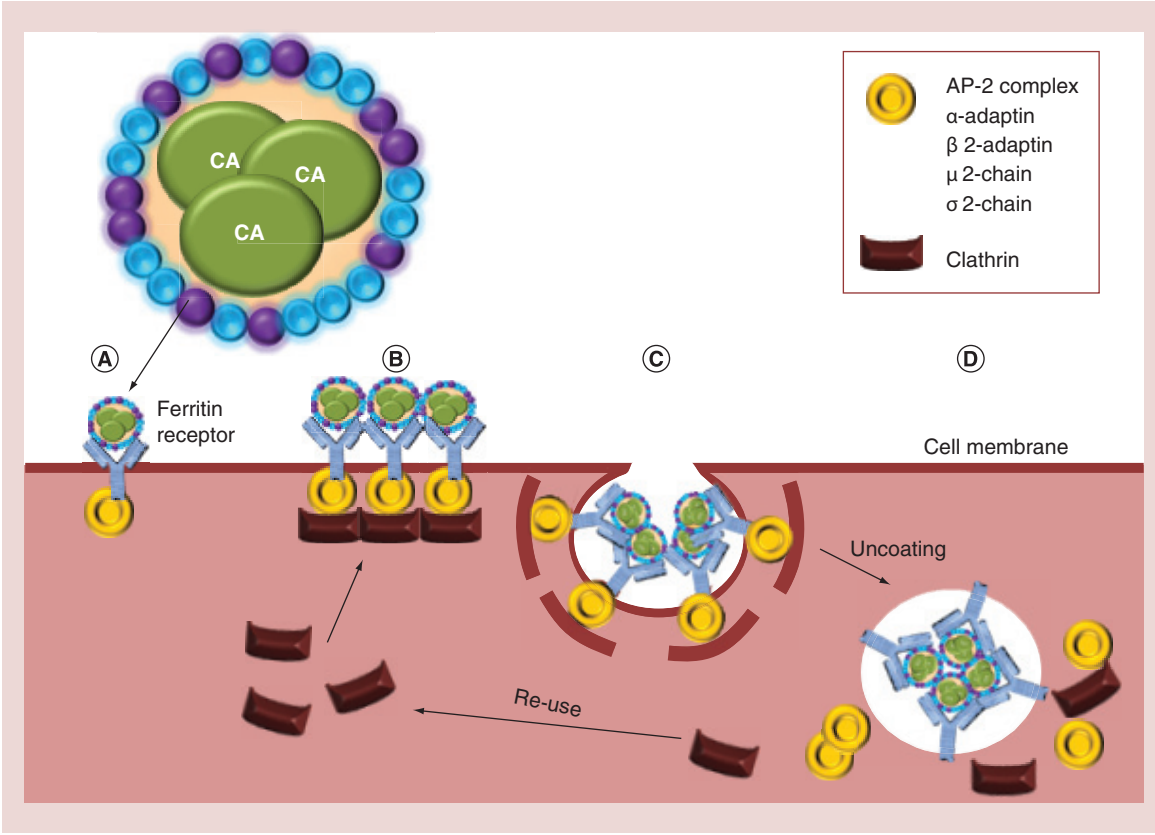

Figure 3. Apoferritin may protect chemotherapeutic agents against the tissue environment and thus significantly decrease the unwanted effects of these substances. A scheme of clathrin-mediated endocytosis is shown, demonstrating how the protein molecule is internalized into most types of cells. **(A)** Apoferritins establish binding with ferritin receptors. **(B)** After binding is established, clathrin polypeptides are attracted by the adaptor complex AP-2 and **(C)** clathrin polypeptides provide a coating of a vesicle lattice. **(D)** After the vesicle is formed, clathrin is removed and used for another purpose. In this fashion, the formed vesicle is transformed into an endosome. Due to endosome acidification, the chemotherapeutic agent may be released into the intracellular space gradually.

achieved [68]. Immunization with this nanostructure exhibited a decrease (more than tenfold) in hemagglutinin antibody titers when compared with licensed inactivated vaccine.

Bionanoparticles with the ability to form stable emulsion droplets decorated with polymer-modified apoferritin with potential to be cross-linked were prepared by grafting thermoresponsive poly(*N*-isopropyl acrylamide) and photo-crosslinkable 2-(dimethyl maleinimido)-*N*-ethyl-acrylamide to the protein surface. This structure allows the formation of capsules with thermoresponsiveness for controlled release purposes [61]. Efficient drug delivery platforms with controllable releasing speeds were constructed using mesoporous apoferritin thin films [62]. Composite nanofibrous dispersions of nanostrands and proteins were formed by assembling negatively charged proteins on the highly positively charged nanostrand surfaces. Moreover, these films also hold promise for applications in recovering dyes from dye waste waters. The structures constructed in this manner show highly diverse possibilities for apoferritin utilization, not only in form of nanotransporters, but also for the formation of functionalized materials with potential extending beyond the boundaries of nanomedicine applications.

Apoferritins in photodynamic therapy

Another form of apoferritin utilization for medical purposes is in photodynamic therapy in cancer treatment. Photodynamic therapy is s a new therapeutic modality that is emerging as a powerful tool against malignant tumors [69]. This strategy is based on the action of photosensitizers (i.e., molecules that may accumulate preferentially inside tumor cells, where they exert a cytotoxic effect after excitation by light at appropriate wavelengths) [70]. Upon the absorption of light, the photosensitizer is promoted to an excited state and undergoes crossing with oxygen, resulting in singlet oxygen, which aggressively attacks any organic compounds, and thus become highly cytotoxic. When used as a delivery system for photosensitizers to the intracellular space, the apoferritin nanocage acts as a

unique transporter that protects loaded photosensitizers from reactive biomolecules in the cell membranes. This enables further targeting of singlet oxygen upon specific light irradiation to tumor cells only (Figure 4). As was shown by Yan and colleagues, a Methylene Blue-encapsulated apoferritin complex exhibits cytotoxic effects, as tested on MCF-7 human breast adenocarcinoma cells, when irradiated using the appropriate wavelength [71]. In addition, it was demonstrated that the encapsulation of Methylene Blue into apoferritin via the reassembly process controlled by pH is useful a tool for photodynamic therapy. When the complex was irradiated at the appropriate wavelength (633 nm), it showed a positive effect on singlet oxygen production and therefore cytotoxic effects on the MCF-7 human breast cancer cell line [72]. It was demonstrated a complex with zinc hexadecafluorophthalocyanine $ZnF_{16}Pc$ [5] to behave as a potent photosensitizer [73]. The surface of the resulting conjugate was modified with RGD4C, formed by Cys–Asp–Cys–Arg–Gly–Asp–Cys–Phe–Cys, and the complex may specifically target tumor tissue through RGD–integrin interactions. Using light irradiation, phototoxicity was induced while leaving normal tissues unaffected. Due to cancer angiogenesis, resulting in an enhanced permeability and retention effect, most types of cancers are especially active in both the uptake and accumulation of nanotransporters carrying drugs and/or photosensitisers [74] This phenomenon makes them vulnerable to photodynamic therapy, and so the utilization of apoferritin as a photosintetizer nanotransporter offers promising prospects for the future of cancer therapy.

Apoferritins in biosensors/bioassays

Apoferritins may also be used as a part of very sensitive bioassays or biosensors. Applications of nanomaterials in electrochemical DNA biosensors and bioassays are reviewed elsewhere [75–77], and apoferritin is one of the more well-discussed nanostructures. In this field of applications, Kim *et al.* genetically engineered apoferritin by fusing GFP to its C-terminus and subsequently used this for chemical conjugation to DNA aptamers via each GFP's cysteine residue that was newly introduced through site-directed mutagenesis [78]. Furthermore, the DNA–aptamer-conjugated complexes were used as a fluorescent reporter probe in the aptamer-based 'sandwich' assay of the PDGF B-chain homodimer, which is considered to be a tumor marker. The limit of detection obtained with this bioassay was lowered to the 100 fM, and the assay sensitivity was significantly enhanced compared with standard immune-based detection. Versatile nanoparticle labels based on apoferritin were demonstrated by Liu *et al.* [79]. Their concept of using hexacyanoferrate(III) and fluorescein as model markers for loading into the cavity of apoferritin with an amino-modified DNA probe conjugated on its surface was used as a label for electrochemical DNA detection in connection with a magnetic bead-based sandwich

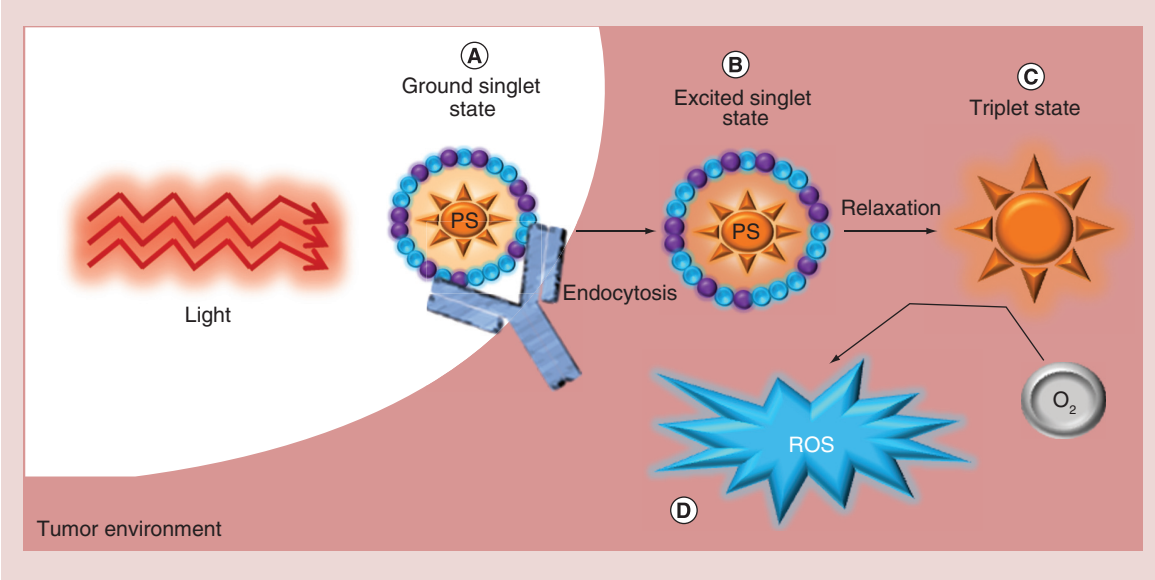

Figure 4. Apoferritins may serve a useful tool in guiding of photosensitizers to the required site of a tissue and protecting photosensitzers against the undesired effects of environment. (A) After irradiation with light, **(B)**photosensitizers absorb a photon, and subsequently, an electron is excited to the first excited singlet state. **(C)**This further relaxes to the more long-living triplet state. **(D)** The triplet-state electron interacts with molecular oxygen, leading to the formation of ROS, thereby damaging cells.
ROS: Reactive oxygen species.

hybridization assay. This method included double-hybridization events with probes linked to the biofunctionalized apoferritin and to magnetic beads, along with magnetic separation of the target DNA-linked magnetic bead–apoferritin assembly. As was mentioned in review by Pumera *et al.*, a number of metals exist that can be introduced into the apoferritin cavity and thus pave the way for different multiplexed assays [80]. Novel nanobioparticles that have been synthesized for these purposes represent a large potential for future applications, bringing new possibilities for the electrochemical biosensing of proteins or DNA.

Apoferritins as precursors for nanoparticles crafting

Because of its unique cavity structure, apoferritin has been widely used as a biotemplate for size-restricted bioinorganic nanocomposite synthesis [22,32,81–86], forming the nanoparticles with consistent size and shape, monodispersion and biocompatibility [87]. These nanocomposites may further find several applications in the field of nanomedicine, such as MRI contrast agents [88,89], as parts of various nanotransporters [90,91] or as smart theranostic platforms [92]. In the case of iron, Fe^{2+} ions are attracted by a negative charge on the outer surface surrounding the hydrophilic threefold channels of the molecule and pass through them. Ions are subsequently condensed and oxidized at negatively charged amino acid sites on the inner surface in order to form iron oxide nanoparticles. The syntheses of Fe_3O_4–γ-Fe_2O_3, MnOOH, CoOOH, CeO_2 or Co_3O_4 typically requires the addition of oxidants, such as O_2 or H_2O_2 [22,93]. For the synthesis of Ca, Ba, Ni or Cr oxoanion compounds, the addition of an oxoanion, such as carbonate or phosphate, is necessary [94,95]. The mechanism of the permeation of positively charged ions through the channels was elucidated using x-ray crystallographic observation of apoferritin metal-binding sites [96]; however, it remains unclear how the anions enter the apoferritin cavity. Solving this issue could enhance the effectiveness of nanoparticle synthesis.

Apoferritin in gene therapy

Gene therapy includes the insertion, removal or modification of defective gene(s) for the treatment of genetically inherited diseases. The commonly used transporters for gene delivery are viral vectors, liposomes, peptides and cationic polymers [97–100]. In addition to excellent knowledge regarding the genetic nature of a disease and the specific gene sequence, it is also important to select a suitable vector. The main requirements of the gene delivery vector are the protection of delivered nucleic acid against nucleases, targeting and the ability to disrupt the endosomal membrane, thus delivering the DNA to the nucleus [101,102]. Among the main obstacles against gene delivery vectors, aggregation, instability, toxicity and the propensity to be captured by the mononuclear phagocyte system [103] are the most significant. There is evidence of the aggregation of nonviral transporters, which could cause embolization [104]. Although the usage of apoferritin as a gene vector has not yet been published, it exhibits a few advantages; however, it is necessary to study apoferritins due to their colloidal behavior, charge, possession of electrostatic repulsion and the stability of the encapsulated DNA. Apoferritin cages possess a net negative charge at neutral pH that ensures its excellent solubility in water [105]. Due to apoferritin's outer surface positive charge, the protein may be easily modified, as was shown in the case of apoferritin with incorporated anionic ligand poly-L-aspartic acid into its structure [57]. In another study, apoferritin was modified by poly(ethylenimine) [106], which was employed for nonviral gene delivery [107,108]. The suggested method of entry of cationic gene delivery systems is by nonspecific adsorptive endocytosis followed by the clathrin-coated pit mechanism [109,110], because negatively charged nonviral vectors present on the cell membrane are able to interact with the positively charged systems.

Conclusion & future perspective

One of the main goals of nanomedicine is to create a nanocarrier that can efficiently and specifically deliver therapeutic agents to target sites in the body. Moreover, in order to enable efficient and specific delivery, a nanocarrier needs to have the ability to be easily modified. The replacement of synthetic materials, such as porous hollow silica nanoparticles, single-wall nanotubes and fullerenes, among others, with natural materials that are more acceptable to many organisms has become an attractive approach in this field of research.

Today, new insights into mechanisms of pH-sensitive vectors are being intensively studied [111–114], because pH values in tumors and other pathologically affected tissues dramatically change [115,116] and pH-sensitive vehicles, such as apoferritin, may serve as a promising tool for gene delivery systems. Apoferritin proteins may self-assemble into multisubunit, hollow, nanoscale cages with affinity towards SCARA5 and/or TfR1, and they have the potential to be modified through synthetic recognition molecules or genetically in order to form chimeric proteins or peptides on its surface. Due to their high stability, special structure and excellent nanotoxicological properties, such as biodegradability, biocompatibility and nontoxicity, apoferritins are the focus of many drug-delivery studies, synthesizing contrast agents in MRI, developing platforms for nanomaterial synthesis or bioas-

says. Particularly for nanomedical purposes, apoferritin meets the special requirement of being a widely used nanotransporter with the capability to protect its cargo against degradation. Moreover, apoferritin may eliminate the early release of its load and thus protect tissues against the adverse effects of various therapeutic agents. Importantly, the size uniformity of protein cages offers simplicity and reproducibility for cargo encapsulation. Protein nanocages also avoid random macromolecular aggregation. Apoferritin also has potential for applications in gene therapy, due to its properties of loading with a cargo and transport it to the required location. However, the lack of human trials of apoferritin means that there are insufficient data to determine whether the use of apoferritin is better than the use of traditional drugs. Despite the fact that apoferritin was previously linked with glomerulonephritis as a results of immune responses in mice [58,117], this may not be a problem when used in humane medicine. In case of undesired immune responses, FRT proteins can be extracted from the patient's body, carrying out the process of iron removal and subsequent drug encapsulation. This protein, which is extracted from bodily tissue, connects the terms 'nanomedicine' and 'personalized medicine' into a powerful weapon that is applicable in fighting various diseases, including cancer.

Financial & competing interests disclosure

The authors gratefully acknowledge financial support from the Grant Agency of the Czech Republic (NANOCHEMO GA CR 14-18344S) and CEITEC CZ.1.05/1.1.00/02.0068. The authors have no other relevant affiliations orfinancial involvement with any organization or entity with a financial interest in or financial conflict with the subject matter or materials discussed in the manuscript apart from those disclosed.

No writing assistance was utilized in the production of this manuscript.

Executive summary

Background

- Nanomaterials of natural origin are of great interest in medicine for the transporting and targeting of drugs.
- The encapsulation of drugs into these nanomaterials can also markedly decrease side effects.

Multitasking apoferritins

- With their self-assembling ability, apoferritins represent promising nanotransporters.
- Due to their ability to encapsulate various molecules, apoferritins may also be used in imaging protocols and photodynamic therapy.
- Biosensing can be considered as a potential field of application due the ability of apoferritins to interact with nucleic acids.
- Apoferritins may also be loaded with various chemicals in order to produce other nanomaterials.

Conclusion & future perspective

- Due to their excellent properties of withstanding various environmental influences, apoferritins may eliminate the early release of their load and thus protect tissues against the adverse effects of various therapeutic agents. Moreover, the cationic nature of the protein's outer surface enables simple surface modification in order to increase transporter specificity.
- There is great potential in the field of gene therapy for this material.

References

Papers of special note have been highlighted as:
• of interest; •• of considerable interest

1 Crichton R. Intracellular iron storage and biomineralisation. In: *Iron Metabolism* (Eds). John Wiley & Sons Ltd, NY, USA, 183–222 (2009).

2 Bou-Abdallah F, Zhao G, Biasiotto G, Poli M, Arosio P, Chasteen ND. Facilitated diffusion of iron(II) and dioxygen substrates into human H-chain ferritin. A fluorescence and absorbance study employing the ferroxidase center substitution Y34W. *J. Am. Chem. Soc.* 130(52), 17801–17811 (2008).

3 Bulvik BE, Berenshtein E, Meyron-Holtz EG, Konijn AM, Chevion M. Cardiac protection by preconditioning is generated via an iron-signal sreated by proteasomal degradation of iron proteins. *PLoS ONE* 7(11), 1–9 (2012).

4 Ullrich A, Horn S. Structural investigations on differently sized monodisperse iron oxide nanoparticles synthesized by remineralization of apoferritin molecules. *J. Nanopart. Res.* 15(8), 1–9 (2013).

5 Zhen ZP, Tang W, Guo CL *et al.* Ferritin nanocages to encapsulate and deliver photosensitizers for efficient photodynamic therapy against cancer. *ACS Nano* 7(8), 6988–6996 (2013).

•• **Reports the effective usage of ferritins in photodynamic therapy.**

6 Smith JL. The physiological role of ferritin-like compounds in bacteria. *Crit. Rev. Microbiol.* 30(3), 173–185 (2004).

7 Liu XF, Theil EC. Ferritins: dynamic management of biological iron and oxygen chemistry. *Acc. Chem. Res.* 38(3), 167–175 (2005).

8 Rakshit T, Mukhopadhyay R. Tuning band gap of holoferritin by metal core reconstitution with Cu, Co, and Mn. *Langmuir* 27(16), 9681–9686 (2011).

9 Rouault TA. The role of iron regulatory proteins in mammalian iron homeostasis and disease. *Nat. Chem. Biol.* 2(8), 406–414 (2006).

10 Zhen ZP, Tang W, Chen HM *et al.* RGD-modified apoferritin nanoparticles for efficient drug delivery to tumors. *ACS Nano* 7(6), 4830–4837 (2013).

11 Hou JX, Yamada S, Kajikawa T *et al.* Role of ferritin in the cytodifferentiation of periodontal ligament cells. *Biochem. Biophys. Res. Commun.* 426(4), 643–648 (2012).

12 Zhao J, Liu ML, Zhang YY, Li HT, Lin YH, Yao SZ. Apoferritin protein nanoparticles dually labeled with aptamer and horseradish peroxidase as a sensing probe for thrombin detection. *Anal. Chim. Acta* 759, 53–60 (2013).

13 Shevchenko EV, Talapin DV, Kotov NA, O'brien S, Murray CB. Structural diversity in binary nanoparticle superlattices. *Nature* 439(7072), 55–59 (2006).

14 Roney C, Kulkarni P, Arora V *et al.* Targeted nanoparticles for drug delivery through the blood–brain barrier for Alzheimer's disease. *J. Control. Release* 108(2–3), 193–214 (2005).

15 Agnihotri SA, Mallikarjuna NN, Aminabhavi TM. Recent advances on chitosan-based micro- and nanoparticles in drug delivery. *J. Control. Release* 100(1), 5–28 (2004).

16 Chomoucka J, Drbohlavova J, Huska D, Adam V, Kizek R, Hubalek J. Magnetic nanoparticles and targeted drug delivering. *Pharmacol. Res.* 62(2), 144–149 (2010).

17 Mundargi RC, Babu VR, Rangaswamy V, Patel P, Aminabhavi TM. Nano/micro technologies for delivering macromolecular therapeutics using poly(D, L-lactide-co-glycolide) and its derivatives. *J. Control. Release* 125(3), 193–209 (2008).

18 Soppimath KS, Aminabhavi TM, Kulkarni AR, Rudzinski WE. Biodegradable polymeric nanoparticles as drug delivery devices. *J. Control. Release* 70(1–2), 1–20 (2001).

19 Andrews SC. Iron storage in bacteria. *Adv. Microb. Physiol.* 40, 281–351 (1998).

20 Andrews SC, Robinson AK, Rodriguez-Quinones F. Bacterial iron homeostasis. *FEMS Microbiol. Rev.* 27(2–3), 215–237 (2003).

• **Provides an overview of the biology of ferritins.**

21 Frolow F, Kalb AJ, Yariv J. Structure of a unique twofold symmetrical heme-binding site. *Nat. Struct. Biol.* 1(7), 453–460 (1994).

22 Douglas T, Stark VT. Nanophase cobalt oxyhydroxide mineral synthesized within the protein cage of ferritin. *Inorg. Chem.* 39(8), 1828–1830 (2000).

23 Chen G, Zhu XL, Meng FB, Yu ZG, Li GX. Apoferritin as a bionanomaterial to facilitate the electron transfer reactivity of hemoglobin and the catalytic activity towards hydrogen peroxide. *Bioelectrochemistry* 72(1), 77–80 (2008).

24 Torti FM, Torti SV. Regulation of ferritin genes and protein. *Blood* 99(10), 3505–3516 (2002).

25 Fukano H, Takahashi T, Aizawa M, Yoshimura H. Synthesis of uniform and dispersive calcium carbonate nanoparticles in a protein cage through control of electrostatic potential. *Inorg. Chem.* 50(14), 6526–6532 (2011).

26 Caskey JH, Jones C, Miller YE, Seligman PA. Human ferritin gene is assigned to chromosome-19. *Proc. Natl Acad. Sci. USA* 80(2), 482–486 (1983).

27 Worwood M, Brook JD, Cragg SJ *et al.* Assignment of human ferritin genes to chromosomes-11 and chromosome-19q13.3–19qter. *Hum. Genet.* 69(4), 371–374 (1985).

28 Harrison PM, Arosio P. The ferritins: molecular properties, iron storage function and cellular regulation. *Biochim. Biophys. Acta* 1275(3), 161–203 (1996).

29 Uto K, Yamamoto K, Kishimoto N, Muraoka M, Aoyagi T, Yamashita I. Characterization of stable, electroactive protein cage/synthetic polymer multilayer thin films prepared by layer-by-layer assembly. *J. Nanopart. Res.* 15(4), 1–11 (2013).

30 De Val N, Declercq JP, Lim CK, Crichton RR. Structural analysis of haemin demetallation by L-chain apoferritins. *J. Inorg. Biochem.* 112, 77–84 (2012).

31 Ciasca G, Chiarpotto M, Campi G *et al.* Reconstitution of aluminium and iron core in horse spleen apoferritin. *J. Nanopart. Res.* 13(11), 6149–6155 (2011).

32 Iwahori K, Yoshizawa K, Muraoka M, Yamashita I. Fabrication of ZnSe nanoparticles in the apoferritin cavity by designing a slow chemical reaction system. *Inorg. Chem.* 44(18), 6393–6400 (2005).

•• **Demonstrates the ability of apoferritins to serve as chemical reactors.**

33 Suzumoto Y, Okuda M, Yamashita I. Fabrication of zinc oxide semiconductor nanoparticles in the apoferritin cavity. *Cryst. Growth Des.* 12(8), 4130–4134 (2012).

34 Galvez N, Sanchez P, Dominguez-Vera JM. Preparation of Cu and CuFe Prussian Blue derivative nanoparticles using the apoferritin cavity as nanoreactor. *Dalton Trans.* (15), 2492–2494 (2005).

35 Tian LX, Cao CQ, Pan YX. The influence of reaction temperature on biomineralization of ferrihydrite cores in human H-ferritin. *Biometals* 25(1), 193–202 (2012).

• **Provides insights into the encapsulation of magnetic particles by apoferritins.**

36 Abe S, Hirata K, Ueno T *et al.* Polymerization of phenylacetylene by rhodium complexes within a discrete space of apo-ferritin. *J. Am. Chem. Soc.* 131(20), 6958–6960 (2009).

37 Liu GD, Wang J, Wu H, Lin YH. Versatile apoferritin nanoparticle labels for assay of protein. *Anal. Chem.* 78(21), 7417–7423 (2006).

38 Liu F, Du BJ, Chai Z, Zhao GH, Ren FZ, Leng XJ. Binding properties of apoferritin to nicotinamide and calcium. *Eur. Food Res. Technol.* 235(5), 893–899 (2012).

39 Uchida M, Flenniken ML, Allen M *et al.* Targeting of cancer cells with ferrimagnetic ferritin cage nanoparticles. *J. Am. Chem. Soc.* 128(51), 16626–16633 (2006).

40 Banyard SH, Stammers DK, Harrison PM. Electron-density map of apoferritin at 2.8-A resolution. *Nature* 271(5642), 282–284 (1978).

41 Dominguez-Vera JM, Colacio E. Nanoparticles of Prussian Blue ferritin: a new route for obtaining nanomaterials. *Inorg. Chem.* 42(22), 6983–6985 (2003).

42 Kim M, Rho Y, Jin KS *et al.* pH-dependent structures of ferritin and apoferritin in solution: disassembly and reassembly. *Biomacromolecules* 12(5), 1629–1640 (2011).

43 Gerl M, Jaenicke R. Mechanism of the self-assembly of apoferritin from horse spleen – cross-linking and spectroscopic analysis. *Eur. Biophys. J. Biophys. Lett.* 15(2), 103–109 (1987).

44 Makino A, Harada H, Okada T *et al.* Effective encapsulation of a new cationic gadolinium chelate into apoferritin and its evaluation as an MRI contrast agent. *Nanomed. Nanotechnol. Biol. Med.* 7(5), 638–646 (2011).

45 Li JY, Paragas N, Ned RM *et al.* Scara5 Is a ferritin receptor mediating non-transferrin iron delivery. *Dev. Cell* 16(1), 35–46 (2009).

46 Aime S, Frullano L, Crich SG. Compartmentalization of a gadolinium complex in the apoferritin cavity: a route to obtain high relaxivity contrast agents for magnetic resonance imaging. *Angew. Chem. Int. Edit.* 41(6), 1017–1019 (2002).

47 Cutrin JC, Crich SG, Burghelea D, Dastru W, Aime S. Curcumin/Gd loaded apoferritin: a novel 'theranostic' agent to prevent hepatocellular damage in toxic induced acute hepatitis. *Mol. Pharm.* 10(5), 2079–2085 (2013).

48 Crich SG, Cutrin JC, Lanzardo S *et al.* Mn-loaded apoferritin: a highly sensitive MRI imaging probe for the detection and characterization of hepatocarcinoma lesions in a transgenic mouse model. *Contrast Media Mol. Imaging* 7(3), 281–288 (2012).

49 Matsumura S, Aoki I, Saga T, Shiba K. A tumor-environment-responsive nanocarrier that evolves its surface properties upon sensing matrix metalloproteinase-2 and initiates agglomeration to enhance T-2 relaxivity for magnetic resonance imaging. *Mol. Pharm.* 8(5), 1970–1974 (2011).

50 Sun CJ, Yang H, Yuan Y *et al.* Controlling assembly of paired gold clusters within apoferritin nanoreactor for *in vivo* kidney targeting and biomedical imaging. *J. Am. Chem. Soc.* 133(22), 8617–8624 (2011).

51 Valero E, Tambalo S, Marzola P *et al.* Magnetic nanoparticles-templated assembly of protein subunits: a new platform for carbohydrate-based MRI nanoprobes. *J. Am. Chem. Soc.* 133(13), 4889–4895 (2011).

52 Simsek E, Kilic MA. Magic ferritin: a novel chemotherapeutic encapsulation bullet. *J. Magn. Magn. Mater.* 293(1), 509–513 (2005).

53 Kilic MA, Ozlu E, Calis S. A novel protein-based anticancer drug encapsulating nanosphere: apoferritin–doxorubicin complex. *J. Biomed. Nanotechnol.* 8(3), 508–514 (2012).

54 Blazkova I, Nguyen HV, Dostalova S *et al.* Apoferritin modified magnetic particles as doxorubicin carriers for anticancer drug delivery. *Int. J. Mol. Sci.* 14(7), 13391–13402 (2013).

55 Yang Z, Wang XY, Diao HJ *et al.* Encapsulation of platinum anticancer drugs by apoferritin. *Chem. Commun.* 43(33), 3453–3455 (2007).

56 Xing RM, Wang XY, Zhang CL *et al.* Characterization and cellular uptake of platinum anticancer drugs encapsulated in apoferritin. *J. Inorg. Biochem.* 103(7), 1039–1044 (2009).

57 Ma-Ham AH, Wu H, Wang J, Kang XH, Zhang YY, Lin YH. Apoferritin-based nanomedicine platform for drug delivery: equilibrium binding study of daunomycin with DNA. *J. Mater. Chem.* 21(24), 8700–8708 (2011).

58 Li M, O'Sullivan KM, Jones LK *et al.* CD100 enhances dendritic cell and $CD4^+$ cell activation leading to pathogenetic humoral responses and immune complex glomerulonephritis. *J. Immunol.* 177(5), 3406–3412 (2006).

59 Liu XY, Wei W, Huang SJ *et al.* Bio-inspired protein–gold nanoconstruct with core–void–shell structure: beyond a chemo drug carrier. *J. Mat. Chem. B* 1(25), 3136–3143 (2013).

60 Bradshaw TD, Junor M, Patane A *et al.* Apoferritin-encapsulated PbS quantum dots significantly inhibit growth of colorectal carcinoma cells. *J. Mat. Chem. B* 1(45), 6254–6260 (2013).

61 Mougin NC, Van Rijn P, Park H, Muller AHE, Boker A. Hybrid capsules via self-assembly of thermoresponsive and interfacially active bionanoparticle–polymer conjugates. *Adv. Funct. Mater.* 21(13), 2470–2476 (2011).

•• **Demonstrates apoferritins as promising aptamer sensors.**

62 Huang HW, Yu Q, Peng XS, Ye ZZ. Mesoporous protein thin films for molecule delivery. *J. Mater. Chem.* 21(35), 13172–13179 (2011).

63 Moss D, Powell LW, Arosio P, Halliday JW. Effect of cell-proliferation on H-ferritin receptor expression in human T-lymphoid (MOLT-4) cells. *J. Lab. Clin. Med.* 120(2), 239–243 (1992).

64 Fargion S, Fracanzani AL, Cislaghi V, Levi S, Cappellini MD, Fiorelli G. Characteristic of the membrane-receptor for human-ferritin. *Curr. Stud. Hematol. Blood Transfus.*(58), 164–170 (1991).

65 Hulet SW, Menzies S, Connor JR. Ferritin binding in the developing mouse brain follows a pattern similar to myelination and is unaffected by the jimpy mutation. *Dev. Neurosci.* 24(2–3), 208–213 (2002).

66 Li L, Fang CJ, Ryan JC *et al.* Binding and uptake of H-ferritin are mediated by human transferrin receptor-1. *Proc. Natl Acad. Sci. USA* 107(8), 3505–3510 (2010).

67 Liu XY, Wei W, Yuan Q *et al.* Apoferritin–CeO_2 nano-truffle that has excellent artificial redox enzyme activity. *Chem. Commun.* 48(26), 3155–3157 (2012).

68 Kanekiyo M, Wei CJ, Yassine HM *et al.* Self-assembling influenza nanoparticle vaccines elicit broadly neutralizing H1N1 antibodies. *Nature* 499(7456), 102–106 (2013).

69 Saboktakin MR, Tabatabaee RM. The novel polymeric systems for photodynamic therapy technique. *Int. J. Biol. Macromol.* 65, 398–414 (2014).

70 Marrelli M, Menichini G, Provenzano E, Conforti F. Applications of natural compounds in the photodynamic therapy of skin cancer. *Curr. Med. Chem.* 21(12), 1371–1390 (2014).

71 Yan F, Zhang Y, Yuan HK, Gregas MK, Vo-Dinh T. Apoferritin protein cages: a novel drug nanocarrier for

photodynamic therapy. *Chem. Commun.* 44(38), 4579–4581 (2008).

72 Yan F, Zhang Y, Kim KS, Yuan HK, Vo-Dinh T. Cellular uptake and photodynamic activity of protein nanocages containing Methylene Blue photosensitizing drug. *Photochem. Photobiol.* 86(3), 662–666 (2010).

73 Garcia AM, Alarcon E, Munoz M, Scaiano JC, Edwards AM, Lissi E. Photophysical behaviour and photodynamic activity of zinc phthalocyanines associated to liposomes. *Photochem. Photobiol. Sci.* 10(4), 507–514 (2011).

74 Liu YY, Chang Y, Yang C *et al.* Biodegradable nanoassemblies of piperlongumine display enhanced anti-angiogenesis and anti-tumor activities. *Nanoscale* 6(8), 4325–4337 (2014).

75 Mao X, Liu GD. Nanomaterial based electrochemical DNA biosensors and bioassays. *J. Biomed. Nanotechnol.* 4(4), 419–431 (2008).

76 Liu GD, Lin YH. Nanomaterial labels in electrochemical immunosensors and immunoassays. *Talanta* 74(3), 308–317 (2007).

77 Liu GD, Wang J, Wu H, Lin YY, Lin YH. Nanovehicles based bioassay labels. *Electroanalysis* 19(7–8), 777–785 (2007).

78 Kim SE, Ahn KY, Park JS *et al.* Fluorescent ferritin nanoparticles and application to the aptamer sensor. *Anal. Chem.* 83(15), 5834–5843 (2011).

79 Liu GD, Wang J, Lea SA, Lin YH. Bioassay labels based on apoferritin nanovehicles. *ChemBioChem* 7(9), 1315–1319 (2006).

80 Pumera M, Sanchez S, Ichinose I, Tang J. Electrochemical nanobiosensors. *Sens. Actuator B Chem.* 123(2), 1195–1205 (2007).

81 Okuda M, Iwahori K, Yamashita I, Yoshimura H. Fabrication of nickel and chromium nanoparticles using the protein cage of apoferritin. *Biotechnol. Bioeng.* 84(2), 187–194 (2003).

82 Ueno T, Suzuki M, Goto T, Matsumoto T, Nagayama K, Watanabe Y. Size-selective olefin hydrogenation by a Pd nanocluster provided in an apo-ferritin cage. *Angew. Chem. Int. Edit.* 43(19), 2527–2530 (2004).

83 Kramer RM, Li C, Carter DC, Stone MO, Naik RR. Engineered protein cages for nanomaterial synthesis. *J. Am. Chem. Soc.* 126(41), 13282–13286 (2004).

84 Yamashita I, Hayashi J, Hara M. Bio-template synthesis of uniform CdSe nanoparticles using cage-shaped protein, apoferritin. *Chem. Lett.* 33(9), 1158–1159 (2004).

85 Douglas T, Dickson DPE, Betteridge S, Charnock J, Garner CD, Mann S. Synthesis and structure of an iron(III) sulfide–ferritin bioinorganic nanocomposite. *Science* 269(5220), 54–57 (1995).

86 Okuda M, Kobayashi Y, Suzuki K *et al.* Self-organized inorganic nanoparticle arrays on protein lattices. *Nano Lett.* 5(5), 991–993 (2005).

87 Meldrum FC, Colfen H. Controlling mineral morphologies and structures in biological and synthetic systems. *Chem. Rev.* 108(11), 4332–4432 (2008).

88 Kim SM, Im GH, Lee DG, Lee JH, Lee WJ, Lee IS. Mn^{2+}-doped silica nanoparticles for hepatocyte-targeted detection of liver cancer in T-1-weighted MRI. *Biomaterials* 34(35), 8941–8948 (2013).

89 Kim SM, Chae MK, Yim MS *et al.* Hybrid PET/MR imaging of tumors using an oleanolic acid-conjugated nanoparticle. *Biomaterials* 34(33), 8114–8121 (2013).

90 Cui YN, Xu QX, Chow PKH, Wang DP, Wang CH. Transferrin-conjugated magnetic silica PLGA nanoparticles loaded with doxorubicin and paclitaxel for brain glioma treatment. *Biomaterials* 34(33), 8511–8520 (2013).

91 Ojer P, Neutsch L, Gabor F, Irache JM, De Cerain AL. Cytotoxicity and cell interaction studies of bioadhesive poly(anhydride) nanoparticles for oral antigen/drug delivery. *J. Biomed. Nanotechnol.* 9(11), 1891–1903 (2013).

92 Wang AF, Qi WX, Wang N *et al.* A smart nanoporous theranostic platform for simultaneous enhanced MRI and drug delivery. *Microporous Mesoporous Mat.* 180, 1–7 (2013).

93 Kang HW, Yeo J, Hwang JO *et al.* Simple ZnO nanowires patterned growth by microcontact printing for high performance field emission device. *J. Phys. Chem. C* 115(23), 11435–11441 (2011).

94 Okuda M, Suzumoto Y, Yamashita I. Bioinspired synthesis of homogenous cerium oxide nanoparticles and two- or three-dimensional nanoparticle arrays using protein supramolecules. *Cryst. Growth Des.* 11(6), 2540–2545 (2011).

95 Meldrum FC, Wade VJ, Nimmo DL, Heywood BR, Mann S. Synthesis of inorganic nanophase materials in supramolecular protein cages. *Nature* 349(6311), 684–687 (1991).

96 Toussaint L, Bertrand L, Hue L, Crichton RR, Declercq JP. High-resolution x-ray structures of human apoferritin H-chain mutants correlated with their activity and metal-binding sites. *J. Mol. Biol.* 365(2), 440–452 (2007).

97 Niidome T, Huang L. Gene therapy progress and prospects: nonviral vectors. *Gene Ther.* 9(24), 1647–1652 (2002).

98 Hosseinkhani H, He WJ, Chiang CH *et al.* Biodegradable nanoparticles for gene therapy technology. *J. Nanopart. Res.* 15(7), 1–15 (2013).

99 Chaturvedi K, Ganguly K, Kulkarni AR *et al.* Cyclodextrin-based siRNA delivery nanocarriers: a state-of-the-art review. *Expert Opin. Drug Deliv.* 8(11), 1455–1468 (2011).

100 Rudzinski WE, Aminabhavi TM. Chitosan as a carrier for targeted delivery of small interfering RNA. *Int. J. Pharm.* 399(1–2), 1–11 (2010).

101 Mahato RI. Non-viral peptide-based approaches to gene delivery. *J. Drug Target.* 7(4), 249–268 (1999).

102 Tan PH, Chan CLH, George AJT. Strategies to improve non-viral vectors – potential applications in clinical transplantation. *Expert Opin. Biol. Ther.* 6(6), 619–630 (2006).

103 Morille M, Passirani C, Vonarbourg A, Clavreul A, Benoit JP. Progress in developing cationic vectors for non-viral systemic gene therapy against cancer. *Biomaterials* 29(24–25), 3477–3496 (2008).

104 Hsu CYM, Uludag H. Nucleic-acid based gene therapeutics: delivery challenges and modular design of nonviral gene

carriers and expression cassettes to overcome intracellular barriers for sustained targeted expression. *J. Drug Target.* 20(4), 301–328 (2012).

105 Valle-Delgado JJ, Molina-Bolivar JA, Galisteo-Gonzalez F, Galvez-Ruiz MJ, Feiler A, Rutland MW. Existence of hydration forces in the interaction between apoferritin molecules adsorbed on silica surfaces. *Langmuir* 21(21), 9544–9554 (2005).

106 Liao N, Zhuo Y, Chai YQ *et al.* Amplified electrochemiluminescent immunosensing using apoferritin-templated poly(ethylenimine) nanoparticles as co-reactant. *Chem. Commun.* 48(61), 7610–7612 (2012).

107 Gosselin MA, Guo WJ, Lee RJ. Efficient gene transfer using reversibly cross-linked low molecular weight polyethylenimine. *Bioconjug. Chem.* 12(6), 989–994 (2001).

108 Fischer D, Bieber T, Li YX, Elsasser HP, Kissel T. A novel non-viral vector for DNA delivery based on low molecular weight, branched polyethylenimine: effect of molecular weight on transfection efficiency and cytotoxicity. *Pharmacol. Res.* 16(8), 1273–1279 (1999).

109 Mcmahon HT, Boucrot E. Molecular mechanism and physiological functions of clathrin-mediated endocytosis. *Nat. Rev. Mol. Cell Biol.* 12(8), 517–533 (2011).

110 Mounkes LC, Zhong W, Cipres-Palacin G, Heath TD, Debs RJ. Proteoglycans mediate cationic liposome–DNA complex-based gene delivery *in vitro* and *in vivo*. *J. Biol. Chem.* 273(40), 26164–26170 (1998).

111 Gaspar VM, Marques JG, Sousa F, Louro RO, Queiroz JA, Correia IJ. Biofunctionalized nanoparticles with pH-responsive and cell penetrating blocks for gene delivery. *Nanotechnology* 24(27), 1–5 (2013).

112 Chen HP, Liu XP, Dou Y *et al.* A pH-responsive cyclodextrin-based hybrid nanosystem as a nonviral vector for gene delivery. *Biomaterials* 34(16), 4159–4172 (2013).

113 Kim HK, Thompson DH, Jang HS, Chung YJ, Van Den Bossche J. pH-responsive biodegradable assemblies containing tunable phenyl-substituted vinyl ethers for use as efficient gene delivery vehicles. *ACS Appl. Mater. Interfaces* 5(12), 5648–5658 (2013).

114 Tseng WC, Su LY, Fang TY. pH responsive PEGylation through metal affinity for gene delivery mediated by histidine-grafted polyethylenimine. *J. Biomed. Mater. Res. B Appl. Biomater.* 101B(2), 375–386 (2013).

115 Zhao QH, Qiu LY. An overview of the pharmacokinetics of polymer-based nanoassemblies and nanoparticles. *Curr. Drug Metab.* 14(8), 832–839 (2013).

116 Gerweck LE, Seetharaman K. Cellular pH gradient in tumor versus normal tissue: potential exploitation for the treatment of cancer. *Cancer Res.* 56(6), 1194–1198 (1996).

117 Iskandar SS, Jennette JC. Interaction of antigen load and antibody-response in determining heterologous protein nephritogenicity in inbred mice. *Lab. Invest.* 48(6), 726–734 (1983).

3.2.3 Metaloenzymy

Enzymy, které jsou závislé na iontech kovu jako kofaktorech, spadají do dvou kategorií: (i) kovem aktivované enzymy a (ii) metalloenzymy. Jak vyplývá z názvu, kovem aktivované enzymy jsou vybuzovány k větší katalytické aktivitě přítomností mono nebo divalentních kovových iontů z okolního prostředí proteinu. Kovy mohou aktivovat substrát (např Mg (II) s ATP), přímo enzymem nebo vstoupit do rovnováhy s využitím iontového náboje enzymu pro poskytnutí vhodných podmínek při vazbě substrátu nebo katalýze. Z tohoto důvodu kovem aktivovaný enzym vyžaduje přebytek kovu asi 2-10 krát vyšší, než je koncentrace enzymu (Medyantseva, E. P., Vertlib, M. G. et al. 1998). Díky slabé vazbě kovu k proteinu, kovem aktivované enzymy typicky ztrácejí aktivitu během jejich purifikace. Příkladem je inaktivace pyruvát kinázy, která během dialýzy ztrácí ionty K^+ potřebné k její aktivitě (Kumar, S. and Barth, A. 2011). Naproti tomu metaloenzymy mají kovový kofaktor pevně navázán do specifického regionu na povrchu proteinu. Některé mohou dokonce vyžadovat více než jeden iont kovu a v méně častých případech může metalloenzym obsahovat dva různé kovové ionty jako je tomu v případě Cu^{2+}, Zn^{2+} superoxid dismutasy (Hoffman, B. M. 2003). Metaloenzymy jsou schopny se přirozeně účastnit většiny katalytických reakcí z hlediska jejich aktivity, selektivity a schopnosti působit za mírných podmínek. Tak jako u ostatních enzymů, tvar aktivního místa metalloenzymů hraje důležitou roli v pro jejich funkci. Iont kovu je často lokalizován v místě, které zapadá do substrátu (Pordea, A. 2015).

3.2.4 Metaloproteiny singnální transdukce

Signální transdukce zahrnuje přenos informace z vnějšku buňky do jejího jádra k vyvolání biologické odezvy pomocí tzv. signálních molekul a na ně reagujících receptorových molekul. Jejich společným rysem je, že dokáží zesílit buněčnou odezvu až 10^4–10^5 krát. Buněčné receptory mají ve své struktuře obvykle dvě domény. Pomocí jedné domény je navázána signální molekula na specifický ligand a pomocí druhé domény je zprostředkována biologická odpověď, tzv. efektorová doména. Příkladem metaloproteinů signální transdukce je kalmodulin (Marshall, C. B., Nishikawa, T. et al.

2015). Jedná se o malý protein, který obsahuje čtyři EF-hand motivy, všechny schopné vázat Ca^{2+} ionty. Ve smyčce EF-hand motivu je Ca^{2+} iont koordinován do pentagonální bipyramidální konfigurace. Šest reziduí molekul kyseliny glutamové a asparagové je zapojeny do této vazby na pozicích 1, 3, 5, 7 a 9 polypeptidového řetězce. Na pozici 1 je glutamátový nebo asparagový ligand, který se chová jako bidentátní a poskytuje dva atomy kyslíku. Devátý zbytek ve smyčce je obsazen glycinem kvůli konformačním požadavkům páteře molekuly. Koordinační sféra vápenatého iontu obsahuje jen karboxylátový atom kyslíku ale nikoliv atom dusíku, což odpovídá pevné povaze vápenatých iontů. Protein má průměrně dvě symetrické domény oddělené flexibilním závěsným regionem. Vazba vápníku pak způsobuje konformační změnu (Kovacs, Erika, Harmat, Veronika et al. 2010). Kalmodulin se podílí na vnitrobuněčné signalizaci, například při regulaci CHR genu (Obrázek 3). V závislosti na buněčném kontextu aktivuje celou řadu enzymů, například adenylátcyklázu, cytosolickou fosfodiesterázu, kinázu lehkého řetězce myosinu, Ca^{2+}/Mg^{2+} ATPázu červených krvinek či fosforyláza kinázu (Penniston, John T., Caride, Ariel J. et al. 2012; Selwa, Edithe, Laine, Elodie et al. 2012; Bisserier, Malik, Berthouze-Duquesnes, Magali et al. 2015; Doroudi, Maryam, Schwartz, Zvis et al. 2015).

Dalším významným kov-vazným proteinem je troponin, který je součástí srdeční a kosterní svaloviny. Produkce svalové síly je zde řízena změnou intracelulární koncentrace vápníku. Obecně, pokud hladina vápníku roste, svaly jsou v kontrakci a pokud hladina vápníku klesá, svaly se dostávají do relaxované formy (Li, Monica X. and Hwang, Peter M. 2015).

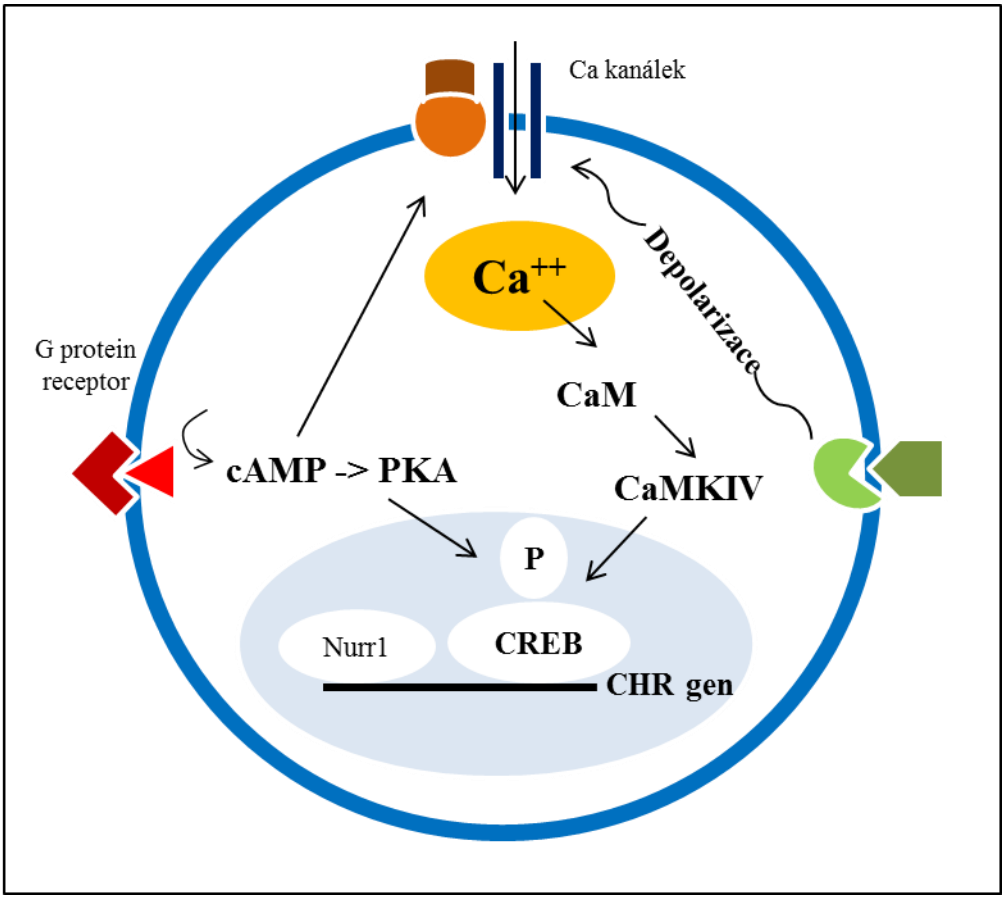

Obrázek 3: Schéma vnitrobuněčné signální dráhy pro regulaci CRH genu (kortikotropin uvolňující hormon). Neurotrasimentr stimuluje adenyl cyklatásu přes G protein, který zvyšuje vnitrobuněčnou koncentraci cAMP, aktivuje PKA enzym a ten poté aktivuje CRH genovou expresi přes fosforylaci (P) CREB (buněčný transkripční faktor). Další neurotransimetr přímo otevírá Ca kanálky, které depolarizuje. Tím dojde ke zvyšení vnitrobuněčné koncentrace vápníku, který aktivuje kalmodulin (CaM) a kalmodulin dependentní protein kinázu (CaMKIV). Následně se zesiluje transkripce CRH genu přes fosforylaci CREB (Převzato z (Yamamori, E., Asai, M. et al. 2004).)

3.2.5 Metaloproteiny transkripční regulace

Metaloproteiny, které jsou zapojeny do regulace genové exprese, mohou být rozděleny na dvě skupiny na základě úlohy iontu kovu. První skupina se vyznačuje schopností iontu kovu se sám o sobě uplatňovat jako efektorová molekula. V druhé skupině se iont kovu prosazuje jako senzorový efektor a často také obsahuje prostetickou skupinu

v proteinové struktuře (Schmidt, Michael H. and Berg, Jeremy M. 1992; LaRochelle, O., Stewart, G. et al. 2001).

Transkripční regulátory, patřící do první skupiny, mohou existovat ve dvou formách: apo a holo formě. V holo formě je iont kovu vázán na proteinovou matrix, zatímco iont kovu působící jako efektor je uvolněn z proteinové matrix v apo formě. Ačkoliv ve všech případech v první skupině je vazba kovových iontů reverzibilní a způsobuje alosterickou konformační změnu pro zachování regulace aktivity transkripčeních regulátorů, regulační mechanismus není stejný pro všechny tyto transkripční regulátory (Massari, M. E. and Murre, C. 2000).

Transkripce genové exprese, která je závislá na externím signálu, může být dokončena transkripční nebo post-transkripční regulací. V uvedeném případě se často uplatňuje dvoukomponentový systém, který zapojuje dva proteiny - senzorovou kinázu a odpovědní regulátor. Senzorová kináza připojuje fosfátovou skupinu z ATP na histidinové zbytky a kontroluje environmentální parametry jako je přítomnost nutrientů a toxinů, kyselost, teplota, osmolarita a vlhkost prostředí (Vincenti, M. P., White, L. A. et al. 1996). Autofosforylace zahrnuje detekci senzor-kinázových proteinů korespondujícím externím signálem, které jsou poté přemístěny z fosforylovaného senzorového proteinu do odpověď-regulátorového proteinu fungujícího jako aktivovaný transkripční regulátor (Hunter, T. and Karin, M. 1992). Mimo uvedený dvoukomponentový systém se metaloproteiny mohou uplatnit v jednokomponentovém systému, kdy obě funkce, senzoru a regulátoru plní jediný protein. V tomto případě iont kovu zprostředkovává celou aktivitu (Rutherford, J. C. and Bird, A. J. 2004).

Posttranskripční regulace genové exprese uplatňuje IRP1 jako cytosolický RNA-vazebný protein, který se váže na vlásenkovou strukturu jako železo-responzivní element (IRE). Tyto elementy jsou lokalizovány na 5´ a 3´ netranslatovaných regionech specifické mRNA, které kódují proteiny zapojené do homeostáze železa, například feritiny, transferiny a trensferinový receptor (Harrison-Findik, D. D., Schafer, D. et al. 2006). Pokud je IRP1 navázán na 5´-IRE, je inhibována translace korespondující mRNA. Tento mechanismus je kontrolován přítomností železa v buňkách. Pokud je přebytek Fe iontů, tak IRP1 ztrácí RNA vazebnou aktivitu (Obrázek 4). V přítomnosti

přebytku železa, IRP1 obsahuje 4Fe-4S klastr, zatímco IRP1 je konvertován na apo-formu. Tato apo-forma je pak s vysokou afinitou navázána na IREs (Huang, L. E., Ho, V. et al. 1997).

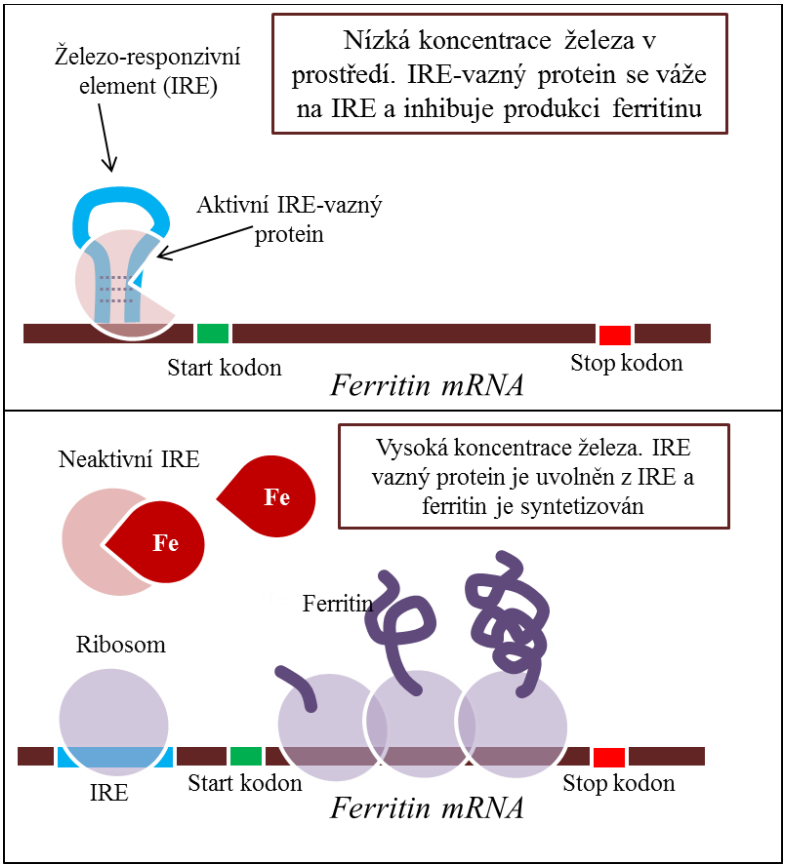

Obrázek 4: Modelové schéma transkripční regulace železo-responzivního elementu (IRE). Nahoře v prostředí s nízkou koncentraci železa, dole v prostředí s vysokou koncentrací železa, které indukuje IRE k produkci ferritinu.

3.2.6 Imunitní metaloproteiny

K omezení nespecifické reaktivity přechodných kovů, potřebuje být jejich dostupnost pevně regulována a obzvláště během probíhajícího ataku infekce. Tento proces se nazývá nutriční imunita a spočívá v zamezení přístupu živin patogenům, které jsou pak následkem ztráty nutrientů inhibovány (Obrázek 5). Mechanismy nutriční imunity se

navzájem liší, avšak většina z nich zahrnuje indukci hepcidinu, hlavního regulačního hormonu, který řídí zásoby železa v organismu (Drakesmith, Hal and Prentice, Andrew M. 2012) a expresi NRAMP1 (Natural Resistance asociated macrophage protein), transportéru Fe iontů pro odčerpání železa a manganu patogenům (Jabado, N., Jankowski, A. et al. 2000; Forbes, J. R. and Gros, P. 2003; Cellier, Mathieu F., Courville, Pascal et al. 2007). Nakonec je uplatňována exprese antimikrobiálních proteinů, které vychytávají ionty kovů v místech infekce (Hood, M. Indriati, Mortensen, Brittany L. et al. 2012; Liu, Janet Z., Jellbauer, Stefan et al. 2012). Hemopexin omezuje množství cirkulujícího železo-vazného hemu a lipokalin-2 vychytává bakteriální železo-pohlcující sideofory, např. enterobaktin (Rocha, E. R., Smith, A. et al. 2001). Během infekce, protizánětlivé mediátory zvyšují expresi kov-vazných proteinů, které poškozují bakterie blokováním jejich mechanismů vychytávat volné kovy. Protizánětlivé cytokiny, IL-17 a IL-22, produkované T-buňkami indukují epiteliální buňky k expresi antimikrobiálních proteinů včetně lipocalinu-2 a kalprotektinu. Navíc aktivované epiteliální buňky sekretují CXC chemokiny, které zásobují centrum infekce neutrofily. Neutrofilní buňky jsou schopné exprimovat velké množství laktoferinu (LF), lipokalinu-2 a kalprotektinu. Mikrobiální infekce může stimulovat produkci hepcidinu v játrech a v makrofázích, což následně redukuje dostupnost železa indukcí degradace buněčného přenašeče železa ferroportinu 1 (Raffatellu, Manuela, George, Michael D. et al. 2009). Transporter divalentních kovů NRAMP1 může exportovat mangan a železo z makrofágů pomocí fágosomu k následnému omezení dostupnosti kovů pro nitrobuněčné patogeny (Portnoy, M. E., Jensen, L. T. et al. 2002). Avšak tyto mechanismy se některé patogenní bakterie naučily překovávat využitím vysoce specializovaných transportérů ABC-typu, které usnadňují příjem kovů navázáním chelátorů hemu a sideroforů (Chandra, R. K. 1996). Ačkoliv lipocalin-2 může pohltit enterobaktin pro omezení přístupu bakterií k železu, některé patogeny používají salmochelin, který nemůže být na lipocalin-2 navázán. Další strategií některých patogenních bakterií je exprese NRAMP transportérů nebo ZIP transportérů pro zvýšení svého příjmu iontů kovů potřebných pro svůj metabolismus (Hornef, M. W., Wick, M. J. et al. 2002).

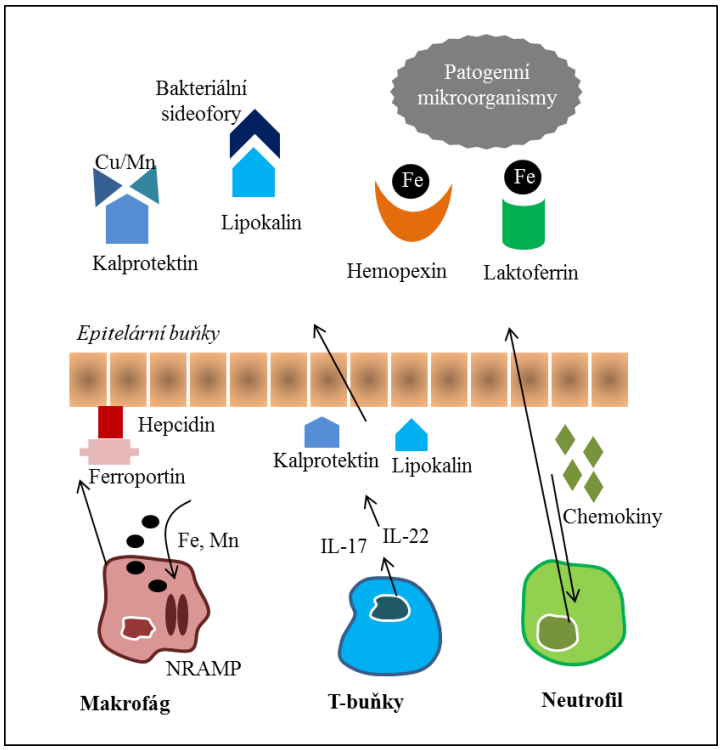

Obrázek 5: Nutriční imunita. Kovy, které patogenní mikroorganismy potřebují pro svoji životaschopnost, jsou vychytávány prostřednictvím kov-vazných proteinů exprimovaných buňkami imunitního systému.

3.2.6.1 Laktoferin

Laktoferin je globulární protein, který se vyskytuje v několika glykosilovaných variantách (Wei, Z., Nishimura, T. et al. 2001). Jeho schopnost vazby železa je až 300x silnější než u ostatních proteinů se stejnou schopností (Moutafchiev, D. A. and Sirakov, L. M. 1981; Birgens, H. S., Kristensen, L. O. et al. 1988). Sekvenační analýza prokázala, že laktoferiny jsou evolučně spojené se sérovými transferiny a například sekvence lidského LF je z 60 % identická se sekvencí transferinů. Obě skupiny proteinů se vyznačují motivy disulfidických vazeb a jsou charakterizovány ze 40 % shodnou 2x složenou interní opakující se strukturou aminokyselinové sekvence (Baker, Heather M. and Baker, Edward N. 2012). Struktura LF je složena do dvou symetrických N a C domén, které jsou dále rozděleny na dvě menší poddomény. Do své struktury je LF

schopen pojmout dva Fe^{3+} ionty, jejichž vysoká afinita (K_D 10^{-20} M) k vazebným místům je vysoce konzervativní a dodává LF unikátní vlastnost udržet ionty železa i při nízkém pH (Baker, H. M. and Baker, E. N. 2004).

LF patří do skupiny multifunkčních proteinů, které vykazují různé biologické aktivity a jsou regulovány různými posttranslačními modifikacemi a alternativním sestřihem. LF zajišťuje široké rozmezí důležitých biologických funkcí jako je regulace a kontrola homeostázi železa, antioxidační aktivita, transport železa a vykazuje antibakteriální, antifungicidní a antivirové vlastnosti. Mimo jiné má vliv na modulaci imunity, protizánětlivé účinky, proteolytickou aktivitu, možnost vázat nukleovou kyselinu, vykazuje RNAsovou aktivitu, podílí se na regulaci transkripce a vykazuje schopnost vázat různé druhy biomolekul a buněk. U LF byla prokázána schopnost interagovat a aktivovat NK buňky, neutrofily a také účast na opravě poškozených tkání (Baker, Heather M. and Baker, Edward N. 2012). Význam LF ve vrozeném imunitním systému byla podrobněji studována v mukonasálním obranném systému, který hraje důležitou roli v ochraně organismu proti bakteriální a virové infekci (Legrand, D., Elass, E. et al. 2005; Ammons, M. C. and Copie, V. 2013). V literatuře byla popsána interakce laktoferinu s rotaviry, lidským respiračním syncyciálním virem, žloutenkou typu C, lidským herpes virem a HIV. U všech byl prokázán inhibiční vliv LF na postupující infekci (Berlutti, Francesca, Pantanella, Fabrizio et al. 2011). Rovněž některé studie potvrdily důležitou roli LF v potlačení časných virových infekcí zabráněním adsorpce a penetrace virových částic do hostitelských buněk (El-Fakharany, Esmail M., Sanchez, Lourdes et al. 2013).

3.3 Analytické metody pro studium významných kov-vazných proteinů

Důležitost významu kov-vazných proteinů potvrzuje široká řada popsaných metod pro jejich studium (Voss, J., Salwinski, L. et al. 1995; Sheardown, H., Cornelius, R. M. et al. 1997; Sommer-Knudsen, J. and Bacic, A. 1997; Atanassova, A., Lam, R. et al. 2004; Mentler, M., Weiss, A. et al. 2005; Carrer, Charlotte, Stolz, Michael et al. 2006; Parsy, Celine B., Chapman, Caroline J. et al. 2007; Atanassova, Anelia, Hoegbom, Martin et al. 2008; Long, Xiufen, Zhang, Caihua et al. 2008; Mohan, Abhilash, Anishetty,

Sharmila et al. 2010; Hynek, David, Krejcova, Ludmila et al. 2012; Zhang, Aming, Zhang, Cheng et al. 2012; Chakravorty, Dhruva K., Wang, Bing et al. 2013; Toyama, Takashi, Shinkai, Yasuhiro et al. 2013; Huang, Li, Hu, Xiumei et al. 2014; Yamanaka, Ryutaro, Hirasaka, Yuka et al. 2014). Všeobecně lze rozdělit tyto metody na základě využití získaných dat. Základem jejich studia je sledovaní krystalografické struktury proteinů a jejich vazby iontů kovů (Hardman, K. D. 1973; Dauter, Z. 2005; Wille, Holger, Grovaerts, Cedric et al. 2007; Isaksson, Johan, Nystom, Susanne et al. 2009; Gao, Zengqiang, Hou, Haifeng et al. 2010), prediktivní studie chování a vlastností těchto proteinů (Babor, Mariana, Gerzon, Sergey et al. 2008; Wang, Chu, Vernon, Robert et al. 2010; Lu, Chih-Hao, Lin, Yu-Feng et al. 2012; AlHazmi, Hassan A., Nachbar, Markus et al. 2014). V molekulární biologii je sledována funkce a role v buněčných mechanismech, stejně tak jako v biochemickém přístupu je zkoumána jejich aktivita a působení na organismus (Hooper, Nigel M., Taylor, David R. et al. 2008; Harley, R. 2011; Drozd, A. and Krezel, A. 2014; Kovuri, Venkata Aditya, Craig, Paul et al. 2014; Besold, Angelique N. and Michel, Sarah L. J. 2015; Kowalski, Konrad, Goszczynski, Tomasz et al. 2015; Vanderslice, N., Messer, A. S. et al. 2015). Řada z metaloproteinů se uplatňuje ve vrozené imunitě a jsou proto hlavním zájmem imunologických metod (Garvey, J. S., Thomas, D. G. et al. 1987; Roesijadi, G. and Morris, J. E. 1988; Saenseeha, Suphakdee, Janwan, Penchom et al. 2014; Uehara, Hiroshi and Rao, V. Ashutosh 2015). V oblasti vývoje a výzkumu léčiv jsou metaloproteiny testovány jako potencionální terapeutika ať už při působení přímo nebo jako nástroje pro genovou terapii (Luo, Q., Guo, W. et al. ; Turunen, P., Puhakka, H. L. et al. 2006; Shi, Kai, Cui, Fude et al. 2013; Price, Robert, Poursaid, Azadeh et al. 2015; Parimelzaghan, Anitha, Anbarasu, Anand et al. 2016). Díky jejich schopnosti uzavřít ve své struktuře ionty kovu, stejně tak jako malé molekuly léčiv, jsou metaloproteiny studovány pro využití v nanotechnologických aplikacích (Giannotti, Marina I., Cabeza de Vaca, Israel et al. 2015; Hu, Yihui, Guo, Wenjing et al. 2015; Ouyang, Chun-Yu, Lin, Yu-Kuan et al. 2016; Qiao, S. P., Lang, C. et al. 2016). V diagnostice mohou metaloproteiny sloužit jako markery některých onemocnění (Shovman, O., Gilburd, B. et al. 2005; Markowski, Jaroslaw, Tyszkiewicz, Tomasz et al. 2009; Rausch, Mary E.,

Beer, Lynn et al. 2011; Skjot-Arkil, H., Schett, G. et al. 2012), jako je tomu v případě metalothioneinu (Raleigh, J. A., Chou, S. C. et al. 2000; Theocharis, S. E., Margeli, A. P. et al. 2003; Knapen, Dries, Reynders, Hans et al. 2007; Pastuszewski, Wojciech, Dziegiel, Piotr et al. 2007). Následující kapitola se bude zabývat hlavními metodami vhodnými pro studium metalloproteinů.

3.3.1 Kapalinová chromatografie

Kapalinová chromatografie je základní a nejvíce využívanou metodou pro separaci proteinů. Gelová permeační chromatografie využívá rozdíly ve velikosti a 3D konfigurace proteinů (Szpunar, J. 2005). Malé rozdíly v náboji proteinů při různém pH dovolují použití iontově výměnné chromatografie v anionickém i kationickém módu (Brunnekreeft, J. W. I. and Eidhof, H. H. M. 1993; Rohrer, J. S. and Avdalovic, N. 1996). Rozdíl v polaritě 20 esenciálních aminokyselin způsobuje rozdíly v hydrfobicitě proteinů, což je využito v chromatografii na reverzních fázích (Chassaigne, H. and Szpunar, J. 1998). Přítomnost prostetické skupiny představuje chemickou odlišnost s velmi specifikou reaktivností, které využívá afinitní chromatografie vynikající precizními výsledky separace (Campanella, Beatrice and Bramanti, Emilia 2014).

Principem gelové chromatografie je separace proteinů na základě jejich molekulové hmotnosti v roztoku, nebo přesněji na základě jejich hydrodynamického objemu. Při separaci kov-vazných proteinů je třeba zajistit, aby molekuly zůstaly intaktní a náplň kolony nereagovala se stanovovaným proteinem (Bai, Yan 2015). Separace probíhá při nižším pH, které nevyvolá uvolnění iontu kovu z molekulové struktury. Redistrubuce kovů může také nastat vlivem nevhodně zvolené stacionární fáze, většinou díky silanolovým skupinám u gelů na bázi siliky. Gelová chromatografie je tedy velmi citlivá na podmínky separace, aby nedocházelo ke změně distribučního profilu a byla zachována rozlišitelnost.

Pro analytickou i preparativní separaci proteinů je velmi využívanou technikou iontově výměnná kapalinová chromatografie (IEC). Principem je separace proteinů na základě jejich elektrického náboje, který závisí na acidobazických vlastnostech separovaného proteinu (Salvalaglio, Matteo, Paloni, Matteo et al. 2015). Tyto vlastnosti jsou určeny

počtem a povahou ionizovatelných postranních řetězců polypeptidu. Často využívané funkční skupiny v IEC jsou alkylované amino skupiny pro anioniové měniče a fosfátové skupiny pro kationtové měniče. Pro separaci pomocí IEC jsou důležité nejen funkční skupiny matrice, ale také samotná struktura kostry stacionární fáze, která může ovlivnit nespecifickou vazbu proteinu. Je proto důležité, aby výplňový materiál kolony byl z interntního materiálu jako je celulosa, dextran, agarosa, silika nebo polymerní materiály (Lang, Katharina M. H., Kittelinann, Joerg et al. 2015). Výhodou IEC jsou mírné podmínky eluce, které pomáhají zachovat strukturu a funkce proteinů intaktní a vysoké separační rozlišení (Duong-Ly, Krisna C. and Gabelli, Sandra B. 2014).

Chromatografie na reverzních fázích separuje proteiny na základě jejich hydrofobicity. Principiálně, čím větší proteiny jsou separovány a čím více jsou hydrofobní, tím je třeba použít stacionární fázi s krátkými alkylovými řetězci, aby nedocházelo ke ztrátě proteinů ireverzibilní vazbou k náplni kolony (Yang, Yuanzhong, Boysen, Reinhard I. et al. 2015). Ačkoliv je tato metoda pro separaci a detekcí proteinů využívaná (Yu, Zitong, Han, Caixia et al. 2013; Bobaly, Balazs, Mikola, Vivien et al. 2015; Yang, Yuanzhong, Boysen, Reinhard I. et al. 2015; Akimoto, Masaru, Hokazono, Eisaku et al. 2016; Cruz-Huerta, Elvia, Martinez Maqueda, Daniel et al. 2016; Tyteca, Eva, De Vos, Jelle et al. 2016), v chromatografii na reverzních fázích se často objevuje nízká návratnost, rozmývání a tvorba vícečetných píků. S ohledem na kov-vazné proteiny, zde velmi často dochází k denaturaci proteinů a vyvázáním kovu ze struktury proteinu díky použití organických rozpouštědel v mobilní fázi.

Konjugované proteiny obsahují chemické skupiny, které nejsou aminokyselinami, ale nazývají se prostetické skupiny (Takeuchi, Toshifumi, Mori, Takuya et al. 2014). V některých případech jejich přítomnost umožňuje separovat proteiny nebo dokonce jejich isoformy pomocí afinitní chromatografie. Tato separační technika je založena na charakteru mnoha proteinů vstupovat do specifických interakcí s některými molekulami (Vunnum, S., Natarajan, V. et al. 1998; Song, Yufeng, Zhang, Hongxiao et al. 2014). Stacionární fáze je chemicky modifikována připojením sloučeniny se specifickou afinitou k cílové sekvenci proteinu. Výplňový materiál kolony musí být inertní a snadno modifikovatelný, například agarosa. Využité ligandy jsou pak biospecifické, tzn.

enzymy, substráty, protilátky, receptory nebo pseudo-biospecifické např. lektiny, barviva nebo síru obsahující skupiny. Absorpce analytu na stacionární fázi je uskutečňována přes elektrostatické síly mezi nabitými skupinami, nepolárními interakcemi, vodíkovými můstky a hydrofobními vazbami (Arakawa, Tsutomu, Kita, Yoshiko et al. 2008). Obecně afinitní chromatografie představuje jednu z nejefektivnějších metod pro purifikaci proteinů, díky tomu, že umožňuje separaci jednoho proteinu z jejich komplexní směsi (Smith, M. C., Furman, T. C. et al. 1988; Arnold, F. H. 1991; Berkovsky, A. L. and Potapov, P. P. 1997; de la Calle Guntinas, M. B., Bordin, G. et al. 2002; Ueda, E. K. M., Gout, P. W. et al. 2003; Dalal, Sohel, Raghava, Smita et al. 2008; Lei, Genhu, Liu, Liting et al. 2008).

3.3.2 Enzymová imunoanalýza

Principem imunochemických metod je využití specifických protilátek ke sledovaným proteinům, tzv. antigenům. Tato technika vyniká vysokou specifitou a možností kvalitativního i kvantitativního stanovení jak protilátek, tak antigenů i ve velmi nízkých koncentracích. Mimoto jsou protilátky schopny se vázat na povrch polymerních materiálů, díky čemuž jsou snadno imobilizovatelné například na mikrotitračních destičkách a tak zajistit promytí nenavázaných komponent směsi. Pro různé analytické postupy mohou být protilátky imobilizované na nanočásticích nebo polymerních nosičích (Cardoso, M. M., Peca, I. N. et al. 2012; Omidfar, Kobra, Khorsand, Fahimeh et al. 2013; Goodall, Stephen, Jones, Martina L. et al. 2015; Shargh, Vahid Heravi, Hondermarck, Hubert et al. 2016). V imunochemii se rozlišuje několik metod na základě detekce konečného produktu, které jsou založeny na stejném principu vazby protilátka-antigen. Jedná se o enzymově značenou imunoanalýzu (Butcher, H., Kennette, W. et al. 2003), radioimunoanalýzu (Butcher, H., Kennette, W. et al. 2003), luminiscenční imunoanalýzu (Riechers, Alexander, Schmidt, Jennifer et al. 2009) nebo metalloimunoanalýzu (Vessieres, A., Salmain, M. et al. 1999).

Antigeny mohou být různé makromolekuly, speciálně proteiny i kov-vazné proteiny, které jsou schopny vyvolat v specifickou imunitní odezvu jak na buněčné, tak na humorální úrovni a specificky interagovat s produkty imunitní odpovědi (Butcher, H.,

Kennette, W. et al. 2003). Imunitní odpověď zahrnuje tvorbu protilátek pomocí plasmatických buněk, které jsou výsledkem diferenciace B lymfocytů po předchozí stimulaci antigenem. Protilátky jsou heterogenní skupina glykoproteinů, immunoglobulinů (Ig). Každý Ig obsahuje nejméně dva lehké a dva těžké řetězce spojené disulfidickými můstky. Lehký řetězec se vyskytuje ve dvou typech kappa a lambda, těžký řetězec existuje v 5 isotypech a určuje třídu Ig (IgG, IgM, IgA, IgD a IgE). C konec obou řetězců je označován za konstantní region, zatímco N konec se může lišit a tvoří část protilátkové molekuly, která váže antigen. Mimo IgM, který má 10 vazebných míst a IgA se 4 vazebnými místy, mají ostatní imunoglobuliny 2 vazebná místa pro antigen (Moreno-Bondi, M. C., Benito-Pena, M. E. et al. 2012). Monoklonální protilátky jsou produktem jednoho klonu plasmových buněk odvozených od B-lymfocytů a jsou přímo určené pro interakci s jedním epitopem. Obvykle vykazují výbornou specifitu, avšak zhoršenou schopnost precipitovat antigen (Brorson, Kurt and Jia, Audrey Y. 2014). Polyklonální protilátky jsou připravovány imunizací zvířat (např. králík, koza, ovce) daným antigenem (Trushinskaya, G. V., Simonov, V. I. et al. 1992). Každý epitop tak stimuluje odlišný klon B-buněk a komplexní antigeny nesou několik antigenů. Polyklonální protilátky tedy vykazují schopnost interakce s mnoha antigeny.

Imunoanalýza je velmi dobře využitelná jak pro proteiny, tak i proteiny se schopností vázat kovy (Casalis, L., Bano, F. et al. 2011; Kumar, Rajesh 2012; He, Xiaohua and Patfield, Stephanie A. 2015). Variantou je také využití kov-vazných proteinů pro detekci těžkých kovů (Liu, Gong-Liang, Wang, Ju-Fang et al. 2006). Imunochemické metody se obecně využívají k diagnostice některých onemocnění na základě detekce specifických protilátek nebo biomarkerů, detekci toxinů, hormonů, proteinů a dalších bioaktivních látek. Výhodou je rozlišení proteinů na úrovni jeho isoformy (Chan, H. M., Cherian, M. G. et al. 1992). Přínosem imunoanalýzy je možnost kombinace s dalšími analytickými přístupy jako jsou například optické detekční metody nebo elektrochemie. Spojení těchto dvou metod lze využít v oblasti biosenzorů jako variantu v pokročilých bioanalytických systémech (Bahadir, Elif Burcu and Sezginturk, Mustafa Kemal 2015). Detekce specifických antigenů je zejména zajištěna vazbou antigenu na protilátkou modifikovaném povrchu elektrody (Xu, Qiao and Davis, Jason J. 2014). Protilátky zde

fungují jako bioreceptor na který se váže cílový analyt. Vazba pak vyvolá odezvu na převodníku detektoru a signál může být kvantifikován. Metodu ELISA lze využít jako biosenzor pro detekci patogenních bakterií v koncentracích nižších než 15 kolonií tvořících jednotek (Cho, Il-Hoon and Irudayaraj, Joseph 2013). V této studii byla využita afinita zlatých nanočástic k proteinům, díky kterým byla vytvořena síť protilátek značených HRP a tím došlo k zesílení detekčního signálu (Obrázek 6). V posledních letech se využívají jak elektrochemické, tak optické metody detekce pro klinickou diagnózu díky jejich jednoduchosti, citlivosti, specifitě, možnosti automatizace, miniaturizace a efektivitě nákladů na provoz (Wu, Jie, Fu, Zhifeng et al. 2007).

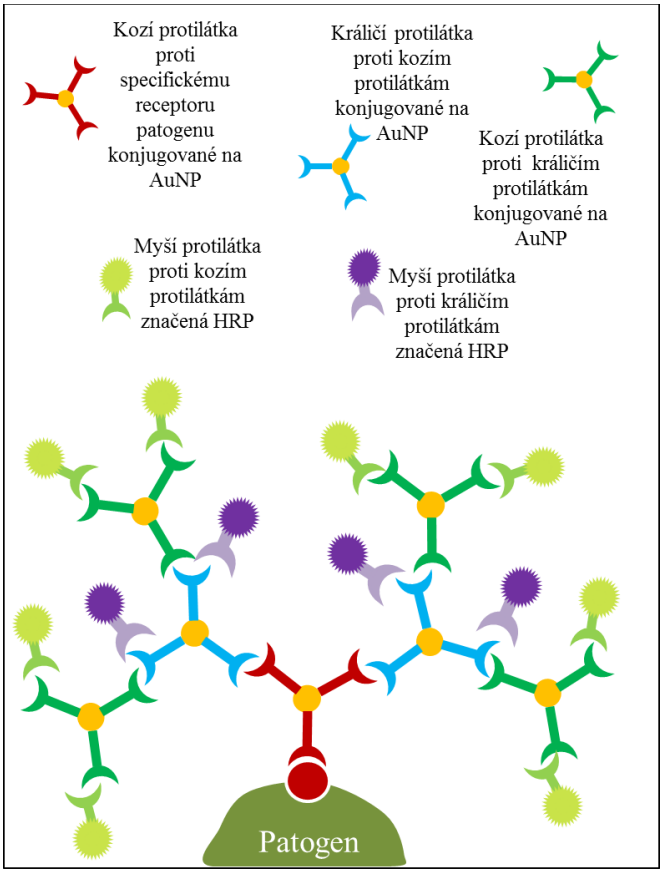

Obrázek 6: Schéma biosenzoru pro detekci patogenních bakterií založený na metodě ELISA. Na specifické protilátky proti patogenu byly postupně konjugovány sekundární (králičí proti primárním) a terciální (kozí proti králičím) protilátky. Pro detekci byly využity myší protilátky proti sekundárním a terciálním protilátkám značeným křenovou

peroxidázou (HRP). Po přidání H_2O_2 a substrátu 3,3',5,5'-Tetramethylbenzidinu (TMB) dochází k barevné změně reagencií, která je přímo úměrná koncentraci patogenní bakterie ve vzorku. Přepracováno z (Cho, Il-Hoon and Irudayaraj, Joseph 2013).

3.3.3 Optické metody pro detekci proteinů

Spektroskopické techniky využívají světlo v interakci s hmotou a poskytují tedy informace o struktuře vzorku. Světlo je elektromagnetické záření, fenomén s různou energií a v závislosti na této energii mohou být určeny vlastnosti molekul. Molekulární substruktury, které jsou zodpovědné za interakci s elektromagnetickým zářením, se označují chromofory. V případě proteinů se jedná o peptidovou vazbu, některé postranní řetězce aminokyselin (zejména tryptofan a tyrosin), prostetické skupiny a koenzymy (Simonian, Michael H. and Smith, John A. 2006). Elektronové přechody peptidové vazby se nachází ve vzdálené oblasti UV při 190 nm a 210 nm. Řada aminokyselin (Asp, Glu, Asn, Gln, Arg a His) vykazuje absorbanční maximum při 210 nm, avšak jsou vždy překryty silnější absorbancí peptidových vazeb. Odlišné absorbanční maximuma mají aromatické aminokyseliny. Pro fenylalanin platí absorbanční maximum 257 nm, pro tyrosin a tryptofan dominují v typickém proteinovém spektru absorbanční maxima 274 a 280 nm. Aminokyselina cystein má slabé absorpční maximum při podobných vlnových délkách jako fenylalanin a to při 250 nm (Gu, HongYan and Chang, WeiShan 2012).

Absorpční spektrum chromoforu je určeno jeho chemickou strukturou a prostředím ve kterém je chromofor rozpuštěn (Goldring, J. P. Dean 2015). Faktory, které nejvíce ovlivňují UV/Vis absorbanci jsou: protonace/deprotonace rozpouštědla, polarita a orientace chromoforu. Naopak změny prostředí v blízkosti chromoforu a změny absorbance jím vyvolané mohou sloužit jako indikátory (Hoff, W. D., Devreese, B. et al. 1996). V prvním případě se posouvá vlnová délka do vyšších hodnot (bathochromní posun) nebo opačným směrem (hypsochromní posun). Dále může nastat nárůst absorbance (hyperchromicita) nebo opačný efekt nazývaný hypochromicita. Protonace či deprotonace je závislá na změně pH nebo na oxidačně-redukčních reakcích, které

z chromoforů vytváří senzitivní reporter změny okolního prostředí. Tyto změny se projevují červeným a hyperchromním posunem absorbančního spektra. Polarita rozpouštědla způsobuje změny mezi základním a excitovaným stavem molekul, takže při přechodu do méně polárního prostředí se objevuje červený posun a hyperchromní efekt, zatímco u přechodu do více polárního prostředí se projevuje modrým a hypochromním posunem (Imamoto, Y., Koshimizu, H. et al. 2001).

Aplikace UV/Vis spektrometrie se často uplatňuje pro kvantifikaci biomolekul, určení konformačních změn, detekci aromatických aminokyselin enzymů a sledování katalytických reakcí chromoforů. Často jsou zde využity i kolorimetrické metody, které využívají barviva, schopná se specificky začlenit do struktury proteinů, což je doprovázeno posunem absorbčního maxima. Tento posun je kvantifikován a je přímo úměrný koncentraci proteinů ve vzorku. Mezi nejčastěji využívané metody jsou pyrogalová červeň (Fiorina, J. C., Aimone-Gastin, I. et al. 2001), metoda dle Bradfordové (Zor, T. and Seliger, Z. 1996), Lowryho metoda (Stauffer, C. E. 1975) nebo Biuretova metoda (Robson, R. M., Goll, D. E. et al. 1968). Spektrofotometrické metody lze využít nejen pro detekci proteinů, ale také i pro detekci navázaných kovů. Ionty kovů jsou spektrofotometricky stanovitelné pomocí chelatačních činidel vykazující optické vlastnosti, například Zincon, který se využívá jako chromofor pro kvantifikaci zinku a mědi ve vodných roztocích. Nevýhodou je nutnost odstranění vázajícího proteinu, aby nedocházelo k ovlivnění analýzy (Saebel, Crystal E., Neureuther, Joseph M. et al. 2010). Použití spektroskopických metod je tedy velmi široké pro analýzu proteinů a často se jedná o primární analýzu proteinů a kov-vazných proteinů, která je schopna studované biomolekuly charakterizovat a kvantifikovat.

3.3.4 Elektrochemické metody

Elektrochemické metody jsou vhodným nástrojem pro studium kov-vazných proteinů (Palecek, E ; Scheller, F ; Wang, J 2005). Jejich redoxní chování může být využito pro sestrojení biosenzorů (Wei, Ming-Yuan, Guo, Liang-Hong et al. 2012), které mohou být použity pro zjišťování koncentrace proteinů (Polanski, Malu and Anderson, N. Leigh 2007) nebo jejich struktury po navázání ligandu, díky kterému dochází k měřitelným

změnám prostředí (Obrázek 7) (Anderson, L. 2005; Diaconu, Iulia, Cristea, Cecilia et al. 2013; Chen, Chao, Xie, Qingji et al. 2013). Je známo, že biologické makromolekuly vykazují pomalejší rychlost heterogenního přenosu elektronů na konvenčních elektrodách, který je přisuzován trojrozměrné struktuře proteinů blokující jejich elektroaktivní centra nebo jejich adsorpci nebo pasivitu na elektrodovém povrchu. Těmto problémům se lze vyhnout přípravou chemicky modifikovaných elektrod (Borgmann, Sabine, Hartwich, Gerhard et al. 2005). Jsou známy dva druhy; v prvním případě je modifikovaná elektroda, která funguje jako prostředník, zatímco promotorová elektroda zůstává v původním stavu. V této situaci je sledována změna signálu mezi modifikovanou a nemodifikovanou elektrodou. Mediátorová elektroda je modifikovaná takovým materiálem, který umožňuje elektronový transfer v požadovaném rozsahu potenciálu. Proto mohou materiály, které slouží jako mediátor přinášet redoxní vlny (Borgmann, Sabine, Hartwich, Gerhard et al. 2005). Potenciálový rozsah proteinů závisí na mnoha faktorech, které mohou být použity pro určení vnitřního redox potenciálu hemových proteinů včetně postranních ligandů, jejich orientaci, konformaci porfyrinu, polarity a hydrofobicity hemové vnitřní kapsy a interakci proteinových ligandů s vnějším prostředím (Kohno, Michiaki, Tanimura, Susumu et al. 2011; Bischoff, Rainer and Schlueter, Hartmut 2012). Použití modifikovaných elektrod má své limity jako je neschopnost ukázat redoxní chování některých proteinů (Butterfield, D. Allan, Reed, Tanea T. et al. 2007), rozlišení mezi metaloproteiny a proteiny bez iontů kovů a také potřeba těchto metod zafixovat mediátory a proteiny na povrch elektrody (Butterfield, D. Allan, Perluigi, Marzia et al. 2006).

Elektrochemické metody vynikají přesností, rychlostí, jednoduchostí, nízkými provozními náklady a možností miniaturizace. Tyto vlastnosti jsou velmi perspektivní pro vývoj nových analytických postupů, monitoring biochemických procesů *in vivo* a *in vitro* nebo i objevení nových potencionálních léčiv.

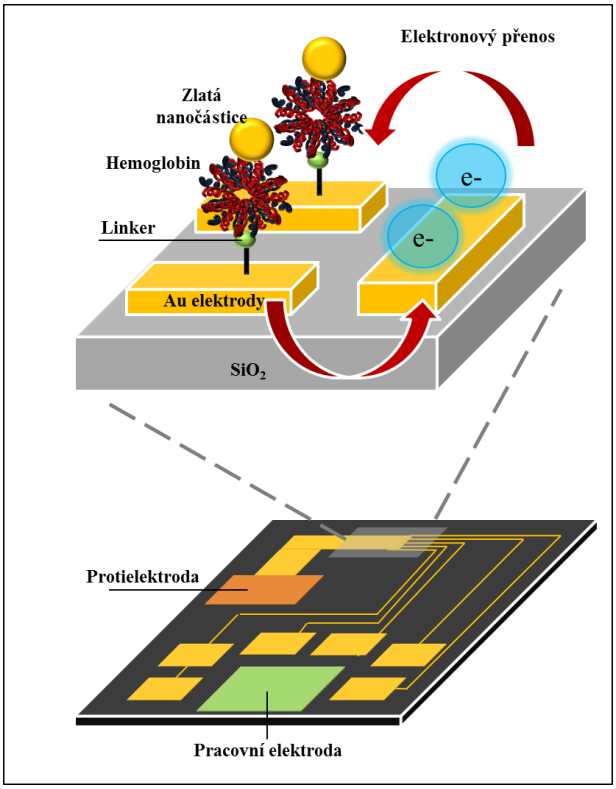

Obrázek 7: Elektrochemický biosenzor na čipu pro detekci H_2O_2. Biosenzor je založen na oxidaci hemoglobinu a změny oxidačního stavu Fe atomů uvnitř proteinu. Tato změna vyvolá přenos elektronů zesílenou zlatým nanočásticemi mezi Au "gap" elektrodou a zlatou protielektrodou. Přepracováno z (Lee, Taek, Kim, Tae-Hyung et al. 2016).

3.4.5 Hmotnostní spektrometrie

Důležitou roli v proteomice a ve studiu kov-vazných proteinů hraje hmotnostní spektrometrie. Tato technika využívá měření poměru hmotnosti *m* a náboje *z* analyzované látky. Princip metody spočívá v ionizaci vzorku vhodnou ionizační technikou, která dodává analyzovaným molekulám náboj. Na základě jejich hmotnosti a dochází k separaci v hmostnostním analyzátoru a detekci pomocí zvoleného detektoru. Oba kroky jsou realizovány ve vakuu, aby bylo zamezeno srážkám iontů a následným fragmentacím vzorku. Výsledkem analýzy je hmotnostní spektrum, ze kterého lze identifikovat konkrétní protein pomocí proteinových databází (Uniprot, NCBI, ExPASy).

Na základě povahy analyzovaných vzorků se využívá buď měkká, nebo tvrdá ionizace. Pro biomolekuly jsou vhodné měkké techniky, jako je ionizace elektrosprejem (Becker, Rene, Schwarz, Gunnar et al. 2015) nebo ionizace laserem za přítomnosti matrice (Rigueira, Leila M. B., Lana, Diogo A. P. D. et al. 2016), které jsou šetrné ke vzorku a omezují vznik fragmentů. Pro studium kov-vazných proteinů se v kombinaci s hmotnostní spektrometrií využívá ionizace indukčně vázaným plazmatem (Moller, Laura Hyrup, Jensen, Celina Stoving et al. 2015), která umožňuje stanovit stopové množství kovů. Tato technika využívá vysokých teplot (6 000 – 10 000 K), díky kterým zanikají chemické vazby v molekulách přítomných sloučenin a vznikají volné atomy kladně nabitých iontů kovů.

Mezi základní typy hmotnostních analyzátorů, ve kterých se separují ionty na základě jejich hmotnosti a náboje, jsou průletové analyzátory (Bonham, Christopher A., Steevensz, Aaron J. et al. 2014), kvadrupóly, iontové pasti (Meier, Samuel M., Babak, Maria V. et al. 2014) a jejich kombinace (Kurahashi, T., Miyazaki, A. et al. 2001). Detektor následně poskytuje signál úměrný počtu dopadajících iontů pomocí elektronového násobiče nebo detekcí elektrického proudu, vznikajícího přímým dopadem iontů.

Hmotnostní spektometrie se pro analýzu proteinů často kombinuje se separačními technikami jako je kapalinová chromatografie (Wang, Y., Li, H. et al. 2014), gelová elektroforéza (Schmidt, A. C., Storr, B. et al. 2011) a kapilární elektroforéza (Nguyen, Tam T. T. N., Ostergaard, Jesper et al. 2015).

4 MATERIÁL A METODY

4.1 Chemikálie

Standard laktoferinu byl zakoupen od firmy Sigma-Aldrich (St. Louis, USA). Paramagnetické částice byly zakoupeny od firmy Invitrogen (Norsko). Polyklonální kozí protilátky proti laktoferinu, monoklonální myší protilátky proti laktoferinu a kuřecí-HRP konjugované protilátky byly zakoupeny od firmy SantaCruz Biotechnology (USA). Polyklonální králičí proti myším protilátky konjugované alkaickou fosfatázou byly zakoupeny od firmy Dako (Dánsko). Fragmenty proteinu metallothioneinu a byly zakoupeny od firmy Clonestar (Česká republika). Ostatní použité chemikálie byly zakoupeny od firmy Sigma Aldrich v ACS čistotě, pokud není uvedeno jinak. Pracovní roztoky použitých standardů byly připravovány denně ředěním zásobních roztoků. Hodnoty pH byly měřeny s použitím WTW inoLab Level 3 (Německo), spojeným s osobním počítačem (Weilheim). pH-elektroda (SenTix-H, WTW) byla pravidelně kalibrována souborem WTW pufrů. K ředění roztoků byla použita demineralizována voda pomocí reverzní osmózy na přístroji Aqua Osmotic 02 (Aqua Osmotic,Česká republika) a dále čištěna pomocí Millipore RG (Millipore Corp., USA, 18 M Ω).

4.2 Příprava CdTe Qds

Kadmium chlorid ($CdCl_2$, 0.04 M, 4 ml) byl naředěn na 42 ml MiliQ vodou a poté byl k roztoku přidán trisodný citrát dihydrit (100 mg). Na_2TeO_3 (0,01 M, 4 ml), MPA (119 mg), and $NaBH_4$ (50 mg) byly ke vzniklé směsi přidány pod neustálým mícháním. Molekulový poměr Cd_2/MPA/Te byl 1:7:0,25 na 10 ml. Připravené prekurzory byly vystaveny mikrovlnnému záření (400 W, Multiwave 3000, Anton-Paar GmbH, Rakousko). Následně byla směs ochlazena a vzniklé kvantové tečky byly vysráženy promocí isopropanolu v objemovém poměru 1:2 a centrifugovány (Eppendorf centrifuge 5417R). Vzniklý pelet byl resuspendován v 500 ml 10 mM Tris pufrem (pH 8.5).

4.3 Biologický materiál

Vzorky slin byly odebírány pomocí odběrových zkumavek Salivette (Sarstedt, Německo). Přiložená buničina byla žvýkána po dobu 2 min. Následovala centrifugace vzorků v Salivette zkumavce při 3000 rpm po dobu 5 min. (Universal 320, Hettich Zentrifugen, Německo). Odebraný vzorek byl naředěn 1:1 s 25 mM Tris-HCl (pH 7) a přefiltrován přes mikrofiltr (microStar 0,45 μm CA, Costar Cambridge). Takto připravené vzorky byly analyzovány pomocí iontově výměnné kapalinové chromatografie s UV detekcí.

Samci Novozélandských králíků o hmotnosti 3 - 3,5 kg (MaK-Bergman, Kocanda, , Česká Republika) byly pod anestezií 30 mg/kg ketamin a 3 mg/kg xylazin (Ve´toquinol Biovet, Francie) vykrveni vpichem do srdce. Jednotlivá játra byla vypreparována a uchována v mrazu. 2g tkáně bylo homogenizováno (Ultra-turrax T8 (Scholler instruments, Německo) v 8 ml 10 mM Tris-HCl (pH 8,6) a centrifugováno (Universal 320, Hettich Zentrifugen, Německo) při 5 000 rpm (30 min, 4 °C). Odebraný supernatant byl zahřát na 99 °C 10 min (Eppendorf thermomixer comfort, Německo) a znovu centrifugován. Odebraný supernatant byl použit k izolaci metalothioneinu pomocí gelové permeační kapalinové chromatografie.

4.4 Kapalinová chromatografie s UV detekcí

Systém kapalinového chromatografu Biologic DuoFlow (Biorad, USA) byl složen ze dvou chromatografických pump pro dopravu elučních pufrů, monolitické kolony s jedním CIM diskem, který byl modifikován $-SO^{3-}$ funkčními skupinami (Bia Separations, Slovinsko) pro separaci laktoferinu a gelovou filtrační kolonou (HiLoad 26/60, 75 PG, GE Healthcare, Švédsko) pro purifikaci metalothioneinu, dávkovacího ventilu s 2ml dávkovací smyčkou, UV-VIS detektoru a automatického sběrače frakcí. Kapalina byla na kolonu dopravována pomocí dvou pump za pomocí vysokotlakého gradientu. Výstup z kolony byl napojen na UV-VIS detektor, který sloužil pro úpravu nastavení sběru frakcí. Jako mobilní fáze I (MFI) byl použit 25 mM Tris-HCl o pH 7, mobilní fáze II (MFII) byla složena z 2 M NaCl v MFI. Průtok mobilní fáze byl 4

$ml.min^{-1}$. Laktoferin byl eluován lineárně se zvyšujícím gradientem NaCl: 0-6 ml (0 % II), 6 → 12 ml (100 % II), 12→16 ml (100 % II), 16→17 ml, (0 % II), 17 → 21 ml (0 % II). Metalothinein byl z kolony eluován v isokratických podmínkách pomocí 150mM NaCl v 10 mM Tris–HCl pufru (pH 8.6). Detektor byl nastaven na 280 nm (maximum při absorpci aromatických aminokyselin). Frakce proteinů o objemu 1 ml byla sbírána pomocí automatického sběrače frakcí (Biorad, USA).

4.5 Spektrofotometrická analýza

Pro spektrometrické analýzy byl použit automatický spektrofotometr BS–200 (Mindray, Čína), který se skládá z kyvetového prostoru (temperovaného na 37 ± 0,1 °C), reagenčního prostoru s karuselem pro reagencie a přípravu vzorků (temperovaného na 4 ± 1 °C) a optického detektoru (Sochor, J., Ryvolova, M. et al. 2010). Zdrojem světla byla halogeno-wolframová žárovka. Přenos vzorků a reagencí zabezpečovalo robotické rameno s dávkovací jehlou (chyba dávkování do 1 % objemu). Kontaminace byla minimalizována díky proplachování jak dávkovací jehly, tak míchadla MilliQ vodou. Ke stanovení laktoferinu pyrogalovou červení bylo ke 200 µl činidla (50 mM sukcinová kyselina, 3,47 mM benzoát sodný, 0,06 mM molybdenát sodný, 1,05 mM oxalát sodný a 0,07 mM pyrogalová červeň) (Pupkova, V. I. and Prasolova, L. M. 2007; Yang, J. Y., Chien, T. I. et al. 2009; Silva, A. S. and Falkenberg, M. 2011) (Skalab-kit, Svitavy Česká republika) přidáno 4 µl vzorku. U metody dle Bradfordové (Seevaratnam, R., Patel, B. P. et al. 2009; Field, A. and Field, J. 2010; Carlsson, Nils, Borde, Annika et al. 2011) bylo k 190 µl činidla (0,01% Coomassie Brilliant Blue G-250, 4,7% etanol, 8,5% kyselina fosforečná v destilované vodě) přidáno 10 µl vzorku (Zor, T. and Seliger, Z. 1996). Detekce u obou metod probíhala při 578 nm a doba reakce byla 10 min. Pro stanovení proteinů biuretovým činidlem bylo do kyvety napipetováno 150 µl biuretového činidla (100 mM vinan sodno-draselný, 100 mM NaOH, 15 mM KI, 6 mM $CuSO_4$) a následně 3 µl vzorku. Po 10 min. inkubaci při 37 °C byla změřena absorbance při vlnové délce 546 nm. Obsah kyvet po nadávkování vzorku byl ihned promíchán automatickým míchadlem a analyzován. Absorbance byla odečítána v čase 18 sekund, kde byla zaznamenána maximální absorbance pro všechny body kalibrace.

4.6 ELISA

Mikrotitrační destička byla pokryta 100 µl polyklonálních kozích protilátek proti lakoferinu (SantaCruz Biotechnology, USA) ředěných 1:5000 nebo 1:3000 0,05 M uhličitanového pufru pH 9,6. Následně byl volný povrch zablokován 150 µl 1 %BSA a po inkubaci 30 min 25 °C byly jamky promyty PBS pufrem. Standard laktoferinu byl v objemu 100 µl nadávkován do každé jamky a směs byla inkubována 30 min 25 °C. Po promytí nenavázaného laktoferinu PBS pufrem, byly na laktoferin navázány monoklonální myší protilátky proti laktoferinu (SantaCruz Biotechnology, USA) ředění 1:5000 nebo 1:1000. Po inkubaci byly jamky promyty a celý komplex byl konjugován s HRP značenými kuřecími protilátkami proti myším protilátkám. Po inkubaci 30 min 25 °C a promytí byl celý komplex detekován jak elektrochemicky, tak spektrofotometricky.

4.7 Injekční analýza v zastaveném toku (SFIA)

Systém byl složen z programovatelné dávkovací jehly pump (Model eVol, SGEAnalytical Science Pty, Austrálie), tříkanálového dvoupozičního ventilu (Valco Instruments, USA) a prototypu miniaturizovaného mikropotenciostatu (910 PSTAT mini, Metrohm, Švýcarsko), dávkovací kapiláry, která vstupovala do elektrochemické průtokové cely (CH Instruments, USA). Vzorek byl do systému injektován v objemu 10 µl. Elektrochemická detekce probíhala na pracovní elektrodě ze skelného uhlíku, pomocné platinové elektrody a Ag/AgCl 3 M KCl referenční elektrody. Parametry pro cyklickou voltametrii byly: cyklus skenu od 0 do 1000 mV a zpět, rychlost skenu 20 mV/s. Parametry diferenční pulzní voltametrie byly následující: vstupní potenciál 0,8 V, konečný potenciál -0,6 V, amplituda 0,05 V, délka pulsu 0,0167 s, perioda pulsu 0,2 s, depoziční potenciál 0,2 V, depoziční čas 30 s a citlivost $2{,}10^{-5}$ A/V. Měření probíhalo v prostředí 0,05 M uhličitanového pufru pH 9,6.

5 VÝSLEDKY A DISKUZE

5.1 Separace a detekce kov-vazných proteinů

5.1.1 Vědecký článek I

Isolation and determination of lactoferrin in human saliva

Skalickova, S., Zitka, O., Krizkova, S., Vlkova, M., Sochor, J., Adam, V. and Kizek, R. *Chem. Listy, 2014, 0009-2770, 56-63*

Podíl autora Skaličková S.: 60 % textové části práce a 70 % experimentální práce

Sliny jsou výměškem slinných žláz člověka a mnoha jiných živočichů. Bylo prokázáno, že složení slin je ovlivněno výskytem několika onemocnění, jako jsou akutní záněty, cystická fibróza nebo karcinom dutiny ústní. Řada vědeckých prací využívá proteinového složení slin pro diagnózu patologických změn v organismu díky jejich funkcím, které ve slinách zastupují (Javaid, Mohammad A., Ahmed, Ahad S. et al. 2016). Významným kov-vazným proteinem slin je laktoferin, u kterého byly prokázány antimikrobiální, antivirotické a antikarcinogenní účinky. Jeho zvýšená hladina v organismu je spojována s probíhajícím zánětlivým onemocněním, celiakií nebo Sjörgenovým syndromem (Mayeur, S., Spahis, S. et al. 2016). Včasná diagnostika těchto onemocnění může zabránit komplikacím a zhoršením stavu pacienta. Mezi metody, které se využívají pro izolaci a detekci kov-vazných proteinů, patří kapalinová chromatografie za využití gelové permeační nebo iontově výměnné separace.

Cílem předkládané studie bylo vyvinout metodu pro izolaci laktoferinu z lidských slin pomocí iontově výměnné kapalinové chromatografie s využitím monolytické kolony a off-line spektrofotometrické detekce metodou Pyrogallová červeň, metodou dle Bradfordové a Biuretovou metodou. Monolytická kolona představuje vhodný nástroj pro separaci a izolaci velkých proteinů jako je laktoferin a ve spojení s kapalinovou chromatografií se jedná o spolehlivou metodu pro separaci tohoto proteinu z různých biologických matric. Účinnost separace a izolace byla ověřena pomocí gelové chromatografie, která potvrdila přítomnost jediného proteinu o přibližné molekulové

hmotnosti jakou má laktoferin. Pro charakterizaci metody byly evaluovány analytické parametry spektrofotometrické detekce jako je lineární dynamický rozsah, relativní směrodatná odchylka stanovení a limit detekce. Z dosažených výsledků je patrné, že nejcitlivější detekční metodou pro laktoferin byla metoda dle Bradfordové. Kalibrační křivka pro laktoferin vykazovala lineární trend v rozsahu 0,06 - 62,5 μg/ml. Limit detekce byl stanoven na 0,01 μg/ml. Optimalizovanou metodou byly analyzovány vzorky slin zdravých subjektů. Průměrná koncentrace laktoferinu byla stanovena 42 ± 4 μg/mg proteinu. U testovaných subjektů byla pozorována 2,5 x vyšší hladina laktoferinu u pacientky s chronickou celiakií. Je známo, že celiakie je autoimunitní onemocnění vyvolané imunitní odezvou na gluten. U tohoto typu onemocnění vzrůstá exprese protizánětlivých látek v organismu. Získané výsledky této práce ukazují, že námi navrhovaný postup s využitím kapalinové chromatografie, monolitické kolony a off-line spektrofotometrickou detekcí pomocí metody dle Bradfordové, je velmi senzitivní a robustní přístup pro izolaci a stanovení laktoferinu z biologické matrice. Námi předkládaná metodika je tak využitelná pro diagnostické účely chorob spojených se změnou koncentrace laktoferinu ve slinách.

LABORATORNÍ PŘÍSTROJE A POSTUPY

IZOLACE A STANOVENÍ LAKTOFERINU Z LIDSKÝCH SLIN

SYLVIE SKALIČKOVÁ[a], ONDŘEJ ZÍTKA[a], SOŇA KŘÍŽKOVÁ[a], MARCELA VLKOVÁ[c], JIŘÍ SOCHOR[a,b], VOJTĚCH ADAM[a,b] a RENÉ KIZEK[a,b]

[a] Ústav chemie a biochemie, Agronomická fakulta, Mendelova univerzita v Brně, Zemědělská 1, 613 00 Brno, [b] Středoevropský technologický institut, Vysoké učení technické v Brně, Technická 10, 616 00 Brno, [c] Ústav klinické imunologie a alergologie, Fakultní nemocnice u Sv. Anny v Brně, Pekařská 53, 656 91 Brno
kizek@sci.muni.cz

Došlo 22.3.12, přepracováno 11.2.13, přijato 24.2.13.

Klíčová slova: laktoferin, sliny, iontově-výměnná kapalinová chromatografie, fotometrická detekce

Úvod

Sliny jsou směsí biologicky významných glykoproteinů, proteinů, enzymů, hormonů, minerálů a elektrolytů rozpuštěných ve vodě a jsou produkovány především párovými velkými slinnými žlázami[1,2]. Obsah vody a v ní rozpuštěných látek kolísá v závislosti na momentálním fyziologickém stavu organismu, přičemž jsou tyto procesy řízené vegetativním nervovým systémem na základě podmíněných a nepodmíněných reflexů[2]. Sliny se podílejí na přenosu chuti k chuťovým pohárkům, zvlhčují dutinu ústní, štěpí sacharidy a tuky na jednodušší sloučeniny, mají antimikrobní, desinfekční a ochranné účinky[3].

Jednou z významných složek slin je laktoferin. Tento glykosylovaný protein o molekulové hmotnosti 80 kDa je složený z 692 aminokyselin[4,5] a jeho isoelektrický bod (pI) byl stanoven na 8–8,5 (cit.[6,7]). Struktura laktoferinu je uspořádána do jednoduchého polypeptidového řetězce strukturovaného do dvou domén (obr. 1, převzato z databáze Expasy). Ty jsou pak schopny vázat ionty kovů, nejčastěji Fe^{2+} nebo Fe^{3+}, ale také i ionty Cu^{2+}, Zn^{2+} a Mn^{2+} (cit.[6,7]). Výskyt tohoto proteinu byl zaznamenán v sekretech několika sliznic (mateřském mléce, slzách, krevní plazmě, slinách, potu spermatu či vaginálním výtoku)[6]. V organismu plní důležitou funkci v nespecifickém imunitním systému díky jeho antimikrobní, fungicidní a antivirové aktivitě, která je podmíněná schopností vázat kovové ionty, které většina bakterií vyžaduje pro svůj růst[8]. Zvýšení hladiny laktoferinu v krvi je často spojené se zánětlivými procesy probíhajícími v organismu[9].

Ze vzorku lze laktoferin izolovat díky podstatně odlišnému isoelektrickému bodu v porovnání s dalšími proteiny přítomnými ve vzorku pomocí iontově výměnné chromatografie[10–14]. Další využívané metody pro izolaci a přečištění laktoferinu jsou enzymově značená imunoanalýza[15], afinitní membránová chromatografie[16] či nověji pseudoafinitní chromatografie[17]. Kvantitativní stanovení se nejčastěji provádí imunoseparačními metodami, jako je enzymově značená imunoanalýza (ELISA)[18–20], radioimunoanalýza (RIA)[21,22], či luminiscenčně založená imunoanalýza (LSA)[23]. Pro tyto metody se limity detekce pohybují v rozmezí 10 ng ml^{-1} – 0,2 mg ml^{-1}. Literatura se však také zmiňuje o stanovení laktoferinu vysoce účinnou kapalinovou chromatografií s detektorem diodového pole (DAD) s limitem detekce 4,5 μg ml^{-1} (cit.[24]). Vzhledem k vhodnosti metod kapilární elektroforézy pro stanovení proteinů[25] byl laktoferin studován i čipovou gelovou elektroforézou[26]. Pro detekci laktoferinu jsou vzhledem k snadné možnosti miniaturizace detekčního zařízení[27] do budoucna použitelné i amperometrické metody (limit detekce (LOD) 35 nM)[28]. Jako další elektrochemické metody vhodné pro stanovení proteinů lze uvést Brdičkovu reakci[29] nebo chronopotenciometrickou rozpouštěcí analýzu, kde je možné pro proteiny či enzymy dosáhnout výrazně nízkých limitů detekce[30,31].

V této práci byla provedena separace proteinu laktoferinu z lidských slin za využití iontově výměnné kapalinové chromatografie s monolitickou kolonou a následně byla optimalizována metoda offline fotometrického stanovení, kde byly porovnány parametry metody stanovení s běžně používanými metodami barvení proteinů pomocí biuretového činidla, pyrogalové červeně a Bradfordova činidla[32]. Nejvhodnější metoda byla využita pro off-line stanovení

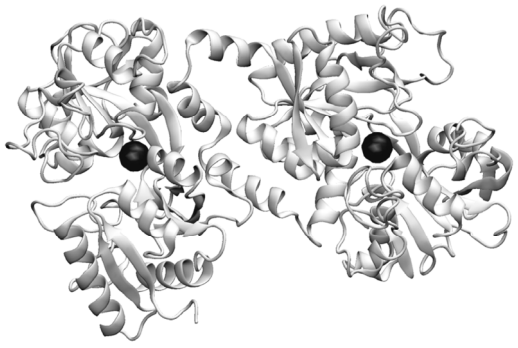

Obr. 1. **3D struktura lidského laktoferinu obsahujícího dva ionty Fe^{2+} vázané v každé z jeho dvou domén** (zdroj:www.expasy.org)

laktoferinu v lidských slinách po přečištění kapalinovou chromatografií.

Experimentální část

Chemikálie

Laktoferin a ostatní chemikálie (Trizma base, HCl, NaCl, Etanol, H_3PO_4, ACS voda, Coomasie brilliant blue) byly zakoupeny od firmy Sigma-Aldrich (St. Louis, USA). Destilovaná voda byla připravena v laboratoři na zařízení AquaOsmotic 02 (AquaOsmotic, Tišnov, Česká republika) a následně přečištěna na zařízení Millipore RG (MilliporeCorp., USA, 18 MΩ) na deionizovanou (MiliQ) vodu.

Odběr a příprava vzorků

K experimentu bylo vybráno 9 zdravých osob ve věku 23–28 let (7 žen a 2 muži) a 1 osoba trpící celiakií (vzorek č. 10, žena). Vzorky slin byly odebírány do odběrových zkumavek Salivette (Sarstedt, Německo). Přiložená buničina byla žvýkána po dobu 2 min. Následovala centrifugace vzorků v Salivette zkumavce při 3000 rpm po dobu 5 min (Universal 320, Hettich Zentrifugen, Německo). Odebraný vzorek byl naředěn 1:1 s 25 mM Tris-HCl pufrem (pH 7) a přefiltrován přes mikrofiltr (microStar 0,45 μm CA, Costar Cambridge). Takto připravený vzorek byl analyzován iontově výměnnou kapalinovou chromatografií s UV detekcí a separované frakce byly off-line fotometricky analyzovány automatickým spektrofotometrem.

Iontově-výměnná kapalinová chromatografie s UV detekcí

Systém kapalinového chromatografu Biologic DuoFlow (Biorad, USA) byl složen ze dvou chromatografických pump pro dopravu elučních pufrů, monolitické kolony s jedním CIM diskem, který byl modifikován -SO_3^- funkčními skupinami (Bia Separations, Slovinsko), dávkovacího ventilu s 2μl dávkovací smyčkou, UV-VIS detektoru a automatického sběrače frakcí (obr. 2A). Kapalina byla na CIM kolonu dopravována dvěma pumpami za pomocí vysokotlakého gradientu. Výstup z kolony byl napojen na UV detektor, který sloužil pro úpravu nastavení sběru frakcí. Jako mobilní fáze I (MFI) byl použit 25 mM Tris-HCl pufr o pH 7, mobilní fáze II (MFII) byla tvořena 2M NaCl v MFI. Průtok mobilní fáze byl 4 ml min^{-1}. Laktoferin byl eluován lineárně se zvyšujícím gradientem NaCl: 0–6 ml (0 % II), 6 → 12 ml (100 % II), 12→16 ml (100 % II), 16→17 ml, (0 % II), 17 → 21 ml (0 % II) (obr. 2B). Detektor byl nastaven na 280 nm (maximum při absorpci aromatických aminokyselin). Frakce laktoferinu o objemu 1 ml byla sbírána v elučním objemu 10,62–11,62 ml automatickým sběračem frakcí (Biorad, USA).

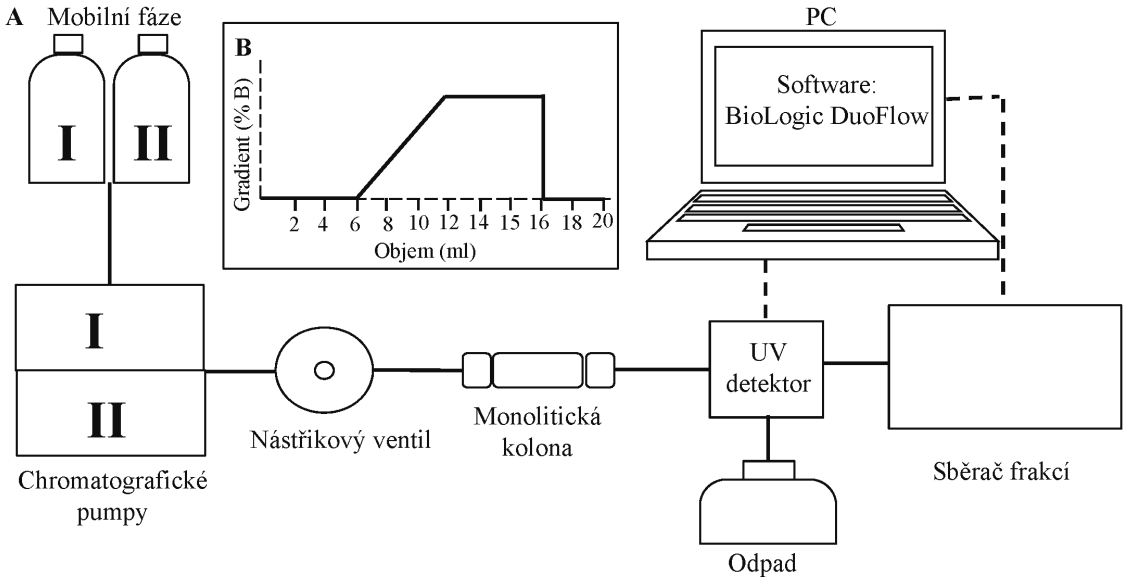

Obr. 2. **(A) Schéma iontově výměnné kapalinová chromatografie využívající monolitickou CIM kolonu s UV detektorem a sběračem frakcí.** Kapalina byla na CIM kolonu dopravována dvěma pumpami za pomocí vysokotlakého gradientu. Výstup z kolony byl napojen na čtyřkanálový UV detektor, který sloužil pro úpravu nastavení sběru frakcí. Jako mobilní fáze I byl použit 25mM Tris-HCl (pH 7), mobilní fáze II se skládala z 2M NaCl v mobilní fázi A. Průtok mobilní fáze činil 4 ml min^{-1} a detekce probíhala při 280 nm. **(B) Znázornění časového průběhu gradientu – koncentrace mobilní fáze B v závislosti na objemu**

Polyakrylamidová gelová elektroforéza

Vyseparované frakce laktoferinu byly analyzovány polyakrylamidovou gelovou elektroforézou v přítomnosti dodecylsulfátu sodného (SDS-PAGE). Pro studium laktoferinu byl použit 7,5% separační gel a koncentrace zaostřovacího gelu byla 5 %. SDS-PAGE probíhala na aparatuře Maxigel od firmy Biometra (Německo). Separace probíhala při napětí 150 V, dokud čelo proteinů nedosáhlo dolního konce gelu (~ 1 h). Během separace byl gel chlazen vodou. SDS-PAGE a detekce proteinů stříbrem byly provedeny podle klasických protokolů[33]. Gel byl inkubován 1 hodinu v roztoku 1 (1,14 % kyseliny octové, 6,4 % methanolu, 0,1 % formaldehydu) s následným propláchnutím 3×15 min v roztoku 2 (methanol s MiliQ vodou v poměru 1:1). Poté byl opět inkubován 1 min v roztoku 3 (0,02 % thiosíranu sodného) a propláchnut 2×20 min destilovanou vodou. Následovala další inkubace 20 min v roztoku 4 (0,02 % $AgNO_3$, 0,076 % formaldehydu) a propláchnutí 20 min destilovanou vodou. Na závěr byl gel inkubován v roztoku 5 (6 % Na_2CO_3, 0,0004 % $Na_2S_2O_3$, 0,05 % formaldehydu) a byl pozorován vznik zbarvení. Po získání optimálního zabarvení (~ 3 min) byl gel ihned propláchnut 2×2 min destilovanou vodou. Pro zafixování byl hotový gel inkubován v roztoku 6 (6,4 % methanolu a 1,14 % kyseliny octové).

Off-line fotometrická analýza

Pro spektrofotometrické analýzy byl použit automatický spektrofotometr BS-200 (Mindray, Čína), který se skládá z kyvetového prostoru (temperovaného na 37±0,1 ° C), reagenčního prostoru s karuselem pro reagencie a přípravu vzorků (temperovaného na 4±1 °C) a optického detektoru[34]. Zdrojem světla byla halogeno-wolframová žárovka. Přenos vzorků a reagencí zabezpečovalo robotické rameno s dávkovací jehlou (chyba dávkování do 1 % objemu). Kontaminace byla minimalizována díky proplachování jak dávkovací jehly, tak míchadla MilliQ vodou. Ke stanovení laktoferinu pyrogalovou červení bylo ke 200 µl činidla (50 mM sukcinová kyselina, 3,47 mM benzoát sodný, 0,06 mM molybdenát sodný, 1,05 mM oxalát sodný a 0,07 mM pyrogalová červeň)[35–37] (Skalabkit, Svitavy Česká republika) přidáno 4 µl vzorku. U metody dle Bradfordové[38–40] bylo k 190 µl činidla (0,01 % Coomassie Brilliant Blue G-250, 4,7 % ethanol, 8,5 % kyselina fosforečná v destilované vodě) přidáno 10 µl vzorku[41]. Detekce u obou metod probíhala při 578 nm a doba reakce byla 10 min. Pro stanovení proteinů biuretovým činidlem bylo do kyvety napipetováno 150 µl biuretového činidla (100 mM vinan sodno-draselný, 100 mM NaOH, 15 mM KI, 6 mM $CuSO_4$) a následně 3 µl vzorku. Po 10 min inkubace při 37 °C byla změřena absorbance při vlnové délce 546 nm. Obsah kyvet po nadávkování vzorku byl ihned promíchán automatickým míchadlem a analyzován. Typické záznamy v podobě kinetických křivek získaných z automatického fotometru BS-200 znázorňující časově závislé měření absorbance různých koncentrací laktoferinu jsou uvedeny na obr. 3. Absorbance byla odečítána v čase18 sekund, kde byla zaznamenána maximální absorbance pro všechny body kalibrace.

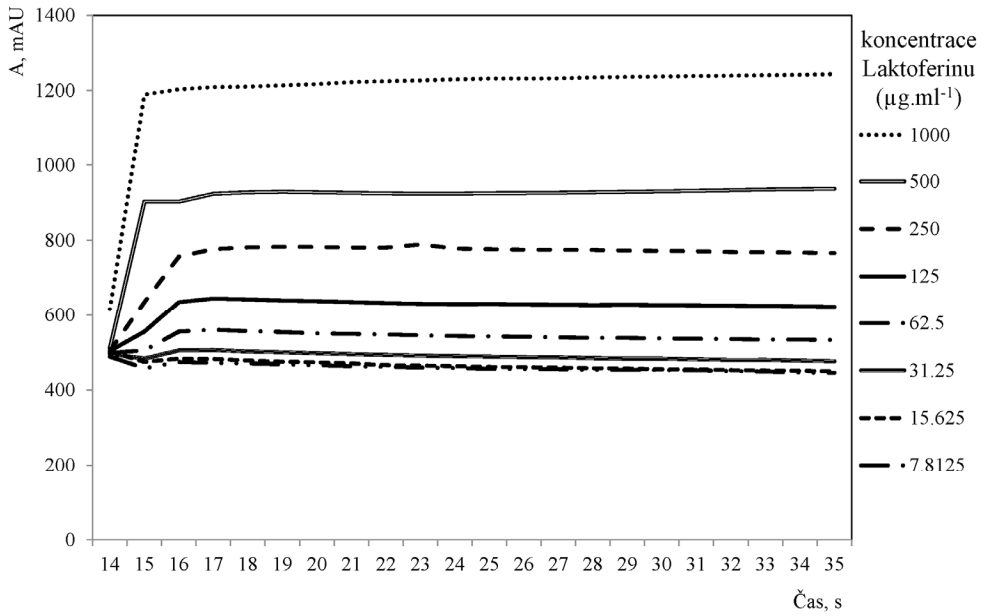

Obr. 3. **Kinetické křivky získané z automatického fotometru BS-200 znázorňující časové závislé měření různých koncentrací laktoferinu metodou dle Bradfordové.** Na obrázku je znázorněna osmibodová kalibrační křivka v rozmezí 7,81 až 1000 µg ml^{-1}

Výsledky a diskuse

Pro separaci laktoferinu jsme využili kapalinový chromatograf, ke kterému byla připojena monolitická kolona. Tato kolona je díky své konstrukci šetrná ke struktuře proteinu, neboť lze separaci provádět při vysokém průtoku a přitom při velmi nízkém tlaku, aniž by došlo k poškození struktury proteinu[26,42]. Strukturní změny proteinů v závislosti na tlaku v koloně byly již v minulosti studovány[43–45]. Pro separaci byl využit postup, jehož parametry byly optimalizovány v práci[42], přičemž byla provedena optimalizace postupu pro izolaci laktoferinu ze slin, kdy jsme pozornost zaměřili na rychlost průtoku mobilní fáze a koncentrace solí obsažených v elučním pufru, a dále jsme se zaměřili na výběr nejvhodnější fotometrické detekce.

Off-line fotometrická detekce

Nejprve jsme se zaměřili na výběr vhodné off-line fotometrické detekce pomocí různých typů barvení. Pro fotometrické stanovení koncentrace laktoferinu z izolovaných frakcí byly vybrány tři metody, které se používají ke stanovení proteinů, a to metoda s pyrogalovou červení[35–37] , metoda dle Bradfordové[38–40] a metoda s biuretovým činidlem[46]. Ke zjištění limitu detekce (3*S/N)[47] metod byla proměřena 15 bodová kalibrační závislost laktoferinu v roztoku 2M NaCl v koncentračním rozmezí od 1

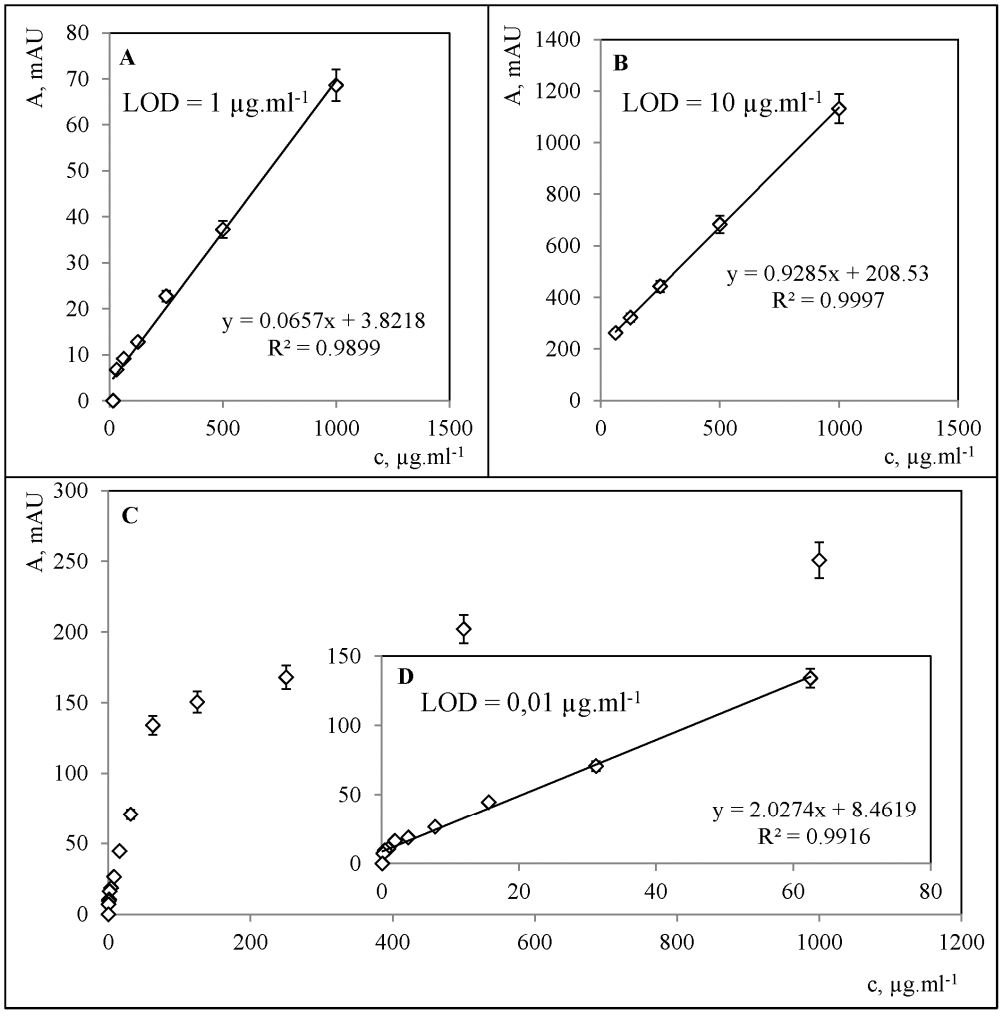

Obr. 4. **Graf závislosti absorbance na koncentraci laktoferinu v získaných frakcích pomocí iontově-výměnné kapalinové chromatografie analyzovaných v off-line provedení pomocí (A) pyrogalové červeně, (B) biuretového činidla a (C) metody dle Bradfordové v koncentračním rozmezí 0,061–1000 µg ml^{-1}. (D) Lineární část kalibrační křivky laktoferinu detegovaného metodou dle Bradfordové od 0,2 do 62,5 µg ml^{-1}**

Tabulka I
Fotometrické stanovení proteinů

Metoda	Rovnice regrese	Lineární dynamický rozsah [μg ml^{-1}]	R^2	LOD[a] [μg ml^{-1}]	LOQ[b] [μg ml^{-1}]	RSD[c] [%]
Pyrogalová červeň	y = 0,0650x + 3,81	16–1000	0,990	1	3	6
Biuretovo činidlo	y = 0,928x + 208	62,5–1000	0,999	10	30	5
dle Bradfordové	y = 2,03x + 8,46	0,1–62,5	0,992	0,01	0,03	4

[a] Limit detekce, [b] limit kvantifikace, [c] relativní směrodatná odchylka

do 1000 μg ml^{-1}. V případě metody využívající pyrogalovou červeň (obr. 4A) byla linearita R^2 = 0,9899 v koncentračním rozmezí 15–1000 μg ml^{-1} s limitem detekce 1 μg ml^{-1} (RSD = 6 %, *n* = 3, tab. I). Linearita kalibrační křivky biuretové metody (obr. 4B) byla R^2 = 0,999 v koncentračním rozmezí 62,5–1000 μg ml^{-1}. Limit detekce 3S/N činil 10 μg ml^{-1} (RSD = 5 %, *n* = 3, tab. I). Kalibrace laktoferinu metodou dle Bradfordové (obr. 4C a D) vykazovala linearitu R^2 = 0,9916 v koncentračním rozmezí 1 do 62,5 μg ml^{-1}. Limit detekce této metody (3 S/N byl 0,01 μg ml^{-1} (RSD = 4 %, *n* = 3, tab. I).

Z těchto výsledků jasně vyplývá, že pro stanovení laktoferinu je nejvhodnější z pohledu limitu detekce metoda dle Bradfordové. Vzhledem k tomu, že v publikovaných studiích byly naměřené koncentrace laktoferinu ve slinách v rozmezí 10,54 μg ml^{-1} (cit.[48]) až 47 μg ml^{-1} (cit.[49]), byla pro off-line detekci zvolena fotometrická metoda dle Bradfordové. Pro ověření detekce i v off-line pro-

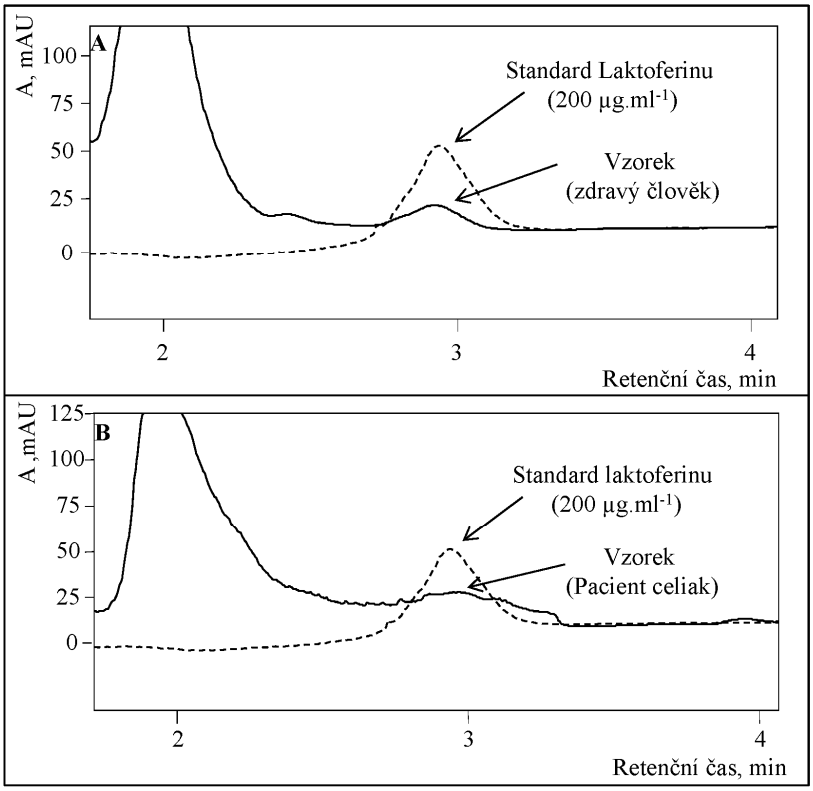

Obr. 5. **(A) Chromatografický záznam vzorku slin zdravého člověka a standardu laktoferinu (200 μg ml^{-1}). (B) Chromatografický záznam vzorku slin pacienta trpícího celiakií v proložení se standardem laktoferinu (200 μg ml^{-1})**

vedení byla 15 bodová kalibrační závislost připravena také v pufru, který je součástí mobilní fáze A pro separaci laktoferinu, a kterým jsou sliny ředěny. Tato kalibrační řada laktoferinu byla analyzována iontově výměnnou kapalinovou chromatografií s následnou fotometrickou detekcí izolovaných frakcí metodou dle Bradfordové. Zjištěné hodnoty absorbance byly při porovnání stejné jako u kalibrace laktoferinu připraveného v prostředí eluentu, tedy mobilní fáze B. V porovnání s ostatními autory (Adam a spol.[42] 100 μg ml^{-1}, Yoshise a spol.[20] 100 μg ml^{-1}, Sykes a spol.[21] 200 μg ml^{-1} a Drackova a spol.[24] 4,5 μg ml^{-1}) vykazuje námi optimalizovaná metoda nižší limity detekce.

Analýza reálných vzorků

Návratnost

Sliny jsou komplexem mnoha látek, které spolu mohou interferovat a tím zkreslovat získané výsledky. Byla tedy studována návratnost stanovení laktoferinu metodou standardního přídavku o koncentraci 50 μg ml^{-1}, kde analýza probíhala dle optimalizované metodiky. Z naměřených hodnot byla vypočítána průměrná návratnost 53±5 % (n=3). Pomocí provedení gelové elektroforézy metodou SDS-PAGE[45,50] byla potvrzeno, že izolovaná frakce obsahovala pouze protein o molekulové hmotnosti 80 kDa, která odpovídá laktoferinu.

Analýza reálných vzorků slin

Před izolací laktoferinu iontově-výměnnou kapalinovou chromatografií byly připravené vzorky slin podrobeny fotometrické analýze metodou dle Bradfordové pro určení celkové koncentrace proteinů. Naměřené absorbance byly přepočítány pomocí následující kalibrační přímky (y = 4,8658x + 7204,7) a zjištěná koncentrace se ve slinách pohybovala v rozmezí 490 až 860 μg ml^{-1}. Stanovené koncentrace korespondují s literaturou, která udává celkové množství proteinů ve slinách od 720 do 2450 μg ml^{-1} (cit.[51,52]). Pro stanovení laktoferinu ze slin byly vzorky izolovány iontově výměnnou kapalinovou chromatografií. Optimalizované podmínky separace byly: průtok mobilní fáze 4 ml min^{-1} a koncentrace NaCl v mobilní fázi B pro vysolení proteinu z kolony 2 M. V elučním objemu 5,26–6,26 ml byla sbírána frakce o objemu 1 ml. Chromatogramy laktoferinu ze vzorku slin pacienta a zdravého člověka jsou uvedeny na obr. 5A a 5B. Odebrané frakce obsahující laktoferin byly následně off-line fotometricky analyzovány metodou dle Bradfordové. Koncentrace laktoferinu se u studovaných zdravých lidí (muži a ženy ve věku 18 až 23 let) po přepočtu na celkový obsah proteinů (hodnoty jsou uvedené jako μg laktoferinu na mg celkových proteinů) pohybovala v rozmezí 32±2 až 100±3 μg mg^{-1} s průměrným obsahem laktoferinu ve slinách 42±4 μg mg^{-1} (n=3). V ostatních publikovaných studiích byly zjištěny koncentrace laktoferinu ve slinách v rozmezí 10,54 μg ml^{-1} (cit.[48]) až 47 μg ml^{-1} (cit.[49]), což odpovídá našim výsledkům, které byly v rozmezí 20–35 μg ml^{-1} (tab. II). U osoby trpící celiakií (vzorek č. 10) byla zjištěna 2,5× vyšší hladina laktoferinu než u průměrných hodnot u zdravých jedinců (tab. II). Vyšší hladinu laktoferinu u celiaků dokládají i další studie[53,54], kde byla zjištěna vyšší koncentrace laktoferinu ve střevní mukóze. U kontrol byl test na laktoferin negativní. Vzhledem k tomu, že se u jedinců trpící touto chorobou po styku nebo pozření lepku vytváří imunitní reakce s následnou tvorbou zánětu střevní sliznice, může tento patologický stav vést ke zvýšené koncentraci laktoferinu v organismu[55].

Tabulka II
Analýza vzorků slin

Vzorek [a]	c (proteiny) [b] [μg ml^{-1}]	c (laktoferin) [μg ml^{-1}]	c (laktoferin/celkové proteiny) [c] [μg/mg proteinů]
1	490 ±30	80 ±7	230 ± 20
2	700 ±50	70 ±6	130 ± 10
3	630 ±70	70 ±6	240 ± 20
4	560 ±40	60 ±5	170 ± 10
5	690 ±50	30 ±2	190 ± 20
6	680 ±50	50 ±4	150 ± 10
7	790 ±60	60 ±5	150 ± 10
8	600 ±40	70 ±6	230 ± 20
9	860 ±60	60 ±5	130 ± 10
10	500 ±40	110 ±10	420 ± 30

[a] Vzorky č. 1–9 byly odebrány (n = 3) od zdravých osob ve věku 23–28 let, vzorek 10 pochází od ženy (28) trpící celiakií, [b] celková koncentrace proteinů byla stanovena pomocí fotometrické metody dle Bradfordové, [c] koncentrace laktoferinu se pohybovala v rozmezí 130±10 až 240±20 μg mg^{-1} s průměrným obsahem laktoferinu ve slinách 170±10 μg mg^{-1}(n=3)

Závěr

Metoda iontově výměnné kapalinové chromatografie s využitím monolitické kolony a následná off-line fotometrická detekce izolovaných frakcí s využitím metody dle Bradfordové je velmi vhodným a robustním postupem pro stanovení laktoferinu v lidských slinách. Kontrola izolovaného laktoferinu byla s pozitivním výsledkem provedena pomocí SDS-PAGE. Optimalizovanou metodou byla stanovena koncentrace laktoferinu u deseti zdravých subjektů. Průměrný obsah laktoferinu ve slinách zdravých osob byl 42±4 μg mg^{-1}, u osoby trpící celiakií byla tato hodnota 2,5× vyšší. Výsledky této práce ukazují, že spojením separační techniky využívající monolitickou kolonu a klasické fotometrické metody dle Bradfordové implementované do automatického analyzátoru je tento postup snadno plně automatizovatelný a vhodný pro tyto typy studia.

Tato práce byla financována z projektu CEITEC CZ.1.05/1.1.00/02.0068.

LITERATURA

1. Schenkels L., Veerman E. C. I., Amerongen A. V. N.: Crit. Rev. Oral Biol. Med. *6*, 161 (1995).
2. Humphrey S. P., Williamson R. T.: J. Prosthet. Dent. *85*, 162 (2001).
3. Amerongen A. V. N., Veerman E. C. I.: Oral Dis. *8*, 12 (2002).
4. Rey M. W., Woloshuk S. L., Deboer H. A., Pieper F. R.: Nucleic Acids Res. *18*, 5288 (1990).
5. Powell M. J., Ogden J. E.: Nucleic Acids Res. *18*, 4013 (1990).
6. Levay P. F., Viljoen M.: Haematologica *80*, 252 (1995).
7. Lonnerdal B., Iyer S.: Annu. Rev. Nutr. *15*, 93 (1995).
8. Arslan S. Y., Leung K. P., Wu C. D.: Oral Microbiol. Immunol. *24*, 411 (2009).
9. Sukharev A. Y., Yermolayeva T. N., Beda N. A., Krylov G. F.: Klin. Lab. Diagnost. *2009*, 38.
10. Hynek R.: Chem. Listy *89*, 93 (1995).
11. Recio I., Visser S.: J. Chromatogr., A *831*, 191 (1999).
12. Salmon V., Legrand D., Georges B., Slomianny M. C., Coddeville B., Spik G.: Protein Expression Purif. *9*, 203 (1997).
13. Ye X. Y., Yoshida S., Ng T. B.: Int. J. Biochem. Cell Biol. *32*, 1143 (2000).
14. Uchida T., Dosako S., Sato K., Kawakami H.: Milchwiss.-Milk Sci. Int. *58*, 482 (2003).
15. Hutchens T. W., Henry J. F., Yip T. T.: Clin. Chem. *35*, 1928 (1989).
16. Wolman F. J., Gonzalez Maglio D., Grasselli A., Cascone O.: J. Membr. Sci. *288*, 132 (2007).
17. Ng P. K., Yoshitake T.: J. Chromatogr. B *878*, 976 (2010).
18. Sato R., Ohki K., Syuto B., Sato J., Naito Y.: International Congress Series; Lactoferrub: Structure, function and applications, *1195*, 111 (2000).
19. Shinmoto H., Kobori M., Tsushida T., Shinohara K.: Biosci. Biotechnol. Biochem. *61*, 1044 (1997).
20. Yoshise R. E., Matsumoto M., Chiji H., Kuwata H., Shin K., Yamauchi K., Tamura Y., Tanaka T., Kumura H., Shimazaki K.: Milchwiss.-Milk Sci. Int. *62*, 446 (2007).
21. Sykes J. A. C., Thomas M. J., Goldie D. J., Turner G. M.: Clin. Chim. Acta *122*, 385 (1982).
22. Boxer L. A., Coates T. D., Haak R. A., Wolach J. B., Hoffstein S., Baehner R. L.: N. Engl. J. Med. *307*, 404 (1982).
23. Maacks S., Yuan H. Z., Wood W. G.: J. Biolumin. Chemilumin. *3*, 221 (1989).
24. Drackova M., Borkovcova I., Janstova B., Naiserova M., Pridalova H., Navratilova P., Vorlova L.: Czech. J. Food Sci. *27*, S102 (2009).
25. Ptacek P.: Chem. Listy *85*, 515 (1991).
26. Zitka O., Krizkova S., Adam V., Horna A., Kukacka J., Prusa R., Zizkova V., Kizek R.: Chem. Listy *104*, 197 (2010).
27. Peckova K., Mocko V., Opekar F., Swain G. M., Zima J., Barek J.: Chem. Listy *100*, 124 (2006).
28. Campanella L., Martini E., Pintore M., Tomassetti M.: Sensors *9*, 2202 (2009).
29. Kizek R., Vacek J., Trnkova L., Klejdus B., Havel L.: Chem. Listy *98*, 166 (2004).
30. Huska D., Adam V., Zitka O., Kukacka J., Prusa R., Kizek R.: Electroanalysis *21*, 536 (2009).
31. Adam V., Petrlova J., Wang J., Eckschlager T., Trnkova L., Kizek R.: PLoS One *5*, 1 (2010).
32. M. B. M.: Anal. Biochem. *72*, 248 (1976).
33. Krizkova S., Hrdinova V., Adam V., Burgess E. P. J., Kramer K. J., Masarik M., Kizek R.: Chromatographia *67*, S75 (2008).
34. Sochor J., Ryvolova M., Krystofova O., Salas P., Hubalek J., Adam V., Trnkova L., Havel L., Beklova M., Zehnalek J., Provaznik I., Kizek R.: Molecules *15*, 8618 (2010).
35. Yang J. Y., Chien T. I., Lu J. Y., Kao J. T.: Clin. Chim. Acta *408*, 75 (2009).
36. Pupkova V. I., Prasolova L. M.: Klin. Lab. Diagnost. 17 (2007).
37. Silva A. S., Falkenberg M.: Clin. Biochem. *44*, 1000 (2011).
38. Seevaratnam R., Patel B. P., Hamadeh M. J.: J. Biochem. *145*, 791 (2009).
39. Field A., Field J.: Food Chem. *121*, 912 (2010).
40. Carlsson N., Borde A., Wolfel S., Akerman B., Larsson A.: Anal. Biochem. *411*, 116 (2011).
41. Zor T., Seliger Z.: Anal. Biochem. *236*, 302 (1996).
42. Adam V., Zitka O., Dolezal P., Zeman L., Horna A., Hubalek J., Sileny J., Krizkova S., Trnkova L., Kizek R.: Sensors *8*, 464 (2008).
43. Kukacka J., Zitka O., Horna A., Stejskal K., Zehnalek J., Adam V., Havel L., Zeman L., Prusa R., Trnkova L., Kizek R.: Faseb J. *21*, A635 (2007).
44. Zitka O., Horna A., Stejskal K., Zehnalek J., Adam V., Havel L., Zeman L., Kizek R.: Acta Chim. Slov.

54, 68 (2007).
45. Zitka O., Krizkova S., Skalickova S., Dospivova D., Adam V., Kizek R.: Electrophoresis *in press*, (2013).
46. Ohnishi S. T., Barr J. K.: Anal. Biochem. *86*, 193 (1978).
47. Long G. L., Winefordner J. D.: Anal. Chem. *55*, A712 (1983).
48. Jentsch H., Sievert Y., Gocke R.: J. Clin. Periodontol. *31*, 511 (2004).
49. Rudney J. D., Smith Q. T.: Infect. Immun. *49*, 469 (1985).
50. Grunert T., Marchetti-Deschmann M., Miller I., Muller M., Allmaier G.: Electrophoresis *29*, 4332 (2008).
51. Bonilla C. A.: J. Dent. Res. *51*, 664 (1972).
52. Jenzano J., Legette Z., Featherstone G., Lundblad R.: FASEB J. *8*, A389 (1994).
53. Barresi G., Tuccari G.: Pathol. Res. Pract. *178*, 111 (1983).
54. Fine K. D., Ogunji F., George J., Niehaus M. D., Guerrant R. L.: Am. J. Gastroenterol. *93*, 1300 (1998).
55. Sollid L. M.: Nat. Rev. Immunol. *2*, 647 (2002).

S. Skaličková[a], O. Zítka[a], S. Křížková[a], M. Vlková[c], J. Sochor[a,b], V. Adam[a,b], and R. Kizek[a,b]
([a] Department of Chemistry and Biochemistry, Faculty of Agronomy, Mendel University, Brno, [b] Central European Institute of Technology, University of Technology, Brno, [c] Department of Clinical Immunology and Allergology, University Hospital, Brno): **Isolation and Determination of Lactoferrin in Human Saliva**

Lactoferrin, a globular glycoprotein, is an important component of saliva. It shows an antibacterial, anticancerogenic and anti-inflammatory activity. The aim of this study was to develop a method of isolation of lactoferrin from human saliva using ion exchange chromatography in a monolithic column and spectrometric detection with Pyrogallol Red by the Bradford and biuret methods. The calibration curve for lactoferrin was linear in the range 0.06–62.5 μg ml^{-1}, limit of detection 0.01 μg ml^{-1}. The lactoferin concentration in saliva of healthy subjects was 42±4 μg mg^{-1}. Patient with celiac disease showed 2.5× times higher concentration of lactoferrin compared with healthy subjects.

5.1.2 Vědecký článek II

Microfluidic tool coupled with electrochemical assay for detection of lactoferrin isolated by antibody-modified paramagnetic beads

Zitka, O., Krizkova, S., Skalickova, S., Dospivova, D., Adam, V. and Kizek, R.

Electrophoresis, 2013, 0173-0835, 2120-2128

Podíl autora Skaličková S.: 50 % textové části práce a 50 % experimentální práce

Laktoferin se nachází v důležitých tělních sekretech jako je mateřské mléko, sliny, pot aj. Díky jeho schopnosti vázat ionty kovů, se uplatňuje v udržování jejich homeostázy v organismu a přispívá k činnosti imunitního systému svými antibakteriálními, antivirovými a antifungicidními účinky. Pro detekci a stanovení laktoferinu byla optimalizována řada metod, z nichž se nejčastěji využívá kapalinová chromatografie. Další vhodné techniky jsou imunochemické metody, kapilární elektroforéza či elektrochemické metody.

Paramagnetické částice jsou dnes často využívané médium pro izolaci a zakoncentrování cílových analytů díky možnosti jejich konjugace s protilátkami proti stanovované látce. Tímto se snižuje čas přípravy vzorků, zvyšuje se reprodukovatelnost a senzitivita analýzy. Mimo jiné paramagnetické částice představují analytický potenciál v biosenzorech.

V této studii jsme vyvinuli imunosenzor pro detekci laktoferinu z biologických vzorků pomocí roboticky ovládané přípravy paramagnetických částic modifikovaných protilátkami proti laktoferinu pomocí automatické pipetovací stanice. V postupu jsme optimalizovali následující kroky: navázání proteinu G na paramagnetické částice, na které byly připojeny kozí protilátky proti LF (10 μg). Laktoferin byl následně přidán do mikrotitrační destičky, která byla pokryta kozími protilátkami proti laktoferinu. Laktoferin byl ve vzniklém komplexu detekován pomocí křenové peroxidázy, která redukuje 3,3',5,5'-Tetramethylbenzidine (TMB). Výsledný produkt byl detekován spektrofotometricky s limitem detekce 5 ng/ml (3 S/N) a také pomocí injekční analýzy v zastaveném průtoku (SFIA) s amperometrickou detekcí. Limit detekce metody byl

stanoven na 0,1 μg/ml. Výsledky obou analýz byly mezi sebou porovnány pomocí korelační analýzy a vypočítaný korelační koeficient R^2 = 0,95 značí, že výsledky jsou v dobré shodě. Výhodou námi navržené metody je možnost její plné automatizace a propojení spektrofotometrické a elektrochemické detekce. Navíc, dynamický rozsah pro SFIA je lepší než u běžně využívané enzymem značené imunoanalýzy.

Ondrej Zitka[1,2]
Sona Krizkova[1,2]
Sylvie Skalickova[1]
Dana Dospivova[1]
Vojtech Adam[1,2]
Rene Kizek[1,2]

[1]Department of Chemistry and Biochemistry, Faculty of Agronomy, Mendel University in Brno, Brno, Czech Republic
[2]Central European Institute of Technology, Brno University of Technology, Brno, Czech Republic

Received November 23, 2012
Revised January 23, 2013
Accepted January 23, 2013

Research Article

Microfluidic tool coupled with electrochemical assay for detection of lactoferrin isolated by antibody-modified paramagnetic beads

Lactoferrin (LF) is approximately 80 kDa iron-binding protein, which is important part of saliva and other body fluids. Due to its ability to bind metal ions, it has many biologically important functions. In this study, a method for the isolation of LF from a biological sample using robotically prepared antibody-modified paramagnetic particles was developed using robotic pipetting station. The method consisted of the following optimised steps. Protein G was bound on the paramagnetic particles, on which goat antibody (10 μg) was linked. LF was subsequently added to microtitration plate, which had affinity to goat antibody and the interaction lasted for 30 min. We found that the highest signals were obtained using the combination of goat antibody 1:3000, murine antibody 1:5000 and conjugate 1:1500. Horseradish peroxidase reducing 3,3′,5,5′-tetramethylbenzidine (TMB) was linked to the merged complex. The resulted product of this reaction was subsequently analysed spectrometrically with detection limit (3 S/N) as 5 ng/mL. In addition, we also determined TMB by stopped flow injection analysis with electrochemical detection. The limit of detection (3 S/N) was estimated as 0.1 μg/mL. To compare spectrometric and electrochemical approach for detection of TMB, calibration range of bead-LF-antibodies complex was prepared and was determined using a least-squares correlation with coefficient R^2 higher than 0.95, indicating a very good agreement of the results obtained.

Keywords:
Electrochemistry / ELISA / Lactoferrin / Magnetic particles / Stopped flow injection analysis
DOI 10.1002/elps.201200631

1 Introduction

Saliva is the product of the salivary gland secretory cells containing glycoproteins, proteins, enzymes, hormones and minerals [1]. Saliva composition varies depending on the current physiological state of an organism and processes controlled by autonomic nervous system on the basis of the conditioned and unconditioned reflexes [1]. Saliva involves in the transfer of flavour to the taste buds, moisturizes the mouth, facilitates dilution and swallowing food, breaks down carbohydrates and fats into simpler compounds and exhibits antimicrobial, antiseptic and protective effects [2]. Lactoferrin (LF), protein contained in saliva, is one of the components of innate immunity due to its antimicrobial, anti-inflammatory effects that result from its structure. It consists from two domains, which have the ability to bind metal ions, mostly Fe^{2+} or Fe^{3+}, but also Cu^{2+}, Zn^{2+} and Mn^{2+} [3, 4], which are required for bacteria growth [5]. The occurrence of this glycoprotein was observed in several mucosal secretions as breast milk, tears, blood, saliva, sweat, semen or vaginal discharge [3]. In addition, the enhanced level of LF in the blood is associated with inflammatory processes in the body [6].

ELISA [7–9], RIA [10, 11] or luminescence-based immunoanalysis [12] are commonly used for determination of LF. This protein can be also determined using other methods like CE [13] and/or flow injection analysis with electrochemical detection [14]. Biosensors with detection limits down to hundreds of pg/mL are suitable for determination of LF in urine samples, where LF is present in very small concentrations [15]. In addition to determination assays, affinity CE was used to investigate the binding of heparin to LF [16].

Nano- and microparticles are increasingly used in immunoassays both for molecules labelling as gold nanoparticles used for CA15–3 antigen determination [17] and for immobilization of target compounds including antibodies [18]. Besides particles without magnetic properties, advantages of paramagnetic particles using are simple separation

Correspondence: Dr. Rene Kizek, Department of Chemistry and Biochemistry, Mendel University in Brno, Zemedelska 1, CZ-613 00 Brno, Czech Republic
E-mail: kizek@sci.muni.cz
Fax: +420-5-4521-2044

Abbreviations: CV, cyclic voltammetry; **FPLC**, fast protein LC; **HRP**, horseradish peroxidase; **LF**, lactoferrin; **SFIA**, stopped flow injection analysis; **TMB**, 3,3′,5,5′-tetramethylbenzidine

Colour Online: See the article online to view Figs. 1–4 in colour.

of immunocomplexes and reactants, relatively large surface area for molecules immobilization, implementation to microdetection systems and therefore possibility to use smaller amounts of sample, to reduce reaction times and to enhance selectivity and reproducibility [19]. Combination of electrokinetic pumping and manipulation in a microfluidic device employing magnetic particles as a solid support was described for detection of rabbit IgG as model protein [20].

In this study, a method for the isolation of LF from a biological sample using antibody-modified paramagnetic particles was developed. The whole process included several steps, which have been optimised. The effectiveness of each step was monitored using spectrophotometric and electrochemical techniques. We also suggested a procedure for the automated preparation of the initial magnetic particle conjugates with antibody. After the isolation of LF by the optimised procedure, concentration of the protein of interest was determined using previously published flow injection analysis with electrochemical detection [21].

2 Materials and methods

2.1 Chemicals and pH measurement

3,3′,5,5′-Tetramethylbenzidine (TMB), Na_2CO_3, $NaHCO_3$, BSA, human IgG, NaCl, Na_2PO_4 and $NaHPO_4$ were purchased from Sigma Aldrich (St. Louis, USA). HPLC-grade methanol (>99.9%; v/v) was from Merck (Dortmund, Germany). Other chemicals were purchased from Sigma Aldrich in ACS purity unless noted otherwise. Stock standard solutions of LF (1 mg/mL) were prepared with ACS water (Sigma-Aldrich) and stored in dark at −20°C. The pH value was measured using WTW inoLab Level 3 with terminal Level 3 (Weilheim, Germany), controlled by software MultiLab Pilot (Weilheim). The pH electrode (SenTix H, pH 0–14/0–100°C/3 mol/L KCl) was regularly calibrated by set of WTW buffers (Weilheim). Polyclonal goat anti-LF, monoclonal murine anti-LF antibodies and chicken-HRP conjugate were purchased from SantaCruz Biotechnology (USA). Polyclonal rabbit anti-mouse conjugate with alkaline phosphatase (AP-conjugated rabbit anti-mouse IgG) was purchased from Dako (Denmark). Magnetic microparticles Dynabeads Protein G were from Invitrogen (Norway). Plastic (tips, DWP plates) used was low retention and low protein binding and was purchased from Eppendorf (Germany).

2.2 Isolation of LF by fast protein LC

LF from human saliva was isolated using fast protein LC (FPLC) protocol by Zitka et al. [22]. The saliva was obtained from healthy man (age 26 years) using Salivette tubes (Sarstedt, Germany). The obtained fractions of LF were dialyzed on cellulose ester membranes 0.1–1 kDa (Float-A-Lyzer G2, Spectra Pro, USA) 24 h, 4°C and lyophilised (Christ Alpha 1–2) 24 h under 1^{-10} mBar and −50°C. Lyophilised LF was dissolved in ACS water to concentration 1 mg/mL and filtered using cut-off filter (Amicon Ultra-2, Ultracel-30 Membrane, 30 kDa, Millipore, Ireland). The concentration of LF standard was measured spectrometrically.

2.3 ELISA

Dilution of the coating, primary and secondary antibodies for LF immunodetection was tested by ELISA. Microtitration plate was coated with 100 μL per well of polyclonal goat anti-LF antibody (SantaCruz Biotechnology) diluted 1:5000 or 1:3000 in 0.05 M carbonate buffer (0.032 M Na_2CO_3 and 0.068 M $NaHCO_3$, pH 9.6) at 4°C for 16 h. After coating the free surface of the wells was blocked with 150 μL per well of 1% BSA w/v in PBS (137 mM NaCl, 2.7 mM KCl, 1.4 mM NaH_2PO_4, and 4.3 mM Na_2HPO_4, pH 7.4) for 30 min at 37°C, then the wells were washed 5× with 350 μL of 0.05% v/v PBS-T (Hydroflex, TECAN, USA). Then, 100 μL of the sample of LF standard was added and the microplate was incubated at 37°C for 1 h. After washing with PBS-T, 100 μL of monoclonal murine anti-LF antibody (SantaCruz Biotechnology) in dilution 1:5000 or 1:10 000 in PBS was added and the plate was incubated for 60 min at 37°C. After washing with PBS-T, 100 μL of chicken anti-mouse-HRP conjugate (SantaCruz Biotechnology) in dilution of 1:1500 or 1:2000 was added and the plate was incubated for 60 min at 37°C. After incubation and washing 100 μL of 0.001% w/v TMB in 0.2 M sodium acetate adjusted to pH 5.8 with citric acid with 0.037% v/v of H_2O_2 was added. After 30 min, the reaction was stopped with 50 μL of H_2SO_4 and after additional 5 min the absorbance was read at 450 nm (Infinite M200 Pro, Tecan, USA).

2.4 Immobilization of antibodies to the paramagnetic beads

The procedure of antibodies preparation and immobilization to the beads was adopted from suppliers manual (Invitrogen). The magnetic beads with protein G (DB-G) (25 μL) were washed twice in the 100 μL of PBS buffer. Goat antibody against LF (10 μg in 100 μL of PBS) was added to DB-G and the Ab-DB-G complex was incubated for 30 min at room temperature in a multi-spin MSC-3000 centrifuge (Biosan, Latvia) to avoid beads sedimentation. During this incubation the antibody was bound to the Dynabeads via its Fc region. After that, tubes were placed on a Dynal Magnetic Particle Concentrator (Invitrogen), thus, the beads migrated to the side of the tube facing the magnet and allowed for easy removal of the supernatant. Unbound antibody was removed and the samples were washed with 100 μL of PBS and the beads were blocked with 0.1 mg/mL of nonspecific human IgG for 30 min in a multi-spin centrifuge. After the washing

the beads were resuspended in 100 μL of PBS with 0.01% Tween-20 and stored for further usage at 4°C.

2.5 Dot-immunobinding assay and SDS-PAGE

Dot-immunobinding assay was used to verify the antibodies binding to LF standards. Two microlitre of the sample was pipetted on a PVDF membrane (Bio-Rad, USA) and let to dry. Then the membrane was blocked with 1% milk and incubated with primary antibodies in dilution of 1:200 in PBS overnight with rotation. Then, the membrane was three times washed with PBS buffer containing 0.05% v/v Tween-20 (PBS-T) and incubated with secondary antibodies in dilution of 1:500 in PBS for 1 h. After the three times washing with PBS-T the membrane was incubated with a chromogenic substrate for HRP (0.4 mg/mL 3-aminoethyl-9-carbazole in 0.5 M acetate buffer with 0.1% H_2O_2, pH 5.5), after the adequate development the reaction was stopped by rinsing with water, dried and scanned.

SDS-PAGE was performed using a Mini Protean Tetra apparatus with gel dimension of 8.3 × 7.3 cm (Bio-Rad). First 12.5% w/v running, then 5% w/v stacking gel was poured. The gels were prepared from 30% w/v acrylamide stock solution with 1% w/v bisacrylamide. The polymerization of the running or stacking gels was carried out at room temperature for 45 or 30 min, respectively. Prior to analysis the samples were mixed with non-reduction sample buffer in a 2:1 ratio. The samples were incubated at 93°C for 3 min, and the sample was loaded onto a gel. For determination of the molecular mass, the protein ladder 'Precision plus protein standards' from Bio-Rad was used. The electrophoresis was run at 150 V for 1 h at laboratory temperature (23°C) (Power Basic, Bio-Rad, USA) in Tris-glycine buffer (0.025 M Trizma-base, 0.19 M glycine and 3.5 mM SDS, pH 8.3). Then the gels were stained with silver according to Krizkova et al. [23].

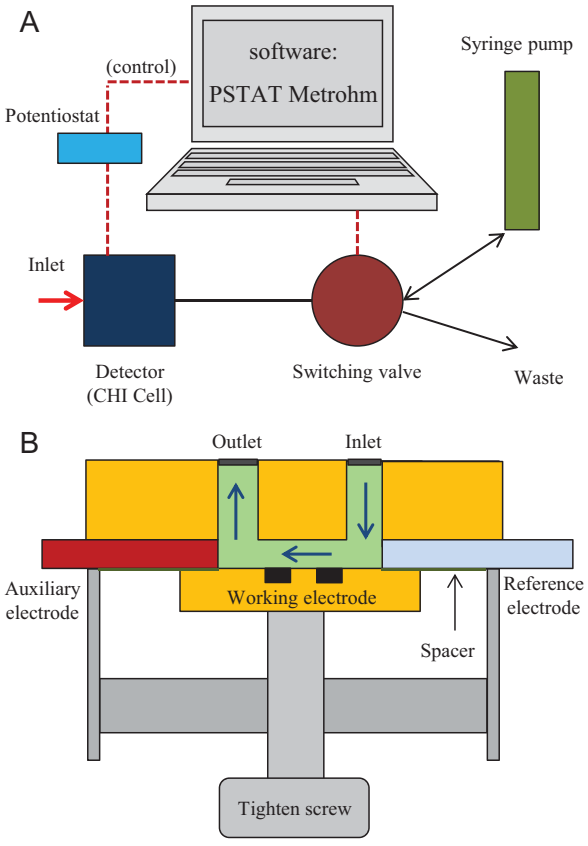

Figure 1. (A) Scheme of SFIA system. (B) Scheme of the electrochemical flow cell (CHI cell).

2.6 Robotic pipetting station

For automated samples handling prior to their electrochemical analysis, an automated pipetting station Ep-Motion 5075 (Eppendorf) with computer controlling was used. Positions C1 and C4 were thermostated (Epthermoadapter PCR96). The samples can be placed in position B3 Ep 0.5/1.5/2 mL adaptor. In B1 position Module Reservoir for washing solutions and waste were placed. Tips were placed in positions A4 (ePtips 50), A3 (ePtips 300) and A2 (ePtips 1000). Transfer was ensured by a robotic arm with pipetting adaptors (TS50, TS300, TS1000 – numeric labelling refers to maximal pipetting volume in microlitre) and a gripper for platforms transport (TG-T). The program sequence was edited and the station was controlled in pEditor 4.0. For samples preparation two platforms were used: Thermorack for 24× 1.5–2 mL microtubes (Position C3), which was used for storage of working solutions, 96-well DPW plate with well volume of 1000 μL (Position C1), which was thermostated. After the immunoseparation and enzymatic reaction, the magnetic particles were forced using Promega magnetic pad at position B4 (Promega, USA) and the solutions were transferred to a new DPW plate, in which HRP determination was performed.

2.7 Stopped flow injection analysis (SFIA)

For electrochemical detection of TMB, miniaturized microfluidic system for low volume coupled with automated electrochemical detection was used [21]. The system is composed from programmed syringe pump (Model eVol, SGE Analytical Science Pty, Australia), three-way 2-position selector valve (made from six-way valve) (Valco Instruments, USA), dosing capillary, which is entered to the electrochemical flow cell (CH Instruments, USA) and a prototype of miniaturized micropotentiostat (910 PSTAT mini (Metrohm, Switzerland)). The scheme of the instrument is shown in Fig. 1A with detailed electrochemical flow cell (Fig. 1B). Programmed syringe pump enables precise sample injections (units of microlitre with error lower than 5%). To prepare a fully automated system, switching valve enabling switching between the off waste and sample flow was placed into the system. Flow cell in volume of 500–1000 nL with electrochemical detection (working electrode: glassy carbon

Table 1. Comparison of immunoreactivity of available LF standards[a)]

Standard	Equation of regression 1:1500	R^2	Equation of regression 1:2000	R^2
1	$y = 0.09 \cdot 10^{-3}x + 7.54 \cdot 10^{-3}$	0.70	$y = 1.14 \cdot 10^{-3}x + 17.70 \cdot 10^{-3}$	0.73
2	ND	ND	$y = 0.1 \cdot 10^{-3}x + 0.86 \cdot 10^{-3}$	0.56
3	$y = 0.21 \cdot 10^{-3}x + 1.62 \cdot 10^{-3}$	0.88	$y = 0.31 \cdot 10^{-3}x + 2.48 \cdot 10^{-3}$	0.90

a) Goat antibodies 1:1500.
ND: not detected.

Table 2. Comparison of immunoreactivity of available LF standards[a)]

Standard	Equation of regression 1:1500	R^2	Equation of regression 1:2000	R^2
1	$y = 0.33 \cdot 10^{-3}x + 0.98 \cdot 10^{-3}$	0.94	$y = 0.27 \cdot 10^{-3}x - 3.08 \cdot 10^{-3}$	0.79
2	ND	ND	$y = 0.23 \cdot 10^{-3}x - 4.01 \cdot 10^{-3}$	0.43
3	$y = 2.48 \cdot 10^{-3}x - 2.70 \cdot 10^{-3}$	0.99	$y = 1.09 \cdot 10^{-3}x + 4.98 \cdot 10^{-3}$	0.96

a) Goat antibodies 1:3000.
ND: not detected.

electrode, auxiliary electrode: platinum, reference electrode: Ag/AgCl 3 M KCl) was used for a measurement.

The sample (10 μL) was injected by automated syringe (SGE Analytical Science, Australia) through flow cell in speed of 1.66 μL/s. The flow cell was cleaned by rinsing with 200 μL ethanol in water (75% v/v), then with 200 μL of 100% methanol and stabilized with 200 μL of the supporting electrolyte. Cleaning was applied after 50 measurements. The data obtained were processed by PSTAT software 1.0 (Metrohm). The experiments were carried out at 20°C.

2.8 Detection of TMB products

Supporting electrolyte for electrochemical detection of TMB was 0.05 M carbonate buffer pH 9.6. Detection parameters of cyclic voltammetry (CV) method were as follows: cyclic scan from 0 to +1000 mV and back to 0 mV, scan rate 20 mV/s. Analysis of calibration curve of TMB was carried out using method of differential pulse voltammetry where parameters were as follows: initial potential E 0.8 V, final potential –0.6 V, amplitude (V) = 0.05, pulse width (s) = 0.0167, pulse period (s) = 0.2, deposition potential (V) = 0.2, deposition time (s) = 30, sensitivity (A/V) 2.10^{-5}.

2.9 Descriptive statistics

Data were processed using Microsoft EXCEL® (USA) and STATISTICA.CZ Version 8.0 (Czech Republic). Results are expressed as mean ± SD unless noted otherwise (EXCEL®). The detection limits (3 S/N) were calculated according to Long and Winefordner [24], whereas N was expressed as standard deviation of noise determined in the signal domain unless stated otherwise.

3 Results and discussion

3.1 ELISA – Testing of LF standards

Immunoreactivity of LF standards with murine and goat anti-LF antibodies was tested by ELISA. Three LF standards were used: LF isolated from human saliva using FPLC according to protocol published by Adam et al. [25], commercially available standards of LF from Biopole and from Sigma-Aldrich, hereafter referred to as standard 1 (human), 2 (Biopole) and 3 (Sigma). LF concentration ranging from 2.5 to 40 ng/mL was prepared. Two dilutions of goat antibodies (1:1500 and 1:3000), three dilutions of murine antibodies (1:5000, 1:10 000 and 1:15 000) and two dilutions of labelled antibodies (1:1500 and 1:2000) were tested. The obtained equations and regression coefficients are shown in Tables 1 and 2. It is apparent that the linearity of the measured lines was strongly dependent on the amount of antibody used for the covering of plate, on the amount of labelled antibody and on the amount standard used. The best linearity ($R^2 = 0.99$) was obtained using standard no. 3 using 1:3000 goat antibody, 1:5000 murine antibody and 1:1500 labelled antibody. In contrast, the addition of 1:1500 goat antibodies did not show good linearity of the calibration curve with $R^2 = 0.70$ using 1:500 labelled antibody, and $R^2 = 0.73$ using 1:2000 labelled antibody. The calibration curve obtained from the analysis of standard no. 2 did not show good linearity and, using 1:1500 labelled antibody, calibration curve showed no trend. It is therefore obvious that the standard no. 2 does not bind to antibodies and therefore cannot be used for further analysis. Standard no. 3 shows good linearity using 1:500 goat antibody and 1:2000 labelled antibody with $R^2 = 0.9$. When applying 1:3000 goat antibody and 1:15 000 labelled antibody, the coefficient of determination of measured dependence was $R^2 = 0.94$. The worse regression coefficient in comparison with standard no. 1 can be associated with

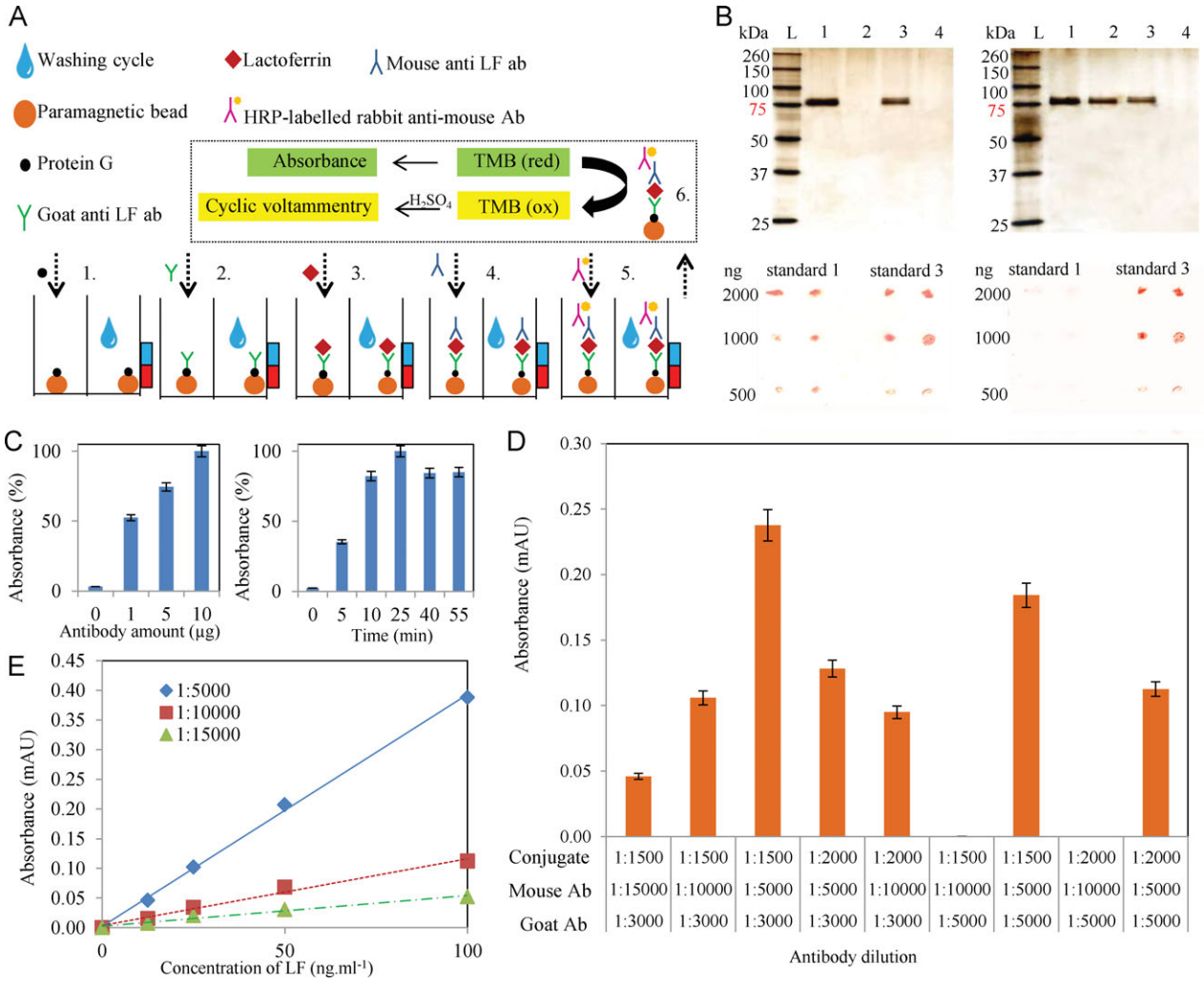

Figure 2. (A) Scheme of bead-LF-antibodies complex. Polyclonal goat antibodies against LF were immobilized onto paramagnetic particles coated with protein G. After binding with LF, monoclonal murine antibody with rabbit conjugate containing HRP against LF was used for detection of this protein. (B) Verifying the functionality of the antibodies and comparison of their immunoreactivity with the standards of LF (standard 1 – Human, standard 3 – Sigma). Left: goat antibodies, right: murine antibodies. SDS-PAGE sample standard after immunoextraction of LF. Lane 1: 500 ng of LF (standard no. 1) before immunoextraction. Lane 2: 500 ng of LF (standard no. 1) after immunoextraction. Lane 3: 500 ng of LF (standard no. 3) before immunoextraction. Lane 4: 500 ng of LF 2 (standard no. 1) after immunoextraction (top) and dot blot of LF standard (bottom). (C) Dependence of signal intensity on amount of coating goat antibodies; 10 µg corresponds to 1:3000 dilution (left), dependence of signal intensity on time of interaction (right). (D) LF signal (80 ng/mL, standard no. 3) measured by using of various combinations of the antibodies and conjugate (goat antibody 1:3000, and conjugate 1:1500). (E) Calibration curve of LF (standard no. 3) measured using various concentration of murine antibody 1:5000, 1:10 000 and 1:15 000.

the fact that standard no. 3 exhibits poor immunoreactivity with used antibodies, probably due to preparation protocol or impurities, which may interfere with the immunoreaction. Based on the results obtained, LF standards nos. 1 and 3 were used in the following experiments.

3.2 Preparation of bead-LF-antibodies complex

In the following part of our study, the immunoseparation of LF was based on magnetic beads modified by sandwich ELISA. Scheme of bead-LF antibodies complex is shown in Fig. 2A. Goat antibody was linked to paramagnetic particles via protein G, subsequently LF was added and murine antibody was bound in the following step. Formation of the immunocomplex was determined with anti-mouse Igs HRP conjugate and TMB. The absorbance of the reaction product was measured at 450 nm.

Before optimising of formation of bead-LF-antibodies complex, the applicability of antibodies for immunoextraction of LF was verified by SDS-PAGE and dot-immunobinding assay. Immunoextraction of LF was designed that 10 µL of beads modified by goat or murine antibody according to the Chapter 2.3 was pipetted to 100 µL of LF (125 µg/mL). Further, samples were shaken for 60 min, then, the liquid was pipetted away and used for SDS-PAGE analysis. For analysis by SDS-PAGE, 500 ng of LF standards before and after

immunoextraction was applied into the wells of a gel. In both standards before immunoextraction, we detected a band with an approximate molecular weight of 80 kDa, which corresponds to LF. After immunoextraction with goat antibodies in standard samples nos. 1 and 3, we did not detect any band after immunoextraction, which indicates that both standards of LF were bound to the antibodies immobilized onto the paramagnetic beads (Fig. 2B, left). When using murine antibodies, we detected weak band in standard no. 1 (Fig. 2B, right). This means that the standard no. 1 bound to murine antibodies on the paramagnetic particles only slightly and remained in solution (Fig. 2B).

Using the dot-blot analysis, it was confirmed that both types of antibodies were able to detect less than 200 ng LF of standard no. 3. In standard no. 1, immunoreactivity was demonstrated only with goat antibodies. Therefore, it can be concluded that this standard was unusable for sandwich type of analysis, which is consistent with results obtained by ELISA (Table 1). It clearly follows from the results obtained that standard no. 3 was used for the following experiments.

Subsequently, the concentration of goat antibodies coupled to paramagnetic particles (1, 5 and 10 μg) was optimised. Detection of antibodies was carried out spectrophotometrically using chicken anti-goat Igs conjugated with HRP. It clearly follows from the results shown in Fig. 2C that the highest absorbance was detected using 10 μg. When optimising interaction time, the following ones were tested as 15, 30, 45 and 60 min. The most suitable time for an interaction of antibodies with LF was 30 min. At higher interaction time, the absorbance slightly decreased (Fig. 2C).

Considering the fact that we planned linking of other antibodies, which also binds to the G protein, we had to block free surface with nonspecific Igs. Blocking increased the detected signal by 3%, which is negligible for our experimental purposes (not shown). The further step was to optimise amount antibodies used for construction bead-LF-antibodies complex. Comparison of signal of LF (80 ng/mL) determined by various concentrations of antibodies, which were selected based on the results obtained by ELISA (combination of goat antibody 1:3000 or 1:5000; murine antibody 1:5000, 1:10 000 or 1:15 000; and conjugate 1:2000 or 1:1500), is shown Fig. 2D. It clearly follows from the results obtained that the highest signals were obtained using the combination of goat antibody 1:3000, murine antibody 1:5000 and conjugate 1:1500. It is also evident that the concentration of murine antibody (the first three columns) was the most critical for obtaining the highest signal heights. Therefore, we aimed our attention at the influence of murine antibodies dilution on LF signal. For this purpose, goat antibody 1:3000 and conjugate 1:1500 was used. There were tested again the following dilution 1:5000, 1:10 000 and 1:15 000. The measured dependence of the signal height on LF concentration within the range from 10 to 100 ng/mL is shown in Fig. 2E. Regression coefficients were greater than 0.97 using all dilutions. Using 1:15 000, the signal was, however, very low. This suggests that the concentration of murine antibody required for further signal amplification was not reached. Using dilution of 1:10 000 increased regression coefficient to 0.99. Using 1:5000, we detected the highest signal and the regression coefficient was greater than 0.99. Sensitivity expressed as slope of the curve enhanced by 22× and/or 78× in the case of using of 1:10 000 and/or 1:5000 dilution, respectively. We confirmed our results that the highest signals were obtained using the combination of goat antibody 1:3000, murine antibody 1:5000 and conjugate 1:1500. Detection limit (3 S/N) was estimated as 5 ng/mL.

Table 3. Analytical parameters of other related methods for determination of LF

Method	Linearity	LOD	Recovery (%)	RSD (%)	Reference
ELISA[a)] (ng/mL)	0.625–40	0.6	98	7.8	[8]
Immunosensor–amperometric detection (μg/mL)	56–8000	24	100	5.4	[26]
CE (μg/mL)	10–400	3	91	2.4	[29]
SFIA (μg/mL)	0.78–100	0.4	93	3.1	–

a) Commercial kit (Abcam, Cambridge, United Kingdom).

3.3 SFIA analysis of TMB

Campanella et al. determined LF using amperometric immunosensor, which consisted of hydrogen peroxide electrode coated with the immobilized antibodies against LF. This method is less time consuming (time accumulation 1 h), but the detection limit was estimated to 3 μg/mL [13, 15, 26, 27]. Amperometric immunosensor was tested for diagnosis of urinary tract infection by determination of LF level with detection limit 145 pg/mL [28]. Short overview of the mostly used methods for LF determination [8, 26, 29] and their comparison with the suggested method is shown in Table 3. To our knowledge there have not been described microfluidic bead-based immunosensor for LF determination. Therefore, we attempted to apply the above-mentioned results for suggestion of microfluidic bead-based immunosensor.

TMB is used as a substrate to generate detectable signal in ELISA. The reaction between the TMB substrate and HRP produces a measurable blue colour change that correlates with analyte level. After adding stop solution (acid), yellow complex is formed (Fig. 3A). TMB also exhibits electrochemical activity and therefore can be measured by using electrochemistry, which is especially useful for miniaturization and sensors [25, 30]. For electrochemical analysis of TMB, SFIA as described by Zitka et al. [21] was used. For observing of redox change of TMB we added 185 μL of stock solution of TMB into the rest of reagents, which were as follows: 1.9 μL of H_2O_2, 92.5 μL of HRP with antibody (diluted 1:10) and finally 1720 μL of substrate buffer. Characterization of conversion of 1 μM TMB within time interval from 5 to 60 min was carried out by CV. When interlaying the obtained cyclic voltammograms showed in Fig. 3B, reduction peaks are detected at approximately 0.25 and 0.35 V. Their height gradually decreased from the beginning of the measurements. The

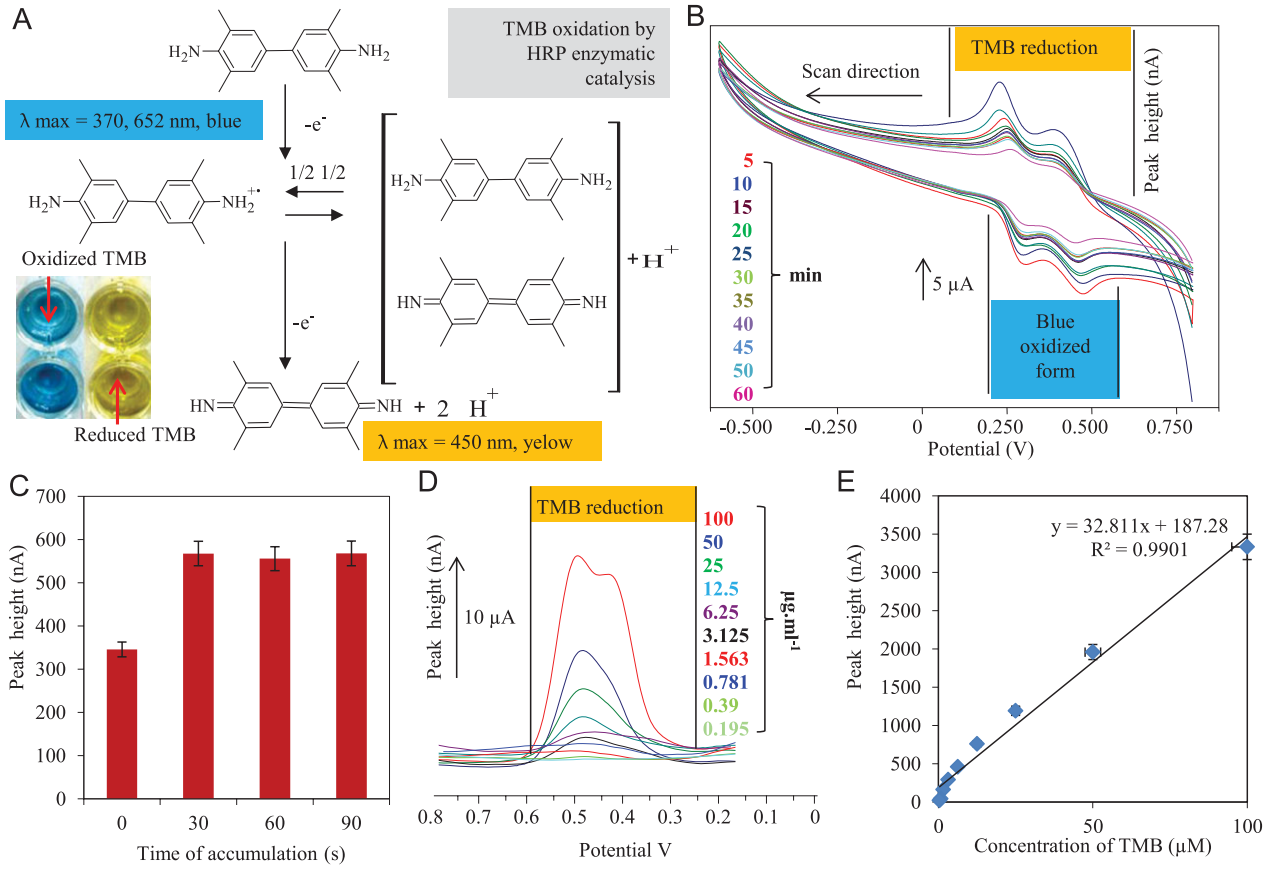

Figure 3. (A) Reaction scheme of the TMB conversion from reduced to oxidized form by HRP. (B) Time dependence of TMB (1 µM) conversion in the presence of 30% H_2O_2 catalysed by HRP as overlay of cyclic voltammetric scans. (C) The influence of time of accumulation on peak height of TMB (1 µM) measured by differential pulse voltammetry (DPV). (D) Differential pulse voltammograms of various concentration of TMB. (E) Calibration curve (0.195–100 µg/mL) of TMB (reduction signals) measured by DPV.

height of the oxidation peaks at 0.260 and 0.280 V slightly increased with a longer interaction time up to 20 min, then, the peaks decreased. Based on the potentials of reduction and oxidation peaks, it is evident that the reaction is reversible.

After that we characterized the basic electrochemical behaviour of TMB, we used differential pulse voltammetry for detection of TMB due to better sensitivity of the measurement compared to CV. Primarily, we optimised accumulation time of TMB (1 µM) at the surface of working electrode (Fig. 3C). It clearly follows from the results obtained that 30 s long interaction time caused marked enhancement of the signal. Under longer accumulation time (60 and 90 s), the signal did no change. Our effort was to develop a sensitive electrochemical detection of TMB, which would be also less time consuming. Therefore, we selected accumulation time of 30 s. Using this accumulation time, calibration curve for TMB within the range from 0.195 to 100 µg/mL was measured (Fig. 3D), which showed a linear trend with the following equation $y = 32.811x + 187.28$, $R^2 = 0.9901$, RSD = 6.7% and $n = 5$ (Fig. 3E). The limit of detection (3 S/N) for TMB was estimated as 100 ng/mL.

3.4 Correlation between spectrophotometric and electrochemical determination

To compare spectrometric and electrochemical approach for detection of TMB, calibration range of bead-LF-antibodies complex was prepared within the range from 2.5 to 80 ng/mL. Standards nos. 1 and 3 were tested and standard 2 was not used, because there was not detected any interaction with antibodies. A linear dependence with $R^2 = 0.99$ was measured using standard no. 3 (Sigma-Aldrich, Fig. 4A). On the other hand, the calibration standard no. 1 showed increasing trend only with $R^2 = 0.91$, which is probably caused by impurities occurring in the sample prepared according to Section 2.2, because the isolated LF was not further purified. Calibration of bead-LF-antibodies complex detected electrochemically was based on reduction signals of TMB (Fig. 4B). Concentration dependence shows a downward trend due to the fact that the decrease of TMB peak is measured. The regression coefficient of standard no. 1 was $R^2 = 0.92$ and of standard no. 3 was $R^2 = 0.98$, which is in good agreement with the spectrophotometric assay.

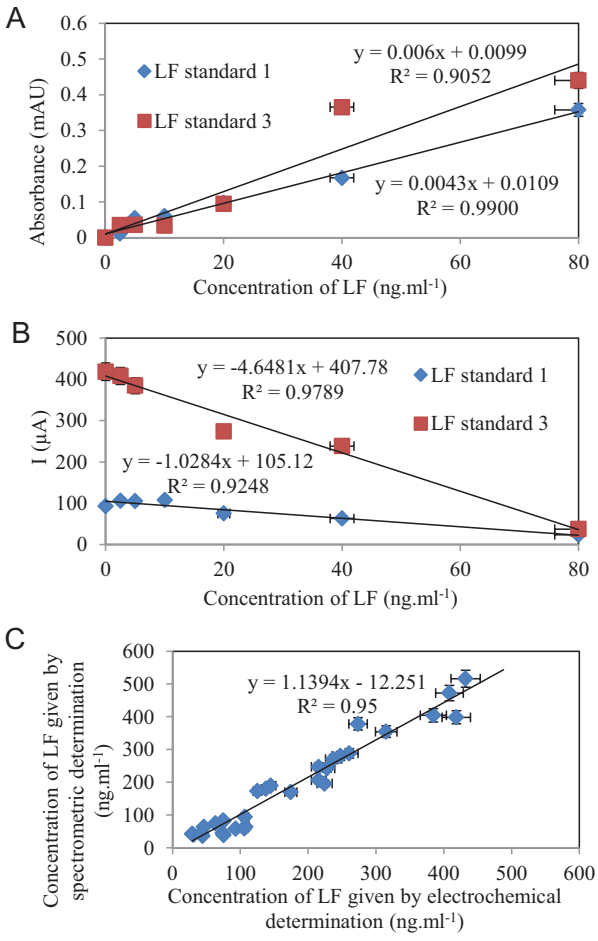

Figure 4. Comparison of the results of electrochemical and spectrometric detection. (A) Calibration curve of LF standards nos. 1 and 3 obtained by spectrometry. (B) Calibration curve of LF standard s nos. 1 and 3 obtained by electrochemistry. (C) Correlation between the concentrations of LF detected by spectrometry and electrochemistry.

The correlation between the concentrations of LF in Sigma-Aldrich standard and in human saliva isolated according to Section 2.2, detected using spectrophotometric and electrochemical assay was determined using a least-squares correlation with coefficient R^2 higher than 0.95, indicating a very good agreement of the results obtained (Fig. 4C).

4 Concluding remarks

In this study, we developed a bead-based immunosensor of LF coupled with electrochemical detection using microfluidic SFIA system with amperometric detection of TMB. Liquid handling during beads preparation was processed by fully automated pipetting system. This immunosensor was further tested for determination of LF obtained by FPLC separation and compared it with determination of commercially available LF standard. It follows from the results obtained that SFIA coupling with bead-based immunoassay has a good potential to be useful for analysis of samples obtaining LF including blood and urine. In comparison with other electrochemical approaches, the suggested tool is more than twofold more sensitive compared to other electrochemical tools. Moreover, dynamic range of the suggested method is better than ELISA.

Financial support from CEITEC CZ.1.05/1.1.00/02.0068 and NanoBioMetalNet CZ.1.07/2.4.00/31.0023 is highly acknowledged.

The authors have declared no conflict of interest.

5 References

[1] Humphrey, S. P., Williamson, R. T., *J. Prosthet. Dent.* 2001, *85*, 162–169.

[2] Amerongen, A. V. N., Veerman, E. C. I., *Oral Dis.* 2002, *8*, 12–22.

[3] Levay, P. F., Viljoen, M., *Haematologica* 1995, *80*, 252–267.

[4] Lonnerdal, B., Iyer, S., *Annu. Rev. Nutr.* 1995, *15*, 93–110.

[5] Arslan, S. Y., Leung, K. P., Wu, C. D., *Oral Microbiol. Immunol.* 2009, *24*, 411–416.

[6] Sukharev, A. Y., Yermolayeva, T. N., Beda, N. A., Krylov, G. F., *Klin. Lab. Diag.* 2009, *2009*, 38–39.

[7] Sato, R., Ohki, K., Syuto, B., Sato, J., Naito, Y., in: Shimazaki, K., Tsuda, H., Tomita, M., Kuwata, T., Perraudin, J. P. (Eds.), *4th International Conference on Lactoferrin Structure, Function and Applications* 1999, Vol. 1195, Sapporo, Japan, pp. 111–116.

[8] Shinmoto, H., Kobori, M., Tsushida, T., Shinohara, K., *Biosci. Biotechnol. Biochem.* 1997, *61*, 1044–1046.

[9] Yoshise, R. E., Matsumoto, M., Chiji, H., Kuwata, H., Shin, K., Yamauchi, K., Tamura, Y., Tanaka, T., Kumura, H., Shimazaki, K., *Milchwiss.-Milk Sci. Int.* 2007, *62*, 446–450.

[10] Sykes, J. A. C., Thomas, M. J., Goldie, D. J., Turner, G. M., *Clin. Chim. Acta* 1982, *122*, 385–393.

[11] Boxer, L. A., Coates, T. D., Haak, R. A., Wolach, J. B., Hoffstein, S., Baehner, R. L., *N. Engl. J. Med.* 1982, *307*, 404–410.

[12] Maacks, S., Yuan, H. Z., Wood, W. G., *J. Biolumin. Chemilumin.* 1989, *3*, 221–226.

[13] Campanella, L., Martini, E., Pintore, M., Tomassetti, M., *Sensors* 2009, *9*, 2202–2221.

[14] Zitka, O., Horna, A., Stejskal, K., Zehnalek, J., Adam, V., Havel, L., Zeman, L., Kizek, R., *Acta Chim. Slov.* 2007, *54*, 68–73.

[15] Pan, Y., Sonn, G. A., Sin, M. L. Y., Mach, K. E., Shih, M. C., Gau, V., Wong, P. K., Liao, J. C., *Biosens. Bioelectron.* 2010, *26*, 649–654.

[16] Heegaard, N. H. H., Brimnes, J., *Electrophoresis* 1996, *17*, 1916–1920.

[17] Ambrosi, A., Airo, F., Merkoci, A., *Anal. Chem.* 2010, *82*, 1151–1156.

[18] Ambrosi, A., Castaneda, M. T., Killard, A. J., Smyth, M. R., Alegret, S., Merkoci, A., *Anal. Chem.* 2007, *79*, 5232–5240.

[19] Richardson, J., Hawkins, P., Luxton, R., *Biosens. Bioelectron.* 2001, *16*, 989–993.

[20] Ambrosi, A., Guix, M., Merkoci, A., *Electrophoresis* 2011, *32*, 861–869.

[21] Zitka, O., Krizkova, S., Krejcova, L., Hynek, D., Gumulec, J., Masarik, M., Sochor, J., Adam, V., Hubalek, J., Trnkova, L., Kizek, R., *Electrophoresis* 2011, *32*, 3207–3220.

[22] Zitka, O., Skalicková, S., Krizkova, S. M. V., Adam, V., Kizek, R., *Chromatographia* 2013, *76*, 611–619.

[23] Krizkova, S., Adam, V., Eckschlager, T., Kizek, R., *Electrophoresis* 2009, *30*, 3726–3735.

[24] Long, G. L., Winefordner, J. D., *Anal. Chem.* 1983, *55*, A712–A724.

[25] Adam, V., Zitka, O., Dolezal, P., Zeman, L., Horna, A., Hubalek, J., Sileny, J., Krizkova, S., Trnkova, L., Kizek, R., *Sensors* 2008, *8*, 464–487.

[26] Campanella, L., Martini, E., Tomassetti, M., *J. Pharm. Biomed. Anal.* 2008, *48*, 278–287.

[27] Campanella, L., Martini, E., Tomassetti, M., *J. Pharm. Biomed. Anal.* 2010, *53*, 186–193.

[28] Pan, Y., Sonn, G. A., Sin, M. L. Y., Mach, K. E., Shih, M. C., Gau, V., Wong, P. K., Liao, J. C., *Biosens. Bioelectron.* 2010, *26*, 649–654.

[29] Li, J., Ding, X. J., Chen, Y. Y., Song, B. H., Zhao, S., Wang, Z., *J. Chromatogr. A* 2012, *1244*, 178–183.

[30] Fanjul-Bolado, P., Gonzalez-Garia, M. B., Costa-Garcia, A., *Anal. Bioanal. Chem.* 2005, *382*, 297–302.

5.2 Studium interakce proteinů s kovy

5.2.1 Vědecký článek III

Single amino acid change in metallothionein metal-binding cluster influences interaction with cisplatin

Zitka, O., Kominkova, M., Skalickova, S., Skutkova, H., Provaznik, I., Eckschlager, T., Stiborova, M., Trnkova, L., Adam, V. and Kizek, R.

Int. J. Electrochem. Sci., 2013, 1452-3981, 2625-2634

Podíl autora Skaličková S.: 30 % textové části práce a 40 % experimentální práce

Cisplatina je jedno z nejefektivnějších cytostatických léčiv na bázi platiny, které se využívá v léčbě onkologických onemocnění. Její mechanismus účinku spočívá v interkalaci do struktury DNA a tvorby kovalentních vazeb mezi cytostatikem a purinovými bázemi, zejména guaninem. To má za následek tvorbu kroslinků, které brání replikaci a transkripci DNA (Dasari, Shaloam and Tchounwou, Paul Bernard 2014). Přes to, že cisplatina je účinné cytostatikum, její využití v léčbě je limitováno vedlejšími účinky a vznikem rezistence. Dosud nebyla rezistence rakovinných buněk plně objasněna, avšak předpokládá se, že základ tohoto procesu jsou interakce cytostatik s biomolekulami, které jsou produkovány nádorovou tkání. Jedním možných mechanismů vysvětlující vznik rezistence některých cytostatik založených na bázi kovu je overexprese metalothioneinu v rakovinných buňkách (Saga, Y., Hashimoto, H. et al. 2004). Metalothionein je nízkomolekulární protein, který vyniká vysokým počtem cysteinových zbytků, které určují jeho kov vazné vlastnosti. Díky tomu je metalothionein schopný do své struktury navázat ionty platiny a podpořit onkogenní buňky vyrovnat se s oxidačním stresem způsobeným léčbou cytostatiky (Doz, F., Roosen, N. et al. 1993). Pro studium metalothioneinu a iontů kovů byla navržena řada postupů. Elektrochemické metody vynikají schopností vyjádřit průběh interakce sledováním redoxního děje.

V této studii jsme se zaměřili na sledování elektrochemického profilu interakce mezi fragmenty kov-vazného proteinu metalothioneinu s hojně využívaným cytostatickým

léčivem cisplatinou. Mechanismus rezistence může být vysvětlen snadnou výměnou zinkových iontů obsažených ve struktuře proteinu s ústředním kovem - platiny v onkologickém léčivu. Abychom posoudily tyto výsledky, byly pro každou interakci navrženy interakční konstanty. Sledovali jsme redoxní parametry vybraných fragmentů metalothioneinu a studovali jsme vliv různých fyzikálních a chemických podmínek jejich interakce s cisplatinou, abychom objasnili vznik rezistence nádorových buněk. Konkrétně jsme se věnovali vlivu teploty (10, 15, 25, 35 a 45 °C), poměru cisplatiny (100 μM) a fragmentu metalothioneinu (50, 100 a 150 μM), a času interakce (1, 2, 3, 4, 5, 6, 7 a 8 hodin). Z dosažených výsledků je patrné, že nejvíce je zvýšená interakce (více jak 100%) u konzervativních aminokyselin, které byly substituovány na více jak jedné pozici vně cysteinových klastrů. Naopak substituce aminokyselin v rámci cysteinových klastrů vedla k redukci interakční konstanty (o více než 10 - 25 % z průměru). Tyto výsledky jasně naznačují, že aminokyseliny mimo cystein-vazný motiv hrají důležitou roli v interakci metalothioneinu s cisplatinou. Na základě těchto výsledků můžeme shrnout, že substituce jednotlivých aminokyselin v peptidovém řetězci proteinu výrazně ovlivňuje interakci metalothioneinu s cisplatinou. Tyto poznatky tak mohou být užitečné při návrhu nových cytostatických léčiv.

Int. J. Electrochem. Sci., 8 **(2013)** 2625 - 2634

International Journal of ELECTROCHEMICAL SCIENCE
www.electrochemsci.org

Single Amino Acid Change in Metallothionein Metal-Binding Cluster Influences Interaction with Cisplatin

Ondrej Zitka[1,2], Marketa Kominkova[1], Sylvie Skalickova[1], Helena Skutkova[3], Ivo Provaznik[3], Tomas Eckschlager[4], Marie Stiborova[5], Libuse Trnkova[1,2], Vojtech Adam[1,2], Rene Kizek[1,2]*

[1] Department of Chemistry and Biochemistry, Faculty of Agronomy, Mendel University in Brno, Zemedelska 1, CZ-613 00 Brno, Czech Republic, European Union
[2] Central European Institute of Technology, Brno University of Technology, Technicka 3058/10, CZ-616 00 Brno, Czech Republic, European Union
[3] Department of Biomedical Engineering, Faculty of Electrical Engineering and Communication, Brno University of Technology, Kolejni 4, CZ-612 00 Brno, Czech Republic, European Union
[4] Department of Paediatric Haematology and Oncology, 2nd Faculty of Medicine, Charles University, and University Hospital Motol, V Uvalu 84, CZ-150 06 Prague 5, Czech Republic, European Union
[5] Department of Biochemistry, Faculty of Science, Charles University, Albertov 2030, CZ-128 40 Prague 2, Czech Republic, European Union
[*]E-mail: kizek@sci.muni.cz

Received: 22 November 2012 / *Accepted:* 19 December 2012 / *Published:* 1 February 2013

The issue of tumour cell resistance to anticancer drugs is a major problem in the treatment of this grave disease and it is still not satisfactorily explained. Its base lies in the interaction of a cytostatic with biomolecules synthesized by tumour cells. One of the generally accepted mechanisms of resistance to some metal based cytostatics is the overexpression of metallothionein in tumour cells. In this study, electrochemical profile of interaction between 23 sulphur-rich fragments of the metal-binding protein metallothionein and cisplatin was studied. To evaluate the results, interaction constants were suggested. Here, we found that the maximum increased interaction (more than 100 %) occurred, when conservative aminoacids were substituted for more than one position outside the cysteine cluster. On the contrary, amino acid substitution within the cysteine cluster led to a reduction in interaction constants (up to 10-25% of average). This result clearly indicates that aminoacids outside cysteine binding motif are of high importance for interactions of metallothionein with cisplatin. Based on the results it can be assumed that the substitution of individual aminoacids in the peptide chain of protein markedly influences the interaction with cisplatin, which could be used for designing new types of cytostatics.

Keywords: Aminoacid Sequence; Interaction Study; Metallothionein Fragments; Cisplatin; High Throughput Analysis; Interaction Constants

1. INTRODUCTION

The issue of tumour cell resistance to anticancer drugs is a major problem in the treatment of this grave disease [1] and it is still not satisfactorily explained [2]. Its base lies in the interaction of a cytostatic with biomolecules synthesized by tumour cells [3]. Developing new types of drugs is conditioned by achieving a higher selectivity and lower occurrence of side effects [4]. An example such development are platinum cytostatics, which have been evolving for more than forty years [5]. They are also one of the longest and most widespread used drugs used for systemic therapy of many cancers, but poor response to this treatment may be caused by interactions of platinum based drugs with proteins or with protein complexes with DNA [6]. One of the generally accepted mechanisms of resistance to some cytostatics is the overexpression of metallothionein in tumour cells [7-10].

From the structural point of view, mammalian metallothioneins (MTs) are low molecular mass (from 5 to 7 kDa, Fig. 1) proteins with unique abundance of cysteine residues (more than 30 % from all aminoacids), which directs their metal binding properties. It has been found 250 various structural forms of MTs [11]. Tertiary structure of MTs is divided into two domains, forming cysteine clusters, where the alpha and beta domains can bind to 4 divalent and 3 metal ions, respectively [12,13].

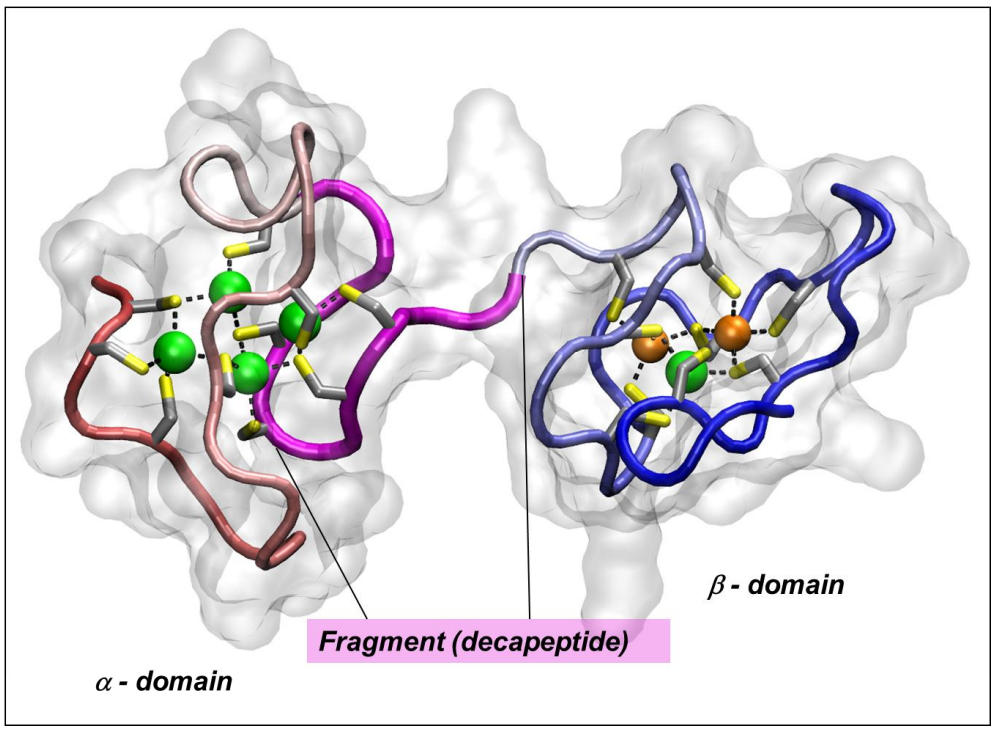

Figure 1. The structure of the protein metallothionein, α – metallothionein domain containing four cadmium atoms (green), β – metallothionein domain containing two zinc atoms (orange) and one atom of cadmium. The position of fragment of metallothionein, which was synthesized for subsequent in vitro interaction studies, is marked by pink. (Source: www.expasy.org).

Due to high abundance of cysteines in the MT structure, several sections of the chain, which contribute significantly to the interaction with the metal ions, can be described. For the purposes of our

in vitro interaction study, metallothionein protein fragments occurring in the metal binding cluster of various vertebrates were selected (Fig. 1). We evaluated redox parameters of the selected fragments of metallothionein (FMT) and studied the effects of various physical and chemical conditions on their interactions with cisplatin due to elucidation of resistance formation in tumour cells against this drug. Particularly, we aimed our attention at i) temperature (10, 15, 25, 35 and 45 °C), ii) ratio of cisplatin (100 μM) and FMT (50, 100 and 150 μM), and iii) time of interaction (1, 2, 3, 4, 5, 6, 7 and 8 hours).

2. EXPERIMENTAL PART

2.1 Bioinformatics

The data source was the internet proteomic database Expasy (www.expasy.org). For data processing software Matlab version 7.9.0 (The MathWorks, Inc., Natik, MA, USA) was used. Alignment was performed by using the conservative sections of the global multiple sequence alignment using the BLOSUM50 substitution matrix. To better assess the similarity of the sequences, distribution was weighted on the number of "characters". Data were processed using MICROSOFT EXCEL® (Microsoft, Prague, Czech Republic) and STATISTICA.CZ Version 8.0 (StatSoft CR s.r.o. Prague, Czech Republic). Results are expressed as mean ± standard deviation (S.D.) unless noted otherwise.

2.2 Chemicals and pH measurement

Standards of fragments of metallothionein (FMTs) were synthesized by Clonestar (Clonestar s.r.o., Brno, Czech Republic). Other chemicals were purchased from Sigma-Aldrich (St.Lois, MO, USA) in ACS purity unless noted otherwise. Stock standard solutions of FMTs (1 mg/ml) was prepared with ACS water (Sigma-Aldrich) and stored in dark at -20 °C. Working standard solutions were prepared daily by dilution of the stock solutions. The pH value was measured using WTW inoLab Level 3 with terminal Level 3 (WTW GmbH, Weilheim, Germany), controlled by software MultiLab Pilot (Weilheim). Deionised water underwent demineralization by reverse osmosis using the instruments Aqua Osmotic 02 (Aqua Osmotic, Tisnov, Czech Republic) and then it was subsequently purified using Millipore RG (Millipore Corp., Billerica, MA, USA, 18 MΩ) – MiliQ water.

2.3 Interaction conditions

Complexes of FMTs with cisplatin were prepared in the following molar ratios cisplatin 100 μM : FMT 50, 100 and 150 μM in the presence of phosphate buffer pH 7.5 (20 mM). Incubation of the complexes was performed in a total volume of 400 μl of the mixture, which was continuously vortexing during incubation in a heating block at 400 rpm.

2.4 FIA-ED system

FIA-ED was consisted of one chromatographic pump and electrochemical detector. Sample (20 µl) was injected by autosampler (Model 542, ESA, Sunnyvale, CA USA). Electrochemical detector Coulochem III (ESA, Sunnyvale, CA USA) was connected directly to the autosampler. For electrochemical detection the electrochemical cell model 5040 (ESA, Sunnyvale, CA USA) was used. This cell is equipped by planar electrode from glassy carbon. Mobile phase was phosphate buffer pH 7.5 (20 mM). Flow rate of mobile phase was 1 ml/min.

3. RESULTS AND DISCUSSION

3.1 Metallothionein fragments selection

Mathematical comparison of different metallothioneins from vertebrates' sequences of length 60 or 61 amino acids was done according to their amino acid sequence of the primary structure. The complete amino acid sequences of a total of 145 metallothioneins were primarily aligned according to conservative sections. There was generated sequence logo representing conservative positions in individual sequences from the aligned sequences (Fig. 2). Ten amino acid long clusters (in position 31-40 or 41) with the highest cysteine content per number of amino acids within the decapeptide with high conservatism that was related to FMT peptide 2, which was the most conservative, i.e. the sum of occurrence of individual amino acids expressed by percent was the highest, were then determined, as it is shown on percentage conservatism: 1 - K (98.62 %), 2 - free (93.79 %), 3 - S (97.93 %), 4 - C (100 %), 5 - C (99.31 %), 6 - S (63.45 %), 7 - C (100 %), 8 - C (99.31 %), 9 - P (100 %), 10 - S (51.72), 11 - G (93.79). Variability positions of 2 and 10 less distant from cysteine residues were < 94 %. Based on these presumptions, we selected fragments that were different at least by just one amino acid. From 145 FMTs, which can be found in nature, twenty three ones fit to this. For each of these 23 sequences, a short fragment within the range from 31 to 40 (41) amino acids was selected. For these 23 fragments, a degree of conservatism of the sequence was estimated. *Pj* is the percentage of degree of conservatism of sequence *j*. It indicates the degree of sequence similarity expressed in relation to the preservation of genetic information of each sequence position. Degree of conservatism calculates as it follows:

$$P_j = \frac{1}{k}\sum_{i=1}^{k}\frac{f_{ij}}{n}\cdot 100, \quad \forall j = 1 \ldots n$$

where *k* is the length of the sequence, *i* is the marker of position in the chain sequence, *j* is the sequence indicator and *n* is the number of sequences. Parameter f_{ij} is the frequency of s_{ij} character on the *i-th* position in the aligned sequences, i.e. a number of times the character located in the *j-th* sequence in the *i-th* position occurs at the same position in all sequences.

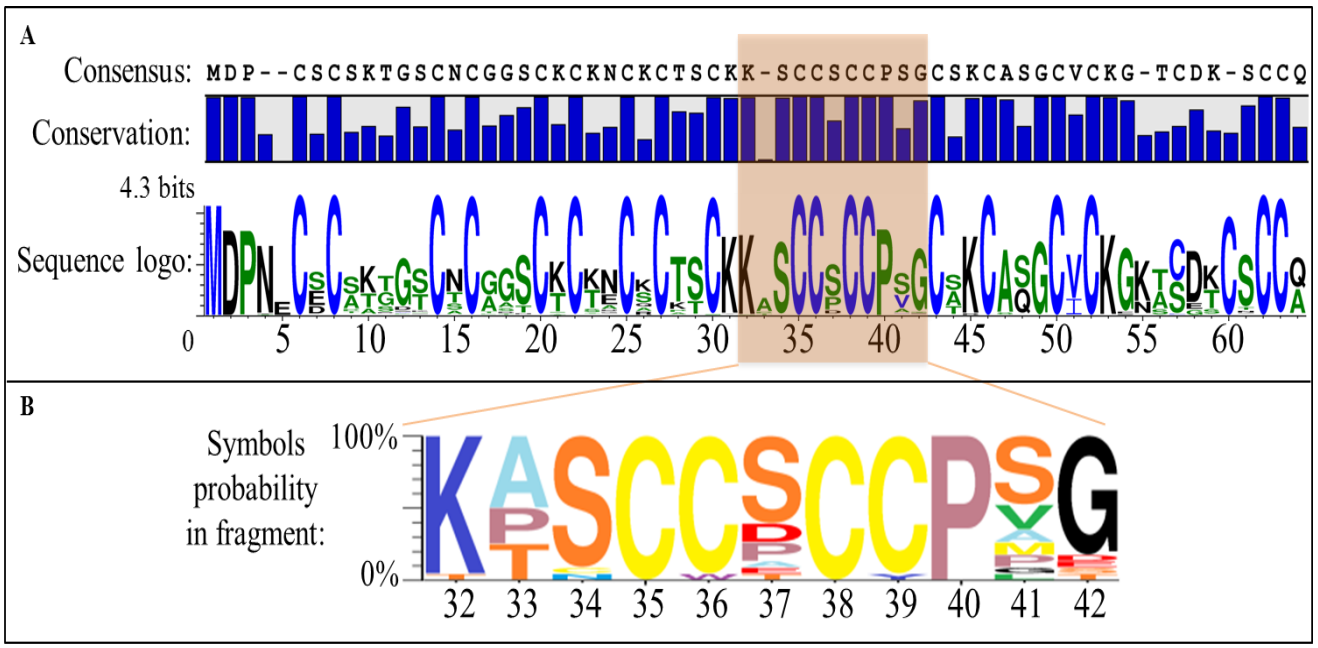

Figure 2. (**A**) Sequence logo assessed for 145 sequences of vertebrate MTs with a length of 60-61 amino acids. (**B**) Modified sequence logo of fragment in positions 32-42 representing the quantity of point mutations single-nucleotide polymorphism of 23 selected sequences.

3.2 Interaction experiment

Samples were incubated for 1, 2, 3, 4, 5, 6, 7 and 8 hours at 10, 15, 25, 35 and 45 °C at a concentration of 100 µM FMT and 50, 100 and 200 µM cisplatin. For each combination from hydrodynamic voltammogram (HDV) was obtained in the potential range from 100 to 1200 mV (n = 3, RSD <15 %). Based on the results obtained, equimolar ratio of 100 µM FMT and 100 µM cisplatin was chosen as the best under 1 h long interaction at 45 °C.

3.3 Data interpretation

Based on the obtained HDVs, regression equations of the dependences measured from the test mixtures (S_{mix}), and platinum itself (S_{Pt}) and fragments themselves (S_{FMT}) were determined. Each mixture dependence was subtracted from platinum and corresponded fragment and gave the value of which presents only the resulting change of the signal due to interaction (S_{int}), which is expressed according to equation No. 1.

Equation No. 1: $S_{int} = (S_{mix} - S_{FMT}) - S_{Pt}$

To determine the influence of various factors on the interactions as ("a 1 – 5", 10 - 45 °C respectively; "b 1 – 8", 1 – 8 hours respectively; "c 1 – 3", 50 - 200 µM respectively), graphical evaluation was done according to $X = S_{(a)}$ versus $Y = \Sigma_{S(a1+a2+a3\ldots)}$, where $S_{(a)} = \Sigma S/p_{parameter}$, for each studied fragment (Figs. 3 and 4).

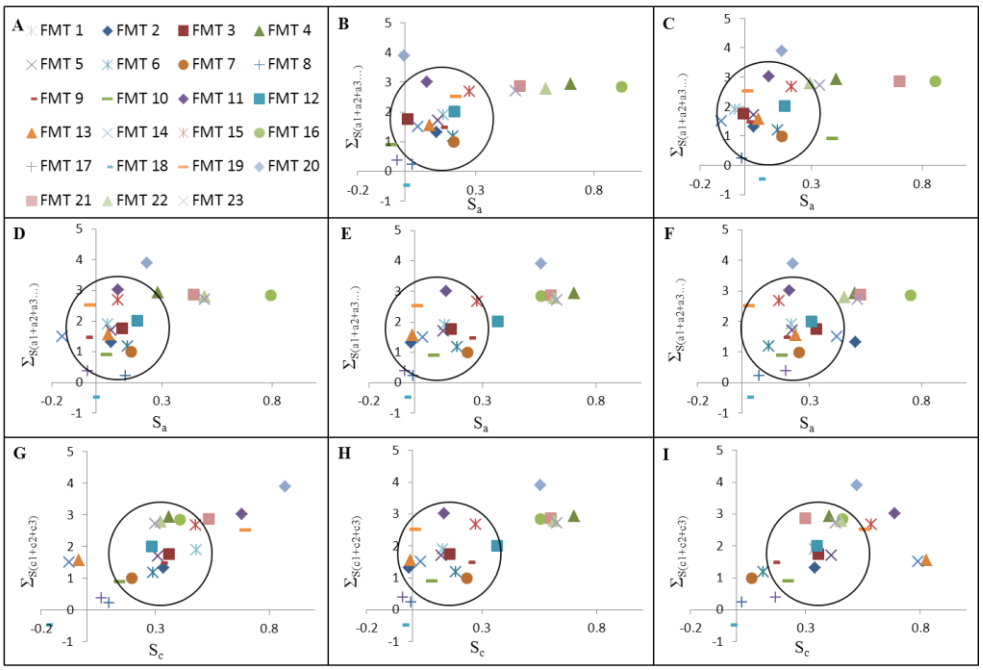

Figure 3. (**A**) Measured fragments of metallothionein. Graphical presentation of slopes affected by certain tested physical and chemical factors as (**B**) Temperature 10 °C; (**C**) Temperature 15 °C; (**D**) Temperature 25 °C; (**E**) Temperature 35 °C; (**F**) Temperature 45 °C; (**G**) Concentration 50 µM; (**H**) Concentration 100 µM; (**I**) Concentration 200 µM.

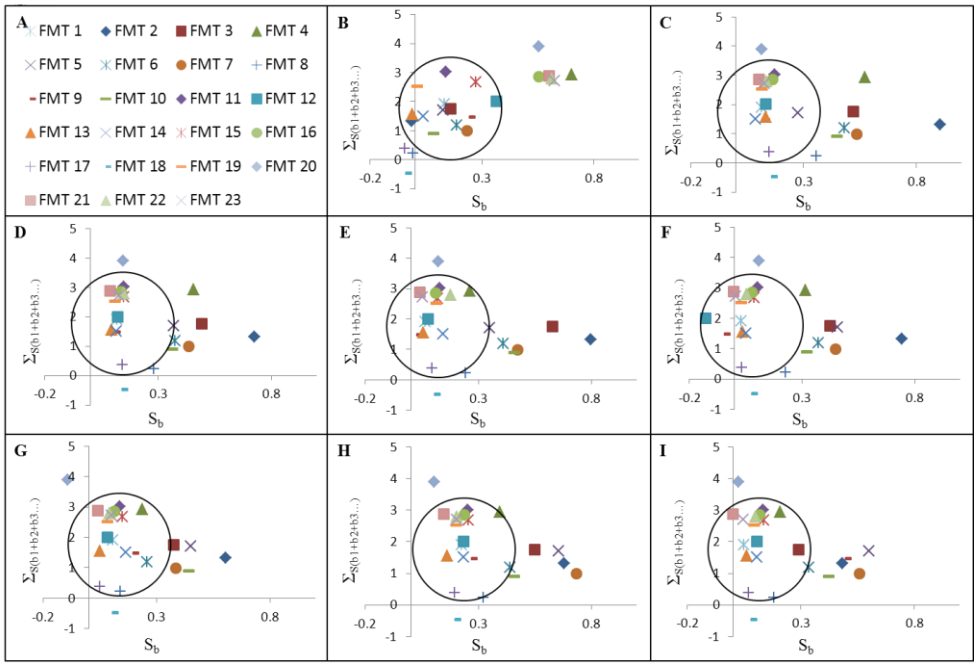

Figure 4. (**A**) Measured fragments of metallothionein. Graphical presentation of slopes affected by certain tested physical and chemical factors as (**B**) Time of interaction 1 h; (**C**) Time of interaction 2 h; (**D**) Time of interaction 3 h; (**E**) Time of interaction 4 h; (**F**) Time of interaction 5 h; (**G**) Time of interaction 6 h; (**H**) Time of interaction 7 h; (**I**) Time of interaction 8 h.

For the selection of only those conditions, under which there were recorded significant increased interaction, a graph with a radius obtained from the relationship Σ_{max}*0.3= 1.17 for y-axis was constructed for the median interval. On the x-axis, the value of the average median interval was $S_{(a)}$=0.16. Points located within the median interval were excluded as insignificant (2× RSD, reliability under 90). On the contrary, values outside the range of median values were found to have significant interactions associated with a diversity of structures of studied FMTs. The values of deviations on x-axis from the edge of the median were further summed on the amount that was interpreted as the total effect of temperature, concentration and interaction time and therefore gave us the interaction constant called IC_{FMT} according to equation No. 2. All fragments except FMT 1 had higher degree of the interaction, i.e. positive IC_{FMT}.

Equation No. 2: $IC_{FMT}= (S_a+S_b+S_c)$

3.4 Influence of aminoacid change on interaction constant

Due to high conservatism of FMT 2, all interactions were associated to this fragment as a percentage change (Fig. 5A). The highest values of IC_{FMT} were found for FMTs 18 and 20, where a marked change in non-neighbouring amino acids directly with cysteines could be observed. At FMT 18, there was found P in position 10 and at FMT 20, position 10 was occupied by V and, moreover, strongly conservative position 1 contained T instead of K. IC_{FMT} values of both mentioned fragments were for more than 100 % higher compared to other studied fragments. On the other hand, FMTs 2, 4, 16 had lower ability to interact with cisplatin despite the fact that there were still conservative amino acids S, S and P next to cysteines. For FMT 4 only there were conservative cysteine clusters surrounded by P instead of S, but the end of peptide was distinguished by substitution of N-terminal D for G, resulting in an overall increase in IC_{FMT} form more than 14 %. It was also observed the increase of IC_{FMT} of FMT 16 for 6 %, which was caused only by substitution of M for S in position No. 10.

Overall, at least conservative peptide FMT 21 of all tested peptides showed the lowest similarity to other tested FMTs. This was caused by replacing a conservative S with N next to the first cysteine cluster in position 3, followed by substitution of C for Y inside the second cysteine cluster in position 8 and finally by the substitution of S for V in position 10, resulting in an overall reduction of IC_{FMT} for more than 10 %. Other reported decreased levels of IC_{FMT} in the order of 25-37% were observed in FMTs 7, 8, 22 and 23. Structure of FMTs 7 and 8 was identical to FMT 2 with the exception of the aminoacid substation in position 6, which was neighboured to both cysteine clusters. Compared to the conservative sequence FMT 2, a mismatch of S for T in position 6 in the case of FMT 8 resulted in the reduction of IC_{FMT} for more than 20 % and a mismatch of S for A in position 6 in the case of FMT 7 caused a decrease in IC_{FMT} for more than 30 %. FMT 22 had aminoacids surrounding the cysteine cluster in positions 3, 6 and 9 as S, P and P, which caused a reduction of IC_{FMT} for more than 25 %. FMT 23 showed at least conservative arrangement (69.92%). In position 2, there were done substitutions of free for A, and of W for C in position 5, and of S for D in position 6, which resulted in the reduction of IC_{FMT} for more than 25 %.

The most significant reduction in the value of IC_{FMT} in the order of 50-100% was observed in all other studied FMTs as 17, 14, 3, 10, 13, 6, 5, 11, 19, 9, 12, 15 and 1, which were majority found within the median range. At FMTs 17, 6, 9 and 1, there was substitution in position 2 for D, E, D and in position 2 for P. The combination of location of P decreased IC_{FMT} mostly. At FMTs 14, 3, 13, 11, 19, 12 and 15, the substitution in position 10 for V, A, M, V, A, G or L was done. In addition to these changes, C was in position 3 at FMT 4, and M in position 10 at FMT 13.

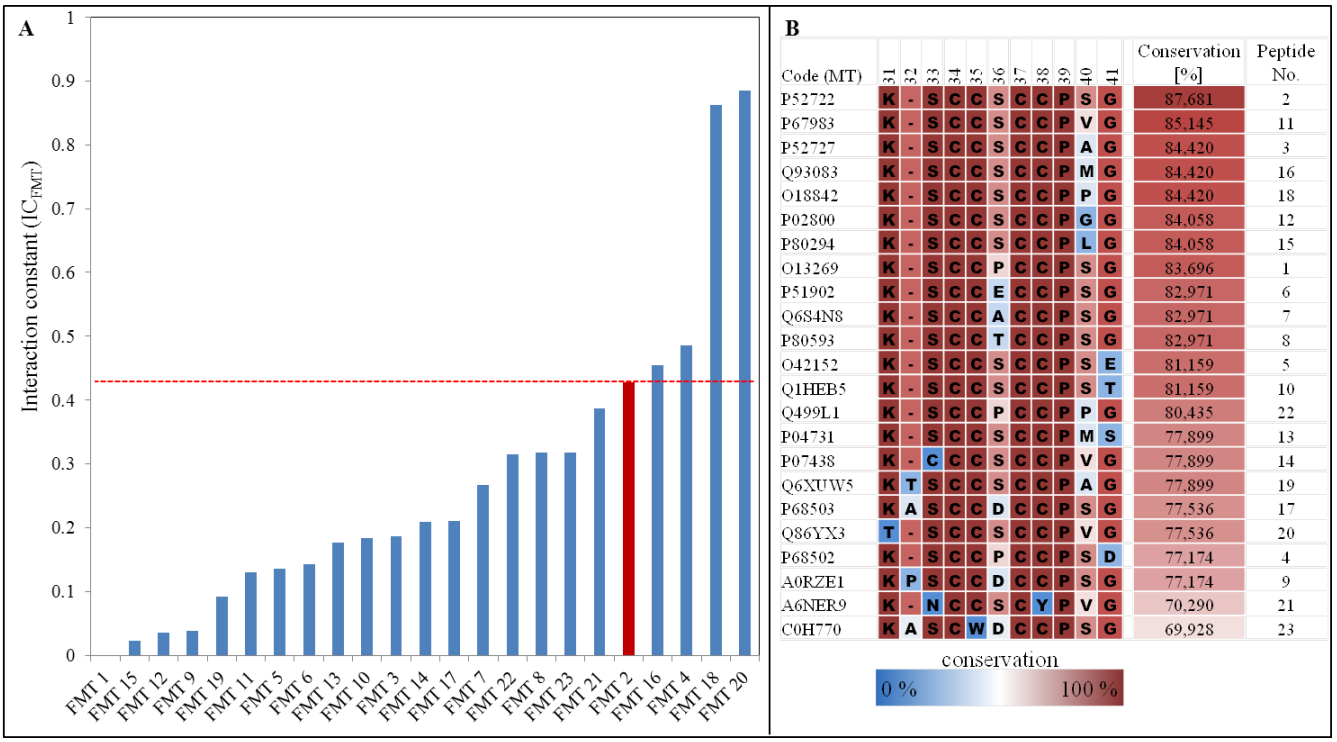

Figure 5. (**A**) Values of IC_{FMT} for all 23 studied metallothionein fragments resulting from the calculation based on the tested parameters (temperature, molar concentration, time of interaction). Value of the most conservative IC_{FMT} 2 (0.43) is highlighted in red. (**B**) Table where you can see the original MT code, amino acid sequence of FMT, which indicates the percentage of similarity in the conservative group and serial number of the peptide. Amino acids significantly affecting the level of interaction are highlighted in blue.

The insertion of these sulphur-containing amino acids at these positions resulted in the reduction of IC_{FMT} for more than 50 %. Moreover, FMT 19 had also changed aminoacid in position 2 to T, which resulted in the decrease in IC_{FMT} for more than 75 %. Compared to similar FMT 20, where K was in front of T and V instead of A in position 10, this was one of the most significant effects characterized by an overall decrease in IC_{FMT} for more than 190 %. The highest effect characterized by a total difference of 201 %, however, was inverse substitution of P in positions 6 and 10 at FMTs 18 and 1. At FMTs 10 and 5, substitution for T and E in position 11 resulted in decreased IC_{FMT} for more than 50 %.

The obtained results show that the greatest influence on the interaction of cisplatin with FMT have aminoacid changes in positions 1 and 10, which are distant by more than one position from the cysteine cluster, where quite significantly affects the overall location of the interaction of aminoacids P, T and V at FMTs 20 and 18. In comparison with these amino acids, aminoacid changes in P and D in positions 6 and 11 at FMT 4 and followed by the M substitution in position 10 at FMT 16 also influenced the interaction with cisplatin but much lower compared to P, T and V.

4. CONCLUSIONS

Metallothionein has been previously studied by electrochemical methods, which are utilizable for this purpose due to high content of cysteine in its structure. In terms of complex formation at the level of aminoacids it is advisable to study only a fragment of this protein [14]. As part of monitoring the effect of histidine, which is not too frequent, on the redox changes in the sequence of MT with the view of the possibility of increasing the coordination of metals was similar to our work. In that study, the authors used a different methodological approach (NMR and ICP-MS) [15], where NMR provides structural information and ICP-MS provides information on the quantity of the elements of the interest. Compared to this multi instrumental approach, our method combines structural and quantitative information. The suitability of electrochemical methods for the study of complex MT with metal has been demonstrated using cathodic stripping voltammetry [16], square wave voltammetry [17] or cyclic voltammetry [18-22]. In addition to these studies, we used FIA-ED method, which was chosen thanks to the experience from the previous studies of interactions between the thiol group of peptide and cisplatin [23,24]. In this study, it is shown in detail that the substitution of individual aminoacids in the peptide chain of protein markedly influence the interaction with cisplatin.

ACKNOWLEDGEMENTS
Financial support from the following projects CEITEC CZ.1.05/1.1.00/02.0068, CYTORES GA CR P301/10/0356, NANOSEMED GA AV KAN20813081, IGA IP23/2012 and by the project for conceptual development of research organization 00064203 is highly acknowledged. The authors wish to express their thanks to Nadezda Spackova for critical evaluation of the paper.

References

1. T. Boehm, J. Folkman, T. Browder and M. S. Oreilly, *Nature*, 390 (1997) 404.
2. W. Sakai, E. M. Swisher, B. Y. Karlan, M. K. Agarwal, J. Higgins, C. Friedman, E. Villegas, C. Jacquemont, D. J. Farrugia, F. J. Couch, N. Urban and T. Taniguchi, *Nature*, 451 (2008) 1116.
3. C. F. Higgins, *Nature*, 446 (2007) 749.
4. C. Sawyers, *Nature*, 432 (2004) 294.
5. D. Wang and S. J. Lippard, *Nat. Rev. Drug Discov.*, 4 (2005) 307.
6. U. M. Ohndorf, M. A. Rould, Q. He, C. O. Pabo and S. J. Lippard, *Nature*, 399 (1999) 708.
7. T. Eckschlager, V. Adam, J. Hrabeta, K. Figova and R. Kizek, *Curr. Protein Pept. Sci.*, 10 (2009) 360.

8. D. Dospivova, K. Smerkova, M. Ryvolova, D. Hynek, V. Adam, P. Kopel, M. Stiborova, T. Eckschlager, J. Hubalek and R. Kizek, *Int. J. Electrochem. Sci*., 7 (2012) 3072.
9. L. Krejcova, I. Fabrik, D. Hynek, S. Krizkova, J. Gumulec, M. Ryvolova, V. Adam, P. Babula, L. Trnkova, M. Stiborova, J. Hubalek, M. Masarik, H. Binkova, T. Eckschlager and R. Kizek, *Int. J. Electrochem. Sci.*, 7 (2012) 1767.
10. J. Sochor, D. Hynek, L. Krejcova, I. Fabrik, S. Krizkova, J. Gumulec, V. Adam, P. Babula, L. Trnkova, M. Stiborova, J. Hubalek, M. Masarik, H. Binkova, T. Eckschlager and R. Kizek, *Int. J. Electrochem. Sci.*, 7 (2012) 2136.
11. M. Capdevila, R. Bofill, O. Palacios and S. Atrian, *Coord. Chem. Rev*., 256 (2012) 46.
12. S. G. Bell and B. L. Vallee, *Chembiochem*, 10 (2009) 55.
13. P. Coyle, J. C. Philcox, L. C. Carey and A. M. Rofe, *Cell. Mol. Life Sci*., 59 (2002) 627.
14. J. Mendieta, J. Chivot, A. Munoz and A. R. Rodriquez, *Electroanalysis*, 7 (1995) 663.
15. C. A. Blindauer, M. T. Razi, D. J. Campopiano and P. J. Sadler, *J. Biol. Inorg. Chem*., 12 (2007) 393.
16. I. Sestakova and P. Mader, *Cell. Mol. Biol*., 46 (2000) 257.
17. O. Nieto and A. R. Rodriguez, *Bioelectrochem. Bioenerg*., 40 (1996) 215.
18. C. Harlyk, G. Bordin, O. Nieto and A. R. Rodriguez, *Electroanalysis*, 9 (1997) 608.
19. N. M. Marshall, D. K. Garner, T. D. Wilson, Y. G. Gao, H. Robinson, M. J. Nilges and Y. Lu, *Nature*, 462 (2009) 113.
20. V. Adam, I. Fabrik, T. Eckschlager, M. Stiborova, L. Trnkova and R. Kizek, *TRAC-Trends Anal. Chem.*, 29 (2010) 409.
21. V. Adam, J. Petrlova, J. Wang, T. Eckschlager, L. Trnkova and R. Kizek, *PLoS ONE*, 5 (2010) e11441.
22. P. Babula, M. Masarik, V. Adam, T. Eckschlager, M. Stiborova, L. Trnkova, H. Skutkova, I. Provaznik, J. Hubalek and R. Kizek, *Metallomics*, 4 (2012) 739.
23. O. Zitka, D. Huska, S. Krizkova, V. Adam, G. J. Chavis, L. Trnkova, A. Horna, J. Hubalek and R. Kizek, *Sensors*, 7 (2007) 1256.
24. O. Zitka, M. Kominkova, S. Skalickova, H. Skutkova, I. Provaznik, T. Eckschlager, M. Stiborova, V. Adam, L. Trnkova and R. Kizek, *Int. J. Electrochem. Sci.*, in press (2012)

5.2.2 Vědecký článek IV

Study of interaction between metallothionein and cdte quantum dots

Skalickova, S., Zitka, O., Nejdl, L., Krizkova, S., Sochor, J., Janu, L., Ryvolova, M., Hynek, D., Zidkova, J., Zidek, V., Adam, V. and Kizek, R.

Chromatographia, 2013, 0009-5893, 345-353

Podíl autora Skaličková S.: 50 % textové části práce a 70 % experimentální práce

Kvantové tečky (QDs) jsou fluoreskující polovodičové nanokrystaly. Jejich potencionální využití se nabízí v biologii a v analytické chemii jako organické fluorofory. Vynikají výjimečnými chemickými a fyzikálními vlastnostmi, které se uplatňují v konstrukci detekčních systému pro detekci iontů, bakterií, virů, nukleotidových sekvencí, proteinů a jiných analytů. Široké uplatnění existuje samozřejmě ve fluorescenční mikroskopii a *in vivo* zobrazování. Součástí QDs jsou ionty kovů jako je kadmium, selen, telur nebo zinek (Michalet, X., Pinaud, F. F. et al. 2005). QDs mohou být snadno navázány do struktury proteinů, což je hlavním parametrem sledování jejich toxicity v oblastech, kde by se QDs mohly uplatnit v *in vivo* zobrazovacích systémech. Toxicita je často způsobena jejich desintegrací na dobře rozpustné anorganické ionty, například kadmium. Řada studií prokázala, že stupeň toxicity QDs je těsně spjat s odlišnými vlastnostmi biologického systému jako je počet buněk, buněčný růst, apoptóza, morfologie buňky a její metabolická aktivita (Chen, Nan, He, Yao et al. 2012). Aby byla zajištěna stabilita QDs, musí být funkcionalizovány biomolekulami obsahujícími thiolovou skupinu, například cystein, merkaptopropionová kyselina, ale také i protein metalothionein, který je bohatý na cysteinové zbytky a vykazuje vysokou afinitu ke kadmiu (Huang, Deping, Geng, Fei et al. 2011).

Cílem této práce bylo navrhnout metodu pro sledování možných interakcí MT s QDs. Pro tento účel byly připraveny QDs s CdTe jádrem. Metalothionein, využitý v naší studii byl izolován z jater kadmiem přikrmovaných králíků, pomocí kapalinové chromatografie s UV detekcí. Účinnost izolace byla ověřena pomocí gelové elektroforézy, která prokázala přítomnost proteinu o přibližné molekulové hmotnosti,

jakou vykazuje metalothionein v izolované frakci. Pro studium interakce byla využita směs obou komponent MT (3,6 μM a CdTE QDs QDs (0, 0.34, 0.68, 1.02, 1.36, 1.7, 2.04 a 2.47 μM). Tato směs byla spektrofotometricky sledována při vlnových délkách 260 a 505 nm. Stejná směs byla také studována pomocí diferenční pulzní voltametrie s Brdičkovou reakcí, speciálně vyvinutou pro detekci MT, která podpořila získaná data. Následně jsme využili kapalinovou chromatografii pro purifikaci QDs-MT konjugátů. Výsledkem bylo získání různých chromatogramů pro 1) Apo-MT, 2) CdTe QDs a 3) MT-QD- komplexu, jehož formace byla potvrzena pomocí fluorescenční spektrofotometrie, která potvrdila vznik tohoto komplexu. V tomto experimentu se nám podařilo vyvinout metodu, která je vhodná, díky vysoké afinitě metallothioneinu ke kademnatým iontům, pro sledování této interakce. Tato metoda nabývá významu z pohledu interakčních studií anorganických nanočástic s biomolekulami jako je DNA a kov-vaznými proteiny pro využití v medicíně.

Chromatographia (2013) 76:345–353
DOI 10.1007/s10337-013-2418-6

ORIGINAL

Study of Interaction between Metallothionein and CdTe Quantum Dots

Sylvie Skalickova · Ondrej Zitka · Lukas Nejdl · Sona Krizkova · Jiri Sochor · Libor Janu · Marketa Ryvolova · David Hynek · Jarmila Zidkova · Vaclav Zidek · Vojtech Adam · Rene Kizek

Received: 19 July 2012 / Revised: 15 January 2013 / Accepted: 31 January 2013 / Published online: 16 February 2013

Abstract Quantum dots (QDs) belong to a new class of fluorescent agent for biochemical, medicinal or other purposes. However, QDs based on cadmium or other metals can be risky for an organism. As one of the mechanism how to detoxify cadmium-based QDs expression of metallothioneins (MT) can be considered. Due to high affinity of metallothionein to cadmium(II) ions, we attempted to develop an approach for studying of possible interaction with QDs. We prepared QDs with CdTe core and studied the interaction with MT, which we isolated from livers of Cd-administered rabbits. To study the interaction, we used the mixture of both components MT (3.6 μM): CdTe QDs (0, 0.34, 0.68, 1.02, 1.36, 1.7, 2.04 and 2.47 μM). The mixtures were studied by spectrophotometry within the range from 200 to 750 nm with detected maxima at 260 and 505 nm. Same mixtures were also analysed by differential pulse voltammetry Brdicka reaction, which supported data from spectrophotometry. Subsequently, we used fast protein liquid chromatography for purification of protein–quantum dot conjugates. We obtained the different chromatograms for (1) Apo MT, (2) CdTe QDs and (3) MT–QD complex. We also collected the fractions and subsequently analysed them on the content of Cd and MT, which confirmed the formation of CdTe QDs–MT complex.

Keywords Fast protein liquid chromatography · Brdicka reaction · Differential pulse voltammetry · Fluorimetry · Spectrophotometry · Separation of quantum dots · ApoMT

Published in the special paper collection "Advances in Chromatography and Electrophoresis and Chiranal 2012" with guest editor Jan Petr.

S. Skalickova · O. Zitka · L. Nejdl · S. Krizkova · J. Sochor · L. Janu · M. Ryvolova · D. Hynek · V. Adam · R. Kizek (✉)
Department of Chemistry and Biochemistry, Faculty of Agronomy, Mendel University in Brno, Zemedelska 1, 613 00 Brno, Czech Republic
e-mail: kizek@sci.muni.cz

O. Zitka · S. Krizkova · J. Sochor · M. Ryvolova · D. Hynek · V. Adam · R. Kizek
Central European Institute of Technology, Brno University of Technology, Technicka 3058/10, 616 00 Brno, Czech Republic

J. Zidkova · V. Zidek
Department of Biochemistry and Microbiology, Institute of Chemical Technology, Technicka 3, 166 28 Prague, Czech Republic

Introduction

Quantum dots (QDs) light-emitting particles on the nanometre scale are emerging as a new class of fluorescent agent for in vivo imaging [1]. QDs often consist of cadmium(II) ions and/or ions of other metal such as selenium, tellurium or zinc [2] and can be used for fluorescent labelling of biomolecules [3, 4]. In addition, these particles can be modified by a recognition molecule such as an antibody and then, QD–antibody complex can be used for identification and visualisation of necrotic lesions or tumour cells [5]. Wang et al. [6] showed that the QDs could be bound by proteins in an organism very easily. However, toxicity of QDs must be considered. Their toxicity is predominantly caused by their disintegration to well-soluble inorganic ions, mostly cadmium(II) [7]. It has been demonstrated that the degree of QDs toxicity is closely connected with different parameters such as cell number, cell growth, apoptosis, cellular morphology or metabolic activity change of targeted tissue [8]. Thus, functionalisation of their surface

by thiol group(s)-containing compounds, such as cysteine, mercaptopropionic acid and glutathione is commonly applied [9]. In spite of this fact, studying of interactions of some protective proteins with QDs is of great interest.

Metallothioneins (MT) are a group of proteins rich in cysteine [10], which are able to bind metal ions especially essential zinc or toxic cadmium [11]. It is not surprising that metallothionein is biosynthesised due to stress caused by heavy metals, respectively, in the response to entering of a metal ion into the intracellular space. This process is realised via binding the metal ion on metal transcription factor-1 (MTF-1), which is zinc finger of the size of 70–80 kDa. MTF-1 subsequently binds to metal response element (MRE) localised in the promoter of gene for metallothionein [12–14], and this process activates transcription of this gene. The process itself is regulated by some factors such as metal-transcription inhibitor (MTI), which inhibits MT transcription by binding to metal responsive element (MRE). After the entry of metal ions into a cell, these ions bind to MTI, and this leads to the change in the conformation and dissociation of MTI from MRE. Therefore, binding site is free and ready for the interaction with MTF-1 [13]. Some studies show that the presence of other heavy-metal ions (not only zinc) may activate other redox-sensitive transcription factors such as NF-kappaB, AP-1and p53 [15].

From the structural point of view, metallothionein is a low-molecular protein of the size of 6–7 kDa of which tertiary structure is based on the presence of two domains, which form cysteine clusters for binding metal ions [16]. Due to the fact that MT contains almost no aromatic amino acids and due to its size, MT forms no secondary structures, thus, it is very difficult to apply analytical methods commonly used in proteomics as gel electrophoresis and mass spectrometry [17–19]. Metallothionein and similar cysteine rich proteins have been studied using the separation methods of affinity chromatography [20], reversed-phase chromatography [21], high-performance liquid chromatography with mass detection [22] and capillary electrophoresis [23–26]. Due to the high content of electrochemically active thiol groups in the structure of MT, electrochemical techniques represent the most sensitive analytical technique for MT quantification [10, 27–30].

Due to high affinity of metallothionein to cadmium(II) ions, in this study, we aim on developing an approach for studying of possible interactions between MT and cadmium-based quantum dots prepared according to [31]. Primarily, we isolated metallothionein from rabbit liver and used it as chelating agent for CdTe QDs. Further, we study the complex formation between MT and CdTe QDs. For that purpose, spectrophotometric, fluorimetric and differential pulse voltammetry were used. Moreover, fast protein liquid chromatography [32–34] was used for CdTe QDs–MT complex observation.

Experimental Section

Chemicals

Trizma base, HCl, NaCl, BSA, TCEP, EDTA, $CdCl_2$, Na_2TeO_3, trisodium citrate dihydrate, mercaptopropionic acid, $Co(NH_3)_6Cl_3$, NH_3(aq) and NH_4Cl of ACS purity used were purchased from Sigma Aldrich Chemical Corp. (Sigma-Aldrich, USA), unless noted otherwise. Deionised water underwent demineralisation by reverse osmosis using the instrument Aqua Osmotic 02 (Aqua Osmotic, Tisnov, Czech Republic) followed by further purification using Millipore RG (Millipore Corp., USA, 18 MΩ)—MiliQ water. The pH was measured using WTW inoLab pH meter (Weilheim, Germany).

QDs Synthesis

QDs were prepared according to Duan et al. [31]. Cadmium chloride solution ($CdCl_2$, 0.04 M, 4 mL) was diluted to 42 mL with ultrapure water, and then trisodium citrate dihydrate (100 mg), Na_2TeO_3 (0.01 M, 4 mL), MPA (119 mg), and $NaBH_4$ (50 mg) were added successively under magnetic stirring. The molar ratio of Cd^{2+}/MPA/Te was 1:7:0.25. 10 mL of the resulting CdTe precursor was put into a Teflon vessel. CdTe QDs were prepared at 95 °C for 10 min under microwave irradiation (400 W, Multiwave 3000, Anton-Paar GmbH, Austria). After microwave irradiation, the mixture was cooled to 50 °C and the CdTe QDs sample was obtained. Re-purification of CdTe QDs was carried out using isopropanol condensing. The CdTe QDs was mixed with isopropanol in ratio 1:2 and then centrifuged for 10 min at 25,000 rpm (Eppendorf centrifuge 5417R). Pellet was dissolved into 500 µL with Tris Buffer (pH 8.5).

Experimental Animals and Preparation of Samples for MT Isolation

The males of New Zealand rabbits weighing 3.0–3.5 kg were kept in separate cages on regular pelleted laboratory chow (MaK-Bergman, Kocanda, Prague, Czech Republic) and allowed free access to drinking water. Rabbits were given the intraperitoneal injection of 10 mg of $CdCl_2$/kg of weight (Sigma-Aldrich) in three equal doses (day 1, day 3 and day 5). In the aforementioned day intervals, animals were anaesthetised with Ketamine: 30 mg/kg and Xylazine: 3 mg/kg, (Vétoquinol Biovet, France). Animals were then bled out by heart puncture, individual livers were collected, weighed and immediately frozen on dry ice.

Preparation of Sample for MT Isolation

Amount of 2 g of defrosted rabbit liver was homogenised on ice using Ultra-turrax T8 (Scholler instruments,

Germany) in 8 mL of 10 mM Tris–HCl buffer (pH 8.6). The obtained sample was subsequently vortexed (Vortex Genuie, Germany) and centrifuged (Universal 320, Hettich Zentrifugen, Germany) at 5,000 rpm (30 min, 4 °C). Taken supernatant was again centrifuged (Eppendorf centrifuge 5417R) in 1.5-mL micro test tube at 4 °C (25,000 rpm, 30 min). The supernatant was subsequently heated in thermomixer (Eppendorf thermomixer comfort, Germany) at 99 °C (10 min) and centrifuged (Eppendorf centrifuge 5417R, Germany) in 1.5-mL micro test tube at 4 °C (25,000 rpm, 30 min). Sample prepared like this was used for isolation of MT.

Fast Protein Liquid Chromatography for Isolation of MT

Fast protein liquid chromatography (FPLC) was purchased from Biologic DuoFlow system (Biorad, USA), which consisted of two chromatographic pumps for the application of elution buffers, a gel-filtration column (HiLoad 26/60, 75 PG, GE Healthcare, Sweden), an injection valve with 2-mL sample loop, an UV–VIS detector and an automated fraction collector. Solution of 150 mM NaCl in 10 mM Tris–HCl buffer (pH 8.6) was used as a mobile phase. Flow of the mobile phase was set to 4 mL/min. Isocratic elution was used for metallothionein separation. Column was washed for 60 min by mobile phase prior to every separation.

Process of metallothionein isolation from rabbit liver after Cd(II) application is shown in (Fig. 1a). Fraction containing metallothionein was collected in elution volume of 240 mL. Signal of metallothionein was well evident due to binding of Cd(II) ions into protein structure, which caused change in the absorbance measured at 254 nm [35]. Dialysis and lyophilisation of corresponding fraction were also carried out in deionised water.

SDS PAGE for MT Assay

The electrophoresis of the fraction containing MT (Fig. 1b) was performed using Maxigel apparatus (Biometr, Germany). First 15 % (w/v) running, then 5 % (w/v) stacking gel was poured. The gels were prepared from 30 % (w/v) acrylamide stock solution with 1 % (w/v) bisacrylamide. The polymerisation of the running or stacking gels was carried out at room temperature for 45 min. Prior to analysis, the samples were mixed with non-reduction sample buffer in a 2:1 ratio. The samples were incubated at 93 °C for 3 min, and the sample was loaded onto a gel. For the determination of the molecular mass, the protein ladder "Precision plus protein standards" from Bio-Rad was used. The electrophoresis was run at 150 V for 1 h at room temperature (Power Basic, Bio-Rad) in Tris–glycine buffer (0.025 M Trizma-base, 0.19 M glycine, and 3.5 mM SDS, pH = 8.3). Then, the gels were stained with Coomassie blue and consequently with silver. The procedure of rapid Coomassie blue staining was adopted from Wong et al. [36], silver staining was performed according to Krizkova et al. [37] with omitting the fixation (1.1 % (v/v) acetic acid, 6.4 % (v/v) methanol, and 0.37 % (v/v) formaldehyde) and first two washing steps (50 % (v/v) methanol).

Differential Pulse Voltammetry for Cadmium(II) Ions Determination

Determination of cadmium(II) ions were performed with 797 VA Stand instrument connected to 889 IC Sample Center (Metrohm, Switze rland). The analyser (797 VA Computrace, Metrohm, Switzerland) employs a conventional three-electrode configuration with a hanging mercury drop electrode (HMDE) working electrode: 0.4 mm^2, Ag/AgCl/3MKCl as reference electrode, and a platinum auxiliary electrode. A sample changer (Metrohm 889 IC Sample

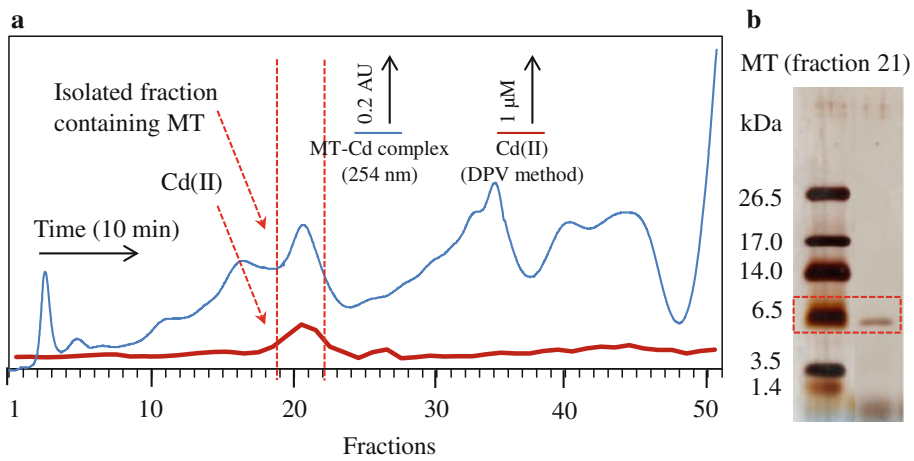

Fig. 1 **a** FPLC chromatogram of real sample of extract from rabbit liver treated with Cd(II) In overlay with determined concentration of cadmium in collected fractions. In the position of MT peak, cadmium(II) was 0.80 µM (determined by differential pulse voltammetry). **b** Electrophoreogram from SDS PAGE analysis of fractions with MT

Center) performs the sequential analysis of 96 samples in plastic test tubes. Differential pulse voltammetric measurements were carried out under the following parameters: deoxygenating with argon 120 s; start potential −0.9 V; end potential −0.3 V; deposition potential −0.9 V; accumulation time 800 s; pulse amplitude 0.025 V; pulse time 0.05 s; step potential 2 mV; time of step potential 0.2 s; volume of injected sample 20 μL; cell was filled with 1,980 μL of electrolyte (0.2 M acetate buffer pH 5.0).

Differential Pulse Voltammetry Brdicka Reaction for MT Determination

Differential pulse voltammetric measurements were performed with 747 VA Stand instrument connected to 693 VA Processor and 695 Autosampler (Metrohm, Switzerland), using a standard cell with three electrodes and cooled sample holder and measurement cell to 4 °C by Julabo F25 (JULABO, Germany). A hanging mercury drop electrode (HMDE) with a drop area of 0.4 mm^2 was the working electrode. An Ag/AgCl/3 M KCl electrode was the reference and platinum electrode was auxiliary. For data processing, VA Database 2.2 by Metrohm CH was employed. The analysed samples were deoxygenated prior to measurements by purging with argon (99.999 %) saturated with water for 120 s. Brdicka supporting electrolyte containing 1 mM $Co(NH_3)_6Cl_3$ and 1 M ammonia buffer (NH_3(aq) + NH_4Cl, pH = 9.6) was used. The supporting electrolyte was exchanged after each analysis. The parameters of the measurement were as follows: initial potential of −0.7 V, end potential of −1.75 V, modulation time 0.057 s, time interval 0.2 s, step potential 2 mV, modulation amplitude −250 mV, E_{ads} = 0 V, volume of injected sample: 25 μL, volume of measurement cell 2 mL (25 μL of sample + 1,975 μL Brdicka solution).

UV–VIS Spectrophotometry

An UV–VIS spectrophotometer Specord 210 (Analytik Jena , Germany) was used for spectrophotometric analyses. This apparatus was equipped by movable carousel with eight positions for cuvettes. Quartz cuvettes Microcuvette (1 cm, total volume of 1.5 mL, Kartell, Italy) were used for the analyses. Carousel was tempered to required temperature by a flow thermostat JULABO F12/ED (JULABO, Germany), where distilled water serves as a medium. All analyses were carried out at 25 °C. The range of wavelengths for the measurement was 200–750 nm. As a blank, we used Tris buffer (pH 7.5) with 150 mM NaCl.

Fluorescence Measurement

Fluorescence spectra were acquired by multifunctional microplate reader Tecan Infinite 200 PRO (TECAN, Switzerland). 350 nm was used as an excitation wavelength and the fluorescence scan was measured within the range from 400 to 750 nm per 2-nm steps. Each intensity value is an average of three measurements. The detector gain was set to 100. The sample (50 μL) was placed in transparent 96 well microplate with flat bottom by Nunc (Thermo Scientific, USA). All measurements were performed at 25 °C controlled by Tecan Infinite 200 PRO (TECAN, Switzerland). As a blank, we used Tris buffer (pH = 7.5) with 150 mM NaCl.

Results and Discussion

Interaction between MT and CdTe QDs was investigated using the multi-instrumental approach. MT was isolated using fast protein liquid chromatography from the homogenate of liver of rabbits treated with cadmium(II) ions according to Demuynck et al. [35]. FPL chromatogram is shown in Fig. 1a. The presence of MT was verified by SDS-PAGE (Fig. 1b). CdTe QDs were prepared according to Duan et al. [31]. Prepared CdTe QDs were further characterised by differential pulse voltammetry (DPV), where concentration of cadmium(II) ions was determined [38–42]. Interaction between MT and CdTe QDs was primarily characterised using UV–VIS spectrophotometry according to [10] and subsequently by fluorimetry and differential pulse voltammetry Brdicka reaction. Finally, size exclusion separation of MT–CdTe QDs complex, where QDs, MT and Cd(II) were determined, was carried out.

Cd Content in the Prepared CdTe QDs

Quantum dots with CdTe core were prepared according to protocol mentioned in "Experimental Section" and the content of cadmium was determined by DPV to quantify prepared QDs. Redox signals of cadmium(II) ions were detected at −0.64 V. Parameters of calibration dependence were as follows: $y = 1.795x$, $R^2 = 0.9996$, $n = 5$ (R.S.D. 3.1 %). Using DPV, method it was determined that prepared stock solution of CdTe QDs contained 68 ± 2 μM ($n = 5$) of cadmium(II) ions.

Spectrophotometry of MT Interacted with CdTe QDs

For verification of the formation of MT–CdTe QDs complex the effect of addition of QDs to MT, which was isolated according to the protocol mentioned in "Experimental Section", was investigated. Firstly, volume of 60 μL of MT (3.6 μM) was mixed with 120 μL of phosphate buffer (pH 7.5, 20 mM). Subsequently, addition of CdTe QDs (68 μM, individual step 1 μL) was carried out. Final concentration of MT in this mixture was 1.2 μM and final concentration of

CdTe QDs was 2.64 μM. Set of ten samples was prepared like this. One sample (1) represented only MT (without QDs addition) at a concentration of 1.2 μM, next sample (2) contained MT in combination with 0.34 μM CdTe QDs, and next samples had increasing concentrations of QDs—0.34, 0.68, 1.02, 1.36, 1.7, 2.04, and 2.47 μM. Total volume of sample, which was applied into cuvette, was always 180 μL. Spectrum within in the range from 200 to 350 nm in 5-min intervals for 30 min was analysed after the individual additions of QDs. It clearly follows from the obtained results that the applications of QDs to MT lead to the increase of absorbance at three wavelengths as 260, 310 and 510 nm (Fig. 2a). Maximum *I* detected at 260 nm was related to MT–QDs complex I, and the second maximum related to MT–QDs complex II was observed at 310 nm, which is in agreement with the previously published results [23], where the increase of absorbance at 240–260 nm as a result of origination of MT–Cd(II) was observed. Addition of CdTe QDs led to the almost linear increase in absorbance for both maxima corresponding to complex I and II, respectively, to complexes of MT (Fig. 2b). The increase of absorbance at 510 nm was caused by CdTe QDs themselves. This fact is well evident in the record of analysis of CdTe QDs at identical concentration without MT presence (Fig. 2a).

Electrochemical Study of CdTe QD–MT Complex

Interaction between CdTe QDs and MT was further monitored using DPV Brdicka reaction. This reaction belongs to the catalytic processes, where nascent signal is influenced by the formation of complexes between analyte with cobalt(III) ions [43]. CdTe QDs complexes with MT gave DP voltammograms, which are shown in Fig. 3a. The voltammograms contain five characteristic signals. RS_2Co, Cat1 and Cat2 are signals associated with MT itself, which have been described in our previous papers [10, 30, 44–46]. Signals X and Y can be related to the interaction between CdTe QDs with the electrolyte and MT. Addition of CdTe QDs leads to the vanishing of signal X and shift of signal Y towards more positive potentials (from −1.05 to −0.98 V). Moreover, signals X and Y formed one composed signal, which narrows with the increasing concentration of CdTe QDs. More detailed description of these processes will be published elsewhere. It follows from the results shown in Fig. 3b that the addition of CdTe QDs to MT causes decrease in catalytic signal Cat2. As it was described in the previous subchapter, the increasing amount of CdTe QDs (0.34, 0.68, 1.02, 1.36, 1.7, 2.04, 2.47, 2.72, 3.06 and 3.4 μM) was gradually added to the 3.4 μM solution of

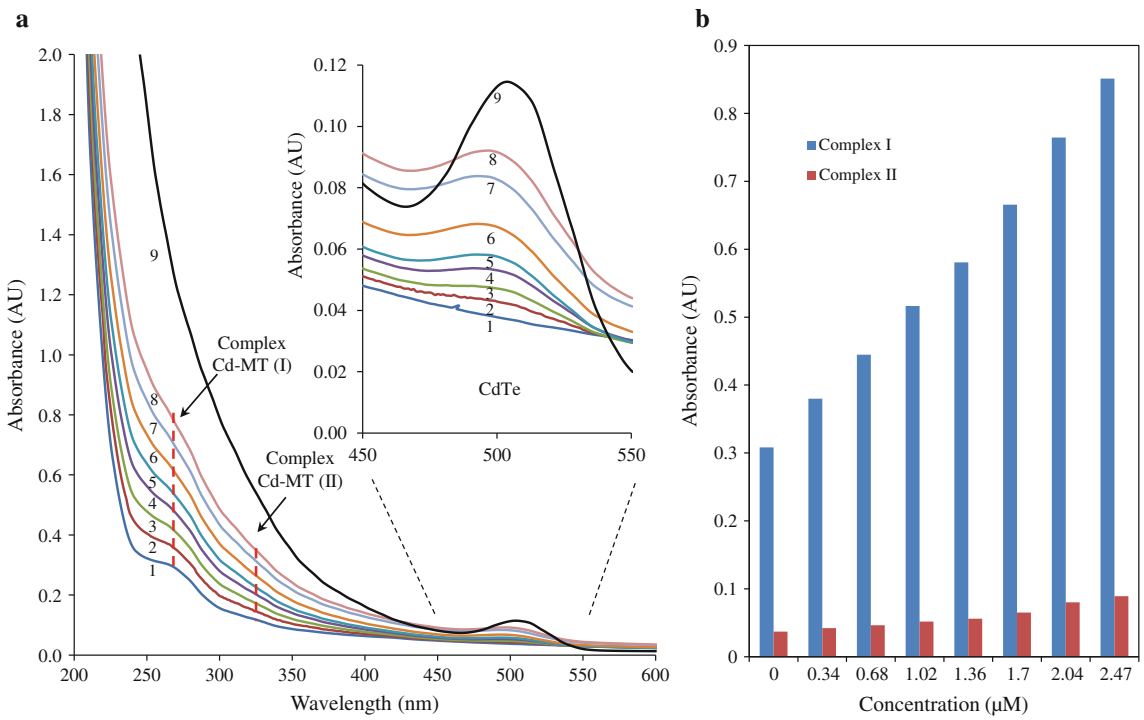

Fig. 2 **a** Overlay of absorption spectra obtained within the range from 200 to 600 nm for mixture of MT (1–1.2 μM), QDs (2–0.34; 3–0.68; 4–1.02; 5–1.36; 6–1.70; 7–2.04; 8–2.47;) and CdTe QDs (9–2.5 μM). Well observable complexes I and II were detected at 254 nm and 310 nm. Detail of spectra maxima of QDs (CdTe) is shown in inset (450–550 nm). **b** The increasing absorbance of complexes I and II after an addition of QDs into MT

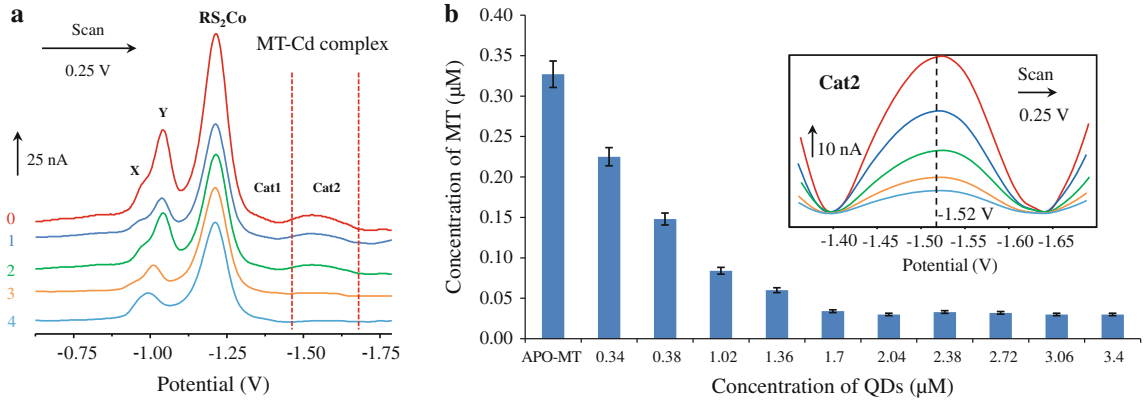

Fig. 3 **a** DP voltammogram of complex MT–CdTe measured in the presence of Brdicka solution. Five various additions of QDs (0.34–34 μM) was mixed with MT solution—voltammogram 0–4. **b** The influence of QDs addition to measured Cat2 MT signal. The parameters of the measurement were as follows: initial potential of 0.75 V, end potential of −1.75 V, modulation time 0.057 s, time interval 0.2 s, step potential 2 mV, modulation amplitude −250 mV, $E_{ads} = 0$ V, volume of injected sample: 25 μL, volume of measurement cell 2 mL (25 μL of sample + 1,975 μL Brdicka solution)

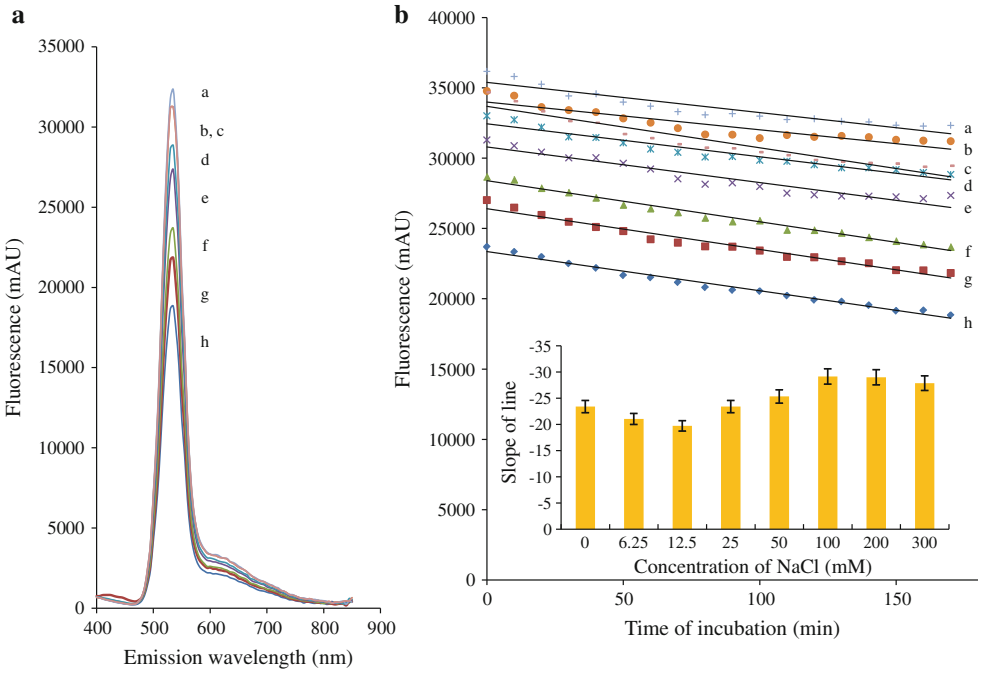

Fig. 4 **a** Emission spectra of QDs (CdTe 3.4 μM) after 3 h under applied concentrations of NaCl (a–0; b, c–12.5, 6.25; d–25; e–50; f–100; g–200; h–300 mM NaCl). **b** Influence of NaCl (0–300 mM) during time dependent measurement (0–1,800 min) on QDs (CdTe 17 μM) signal at 535 nm (excitation at 350 nm); in inset: the slope development owing to decrease of signal is shown

MT. Cat2 signal was decreased for more than 85 % compared to MT itself after the addition of 1.36 μM of CdTe QDs. However, further decrease of Cat2 signal was not observable with the increasing CdTe QDs concentrations (inset in Fig. 3b), which can be related to the saturation of MT moieties for metal interactions by QDs.

Quenching of QDs Emission by NaCl

Further, we aimed our attention on the isolation of QDs–MT complexes. Stability of QDs and their ability to emit radiation after excitation in the higher NaCl concentrations, which was necessary for effective separation of QD–MT using FPLC, was investigated by fluorimetry. Solution of NaCl (0, 6, 12, 25, 50, 100, 200 and 300 mM) was added to 3.4 μM solution of CdTe QDs in Tris buffer. Then, we performed time-dependent fluorimetric analysis for 3 h with 10-min steps. As it is obvious from the obtained results, the increasing concentration of NaCl and time of interaction lead to the decrease of fluorescence of CdTe QDs (emission at 535 nm). The most significant reduction of the emission was detected at the highest applied NaCl concentration (300 mM) as 45 % after 3 h of incubation (Fig. 4a). For the evaluation of the trend of the reduction of the emission, the obtained dependences were plotted with linear lines (Fig. 4b). The least sharp decrease was detected

in the case of 6.25 and 12.5 mM NaCl. On the other hand, the sharpest increase was detected at 100 and 200 mM (in inset Fig. 4b). These results give evidence about the possible effect of ionic strength on CdTe QDs fluorescence quenching. It is necessary to apply higher ionic strength (100–200 mM NaCl) for the size exclusion separation, which was most suitable for the separation/characterisation of MT–QD complex. This fact is based on the necessity to eliminate possible non-specific interactions and other electrostatic and hydrophobic interactions. On the other hand, lower recovery rate must be carefully considered in the case like separated CdTe QDs. The decrease of emission after 2 h is for about 30 % in the case of 150 mM concentration, which must be taken into account as we discussed above.

Quenching of QDs Emission by MT Interaction

Due to the decrease of electrochemical signal of MT observed in QD–MT complex studied using the Brdicka reaction, we decided to determine the emission of CdTe QDs complex with MT. We carried out a time-dependent measurement of QDs emission within the range from 400 to 850 nm under the excitation of 350 nm for individual MT additions (0.43–1.7 μM) to CdTe QDs (1.7 μM) in the presence of Tris buffer (pH = 7.5). The results obtained are shown in Fig. 5a. It clearly follows from the obtained results that additions of 0.43 and 0.64 μM of MT did not influence the intensity of emission. However, addition of 0.85 μM of MT led to the decrease of the intensity of the emission by 20 % during 120 min of incubation. Higher concentrations as 1.28 and 1.7 μM of MT caused emission decrease almost immediately by 60 %, respectively, 90 % with only minimal progression during 120-min-long incubation. In general, change of the emission intensity during incubation was minimal (up to 10 %) in all applied MT concentrations. These results indicate that the complex between MT and CdTe is formed rapidly (already in the time 0) and is stable for 120 min at least. The obtained slopes of linear regression characterise the decrease in emission with the increasing MT concentration with the linearity of $R^2 = 0.8874$ (Fig. 5b).

Separation of QD–MT Complex Using FPLC

For the verification of the formation of MT–QDs complex as well as for separation of this complex, we performed fast protein liquid chromatography with the application of Sephadex FPLC column (HiLoad 26/60, 75 PG, GE Healthcare, Sweden). For the monitoring of complex formation, mixture of 1.7 μM MT and 1.7 μM CdTe QDs was prepared. Volume of sample applied into system was 1 mL. Visible spectra detection of CdTe QDs was performed at 505 nm due to detection of CdTe QDs themselves. Fractions were collected during the whole separation (2 mL for 70 min). In addition to actual absorbance (505 nm) monitored behind the output of column, fractions were subjected to analysis of Cd(II) content and also MT content using the Brdicka's reaction (Fig. 6c). Obtained chromatogram (VIS detection) shows two distinct signals (signal *a* and signal *b*), where signal *a* represents probably a formed complex of QD and MT and signal *b* represents CdTe QDs. Application of only QDs leads to the formation of signal in the same position as signal *b* (Fig. 6b). Signal of metallothionein was observed in the same position as signal *a* (Fig. 6a). Application of Cd(II) ions did not affect the position of both signals as well as the formation of "new" signal. This presumption was supported by the determination of MT in very low concentration (0.2 μM) in the elution time of signal *a*. This fact

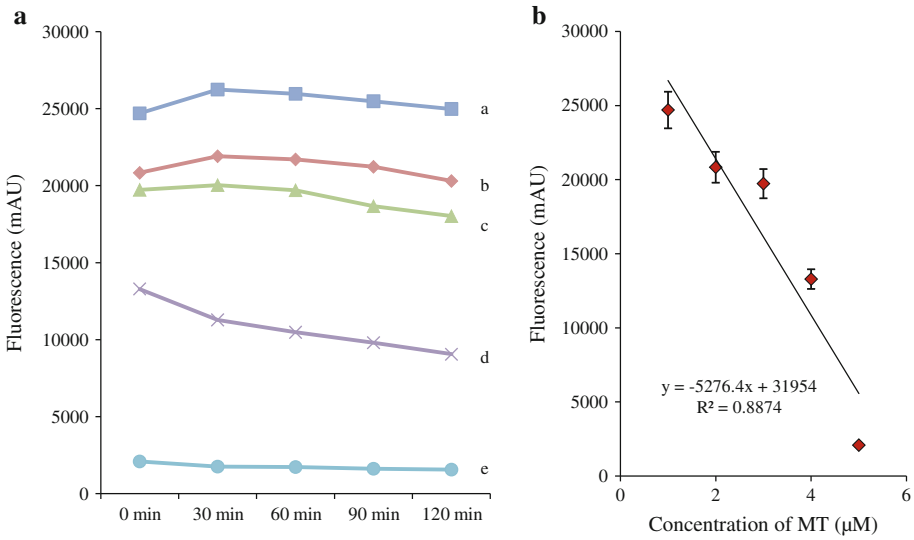

Fig. 5 **a** The influence of addition of apoMT (a–0.43; b–0.64; c–0.85; d–1.28; e–1.70 μM) on QDs (CdTe 1.7 μM) fluorescence at 535 nm (excitation at 350 nm) during time dependent measurement (0–120 min). **b** Calibration curve of addition of apoMT to QDs

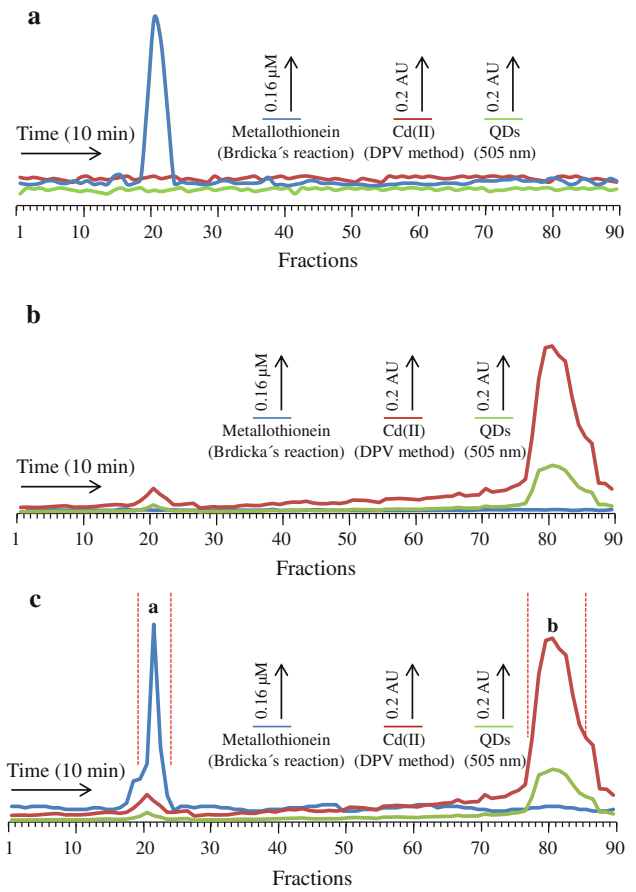

Fig. 6 Chromatogram of MT (1.7 µM) + QDs (1.7 µM) mixture separated by FPLC system and recorded at 505 nm (*green line*). Collected fractions (2 mL) were than analysed by DPV method for Cd content determination (*red line*) and by Brdicka's method for MT content determination (*blue line*) where **a** is analysis of apoMT, **b** is analysis of QDs, and **c** is analysis of the mixture. All measurements were carried out with Sephadex FPLC column (HiLoad 26/60, 75 PG, GE Healthcare, Sweden)

corresponds to the finding introduced in "Experimental Animals and Preparation of Samples for MT Isolation", because, in the case of complex, the signal is reduced by almost 85 %. Observed signal *a* representing complex of MT and QD is eluted 40 min earlier than CdTe QDs represented by signal *b* at applied flow rate of 4 mL/min.

Conclusions

Interaction of inorganic-based nanoparticles with biomolecules including DNA and proteins can be used for diagnosis and treatment purposes in medicine [47–49]. Therefore, there is a need for hyphenating of analytical methods using QDs for this purpose. In this study, we verified the formation of MT–QDs complex by the use of spectrophotometric and fluorimetric methods with subsequent separation using FPLC method. Considering that role of MT in cancerogenesis is discussed [19, 50–57], these results could be considered as a base for some imaging technologies for MT in vivo visualisation.

Acknowledgments Financial support from the following projects IGA TP 6/2012, NANIMEL GACR 102/08/1546, CEITEC CZ.1.05/1.1.00/02.0068 and IAA600110902 is highly acknowledged. The authors thank Pavel Kopel for the technical support.

References

1. Gao XH, Yang LL, Petros JA, Marshal FF, Simons JW, Nie SM (2005) Curr Opin Biotechnol 16:63–72
2. Michalet X, Pinaud FF, Bentolila LA, Tsay JM, Doose S, Li JJ, Sundaresan G, Wu AM, Gambhir SS, Weiss S (2005) Science 307:538–544
3. Wang F, Tan WB, Zhang Y, Fan XP, Wang MQ (2006) Nanotechnology 17:R1–R13
4. Jaiswal JK, Goldman ER, Mattoussi H, Simon SM (2004) Nat Methods 1:73–78
5. Chen FQ, Gerion D (2004) Nano Lett 4:1827–1832
6. Wang QS, Liu PF, Zhou XL, Zhang XL, Fang TT, Liu P, Min XM, Li X (2012) J Photochem Photobiol A Chem 230:23–30
7. Derfus AM, Chan WCW, Bhatia SN (2004) Nano Lett 4:11–18
8. Chen N, He Y, Su YY, Li XM, Huang Q, Wang HF, Zhang XZ, Tai RZ, Fan CH (2012) Biomaterials 33:1238–1244
9. Huang DP, Geng F, Liu YH, Wang XQ, Jiao JJ, Yu L (2011) Colloid Surf A Physicochem Eng Asp 392:191–197
10. Adam V, Krizkova S, Zitka O, Trnkova L, Petrlova J, Beklova M, Kizek R (2007) Electroanalysis 19:339–347
11. Cosson RP, Amiardtriquet C, Amiard JC (1991) Water Air Soil Pollut 57–8:555–567
12. Ghoshal K, Jacob ST (2001) Regulation of metallothionein gene expression. In: Progress in Nucleic Acid Research and Molecular Biology Academic Press Inc, San Diego, pp 357–384
13. Gunes C, Heuchel R, Georgiev O, Muller KH, Lichtlen P, Bluthmann H, Marino S, Aguzzi A, Schaffner W (1998) EMBO J 17:2846–2854
14. Klassen RB, Crenshaw K, Kozyraki R, Verroust PJ, Tio L, Atrian S, Allen PL, Hammond TG et al (2004) Am J Physiol Renal Physiol 287:F393–F403
15. Valko M, Morris H, Cronin MTD (2005) Curr Med Chem 12:1161–1208
16. Coyle P, Philcox JC, Carey LC, Rofe AM (2002) Cell Mol Life Sci 59:627–647
17. Bell SG, Vallee BL (2009) ChemBioChem 10:55–62
18. Adam V, Fabrik I, Eckschlager T, Stiborova M, Trnkova L, Kizek R (2010) TRAC Trends Anal Chem 29:409–418
19. Ryvolova M, Krizkova S, Adam V, Beklova M, Trnkova L, Hubalek J, Kizek R (2011) Curr Anal Chem 7:243–261
20. Kabzinski AKM (1993) Chromatographia 35:439–447
21. Bordin G, Raposo FC, Rodriguez AR (1994) Chromatographia 39:146–154
22. van Vyncht G, Bordin G, Rodriguez AR (2000) Chromatographia 52:745–752
23. Krizkova S, Masarik M, Eckschlager T, Adam V, Kizek R (2010) J Chromatogr A 1217:7966–7971
24. Virtanen V, Bordin G, Rodriguez AR (1998) Chromatographia 48:637–642
25. Virtanen V, Bordin G (1999) Chromatographia 49:S83–S86
26. Ryvolova M, Adam V, Kizek R (2012) J Chromatogr A 1226:31–42
27. Olafson RW, Olsson PE (1991) Method Enzymol 205:205–213

28. Adam V, Petrlova J, Potesil D, Zehnalek J, Sures B, Trnkova L, Jelen F, Kizek R (2005) Electroanalysis 17:1649–1657
29. Petrlova J, Potesil D, Mikelova R, Blastik O, Adam V, Trnkova L, Jelen F, Prusa R, Kukacka J, Kizek R (2006) Electrochim Acta 51:5112–5119
30. Adam V, Blastik O, Krizkova S, Lubal P, Kukacka J, Prusa R, Kizek R (2008) Chem Listy 102:51–58
31. Duan JL, Song LX, Zhan JH (2009) Nano Res 2:61–68
32. McGreavy C, Andrade JS, Rajagopal K (1990) Chromatographia 30:639–644
33. Lemieux L, Piot JM, Guillochon D, Amiot J (1991) Chromatographia 32:499–504
34. Shalliker RA, Kavanagh PE, Russell IM, Hawthorne DG (1992) Chromatographia 33:427–433
35. Demuynck S, Grumiaux F, Mottier V, Schikorski D, Lemiere S, Lepretre A (2006) Comp Biochem Physiol C Toxicol Pharmacol 144:34–46
36. Wong C, Sridhara S, Bardwell JCA, Jakob U (2000) Biotechniques 28:426–432
37. Krizkova S, Adam V, Eckschlager T, Kizek R (2009) Electrophoresis 30:3726–3735
38. Huska D, Zitka O, Krystofova O, Adam V, Babula P, Zehnalek J, Bartusek K, Beklova M, Havel L, Kizek R (2010) Int J Electrochem Sci 5:1535–1549
39. Hynek D, Krejcova L, Sochor J, Cernei N, Kynicky J, Adam V, Trnkova L, Hubalek J, Vrba R, Kizek R (2012) Int J Electrochem Sci 7:1802–1819
40. Kleckerova A, Sobrova P, Krystofova O, Sochor J, Zitka O, Babula P, Adam V, Docekalova H, Kizek R (2011) Int J Electrochem Sci 6:6011–6031
41. Krystofova O, Trnkova L, Adam V, Zehnalek J, Hubalek J, Babula P, Kizek R (2010) Sensors 10:5308–5328
42. Sochor J, Majzlik P, Salas P, Adam V, Trnkova L, Hubalek J, Kizek R (2010) Listy Cukrov Reparske 126:414–415
43. Raspor B (2001) J Electroanal Chem 503:159–162
44. Trnkova L, Kizek R, Vacek J (2002) Bioelectrochemistry 56:57–61
45. Fabrik I, Krizkova S, Huska D, Adam V, Hubalek J, Trnkova L, Eckschlager T, Kukacka J, Prusa R, Kizek R (2008) Electroanalysis 20:1521–1532
46. Krizkova S, Fabrik I, Adam V, Kukacka J, Prusa R, Chavis GJ, Trnkova L, Strnadel J, Horak V, Kizek R (2008) Sensors 8:3106–3122
47. Medintz IL, Uyeda HT, Goldman ER, Mattoussi H (2005) Nat Mater 4:435–446
48. Zitka O, Ryvolova M, Hubalek J, Eckschlager T, Adam V, Kizek R (2012) Curr Drug Metab 13:306–320
49. Drbohlavova J, Adam V, Kizek R, Hubalek J (2009) Int J Mol Sci 10:656–673
50. Krejcova L, Fabrik I, Hynek D, Krizkova S, Gumulec J, Ryvolova M, Adam V, Babula P, Trnkova L, Stiborova M, Hubalek J, Masarik M, Binkova H, Eckschlager T, Kizek R (2012) Int J Electrochem Sci 7:1767–1784
51. Krizkova S, Adam V, Kizek R (2009) Electrophoresis 30:4029–4033
52. Krizkova S, Ryvolova M, Gumulec J, Masarik M, Adam V, Majzlik P, Hubalek J, Provaznik I, Kizek R (2011) Electrophoresis 32:1952–1961
53. Sochor J, Hynek D, Krejcova L, Fabrik I, Krizkova S, Gumulec J, Adam V, Babula P, Trnkova L, Stiborova M, Hubalek J, Masarik M, Binkova H, Eckschlager T, Kizek R (2012) Int J Electrochem Sci 7:2136–2152
54. Zitka O, Krizkova S, Huska D, Adam V, Hubalek J, Eckschlager T, Kizek R (2011) Electrophoresis 32:857–860
55. Eckschlager T, Adam V, Hrabeta J, Figova K, Kizek R (2009) Curr Protein Pept Sci 10:360–375
56. Krizkova S, Fabrik I, Adam V, Hrabeta J, Eckschlager T, Kizek R (2009) Bratisl Med J Bratisl Lek Listy 110:93–97
57. Babula P, Masarik M, Adam V, Eckschlager T, Stiborova M, Trnkova L, Skutkova H, Provaznik I, Hubalek J, Kizek R (2012) Metallomics 4:739–750

5.2.3 Vědecký článek V

Use of nucleic acids anchor system to reveal apoferritin modification by cadmium telluride nanoparticles

Kudr, J., Nejdl, L., Skalickova, S., Zurek, M., Milosavljevic, V., Kensova, R., Ruttkay-Nedecky, B., Kopel, P., Hynek, D., Novotna, M., Adam, V. and Kizek, R.

J. Mat. Chem. B, 2015, 2050-750X, 2109-2118

Podíl autora Skaličková S.: 20 % textové části práce a 30 % experimentální práce

Feritiny jsou univerzální proteiny, které jsou schopny do své struktury uzavřít ionty různých anorganických látek, transportovat je a ve vhodných podmínkách tyto ionty opět uvolnit do okolního prostředí. Díky těmto vlastnostem se staly feritiny významným předmětem výzkumu v oblasti nanotechnologií. Výhodou využití feritinů je jejich organický původ a tak se stává jedním z perspektivních nanotransportérů, které hrají důležitou roli v diagnostice a *in vivo* zobrazování. Nedílnou součástí těchto oborů je pokrok ve vývoji kvantových teček, které vykazují vysoké kvantové výtěžky a stávají se novým diagnostickým přístupem. V nedávných studiích byla popsána syntéza různých nanomateriálů uvnitř apoferitinové struktury. Výhodou takového systému může být využití v *in vivo* zobrazovaní, kdy vnější proteinová klec chrání do ní uzavřené nanostruktury, které vykazují specifické vlastnosti, například fluorescenci (Sun, Cuiji, Yang, Hui et al. 2011). Mimo jiné může být vnější klec různě funkcionalizována nebo modifikována pro zajištění specifity, anebo pro cílený transport. Jednou z možností je využití specifické interakce mezi cysteinovými aminokyselinovými zbytky ve struktuře apoferitinu a jejich specifické interakce se zlatými nanočásticemi značenými oligonukleotidovou sondou modifikovanými paramagnetickými částicemi, které umožňovaly purifikaci celého nanokonstruktu.

Cílem této práce bylo syntetizovat apoferitin modifikovaný kadmium teluridovými nanočásticemi, které byly vytvořeny uvnitř apoferitinové kostry vlivem srážení při vysokých teplotách. Z tohoto důvodu byla prověřena termostabilita apoferitinu jehož denaturace začíná při teplotě 70 °C. Pomocí měření absorbančních spekter a

fluorescence byla sledována tvorba CdTe QDs. Z výsledků je patrná změna signálu při jednotlivých krocích syntézy a posun absorbčních a fluorescenčních maxim, které dokazují vytvoření CdTe QDs uvnitř apoferitinové klece. Pro izolaci apoferitinu s uzavřenými QDs, byl povrch proteinu modifikován zlatými nanočásticemi a přes thiolové skupiny oligonukleotidu upevněn k paramagnetickým částicím, za pomocí kterých byl celý konstrukt izolován od zbytku nenavázaných složek směsi. Tvorba cílového nanokonstruktu byla monitorována pomocí skenovacího elektronového mikroskopu. Jednotlivé kroky tvorby nanokonstruktu vedly ke snížení celkového protékajícího proudu mezi povrchem pracovní a pomocí elektrody, což dokazuje vznik celé nanokonstrukce.

V tomto experimentu se podařilo monitorovat a prokázat tvorbu CdTe QDs uvnitř apoferitinové klece pomocí spektrofotometrie a fluorescence. Díky interakci zlatých nanočástic s povrchem apoferitinu byla umožněna konjugace k oligonukleotidové probě značenou paramagnetickými částicemi. Vzniklý nanokonstrukt vyniká možností purifikace a manipulace díky paramagnetickým částicím a stává se tak možným nástrojem v *in vivo* zobrazovacích technikách díky vysokému kvantovému výtěžku CdTe QDs.

Journal of Materials Chemistry B

PAPER

View Article Online
View Journal | View Issue

Cite this: J. Mater. Chem. B, 2015, 3, 2109

Use of nucleic acids anchor system to reveal apoferritin modification by cadmium telluride nanoparticles

Jiri Kudr,[ab] Lukas Nejdl,[ab] Sylvie Skalickova,[a] Michal Zurek,[b] Vedran Milosavljevic,[ab] Renata Kensova,[ab] Branislav Ruttkay-Nedecky,[ab] Pavel Kopel,[ab] David Hynek,[ab] Marie Novotna,[ab] Vojtech Adam[ab] and Rene Kizek*[ab]

Received 11th August 2014
Accepted 15th January 2015

DOI: 10.1039/c4tb01336k

www.rsc.org/MaterialsB

The aim of this study was to synthesize cadmium telluride nanoparticles (CdTe NPs) modified apoferritin, and examine if apoferritin is able to accommodate CdTe NPs. Primarily, the thermostability of horse spleen apoferritin was tested and it's unfolding at 70 °C was observed. Cadmium telluride nanoparticles (CdTe NPs) were synthesized both within apoferritin protein cage and on its surface. The thermal treatment of apoferritin with CdTe NPs resulted in the aggregation of cores, which was indicated by changes in the absorption spectra and the shape of apoferritin tryptophan fluorescence. The apoferritin modified with CdTe NPs was additionally modified with gold nanoparticles and attached to magnetic particles *via* oligonucleotide using gold affinity to thiol group. This anchor system was used to separate the construct using external magnetic field and to analyse the molecules attached to apoferritin.

1. Introduction

Nanoparticles have been attracting a great attention due to their wide potential of application,[1] where their different shapes, sizes and compositions enhance a possibility of broad range of their use.[2–4] For nanotechnology and biotechnology applications, there is a strong demand on uniformity of nanoparticles properties. However, there are still technical challenges regarding the preparation of nanoparticles with homogeneous size distribution.[5]

Various nanoparticles fabrication methods have been reported.[6–8] It was shown that biomolecules, such as protein cages or viruses, can serve as a template for the synthesis of nanoparticles.[9,10] The cage-like proteins are able to bio-mineralize inorganic materials; moreover, they can be used as a spatially restricted chemical chamber (nanoreactor). Among all protein cages, apoferritin is favoured for its remarkably stable structure under various acidity and temperature.[11,12] Apoferritin is an iron storage protein, which is ubiquitous in animals. It is composed of 24 polypeptide subunits. These heavy and light subunits self-assemble into a hollow protein sphere with outer and inner diameters of 12 and 8 nm, respectively.[13] Horse-spleen apoferritin is composed of nearly of 90% of L-subunit (one tryptophan per L and H subunit at the same position of polypeptide chain). Specific threefold channels at the interface of the subunits are responsible for the flow of positive ions to the hollow core. In recent research, apoferritin has been used to synthesize various metal nanoparticles and semiconductor nanocrystals.[14–20] In these cases, aspartate and glutamate on the inner surface proved to promote the formation of nanoparticles.[17] In addition, apoferritin is used in many biomedical applications.[21–23]

Magnetic particles have important applications in biochemistry and analytical chemistry such as analyte preconcentration, separation and identification.[24–26] The target molecule can be recognized by specific magnetic particle surface modification and the magnetic force enables the separation of adsorbed target molecule from a complex sample.[27,28] The modification of magnetic particles with oligonucleotide probe is broadly used for biosensors fabrication and medical applications due to their unique biorecognition properties based on the ability to hybridize target sequence and to eliminate non-specific adsorption.[29–33]

As it was mentioned above protein cages, including apoferritin, are broadly used in the field of material science. Therefore, the aim of this study was to synthesize CdTe NPs modified apoferritin, and examine if apoferritin is able to accommodate CdTe NPs. Moreover, we designed the anchor system based on modified magnetic particles to prove apoferritin modification by CdTe NPs. The advantage of the proposed system is not only in the synthesis of nanoparticles within the apoferritin cage but also in the possibility to purify this nanoreactor from the unreacted components of the synthesis, as well as to transfer it to the desired location by

[a]Department of Chemistry and Biochemistry, Faculty of Agronomy, Mendel University in Brno, Zemedelska 1, CZ-613 00 Brno, Czech Republic, European Union. E-mail: kizek@sci.muni.cz; Fax: +420-5-4521-2044; Tel: +420-5-4513-3350

[b]Central European Institute of Technology, Brno University of Technology, Technicka 3058/10, CZ-616 00 Brno, Czech Republic, European Union

external magnetic field manipulation due to the conjugation with magnetic field responsive particles.

2. Material and methods

2.1. Chemicals

Water, cadmium acetate dihydrate, sodium tellurite, sodium borohydride and other chemicals were purchased from Sigma-Aldrich (St. Louis, USA) in ACS purity (chemicals meet the specifications of the American Chemical Society), unless noted otherwise. Apoferritin from equine spleen (0.2 μm filtered) and the oligonucleotides were also purchased from Sigma-Aldrich (St. Louis, USA). Magnetic particles Dynabeads Oligo$(dT)_{25}$ were bought from Thermo Fisher Scientific (Waltham, USA). pH was measured with a pH meter WTW (inoLab, Weilheim, Germany).

2.2. Sample preparation

The apoferritin with CdTe NPs (ApoCdTe NPs) was prepared as follows. The horse spleen apoferritin (20 μl, 7.3 μg μl^{-1}) was pipetted into water (300 μl). Then, cadmium acetate (20 μl, 20 mM) and ammonium (4.5 μl, 1 M) were added. After shaking (30 min, 37 °C, 500 rpm) on a thermomixer (Eppendorf, Hamburg, Germany), and then sodium tellurite (3.75 μl, 20 mM) was added to the solution (pH 9.5). To obtain the ApoCdTe NPs sample, sodium borohydride was added to the solution. The control sample (CdTe NPs sample) was prepared in the same way by adding 20 μl of water, instead of apoferritin. The water solution of apoferritin (0.4 mg ml^{-1}) was used to compare the ApoCdTe NPs and apoferritin fluorescence and absorption. After incubation (20 h, 60 °C, 500 rpm) on a thermomixer (Eppendorf, Germany), all the samples were filtered using the Amicon Ultra-0.5 ml Centrifugal Filters with 50 kDa cut-off (Merck Millipore, Billerica, USA) according to the manufacturer instructions.

2.3. Preparation of gold nanoparticles (Au NPs)

Gold nanoparticles were prepared using citrate method at room temperature as reported elsewhere.[34,35] Briefly, an aqueous solution of sodium citrate (0.5 ml, 40 mM) was added to a solution of $HAuCl_4 \cdot 3H_2O$ (10 ml, 1 mM). The colour of the solution slowly changed from yellow to violet. The mixture was stirred overnight. The smallest Au NPs from the top layer of the flask were used for apoferritin modification according to the following protocol. The ApoCdTe NPs, CdTe NPs and apoferritin sample (100 μl) were mixed with the Au NPs (10 μl) and incubated (24 h, 500 rpm, 37 °C) in a thermomixer (Eppendorf, Germany).

2.4. Preparation of anchor system

Buffers used for the isolation step were phosphate buffer I (pH 6.5, 0.1 M NaCl, 0.05 M Na_2HPO_4, and 0.05 M NaH_2PO_4), phosphate buffer II (0.2 M NaCl, 0.1 M Na_2HPO_4, and 0.1 M NaH_2PO_4) and hybridization buffer (100 mM Na_2HPO_4, 100 mM NaH_2PO_4, 0.5 M NaCl, 0.6 M guanidium thiocyanate, and 0.15 M trizma base, pH was adjusted to 7.5 using HCl). 10 μl of the resuspended magnetic particles were placed on the magnetic stand and washed 3-times with phosphate buffer I (100 μl). The magnetic particles were resuspended in the solution containing hybridization buffer (10 μl) and oligonucleotide with polyadenine terminus (10 μl, 100 μg ml^{-1}, 5′-TCTGCATTCCA GATGGGAGCATGAGATGAAAAA). Subsequently, this solution was incubated (30 min, 500 rpm, 37 °C) on thermomixer (Eppendorf, Germany) and the particles were washed with phosphate buffer I (100 μl) in order to remove unattached oligonucleotide. The particles were then resuspended in the solution containing hybridization buffer (10 μl) and thiolated oligonucleotide (10 μl, 100 μg ml^{-1}, 5′-CATCTCATGCTCC CATCTGGAATGCAGA–SH). After incubation (30 min, 500 rpm, 37 °C), the unbounded oligonucleotides were washed away. The product was the modified magnetic particles without any fluid. The prepared construct was used to anchor the gold modified ApoCdTe NPs, apoferritin and CdTe NPs samples.

The samples with different ApoCdTe NPs concentrations and modified by Au NPs were obtained by diluting the stock solution of ApoCdTe NPs with water in different ratios (undiluted ApoCdTe NPs stock solution, 1 : 1, 1 : 3, 1 : 7, 1 : 15 and 1 : 39). The gold modified apoferritin sample (5 μl) and CdTe NPs sample mixed with Au NPs (5 μl) were also mixed with water (35 μl) and used as controls for cadmium detection after separation conducted by the anchor system. In addition, these samples (40 μl) were mixed with the prepared modified magnetic particles and incubated (1 h, 25 °C, 500 rpm). Subsequently, the magnetic particles were washed with phosphate buffer I (100 μl), and phosphate buffer II was added (10 μl) in order to split the hybridized oligonucleotides. The magnetic particles were immobilized by the magnetic field and the supernatants were analysed using atomic absorption spectrometry (AAS).

2.5. Instrumentation

Absorption and fluorescence spectra were measured using an Infinite 200 PRO multimode reader with top heating (Tecan, Männedorf, Switzerland). Gel electrophoresis was performed using a PowerPac Universal Power Supply (Bio-Rad, Hercules, USA). Average current levels were obtained using a Scanning electrochemical microscope 920C (CH Instruments, Austin, USA). Spectro Xepos (Spectro Analytical Instruments, Kleve, Germany) was used to measure X-ray fluorescence spectra. The determination of cadmium was carried out on a 280Z Agilent Technologies atomic absorption spectrometer (Agilent, Santa Clara, USA) with electrothermal atomization and Zeeman background correction. Average particle size and size distribution were determined by quasielastic laser light scattering with Malvern zetasizer Nano-ZS (Malvern Instruments Ltd., Worcestershire, U.K.).

2.6. Apoferritin thermostability

The unfolding of apoferritin was monitored spectrophotometrically using a computer-controlled Peltier thermostat (Labortechnik, Wasserburg, Germany). The sample (35 μg ml^{-1}) was incubated at different temperatures for 5 min, and thereafter the absorbance was measured at 230 nm. Changes in sample

absorbance were recorded using a spectrophotometer Specord S600 with a diode detector (Analytik Jena, Jena, Germany). The thermostability of apoferritin was also tested using gel electrophoresis. The solution of apoferritin (35 μg ml^{-1}) was shaken (500 rpm) and heated with a thermomixer. The samples (10 μl) were removed from the solution during heating when the temperature reached 30, 35, 40, 45, 50, 55, 60, 65, 70 and 75 °C for 5 minutes. These samples were further analysed by native (non-denaturing) polyacrylamide gel electrophoresis (native-PAGE).

2.7. Non-denaturing polyacrylamide gel electrophoresis

The samples were analysed in 6% non-denaturing PAGE in 60 mM 4-(2-hydroxyethyl)-1-piperazineethanesulfonic acid and 40 mM imidazole pH 7.4 buffer as described by Kilic *et al.*[36] Briefly, the samples (10 μl) were mixed with 2 μl of 30% glycerol. The gels (2.4 ml of acrylamide/bis-acrylamide 30% solution, 9.6 ml of running buffer, 9.96 μl of *N*,*N*,*N*′,*N*′-tetramethylethylenediamine and 60 μl of ammonium persulfate) were run at 10 mA for 2 hours (30 minutes for apoferritin thermostability experiment) and were stained with Coomassie Brilliant Blue R stain.

2.8. The scanning electrochemical microscope measurements

Scanning electrochemical microscope (SECM) consisted of 100 mm measuring platinum disc probe electrode with a potential of +0.2 V. During the scanning, particles were attached to the conducting substrate plate coated with gold *via* magnetic force from neodymium magnet. The working distance of the platinum measuring electrode was set at 20 μm above the surface. The mixture consisted of 5% ferrocene in methanol mixed in 1 : 1 ratio with 0.05% KCl with water (v/v).

2.9. Stern–Volmer constant

Fluorescence spectra (excitation wavelength 400 nm) of CdTe NPs (emission wavelength 600 nm) QDs without any capping agent (50 μl) were measured in the presence of 0, 0.3, 0.6, 0.8, 1.1 and 1.4 μM of apoferritin (5 μl) and also at different temperatures (20, 25, 30, 35 and 40 °C). The CdTe NPs fluorescence quenching by apoferritin can be described by Stern–Volmer equation:

$$\frac{F_0}{F} = 1 + k_q\tau_0[Q] = 1 + K_{SV}[Q]$$

where F_0 and F are fluorescence intensities of CdTe NPs in the absence and presence of apoferritin quencher, respectively, k_q is biomolecular quenching constant, τ_0 is the lifetime of the fluorophore without quencher, [Q] is the concentration of the quencher and K_{SV} is the Stern–Volmer quenching constant.[37] The quenching constant K_{SV} was calculated by the linear regression of a plot of $(F_0 - F)/F$ against [Q].[38]

3. Results and discussion

3.1. The synthesis of CdTe NPs within apoferritin

The H subunits (represents 10–15% of horse spleen apoferritin) include the ferroxidase centre, which is responsible for the oxidation of ferrous oxide to ferric oxide and prevents free radicals production. Apoferritin cavity *in vivo* was able to accommodate 4000 iron atoms stored as a mineral ferrihydrite. The hydrophobic fourfold channels represent large energy barrier for divalent and monovalent ions uptake.[39] Apart from that, the hydrophylic threefold channels transferred monovalent and divalent ions into the apoferritin cavity. This ability was broadly used for nanoparticle synthesis within the cavity. As it was previously proved, the apoferritin cavity was able to accommodate several metal ions and inorganic molecules.[14,15,40] From these, cadmium ions were used for ferritin and apoferritin crystallization due to its large coordination numbers,[41] and were also able to bridge the otherwise repulsive carboxyl groups of opposing aspartate and glutamine side chains.[42]

Protein contains three intrinsic fluorophores: phenylalanine, tyrosine and tryptophan, which are also responsible for protein absorption in the UV-region. Tryptophan has longer excitation and emission wavelengths and good quantum yield. Due to the fact that phenylalanine has very low quantum yield and tyrosine is often totally quenched when is located near amino or carboxyl group, protein intrinsic fluorescence mostly arises from tryptophan (its indole ring).[37] Changes in the tryptophan fluorescence intensity, band shape, wavelength maximum and fluorescence lifetime depend on the tryptophan local environment and are used in various applications such as substrate binding or quencher accessibility.[38,43–45] Both, the H and L-chains of apoferritin contain single tryptophan residue, thus 24 tryptophan residues are presented within apoferritin. Therefore, we monitored apoferritin emission spectra after excitation at 230 nm and observed the changes during the sample preparations.

The preparation of ApoCdTe NPs (apoferritin modified with CdTe NPs) is schematically depicted in Fig. 1A. More precisely, ammonium (4.5 μl, 1 M) and cadmium acetate (20 μl, 20 mM) were added to apoferritin solution (0.4 mg ml^{-1}). Cadmium ions were stabilized by ammonium ions and created positively charged tetraminecadmium ions, which were partly transported to the apoferritin cavity.[46] Then, sodium tellurite (3.75 μl, 20 mM) was added and the tellurite ions were reduced to telluride by the addition of sodium borohydride, which resulted in CdTe cores formation. Subsequent heating was applied to allow CdTe cores to aggregate.

The individual steps of ApoCdTe NPs synthesis were monitored using UV-Vis and fluorescence spectroscopy to confirm the CdTe NPs creation. The absorption (230–800 nm) and fluorescence spectra (280–480 nm) were measured and compared with two control samples as (i) CdTe NPs solution without any capping agent and apoferritin (CdTe NPs sample), and (ii) apoferritin water solution. The characteristic absorption peak of protein (apoferritin) was observed at 280 nm in the cases of apoferritin solution with cadmium and tellurite ions

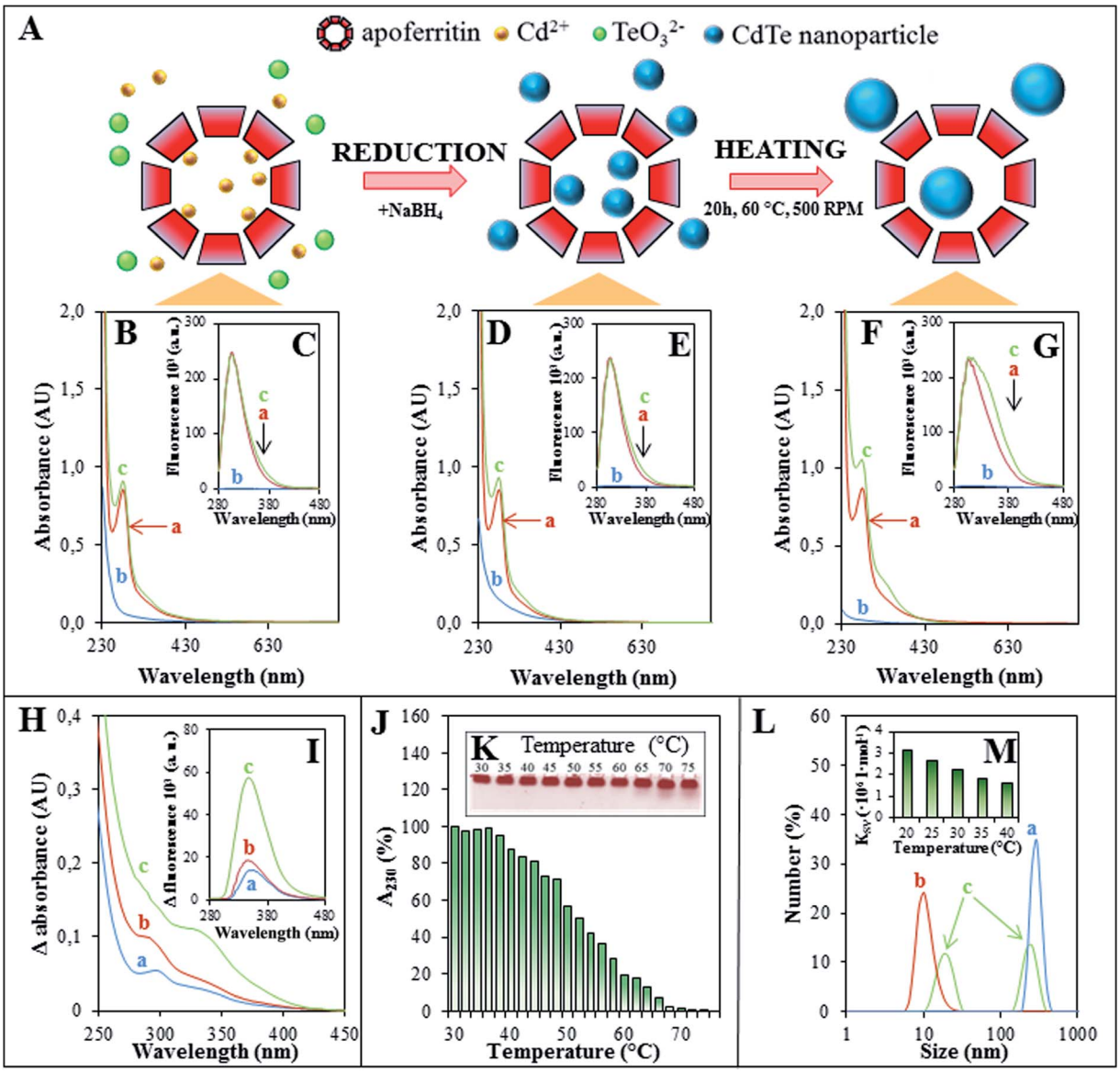

Fig. 1 Individual steps of CdTe NPs synthesis within apoferritin (ApoCdTe NPs) and their characterization. (A) The scheme of the ApoCdTe NPs synthesis, which was monitored using UV-vis spectrometry and fluorescence spectroscopy and compared with the control samples. The absorption and fluorescence spectra of (a) apoferritin solution, (b) cadmium acetate, ammonium and sodium tellurite water solution and (c) same mixture with addition of apoferritin were measured (B and C) before reduction step, (D and E) after reduction and (F and G) after heating. To highlight the differences between ApoCdTe NPs and apoferritin sample the differential (H) absorption and (I) fluorescence spectra (a) before reduction, (b) after reduction and (c) after incubation were calculated. (J) To encourage CdTe creation heating is required, thus apoferritin thermostability was determined. The absorbance of apoferritin solution at 230 nm during the heating depicted as percentages of decrease and (K) the native PAGE of heated apoferritin solution to particular temperature. (L) The size distribution of (a) CdTe colloids, (b) apoferritin in its spherical state and (c) particles presented within ApoCdTe NPs sample. (M) Stern–Volmers K_{SV} constants were determined to elucidate the interaction mechanism between CdTe NPs by apoferritin at different temperatures.

($A_{280} = 0.91$ AU) and apoferritin solution ($A_{280} = 0.86$ AU) before the addition of $NaBH_4$. No absorption peak was observed in the case of cadmium and tellurite ions solution (Fig. 1B). The fluorescence spectra of all three samples were also measured (Fig. 1C). The emission peaks of apoferritin and apoferritin in the presence of ions were observed at 308 nm. The sample with cadmium and tellurite ions without apoferritin exhibited emission spectra with no peak. In comparison to the sample of ions before the addition of reducing agent, the absorption maximum of reduced sample increased in the range from 246 nm to 450 nm due to CdTe cores creation (Fig. 1D), which is in good agreement with Han *et al.*[47] The absorption spectra of ApoCdTe NPs and apoferritin sample remained nearly the same after reduction process. The emission of ApoCdTe NPs and apoferritin samples were lowered by 4% and 3% respectively, compared to the unreduced samples (Fig. 1E). The fluorescence measurement of CdTe NPs sample immediately after reduction revealed no emission peak (excitation wavelength 230 nm), but

emission maxima was observed at 584 nm when excited at 400 nm (not shown). We assume that the presence of CdTe quantum dots in the solution was responsible for this emission maximum. In the next step, the samples were heated (20 h, 60 °C, 500 rpm) to encourage the aggregation of CdTe NPs according to Khalavka *et al.*[48] The measurement of samples absorption spectra after the heating step resulted in the increase of ApoCdTe NPs local maxima at 280 nm by 14% (compared with reduced ApoCdTe NPs sample) and the formation of local maxima at 330 nm, although the absorption spectra of apoferritin sample remained nearly the same (Fig. 1F). The similar absorption spectra of nanoparticle within apoferritin were reported for Pd and Cd.[16,49] Strong decrease in CdTe NPs sample absorption at UV wavelengths was detected after heating and we assume that this is the result of bulk CdTe colloids precipitation (Fig. 1F). Although, the fluorescence of apoferritin and ApoCdTe NPs sample with the maxima at 306 nm remained the same after incubation, the peak width changed (Fig. 1G). The emission of CdTe NPs was not observed and the mechanism of quenching is discussed afterwards. Xiao *et al.* determined the interaction of CdTe quantum dots stabilized by mercapropropionic acid with the human serum albumin by the decrease in albumin fluorescence intensity, however quantum dot properties are strongly affected by the capping agent.[50] Peak width at half height of ApoCdTe NPs (calculated as a distance from the front slope of the peak to the back slope of the peak measured at 50% of the maximum peak height) increased by 54% in comparison with the emission peak before heating and also increased by 30% in the case of apoferritin solution. After the heating, no emission peak of CdTe NPs sample was observed when excited at 230 nm and the emission peak also disappeared when excited at 400 nm (not shown). Without any capping agent, heating of quantum dots resulted in their aggregation.

We also calculated the difference spectra. The absorption and fluorescence spectra of apoferritin solution in a particular synthesis step were subtracted from the spectra of ApoCdTe NPs sample. The differential absorption spectra highlighted the differences between samples at 300 nm before and after reduction step and the local maxima increase at 330 nm (Fig. 1H). The heating of ApoCdTe NPs sample resulted in the difference fluorescence maxima evolving. The differential fluorescence spectra revealed the increasing peak at 350 nm (Fig. 1I). The difference emission of heated ApoCdTe NPs and heated apoferritin increased 3-times in comparison with difference emission of the unheated samples.

In addition, the thermostability of apoferritin spherical structure was examined using UV-Vis spectrophotometry and gel electrophoresis. UV-Vis absorbance measurement is a simple method used to examine the structural changes and formation of complexes.[33,51,52] The protein absorption spectra showed the peak at 280 nm due to the absorption of aromatic side chains of phenylalanine, tyrosine, and due to disulphide bonds, which are responsible for the dimerization of apoferritin H-chains, and mostly by tryptophan.[53] The tryptophan and tyrosine content in various proteins remains constant, and therefore this wavelength is commonly used to determine protein concentration in a reagentless nondestructive way. External conditions like temperature, pH and ionic strength cause changes in the protein conformation, which results in the change of amino acids exposure to the solvent and the absorption spectra.[54–57] Although the UV absorption spectra of proteins show slopes only at app. 230 nm, according to Liu *et al.*,[58] it can be used as a convenient structural probe to find the thermodynamic stability and kinetics of proteins unfolding. The monitoring of absorbance at 230 nm (A_{230}) during the heating was used as structural probe for studying apoferritin. The steady decrease of A_{230} was observed from 30 °C to 76 °C during the heating of apoferritin solution (Fig. 1J). The absorbance of apoferritin solution at 30 °C and 76 °C was expressed as 100% and 0%, respectively. The lowest absorbance (A_{230} = 1.28 AU) was measured after the temperature of the solution reached 76 °C; however, the absorbance of solutions heated to 68 °C and more were nearly the same. We suggest that the heating of apoferritin above the body temperature resulted in the conformation changes of the apoferritin subunits and total denaturation at 68 °C was observed; nevertheless, the substantial reversibility of horse spleen apoferritin denaturation was observed up to a few degrees below denaturation temperature.[11] The UV spectra of folded and unfolded protein commonly shows downward peak (UV absorption of unfolded protein is lower).[58]

The unfolding and denaturation of apoferritin were also examined using the native polyacrylamide gel electrophoresis (Fig. 1K). Smears corresponding to the release of apoferritin subunits were observed in case of samples heated above 65 °C but it seems to have reached a higher intensity at 70 °C. Taking together data from UV absorption and gel electrophoresis, we conclude that the spherical structure of apoferritin degrades in temperature above 65 °C. Based on previous results, we have chosen 60 °C as a safe temperature for CdTe NPs aggregation in the presence of the spherical state of apoferritin. Stefanini *et al.* (1996) suggests that the horse spleen apoferritin should not be heated to 80 °C to avoid its irreversible denaturation.[11] Our results confirm the high thermostability of horse spleen apoferritin, which is consistent with the thermostability of the entire ferritin group as it was determined in the case of ferritin from hyperthermophile *Pyrococcus furiosus*, which is stable up to 120 °C.[14]

The average particle sizes and particle size distribution within samples were determined using a zetasizer; nevertheless, electrochemical methods were suggested to be able to determine nanoparticle sizes (Fig. 1L).[59] Average CdTe colloid was 295 nm in diameter after heating, although we assume that their size without capping agent is not stable. The average size of spherical apoferritin was found to be 11 nm, which correspond with the commonly accepted size of apoferritin (12 nm). Two main particle fractions were detected in the case of ApoCdTe NPs sample as (i) CdTe colloids with average sizes of 255 nm and (ii) apoferritin modified by CdTe NPs with average diameter of 18 nm.

As we observed the quenching of CdTe NPs fluorescence by apoferritin and *vice versa*, we used the calculations of Stern–Volmers constants to elucidate the interaction of CdTe NPs and

apoferritin surface. Fluorescence quenching mechanism is usually described as either dynamic or static and can be determined using different temperature dependence.[60] As it is shown in Fig. 1M, the calculated Stern–Volmer quenching constants K_{SV} of CdTe NPs were inversely correlated with the increasing temperature. This phenomenon is often observed in the case of static quenching and suggests that the quenching of CdTe NPs was the result of them binding to the surface of apoferritin, rather than by dynamic collision.[61]

3.2. Anchoring of the apoferritin samples

The utilization of the apoferritin cage as a nanoreactor provides variety of advantages; however, the manipulation of such a molecule by external stimuli is of an interest mainly to enable the reaction to take place at the desired place, and subsequently transfer the product to the site of action. Therefore, an elegant approach of application of magnetic particles can be used. For this reason, a simple connection using gold nanoparticles and complementary oligonucleotides was proposed, enabling to simply connect the cage to the magnetic particle and spatially manipulate the nanoreactor.

In the following experiments, apoferritin, CdTe NPs and ApoCdTe NPs samples were mixed with the gold nanoparticles (Au NPs). Covalent bond between Au and S is the most widely used interaction to achieve stable conjugation between Au NPs and oligonucleotides or proteins containing cysteine.[62–64] The citrate capped Au NPs are known as one of the easily synthesized NPs, thus are frequently used for biosensors fabrication and biomolecule labelling.[65–67] The exposed citrate is responsible for the negative charge of Au NPs surface.[68] Due to the fact that the apoferritin inner surface has a negative electrostatic potential due to the presence of many acidic amino acids residues, which is important to attract metal ions from solution during biomineralization, the electrostatic binding between Au NPs and apoferritin (horse spleen apoferritin p*I* is between 4.1–5.5) is impossible in neutral pH.[69] Our concept of apoferritin modification with Au NPs relies on the apoferritin's ability to displace the citrate on nanoparticle surface as a result of the direct interaction of amino acids functional group (thiol of cysteine, amine of lysine or imidazole of histidine) with the gold surface. The forming of chemical bond between sulphur from apoferritin cysteine and gold was previously reported.[70]

The integrity of apoferritin structure during the CdTe NPs synthesis was examined using gel electrophoresis (Fig. 2A). The apoferritin sample and apoferritin sample after Au NPs modification was run in the gel (Fig. 2Aa and e). The band of native apoferritin nanosphere was found to be app. 1 cm from the beginning (Fig. 2A red arrow), which was reported by Kilic *et al.* under these conditions.[71] The faint band attributed to the dimeric form of apoferritin sphere was also observed (Fig. 2A green arrow), which was in good agreement with Kilic *et al.*[36] After apoferritin sample heating (20 h, 60 °C, 500 rpm), the sample was filtered using filter unit with 50 kDa cut off and the filtrate was analysed on PAGE (Fig. 2Ac). There was no apoferritin subunit band detected (both approximately 20 kDa), thus we concluded that the integration of apoferritin was mostly preserved after heating. The ApoCdTe NPs sample was treated in the same way. In Fig. 2Ab, d and f shows the ApoCdTe NPs sample after synthesis and its filtrate and ApoCdTe NPs modified by Au NPs. The positions of ApoCdTe NPs sample bands were similar to bands of apoferritin sample. Only slight shifts of ApoCdTe NPs bands were observed. We assume that the protein charge was not changed. Therefore, we came to the conclusion that it was the result of CdTe NPs attachment to the apoferritin surface and the increase of its hydrodynamic size, as also suggested by the particles size distribution and static quenching of CdTe NPs fluorescence by apoferritin (Fig. 1L).

In conclusion, no shifts of the bands of apoferritin and ApoCdTe NPs were observed after their modification with gold

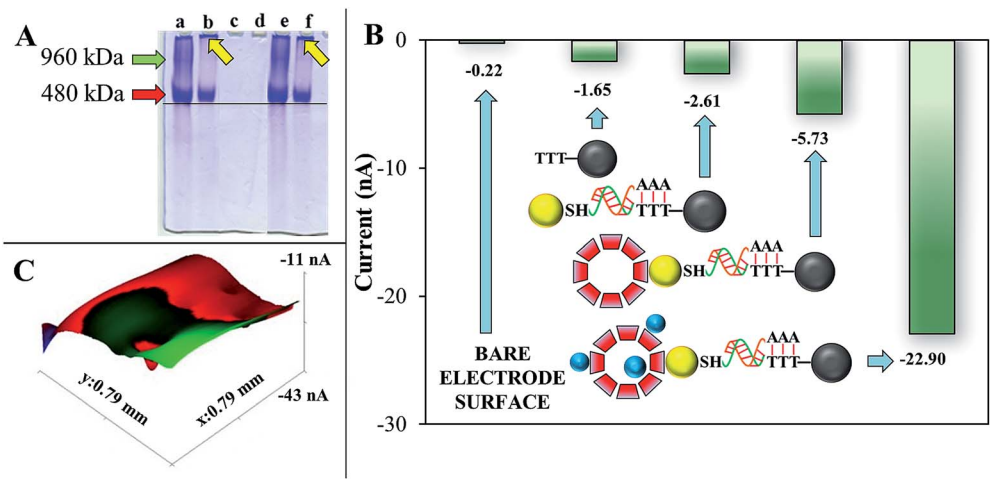

Fig. 2 Creation of anchor system. (A) The native PAGE shows the (a) apoferritin sample, (b) the ApoCdTe NPs sample after heating, (c and d) the filtrate obtained by filtration of apoferritin and ApoCdTe NPs sample through filter unit after heating, and (e and f) apoferritin and ApoCdTe NPs sample after Au NPs modification. (B) The average current levels of individual parts of nanoconstruct measured by SECM confirmed individual steps of anchor system creation. (C) The image of ApoCdTe NPs anchored to magnetic particles obtained by SECM.

nanoparticles. The bands intensities of ApoCdTe NPs and ApoCdTe NPs modified with Au NPs were not so well-marked as the apoferritin bands. The thermostability of apoferritin seems to be partly influenced by CdTe NPs presence. Heating (60 °C for 20 h) resulted in apoferritin portion unfolding, indicated by polypeptide aggregates, which cannot go through the native-PAGE and for this reason stacked at the beginning of the gel (Fig. 2A yellow arrow) and they were also not able to go through the filter unit with 50 kDa cut-off.

The individual steps of nanoconstruct formation were examined using SECM (Fig. 2B). The bare gold plate was first scanned and the average current level was calculated (−0.22 nA). The magnetic particles attached to the gold plate due to magnetic field had an average current level of −1.65 nA. The oligonucleotide with terminal polyA sequence was hybridized to magnetic particles. This complex was then hybridized to complementary oligonucleotide with thiolated terminus and Au NPs were immobilized on its thiol groups. This part of construct decreased the reduction signal by 0.96 nA to −2.61 nA. The construct extended by apoferritin resulted in the decrease of the signal by 3.12 nA to −5.73 nA, therefore the apoferritin addition increased the amount of reducible substances by 120%. The presence of CdTe NPs within the apoferritin cavity and on the apoferritin surface decreased the average current level four-times to −22.90 nA. The SECM record of ApoCdTe NPs immobilized on the surface of gold electrode using anchor system and applying of external magnetic field is shown in Fig. 2C.

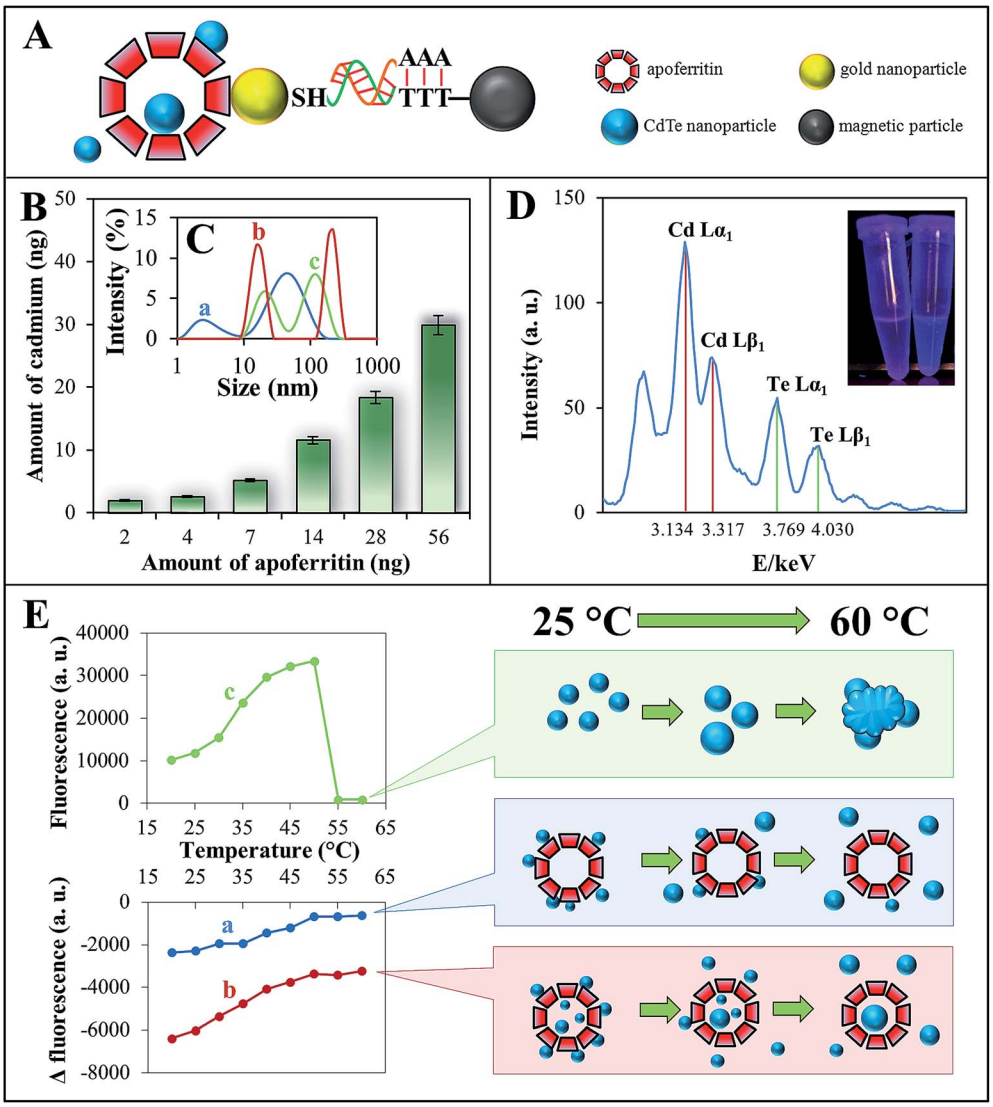

Fig. 3 Proving of apoferritin modification with CdTe NPs. (A) The scheme of ApoCdTe NPs anchored to the separative nanoconstruct used to prove the dependence of the detected cadmium amount on the amount of anchored apoferritin (B). (C) The sizes of gold nanoparticles (a) used for apoferritin modification, (b) particles presented within the ApoCdTe NPs sample and (c) the particles separated by anchor system. (D) The XRF spectra shows that Cd and Te ions were presented in ApoCdTe NPs sample separated by the anchor system. Inset: the image of water on the left and ApoCdTe NPs on the right side after excitation by 312 nm. (E) The dependence of fluorescence on the heating temperature for (a) CdTe solution with apoferritin added after CdTe synthesis, (b) ApoCdTe NPs and (c) the CdTe without any capping agent suggests that portion of CdTe NPs is presented within apoferritin cavity.

3.3. The presence of CdTe nanoparticles within apoferritin

The Au NPs were added to apoferritin, CdTe NPs and ApoCdTe NPs samples. After incubation of the samples with the Au NPs, we used the anchor system to capture the Au NPs and molecules attached to them (Fig. 3A). Oligonucleotide probes with terminal AAA sequence were hybridized to magnetic particles with TTT sequence bound to theirs surface. Second probes with thiol groups were hybridized to the first one and together formed a system capable of anchoring gold modified biomolecules. The different concentrations of ApoCdTe NPs sample modified with Au NPs were added to oligonucleotides with attached magnetic particles. CdTe NPs solution was added to the magnetic particle as a control. After incubation (1 h, 25 °C), these constructs were separated from the solution of unattached molecules by applying external magnetic field. Subsequently, the hybridized oligonucleotides in the constructs were disrupted due to chemical denaturation and the magnetic particles were removed from the samples. Finally, the samples were analysed using AAS. No trace of cadmium was detected in the control samples. It means that no CdTe NPs were modified by Au NPs and anchored. Apart from that, ApoCdTe NPs was successfully modified by Au NPs and attached to the anchor system. The dependence of detected amount of total cadmium on the volume of ApoCdTe NPs applied to the anchor system proved the modification of apoferritin by CdTe NPs and it is shown in Fig. 3B. Furthermore, we calculated that the ratio of the detected cadmium to one apoferritin anchored molecule to be 2700 : 1. The sizes and size distributions of gold nanoparticles used for apoferritin modification and particles separated from ApoCdTe NPs solution were measured and compared with the size distribution of the particles presented within the ApoCdTe NPs solution (Fig. 3C). We observed that gold nanoparticles with average diameter of 4 nm exhibited a broad size distribution from 1 to 8 nm. In this case, we suggested that the gold nanoparticles aggregation and cluster formation was partly responsible for this size distribution and also for the presence of second size distribution peak from 10 to 120 nm. The size distribution of ApoCdTe NPs sample consisted of two peaks. The first peak, at app. 18 nm, was assigned to the apoferritin with CdTe NPs present on its surface and the second to the CdTe colloids with sizes from 165 to 340 nm. The size distribution of particles separated from the ApoCdTe NPs solution by anchor system shows that the apoferritin was modified by Au NPs and probably also attached to the Au NPs clusters. The size distribution of particles attributed to apoferritin modified with CdTe NPs and Au NPs was from 12 to 42 nm with the biggest intensity at 21 nm. We assume that the thiolated oligonucleotide was still bound to the apoferritin and contributed to the peak shift. Particles with size of 105 nm were also separated from ApoCdTe NPs solution, which suggests that the aggregated Au NPs were also anchored. Although the small overlap of CdTe NPs colloids size distribution from ApoCdTe NPs sample and size distribution of particles separated from ApoCdTe NPs sample was observed, we concluded that no CdTe NPs colloids were anchored, because no fraction bigger than CdTe NPs colloids was observed in the size distribution of the anchored particles, which confirms the results from AAS measurement of the control sample. The sample, where the highest concentration of cadmium was proven, was also analysed by X-ray fluorescence (XRF). The measurement of XRF spectra confirmed the presence of tellurium (the $L\alpha_1$ line energy corresponds to 3.134 keV and $L\beta_1$ to 3.317 keV) and also cadmium (the $L\alpha_1$ corresponds to 3.769 keV and $L\beta_1$ to 4.030 keV) in the solution containing ApoCdTe NPs (Fig. 3D).

We also tested the effect of CdTe NPs nanoparticles on the fluorescence of tryptophan in apoferritin. The fluorescence spectra of ApoCdTe NPs sample were compared with the spectra of CdTe NPs solution with added apoferritin. Apoferritin emissions in the presence of cadmium, tellurite and ammonium ions were measured and subtracted from the emissions of ApoCdTe NPs and the mixture of CdTe NPs and apoferritin, which were monitored during heating (20, 25, 30, 35, 40, 45, 50, 55 and 60 °C) using an excitation wavelength of 380 nm. This excitation wavelength was chosen in order to observe changes in the apoferritin emission peak width rather than emission maxima and to enable observing the subtle changes of tryptophan fluorescence. The addition of apoferritin to CdTe NPs solution resulted in the complete disappearance of CdTe NPs peak at 602 nm, which was replaced by the emission of tryptophan at 450 nm (excitation wavelength 380 nm). The concentration dependent ability of protein to quench different types CdTe quantum dots was previously described by Wang *et al.*[72] and the mechanism of apoferritin interaction with CdTe NPs without surface stabilisation was described by Stern–Volmer equation described above. In addition, we compared the fluorescence intensities of ApoCdTe NPs and apoferritin covered with CdTe NPs. In the case of both the samples, the fluorescence of apoferritin tryptophan was statically quenched (fluorescence was decreased) by the presence of CdTe NPs on apoferritin surface, whereas it was reported previously that hydrous ferric oxides emerging at ferroxidase centres are able to quench tryptophan fluorescence.[73] The increasing temperatures resulted in the growing and, finally, aggregation of CdTe NPs, which is in good agreement with results obtained by Shen *et al.*[74] It also induced release of growing CdTe NPs from apoferritin surface and led to the increase of apoferritin fluorescence (Fig. 3E). The total release was observed at 50 °C. After the release of CdTe NPs from apoferritin surface, the fluorescence of apoferritin with CdTe NPs within the cavity was still partly quenched (Fig. 3Eb). On the contrary, the fluorescence of apoferritin with CdTe only on its surface was almost same as apoferritin control after heating.

4. Conclusions

Apoferritin is an appealing molecule due to its inner cavity, and is extensively investigated as a nanoreactor or drug carrier. We designed the nanoconstruct, which is able to selectively bind apoferritin molecules modified by gold nanoparticles and separate them from the solution of unreacted components and therefore to purify the required product. This simple anchor system enables to analyse the anchored molecule modification

with the target analyte, also its degree or amount of encapsulated analyte. In order to test this concept we utilized apoferritin cavity as a nanoreactor and synthesized apoferritin modified by CdTe nanoparticles, which proved to be presented on the surface and within the apoferritin cavity.

Acknowledgements

The financial support from the following project NANOLABSYS CZ.1.07/2.3.00/20.0148 is highly acknowledged. The authors thank Dagmar Uhlirova, Martina Stankova and Radek Chmela for technical assistance.

References

1 G. M. Whitesides, *Small*, 2005, **1**, 172–179.
2 L. Sironi, S. Freddi, M. Caccia, P. Pozzi, L. Rossetti, P. Pallavicini, A. Dona, E. Cabrini, M. Gualtieri, I. Rivolta, A. Panariti, L. D'Alfonso, M. Collini and G. Chirico, *J. Phys. Chem. C*, 2012, **116**, 18407–18418.
3 B. S. Yin, S. W. Zhang, Y. Jiao, Y. Liu, F. Y. Qu, Y. J. Ma and X. Wu, *J. Nanosci. Nanotechnol.*, 2014, **14**, 7157–7160.
4 H. Zhang, S. S. Jia, M. Lv, J. Y. Shi, X. L. Zuo, S. Su, L. H. Wang, W. Huang, C. H. Fan and Q. Huang, *Anal. Chem.*, 2014, **86**, 4047–4051.
5 G. D. Liu, H. Wu, J. Wang and Y. H. Lin, *Small*, 2006, **2**, 1139–1143.
6 H. L. Li, Y. C. Zhu, S. G. Chen, O. Palchik, J. P. Xiong, Y. Koltypin, Y. Gofer and A. Gedanken, *J. Solid State Chem.*, 2003, **172**, 102–110.
7 H. Y. Hsueh, H. Y. Chen, Y. C. Hung, Y. C. Ling, S. Gwo and R. M. Ho, *Adv. Mater.*, 2013, **25**, 1780–1786.
8 W. Zhou, K. Zheng, L. He, R. M. Wang, L. Guo, C. P. Chen, X. Han and Z. Zhang, *Nano Lett.*, 2008, **8**, 1147–1152.
9 K. Uto, K. Yamamoto, N. Kishimoto, M. Muraoka, T. Aoyagi and I. Yamashita, *J. Nanosci. Nanotechnol.*, 2014, **14**, 3193–3201.
10 C. B. Mao, D. J. Solis, B. D. Reiss, S. T. Kottmann, R. Y. Sweeney, A. Hayhurst, G. Georgiou, B. Iverson and A. M. Belcher, *Science*, 2004, **303**, 213–217.
11 S. Stefanini, S. Cavallo, C. Q. Wang, P. Tataseo, P. Vecchini, A. Giartosio and E. Chiancone, *Arch. Biochem. Biophys.*, 1996, **325**, 58–64.
12 R. R. Crichton and C. F. A. Bryce, *Biochem. J.*, 1973, **133**, 289–299.
13 M. Uchida, M. T. Klem, M. Allen, P. Suci, M. Flenniken, E. Gillitzer, Z. Varpness, L. O. Liepold, M. Young and T. Douglas, *Adv. Mater.*, 2007, **19**, 1025–1042.
14 M. J. Parker, M. A. Allen, B. Ramsay, M. T. Klem, M. Young and T. Douglas, *Chem. Mater.*, 2008, **20**, 1541–1547.
15 I. Yamashita, J. Hayashi and M. Hara, *Chem. Lett.*, 2004, **33**, 1158–1159.
16 T. Ueno, M. Suzuki, T. Goto, T. Matsumoto, K. Nagayama and Y. Watanabe, *Angew. Chem., Int. Ed.*, 2004, **43**, 2527–2530.
17 R. Tsukamoto, K. Iwahori, M. Muraoka and I. Yamashita, *Abstr. Pap. Am. Chem. Soc.*, 2005, **229**, U938–U939.
18 B. Hennequin, L. Turyanska, T. Ben, A. M. Beltran, S. I. Molina, M. Li, S. Mann, A. Patane and N. R. Thomas, *Adv. Mater.*, 2008, **20**, 3592–3596.
19 T. D. Bradshaw, M. Junor, A. Patane, P. Clarke, N. R. Thomas, M. Li, S. Mann and L. Turyanska, *J. Mater. Chem. B*, 2013, **1**, 6254–6260.
20 X. Y. Liu, W. Wei, S. J. Huang, S. S. Lin, X. Zhang, C. M. Zhang, Y. G. Du, G. H. Ma, M. Li, S. Mann and D. Ma, *J. Mater. Chem. B*, 2013, **1**, 3136–3143.
21 K. L. Fan, L. Z. Gao and X. Y. Yan, *Wiley Interdiscip. Rev.: Nanomed. Nanobiotechnol.*, 2013, **5**, 287–298.
22 E. Fantechi, C. Innocenti, M. Zanardelli, M. Fittipaldi, E. Falvo, M. Carbo, V. Shullani, L. D. Mannelli, C. Ghelardini, A. M. Ferretti, A. Ponti, C. Sangregorio and P. Ceci, *ACS Nano*, 2014, **8**, 4705–4719.
23 I. Blazkova, H. V. Nguyen, S. Dostalova, P. Kopel, M. Stanisavljevic, M. Vaculovicova, M. Stiborova, T. Eckschlager, R. Kizek and V. Adam, *Int. J. Mol. Sci.*, 2013, **14**, 13391–13402.
24 B. H. Jun, M. S. Noh, G. Kim, H. Kang, J. H. Kim, W. J. Chung, M. S. Kim, Y. K. Kim, M. H. Cho, D. H. Jeong and Y. S. Lee, *Anal. Biochem.*, 2009, **391**, 24–30.
25 D. Huska, J. Hubalek, V. Adam, D. Vajtr, A. Horna, L. Trnkova, L. Havel and R. Kizek, *Talanta*, 2009, **79**, 402–411.
26 J. H. Min, M. K. Woo, H. Y. Yoon, J. W. Jang, J. H. Wu, C. S. Lim and Y. K. Kim, *Anal. Biochem.*, 2014, **447**, 114–118.
27 S. H. Lim, F. Bestvater, P. Buchy, S. Mardy and A. D. C. Yu, *Sensors*, 2009, **9**, 5590–5599.
28 L. B. Nie, X. L. Wang, S. Li and H. Chen, *Anal. Sci.*, 2009, **25**, 1327–1331.
29 F. Patolsky, Y. Weizmann, E. Katz and I. Willner, *Angew. Chem., Int. Ed.*, 2003, **42**, 2372–2376.
30 Y. S. Xing, P. Wang, Y. C. Zang, Y. Q. Ge, Q. H. Jin, J. L. Zhao, X. Xu, G. Q. Zhao and H. J. Mao, *Analyst*, 2013, **138**, 3457–3462.
31 C. L. Cowles and X. S. Zhu, *Anal. Methods*, 2013, **5**, 801–804.
32 P. Hu, C. Z. Huang, Y. F. Li, J. Ling, Y. L. Liu, L. R. Fei and J. P. Xie, *Anal. Chem.*, 2008, **80**, 1819–1823.
33 X. L. Han, P. Mei, Y. Liu, Q. Xiao, F. L. Jiang and R. Li, *Spectrochim. Acta, Part A*, 2009, **74**, 781–787.
34 J. Kimling, M. Maier, B. Okenve, V. Kotaidis, H. Ballot and A. Plech, *J. Phys. Chem. B*, 2006, **110**, 15700–15707.
35 J. Polte, T. T. Ahner, F. Delissen, S. Sokolov, F. Emmerling, A. F. Thunemann and R. Kraehnert, *J. Am. Chem. Soc.*, 2010, **132**, 1296–1301.
36 M. A. Kilic, S. Spiro and G. R. Moore, *Protein Sci.*, 2003, **12**, 1663–1674.
37 J. R. Lakowicz, *Principles of Fluorescence Spectroscopy*, Springer, New York, 2006.
38 Q. Xiao, H. N. Qiu, S. Huang, C. S. Huang, W. Su, B. Q. Hu and Y. Liu, *Mol. Biol. Rep.*, 2013, **40**, 5781–5789.
39 T. Takahashi and S. Kuyucak, *Biophys. J.*, 2003, **84**, 2256–2263.
40 S. Aime, L. Frullano and S. G. Crich, *Angew. Chem., Int. Ed.*, 2002, **41**, 1017–1019.

41 K. Bartling, A. Sambanis and R. W. Rousseau, *Cryst. Growth Des.*, 2007, **7**, 569–575.
42 D. M. Lawson, P. J. Artymiuk, S. J. Yewdall, J. M. A. Smith, J. C. Livingstone, A. Treffry, A. Luzzago, S. Levi, P. Arosio, G. Cesareni, C. D. Thomas, W. V. Shaw and P. M. Harrison, *Nature*, 1991, **349**, 541–544.
43 A. Datta, S. Chatterjee, A. K. Sinha, S. N. Bhattacharyya and A. Saha, *J. Lumin.*, 2006, **121**, 553–560.
44 J. T. Vivian and P. R. Callis, *Biophys. J.*, 2001, **80**, 2093–2109.
45 A. Kowalska-Baron, K. Galecki, K. Rozniakowski, B. Kolesinska, Z. J. Kaminski and S. Wysocki, *Spectrochim. Acta, Part A*, 2014, **128**, 830–837.
46 I. Yamashita, *Abstr. Pap. Am. Chem. Soc.*, 2005, **229**, U906.
47 H. Y. Han, Z. H. Sheng and H. G. Liang, *Mater. Lett.*, 2006, **60**, 3782–3785.
48 Y. Khalavka, B. Mingler, G. Friedbacher, G. Okrepka, L. Shcherbak and O. Panchuk, *Phys. Status Solidi A*, 2010, **207**, 370–374.
49 K. K. W. Wong and S. Mann, *Adv. Mater.*, 1996, **8**, 928.
50 J. B. Xiao, Y. L. Bai, Y. F. Wang, J. W. Chen and X. L. Wei, *Spectrochim. Acta, Part A*, 2010, **76**, 93–97.
51 J. Zhang, L. N. Chen, B. R. Zeng, Q. L. Kang and L. Z. Dai, *Spectrochim. Acta, Part A*, 2013, **105**, 74–79.
52 H. Herberhold, S. Marchal, R. Lange, C. H. Scheyhing, R. F. Vogel and R. Winter, *J. Mol. Biol.*, 2003, **330**, 1153–1164.
53 D. W. Yang, K. Matsubara, M. Yamaki, S. Ebina and K. Nagayama, *Biochim. Biophys. Acta, Protein Struct. Mol. Enzymol.*, 1994, **1206**, 173–179.
54 M. Weik and J. P. Colletier, *Acta Crystallogr., Sect. D: Biol. Crystallogr.*, 2010, **66**, 437–446.
55 H. Wu, S. H. Fan, H. Chen, J. Shen, Y. Y. Geng, L. Peng and H. L. Du, *Anal. Methods*, 2014, **6**, 4729–4733.
56 Z. Kriz, J. Klusak, Z. Kristofikova and J. Koca, *PLoS One*, 2013, **8**, 1–14.
57 R. Esfandiary, J. S. Hunjan, G. H. Lushington, S. B. Joshi and C. R. Middaugh, *Protein Sci.*, 2009, **18**, 2603–2614.
58 P. F. Liu, L. V. Avramova and C. Park, *Anal. Biochem.*, 2009, **389**, 165–170.
59 M. Giovanni and M. Pumera, *Electroanalysis*, 2012, **24**, 615–617.
60 Y. J. Hu, C. H. Chen, S. Zhou, A. M. Bai and Y. Ou-Yang, *Mol. Biol. Rep.*, 2012, **39**, 2781–2787.
61 M. Hossain, A. Y. Khan and G. S. Kumar, *PLoS One*, 2011, **6**, 1–12.
62 F. Li, H. Q. Zhang, B. Dever, X. F. Li and X. C. Le, *Bioconjugate Chem.*, 2013, **24**, 1790–1797.
63 B. L. V. Prasad, C. M. Sorensen and K. J. Klabunde, *Chem. Soc. Rev.*, 2008, **37**, 1871–1883.
64 A. Vallee, V. Humblot and C. M. Pradier, *Acc. Chem. Res.*, 2010, **43**, 1297–1306.
65 F. Y. Yeh, T. Y. Liu, I. H. Tseng, C. W. Yang, L. C. Lu and C. S. Lin, *Biosens. Bioelectron.*, 2014, **61**, 336–343.
66 R. Luo, Y. H. Li, X. J. Lin, F. Dong, W. Zhang, L. Yan, W. Cheng, H. X. Ju and S. J. Ding, *Sens. Actuators, B*, 2014, **198**, 87–93.
67 M. Pumera, M. Aldavert, C. Mills, A. Merkoci and S. Alegret, *Electrochim. Acta*, 2005, **50**, 3702–3707.
68 G. Tomoaia, P. T. Frangopol, O. Horovitz, L. D. Bobos, A. Mocanu and M. Tomoaia-Cotisel, *J. Nanosci. Nanotechnol.*, 2011, **11**, 7762–7770.
69 P. Arosio, T. G. Adelman and J. W. Drysdale, *J. Biol. Chem.*, 1978, **253**, 4451–4458.
70 J. W. Kim, A. E. Posey, G. D. Watt, S. H. Choi and P. T. Lillehei, *J. Nanosci. Nanotechnol.*, 2010, **10**, 1771–1777.
71 M. A. Kilic, E. Ozlu and S. Calis, *J. Biomed. Nanotechnol.*, 2012, **8**, 508–514.
72 S. S. Wang, X. T. Wang, M. M. Guo and J. S. Yu, *Chem. J. Chin. Univ.*, 2012, **33**, 1195–1204.
73 F. Bou-Abdallah, G. Zhao, G. Biasiotto, M. Poli, P. Arosio and N. D. Chasteen, *J. Am. Chem. Soc.*, 2008, **130**, 17801–17811.
74 M. Shen, W. P. Jia, Y. J. You, Y. Hu, F. Li, S. D. Tian, J. Li, Y. X. Jin and D. M. Han, *Nanoscale Res. Lett.*, 2013, **8**, 1–6.

6 ZÁVĚR

Práce se zabývá studiem interakcí proteinů s kovy s využitím multiinstrumentálního přístupu. V literárním přehledu jsou popsány významné skupiny kov-vazných proteinů rozdělené na základě jejich funkce v organismu. Jedná se o transportní a zásobní kov-vazné proteiny, metaloenzymy, metaloproteiny singnální transdukce, metaloproteiny transkripční regulace a imunitní metaloproteiny. Literární část je doplněna přehledovým článkem o využití apoferitinu v nanomedicíně publikovaném v časopise Nanomedicine. Dále je pak podán přehled o využití běžně využívaných analytických metod pro sledování těchto biomolekul; kapalinová chromatografie, imunochemické metody, spektrofotometrické a elektrochemické metody.

Výsledková část je rozdělena na dva celky. První je zaměřen na separaci a detekci kov-vazného proteinu laktoferinu za využití iontově výměnné kapalinové chromatografie s využitím monolytické kolony a off-line fotometrickou detekcí pomocí Pyrogallové červeně, Biuretova a Bradfordova činidla. Optimalizovanou metodou byly analyzovány vzorky slin. Z výsledků byla patrná vyšší hladina laktoferinu u osoby trpící celiakií. Dále byla navržena a popsána metodika využívající izolaci a separaci laktoferinu pomocí paramagnetických částic modifikovaných protilátkami proti laktoferinu. Pro detekci byly využity protilátky značené křenovou peroxidázou a jejich interakce v prostředí substrátu TMB. Detekce výsledného produktu byla realizována jak elektrochemicky, tak spektrofotometricky a obě metody byly mezi sebou korelovány.

V druhé části se práce zabývá studiem interakce proteinů s kovy. Prvním dílčím cílem bylo sledování interakce fragmentů metalothioneinu s cisplatinou pro objasnění vzniku rezistence organismu na cytostatická léčiva. V rámci studie byly sledovány redoxní parametry vybraných fragmentů metalothioneinu za různých fyzikálních a chemických podmínek. Z dosažených výsledků je patrné, že nejvíce je zvýšená interakce u konzervativních aminokyselin, které byly substituovány na více jak jedné pozici vně cysteinových klastrů. Další dílčí část je formulována do dvou článků zaměřených na interakci kov-vazných proteinů s CdTe kvantovými tečkami. Ve článku „Study of interaction between metallothionein and CdTe quantum dots“ byl korelován průběh

chromatogramu metalothioneinu, CdTe QDs a jejich interakce. Celá studie byla podpořena spektrofotometrickou a elektrochemickou analýzou poskytující ucelený pohled na probíhající interakci. Poslední článek disertační práce se zabývá vývojem postupu pro syntézu CdTe QDs uvnitř struktury apoferitinu a jeho následnou interakcí se zlatými nanočásticemi konjugovaných s paramagnetickými částicemi značenou oligonukleotidovou sondou. Tvorba nanokonstruktu byla ověřena pomocí spektrofotometrických a elektrochemických metod. Práce ukazuje, že multiinstrumentální přístup může být velmi vhodným nástrojem pro studium kovů s proteiny v oblasti jejich separace, ale také pro sledování jejich vzájemné interakce.

7 ZDROJE INFORMACÍ

AKIMOTO, M., E. HOKAZONO, et al., Highly sensitive reversed-phase high-performance liquid chromatography assay for the detection of Tamm-Horsfall protein in human urine. *Annals of Clinical Biochemistry*.2016, **53**(1): 75-84.

ALHAZMI, H. A., M. NACHBAR, et al., Affinity capillary electrophoresis (ACE) for fast prediction of protein selectivity to metal ions. *Journal of Biological Inorganic Chemistry*.2014, **19**: S876-S877.

AMMONS, M. C. and V. COPIE, Mini-review: Lactoferrin: a bioinspired, anti-biofilm therapeutic. *Biofouling*.2013, **29**(4): 443-455.

AMREIN, B., M. SCHMID, et al., Identification of two-histidines one-carboxylate binding motifs in proteins amenable to facial coordination to metals. *Metallomics*.2012, **4**(4): 379-388.

ANDERSON, L., Candidate-based proteomics in the search for biomarkers of cardiovascular disease. *Journal of Physiology-London*.2005, **563**(1): 23-60.

ARAKAWA, T., Y. KITA, et al., Solvent modulation of column chromatography. *Protein and Peptide Letters*.2008, **15**(6): 544-555.

ARNOLD, F. H., METAL-AFFINITY SEPARATIONS - A NEW DIMENSION IN PROTEIN PROCESSING. *Bio-Technology*.1991, **9**(2): 151-156.

ASKWITH, C. and J. KAPLAN, Iron and copper transport in yeast and its relevance to human disease. *Trends in Biochemical Sciences*.1998, **23**(4): 135-138.

ATANASSOVA, A., M. HOEGBOM, et al. (2008). High throughput methods for analyzing transition metals in proteins on a microgram scale. Methods in Molecular Biology. B. Kobe, M. Guss and T. Huber. **426:** 319-330.

ATANASSOVA, A., R. LAM, et al., A high-performance liquid chromatography method for determining transition metal content in proteins. *Analytical Biochemistry*.2004, **335**(1): 103-111.

BABOR, M., S. GERZON, et al., Prediction of transition metal-binding sites from apo protein structures. *Proteins-Structure Function and Bioinformatics*.2008, **70**(1): 208-217.

BAHADIR, E. B. and M. K. SEZGINTURK, Applications of electrochemical immunosensors for early clinical diagnostics. *Talanta*.2015, **132**: 162-174.

BAI, Y. (2015). Detecting Protein-Protein Interactions by Gel Filtration Chromatography. Protein-Protein Interactions: Methods and Applications, 2nd Edition. C. L. Meyerkord and H. Fu. **1278:** 223-232.

BAKER, H. M. and E. N. BAKER, Lactoferrin and iron: structural and dynamic aspects of binding and release. *Biometals*.2004, **17**(3): 209-216.

BAKER, H. M. and E. N. BAKER, A structural perspective on lactoferrin function. *Biochemistry and Cell Biology*.2012, **90**(3): 320-328.

BAKER, H. M. and E. N. BAKER, A structural perspective on lactoferrin function. *Biochemistry and Cell Biology-Biochimie Et Biologie Cellulaire*.2012, **90**(3): 320-328.

BARBATO, J. C., O. CATANESCU, et al., Targeting of metallothionein by L-homocysteine - A novel mechanism for disruption of zinc and redox homeostasis. *Arteriosclerosis Thrombosis and Vascular Biology*.2007, **27**(1): 49-54.

BARONDEAU, D. P., C. J. KASSMANN, et al., Nickel superoxide dismutase structure and mechanism. *Biochemistry*.2004, **43**(25): 8038-8047.

BECKER, R., G. SCHWARZ, et al., Software assisted data analysis for relative quantification of differentially metal labeled proteins based on HPLC/ESI-MS and -MS/MS experiments. *Journal of Mass Spectrometry*.2015, **50**(10): 1120-1123.

BERKOVSKY, A. L. and P. P. POTAPOV, Development of a purification procedure for the placental protein 14 involving metal-chelate affinity chromatography and hydrophobic interaction chromatography. *Journal of Chromatography B*.1997, **692**(2): 273-279.

BERLUTTI, F., F. PANTANELLA, et al., Antiviral Properties of Lactoferrin-A Natural Immunity Molecule. *Molecules*.2011, **16**(8): 6992-7018.

BESOLD, A. N. and S. L. J. MICHEL, Neural Zinc Finger Factor/Myelin Transcription Factor Proteins: Metal Binding, Fold, and Function. *Biochemistry*.2015, **54**(29): 4443-4452.

BIRGENS, H. S., L. O. KRISTENSEN, et al., Lactoferrin-mediated transfer of iron to intracellular ferritin in human-monocytes. *European Journal of Haematology*.1988, **41**(1): 52-57.

BISCHOFF, R. and H. SCHLUETER, Amino acids: Chemistry, functionality and selected non-enzymatic post-translational modifications. *Journal of Proteomics*.2012, **75**(8): 2275-2296.

BISSERIER, M., M. BERTHOUZE-DUQUESNES, et al., Carabin Protects Against Cardiac Hypertrophy by Blocking Calcineurin, Ras, and Ca2+/Calmodulin-Dependent Protein Kinase II Signaling. *Circulation*.2015, **131**(4): 390-U449.

BOBALY, B., V. MIKOLA, et al., Recovery of Proteins Affected by Mobile Phase Trifluoroacetic Acid Concentration in Reversed-Phase Chromatography. *Journal of Chromatographic Science*.2015, **53**(7): 1078-1083.

BONHAM, C. A., A. J. STEEVENSZ, et al., Investigating redox regulation of protein tyrosine phosphatases using low pH thiol labeling and enrichment strategies coupled to MALDI-TOF mass spectrometry. *Methods*.2014, **65**(2): 190-200.

BORGMANN, S., G. HARTWICH, et al. (2005). Amperometric Enzyme Sensors based on Direct and Mediated Electron Transfer. Electrochemistry of Nucleic Acids and Proteins: Towards Electrochemical Sensors for Genomics and Proteomics. E. Palecek, F. Scheller and J. Wang. **1:** 599-655.

BOZHKOV, A., V. PADALKO, et al., Resistance to heavy metal toxicity in organisms under chronic exposure. *Indian Journal of Experimental Biology*.2010, **48**(7): 679-696.

BRADLEY, J. M., N. E. LE BRUN, et al., Ferritins: furnishing proteins with iron. *Journal of Biological Inorganic Chemistry*.2016, **21**(1): 13-28.

BRORSON, K. and A. Y. JIA, Therapeutic monoclonal antibodies and consistent ends: terminal heterogeneity, detection, and impact on quality. *Current Opinion in Biotechnology*.2014, **30**: 140-146.

BRUNNEKREEFT, J. W. I. and H. H. M. EIDHOF, Improved rapid procedure for simultaneous determinations of hemoglobins a(1a) a(1b), a(1c), f, c, and s, with indication for acetylation or carbamylation by cation-exchange liquid-chromatography. *Clinical Chemistry*.1993, **39**(12): 2514-2518.

BUERGERS, A. C. and E. LAMMERT, Extraerythrocytic hemoglobin - A possible oxygen transporter in human malignant tumors. *Medical Hypotheses*.2011, **77**(4): 580-583.

BUTCHER, H., W. KENNETTE, et al., A sensitive time-resolved fluorescent immunoassay for metallothionein protein. *Journal of Immunological Methods*.2003, **272**(1-2): 247-256.

BUTTERFIELD, D. A., M. PERLUIGI, et al., Oxidative stress in Alzheimer's disease brain: New insights from redox proteomics. *European Journal of Pharmacology*.2006, **545**(1): 39-50.

BUTTERFIELD, D. A., T. T. REED, et al., Elevated levels of 3-nitrotyrosine in brain from subjects with amnestic mild cognitive impairment: Implications for the role of nitration in the progression of Alzheimer's disease. *Brain Research*.2007, **1148**: 243-248.

CAMPANELLA, B. and E. BRAMANTI, Detection of proteins by hyphenated techniques with endogenous metal tags and metal chemical labelling. *Analyst*.2014, **139**(17): 4124-4153.

CARDOSO, M. M., I. N. PECA, et al., Antibody-Conjugated Nanoparticles for Therapeutic Applications. *Current Medicinal Chemistry*.2012, **19**(19): 3103-3127.

CARLSSON, N., A. BORDE, et al., Quantification of protein concentration by the Bradford method in the presence of pharmaceutical polymers. *Anal. Biochem*.2011, **411**(1): 116-121.

CARRER, C., M. STOLZ, et al., Removing coordinated metal ions from proteins: a fast and mild method in aqueous solution. *Analytical and Bioanalytical Chemistry*.2006, **385**(8): 1409-1413.

CASALIS, L., F. BANO, et al., Ultrasensitive protein detection in nano-immuno assays based on DNA directed immobilization and atomic force microscopy nanografting. *European Biophysics Journal with Biophysics Letters*.2011, **40**: 41-41.

CELLIER, M. F., P. COURVILLE, et al., Nramp1 phagocyte intracellular metal withdrawal defense. *Microbes and Infection*.2007, **9**(14-15): 1662-1670.

CRUZ-HUERTA, E., D. MARTINEZ MAQUEDA, et al., Short communication: Identification of iron-binding peptides from whey protein hydrolysates using iron (III)-immobilized metal ion affinity chromatography and reversed phase-HPLC-tandem mass spectrometry. *Journal of Dairy Science*.2016, **99**(1): 77-82.

DAI, Y., J. ZHEN, et al., Analysis of the complex formation, interaction and electron transfer pathway between the "open" conformation of NADPH-cytochrome P450 reductase and aromatase. *Steroids*.2015, **101**: 116-124.

DALAL, S., S. RAGHAVA, et al., Single-step purification of recombinant green fluorescent protein on expanded beds of immobilized metal affinity chromatography media. *Biochemical Engineering Journal*.2008, **42**(3): 301-307.

DASARI, S. and P. B. TCHOUNWOU, Cisplatin in cancer therapy: Molecular mechanisms of action. *European Journal of Pharmacology*.2014, **740**: 364-378.

DAUTER, Z., Use of polynuclear metal clusters in protein crystallography. *Comptes Rendus Chimie*.2005, **8**(11-12): 1808-1814.

DE LA CALLE GUNTINAS, M. B., G. BORDIN, et al., Identification, characterization and determination of metal-binding proteins by liquid chromatography. A review. *Analytical and Bioanalytical Chemistry*.2002, **374**(3): 369-378.

DIACONU, I., C. CRISTEA, et al., Electrochemical immunosensors in breast and ovarian cancer. *Clinica Chimica Acta*.2013, **425**: 128-138.

DOROUDI, M., Z. SCHWARTZ, et al., Membrane-mediated actions of 1,25-dihydroxy vitamin D3: A review of the roles of phospholipase A(2) activating protein and Ca2+/calmodulin-dependent protein kinase II. *Journal of Steroid Biochemistry and Molecular Biology*.2015, **147**: 81-84.

DOZ, F., N. ROOSEN, et al., Metallothionein and anticancer agents - the role of metallothionein in cancer-chemotherapy. *Journal of Neuro-Oncology*.1993, **17**(2): 123-129.

DRAKESMITH, H. and A. M. PRENTICE, Hepcidin and the Iron-Infection Axis. *Science*.2012, **338**(6108): 768-772.

DROZD, A. and A. KREZEL, Zn(II)-binding diversity of human metallothioneins isoforms - insights into protein stability and cellular functions. *Febs Journal*.2014, **281**: 542-542.

DUONG-LY, K. C. and S. B. GABELLI (2014). Using Ion Exchange Chromatography to Purify a Recombinantly Expressed Protein. Laboratory Methods in Enzymology: Protein, Pt C. J. Lorsch. **541:** 95-103.

EIDE, D. J., The molecular biology of metal ion transport in Saccharomyces cerevisiae. *Annual Review of Nutrition*.1998, **18**: 441-469.

EL-FAKHARANY, E. M., L. SANCHEZ, et al., Effectiveness of human, camel, bovine and sheep lactoferrin on the hepatitis C virus cellular infectivity: comparison study. *Virology Journal*.2013, **10**: 199-Article No.: 199.

ERIKSON, K. M., J. L. BEARD, et al., Distribution of brain iron, ferritin, and transferrin in the 28-day-old piglet. *Journal of Nutritional Biochemistry*.1998, **9**(5): 276-284.

FIELD, A. and J. FIELD, Melamine and cyanuric acid do not interfere with Bradford and Ninhydrin assays for protein determination. *Food Chem*.2010, **121**(3): 912-917.

FIORINA, J. C., I. AIMONE-GASTIN, et al., Total urinary protein assays: pyrogallol red versus coomassie blue. *Annales De Biologie Clinique*.2001, **59**(2): 187-192.

FORBES, J. R. and P. GROS, Iron, manganese, and cobalt transport by Nramp1 (Slc11a1) and Nramp2 (Slc11a2) expressed at the plasma membrane. *Blood*.2003, **102**(5): 1884-1892.

FRAGA, C. G., Relevance, essentiality and toxicity of trace elements in human health. *Molecular Aspects of Medicine*.2005, **26**(4-5): 235-244.

GAO, Z., H. HOU, et al. (2010). Protein Crystallography for Metalloproteins.

GARVEY, J. S., D. G. THOMAS, et al. (1987). Elisa for metallothionein. Kagi, J. H. R. And Y. Kojima**:** 335-342.

GIANNOTTI, M. I., I. CABEZA DE VACA, et al., Direct Measurement of the Nanomechanical Stability of a Redox Protein Active Site and Its Dependence upon Metal Binding. *Journal of Physical Chemistry B*.2015, **119**(36): 12050-12058.

GIORGIO, M., E. MIGLIACCIO, et al., Electron transfer between cytochrome c and p66(Shc) generates reactive oxygen species that trigger mitochondrial apoptosis. *Cell*.2005, **122**(2): 221-233.

GOLDRING, J. P. D. (2015). Spectrophotometric Methods to Determine Protein Concentration. Western Blotting: Methods and Protocols. B. T. Kurien and R. H. Scofield. **1312:** 41-47.

GONZALEZ-IGLESIAS, H., L. ALVAREZ, et al., Metallothioneins (MTs) in the human eye: a perspective article on the zinc-MT redox cycle. *Metallomics*.2014, **6**(2): 201-208.

GOODALL, S., M. L. JONES, et al., Monoclonal antibody-targeted polymeric nanoparticles for cancer therapy-future prospects. *Journal of Chemical Technology and Biotechnology*.2015, **90**(7): 1169-1176.

GU, H. and W. CHANG, Three-dimensional protein shape rendering in magnetized solution with Lambert-Beer law. *Applied Optics*.2012, **51**(20): 4827-4832.

GUO, L., L. A. LICHTEN, et al., STAT5-glucocorticoid receptor interaction and MTF-1 regulate the expression of ZnT2 (Slc30a2) in pancreatic acinar cells. *Proceedings of the National Academy of Sciences of the United States of America*.2010, **107**(7): 2818-2823.

HARDING, M. M., M. W. NOWICKI, et al., Metals in protein structures: a review of their principal features. *Crystallography Reviews*.2010, **16**(4): 247-302.

HARDISON, R. C., Evolution of Hemoglobin and Its Genes. *Cold Spring Harbor Perspectives in Medicine*.2012, **2**(12).

HARDMAN, K. D., Crystallography of a metal-containing protein, concanavalin A. *Advances in experimental medicine and biology*.1973, **40**: 103-123.

HARLEY, R., Pulmonary fibrosis in alveolar proteinosis: metals and mechanisms. *Virchows Archiv*.2011, **459**: S133-S133.

HARRISON-FINDIK, D. D., D. SCHAFER, et al., Alcohol metabolism-mediated oxidative stress down-regulates hepcidin transcription and leads to increased duodenal iron transporter expression. *Journal of Biological Chemistry*.2006, **281**(32): 22974-22982.

HE, X. and S. A. PATFIELD, Immuno-PCR Assay for Sensitive Detection of Proteins in Real Time. *Methods in molecular biology (Clifton, N.J.)*.2015, **1318**: 139-148.

HEDIGER, M. A., Membrane permeability - The diversity of transmembrane transport processes. *Current Opinion in Cell Biology*.1997, **9**(4): 543-546.

HOFF, W. D., B. DEVREESE, et al., Chemical reactivity and spectroscopy of the thiol ester-linked p-coumaric acid chromophore in the photoactive yellow protein from Ectothiorhodospira halophila. *Biochemistry*.1996, **35**(4): 1274-1281.

HOFFMAN, B. M., ENDOR of metalloenzymes. *Accounts of Chemical Research*.2003, **36**(7): 522-529.

HOOD, M. I., B. L. MORTENSEN, et al., Identification of an Acinetobacter baumannii Zinc Acquisition System that Facilitates Resistance to Calprotectin-mediated Zinc Sequestration. *Plos Pathogens*.2012, **8**(12).

HOOPER, N. M., D. R. TAYLOR, et al., Mechanism of the metal-mediated endocytosis of the prion protein. *Biochemical Society Transactions*.2008, **36**: 1272-1276.

HORNEF, M. W., M. J. WICK, et al., Bacterial strategies for overcoming host innate and adaptive immune responses. *Nature Immunology*.2002, **3**(11): 1033-1040.

HU, Y., W. GUO, et al., Protein- and Peptide-directed Approaches to Fluorescent Metal Nanoclusters. *Israel Journal of Chemistry*.2015, **55**(6-7): 682-697.

HUANG, D., F. GENG, et al., Biomimetic interactions of proteins with functionalized cadmium sulfide quantum dots. *Colloids and Surfaces a-Physicochemical and Engineering Aspects*.2011, **392**(1): 191-197.

HUANG, L., X. HU, et al., Rapid Detection of New Delhi Metallo-beta-Lactamase Gene and Variants Coding for Carbapenemases with Different Activities by Use of a

PCR-Based In Vitro Protein Expression Method. *Journal of Clinical Microbiology*.2014, **52**(6): 1947-1953.

HUANG, L. E., V. HO, et al., Erythropoietin gene regulation depends on heme-dependent oxygen sensing and assembly of interacting transcription factors. *Kidney International*.1997, **51**(2): 548-552.

HUNTER, T. and M. KARIN, The regulation of transcription by phosphorylation. *Cell*.1992, **70**(3): 375-387.

HYNEK, D., L. KREJCOVA, et al., Metallomics Study of Lead-Protein Interactions in Albumen by Electrochemical and Electrophoretic Methods. *International Journal of Electrochemical Science*.2012, **7**(2): 943-964.

CHAKRAVORTY, D. K., B. WANG, et al., Solution NMR refinement of a metal ion bound protein using metal ion inclusive restrained molecular dynamics methods. *Journal of Biomolecular Nmr*.2013, **56**(2): 125-137.

CHAN, H. M., M. G. CHERIAN, et al., Quantification of metallothionein isoforms using an enzyme-linked-immunosorbent-assay (elisa) with 2 specific antisera. *Toxicology and Applied Pharmacology*.1992, **116**(2): 267-270.

CHANDRA, R. K., Nutrition, immunity and infection: From basic knowledge of dietary manipulation of immune responses to practical application of ameliorating suffering and improving survival. *Proceedings of the National Academy of Sciences of the United States of America*.1996, **93**(25): 14304-14307.

CHASSAIGNE, H. and J. SZPUNAR, The coupling of reversed-phase HPLC with ICP-MS in bioinorganic analysis. *Analusis*.1998, **26**(6): M48-M51.

CHEN, C., Q. XIE, et al., Recent advances in electrochemical glucose biosensors: a review. *Rsc Advances*.2013, **3**(14): 4473-4491.

CHEN, N., Y. HE, et al., The cytotoxicity of cadmium-based quantum dots. *Biomaterials*.2012, **33**(5): 1238-1244.

CHO, I.-H. and J. IRUDAYARAJ, In-situ immuno-gold nanoparticle network ELISA biosensors for pathogen detection. *International Journal of Food Microbiology*.2013, **164**(1): 70-75.

IMAMOTO, Y., H. KOSHIMIZU, et al., Roles of amino acid residues near the chromophore of photoactive yellow protein. *Biochemistry*.2001, **40**(15): 4679-4685.

ISAKSSON, J., S. NYSTOM, et al., Does a Fast Nuclear Magnetic Resonance Spectroscopy- and X-Ray Crystallography Hybrid Approach Provide Reliable

Structural Information of Ligand-Protein Complexes? A Case Study of Metalloproteinases. *Journal of Medicinal Chemistry*.2009, **52**(6): 1712-1722.

ISLAM, E. U., E. YANG XIAO, et al., Assessing potential dietary toxicity of heavy metals in selected vegetables and food crops. *Journal of Zhejiang University-Science B*.2007, **8**(1): 1-13.

JABADO, N., A. JANKOWSKI, et al., Natural resistance to intracellular infections: Natural resistance-associated macrophage protein 1 (NRAMP1) functions as a pH-dependent manganese transporter at the phagosomal membrane. *Journal of Experimental Medicine*.2000, **192**(9): 1237-1247.

JAVAID, M. A., A. S. AHMED, et al., Saliva as a diagnostic tool for oral and systemic diseases. *Journal of oral biology and craniofacial research*.2016, **6**(1): 66-75.

KIMURA, T., N. ITOH, et al., Mechanisms of Heavy Metal Sensing by Metal Response Element-binding Transcription Factor-1. *Journal of Health Science*.2009, **55**(4): 484-494.

KNAPEN, D., H. REYNDERS, et al., Metallothionein gene and protein expression as a biomarker for metal pollution in natural gudgeon populations. *Aquatic Toxicology*.2007, **82**(3): 163-172.

KOHNO, M., S. TANIMURA, et al., Targeting the Extracellular Signal-Regulated Kinase Pathway in Cancer Therapy. *Biological & Pharmaceutical Bulletin*.2011, **34**(12): 1781-1784.

KOVACS, E., V. HARMAT, et al., Structure and mechanism of calmodulin binding to a signaling sphingolipid reveal new aspects of lipid-protein interactions. *Faseb Journal*.2010, **24**(10): 3829-3839.

KOVURI, V. A., P. CRAIG, et al., Recognition of metal ions using ProMOL to improve protein function assignation. *Faseb Journal*.2014, **28**(1).

KOWALSKI, K., T. GOSZCZYNSKI, et al., Synthesis of Lysozyme-Metallacarborane Conjugates and the Effect of Boron Cluster Modification on Protein Structure and Function. *Chembiochem*.2015, **16**(3): 424-431.

KUMAR, R., A real-time immuno-PCR assay for the detection of transgenic Cry1Ab protein. *European Food Research and Technology*.2012, **234**(1): 101-108.

KUMAR, S. and A. BARTH, Effects of Ions on Ligand Binding to Pyruvate Kinase: Mapping the Binding Site with Infrared Spectroscopy. *Journal of Physical Chemistry B*.2011, **115**(20): 6784-6789.

KURAHASHI, T., A. MIYAZAKI, et al., Extensive investigations on oxidized amino acid residues in H2O2-treated Cu,Zn-SOD protein with LC-ESI-Q-TOF-MS, MS/MS for the determination of the copper-binding site. *Journal of the American Chemical Society*.2001, **123**(38): 9268-9278.

LANG, K. M. H., J. KITTELINANN, et al., A comprehensive molecular dynamics approach to protein retention modeling in ion exchange chromatography. *Journal of Chromatography A*.2015, **1381**: 184-193.

LANGMADE, S. J., R. RAVINDRA, et al., The transcription factor MTF-1 mediates metal regulation of the mouse ZnT1 gene. *Journal of Biological Chemistry*.2000, **275**(44): 34803-34809.

LAROCHELLE, O., G. STEWART, et al., Characterization of the mouse metal-regulatory-element-binding proteins, metal element protein-1 and metal regulatory transcription factor-1. *Biochemical Journal*.2001, **353**: 591-601.

LAZO, J. S., Y. KONDO, et al., Enhanced sensitivity to oxidative stress in cultured embryonic-cells from transgenic mice deficient in metallothionein-i and metallothionein-ii genes. *Journal of Biological Chemistry*.1995, **270**(10): 5506-5510.

LEE, T., T.-H. KIM, et al., Investigation of Hemoglobin/Gold Nanoparticle Heterolayer on Micro-Gap for Electrochemical Biosensor Application. *Sensors (Basel, Switzerland)*.2016, **16**(5).

LEGRAND, D., E. ELASS, et al., Lactoferrin: a modulator of immune and inflammatory responses. *Cellular and Molecular Life Sciences*.2005, **62**(22): 2549-2559.

LEI, G., L. LIU, et al., New alpha-amino phenylalanine tetrazole ligand for immobilized metal affinity chromatography of proteins. *Journal of Separation Science*.2008, **31**(16-17): 3002-3008.

LI, M. X. and P. M. HWANG, Structure and function of cardiac troponin C (TNNC1): Implications for heart failure, cardiomyopathies, and troponin modulating drugs. *Gene*.2015, **571**(2): 153-166.

LI, W., A. HELLSTEN, et al. (2004). Enhanced expression of natural resistance-associated macrophage protein 1 in atherosclerotic lesions may be associated with oxidized lipid-induced apoptosis. Signal Transduction Pathways, Chromatin Structure, and Gene Expression Mechanisms as Therapeutic Targets. M. Diederich. **1030:** 202-207.

LIDDINGTON, R. (1994). X-ray crystallography of partially liganded structures. Methods in Enzymology; Hemoglobins, Part C: Biophysical methods. J. Everse, K. D. Vandegriff and R. M. Winslow. **232:** 15-26.

LICHTEN, L. A., M.-S. RYU, et al., MTF-1-Mediated Repression of the Zinc Transporter Zip10 Is Alleviated by Zinc Restriction. *Plos One*.2011, **6**(6).

LIN, M.-C., Y.-C. LIU, et al., PTEN interacts with metal-responsive transcription factor 1 and stimulates its transcriptional activity. *Biochemical Journal*.2012, **441**: 367-377.

LIU, G.-L., J.-F. WANG, et al., Advances in heavy metal ions immunoassay. *Sheng wu gong cheng xue bao = Chinese journal of biotechnology*.2006, **22**(6): 877-881.

LIU, J. Z., S. JELLBAUER, et al., Zinc Sequestration by the Neutrophil Protein Calprotectin Enhances Salmonella Growth in the Inflamed Gut. *Cell Host & Microbe*.2012, **11**(3): 227-239.

LONG, X., C. ZHANG, et al., A novel method for study of the aggregation of protein induced by metal ion aluminum(III) using resonance Rayleigh scattering technique. *Spectrochimica Acta Part a-Molecular and Biomolecular Spectroscopy*.2008, **69**(1): 71-77.

LU, C.-H., Y.-F. LIN, et al., Prediction of Metal Ion-Binding Sites in Proteins Using the Fragment Transformation Method. *Plos One*.2012, **7**(6).

MARKOWSKI, J., T. TYSZKIEWICZ, et al., Metal-proteinase ADAM12, kinesin 14 and checkpoint suppressor 1 as new molecular markers of laryngeal carcinoma. *European Archives of Oto-Rhino-Laryngology*.2009, **266**(10): 1501-1507.

MARSHALL, C. B., T. NISHIKAWA, et al., Calmodulin and STIM proteins: Two major calcium sensors in the cytoplasm and endoplasmic reticulum. *Biochemical and Biophysical Research Communications*.2015, **460**(1): 5-21.

MASSARI, M. E. and C. MURRE, Helix-loop-helix proteins: Regulators of transcription in eucaryotic organisms. *Molecular and Cellular Biology*.2000, **20**(2): 429-440.

MAYEUR, S., S. SPAHIS, et al., Lactoferrin, a Pleiotropic Protein in Health and Disease. *Antioxidants & Redox Signaling*.2016, **24**(14): 813-835.

MEDYANTSEVA, E. P., M. G. VERTLIB, et al., Metal ions as effectors of enzymes. *Uspekhi Khimii*.1998, **67**(3): 252-260.

MEIER, S. M., M. V. BABAK, et al., Efficiently Detecting Metallodrug-Protein Adducts: Ion Trap versus Time-of-Flight Mass Analyzers. *Chemmedchem*.2014, **9**(7): 1351-1355.

MENTLER, M., A. WEISS, et al., A new method to determine the structure of the metal environment in metalloproteins: investigation of the prion protein octapeptide repeat Cu2+ complex. *European Biophysics Journal with Biophysics Letters*.2005, **34**(2): 97-112.

MICHALET, X., F. F. PINAUD, et al., Quantum dots for live cells, in vivo imaging, and diagnostics. *Science*.2005, **307**(5709): 538-544.

MOHAN, A., S. ANISHETTY, et al., Global metal-ion binding protein fingerprint: a method to identify motif-less metal-ion binding proteins. *Journal of Bioinformatics and Computational Biology*.2010, **8**(4): 717-726.

MOLLER, L. H., C. S. JENSEN, et al., Evaluation of a membrane desolvator for LC-ICP-MS analysis of selenium and platinum species for application to peptides and proteins. *Journal of Analytical Atomic Spectrometry*.2015, **30**(1): 277-284.

MOOS, T. and E. H. MORGAN, The metabolism of neuronal iron and its pathogenic role in neurological disease: review. *Ann N Y Acad Sci*.2004: 14-26.

MORENO-BONDI, M. C., M. E. BENITO-PENA, et al. (2012). Immuno-Like Assays and Biomimetic Microchips. Molecular Imprinting. K. Haupt. **325:** 111-164.

MOUTAFCHIEV, D. A. and L. M. SIRAKOV, Transferrin binding to the membranes of lactating rabbit mammary gland. Iron transfer from membranes to lactoferrin. *Zeitschrift fur medizinische Laboratoriumsdiagnostik*.1981, **22**(5): 264-271.

NARA, M. and M. TANOKURA, Infrared spectroscopic study of the metal-coordination structures of calcium-binding proteins. *Biochemical and Biophysical Research Communications*.2008, **369**(1): 225-239.

NELSON, N., Metal ion transporters and homeostasis. *Embo Journal*.1999, **18**(16): 4361-4371.

NGUYEN, T. T. T. N., J. OSTERGAARD, et al., A method for studies on interactions between a gold-based drug and plasma proteins based on capillary electrophoresis with inductively coupled plasma mass spectrometry detection. *Analytical and Bioanalytical Chemistry*.2015, **407**(28): 8497-8503.

OMIDFAR, K., F. KHORSAND, et al., New analytical applications of gold nanoparticles as label in antibody based sensors. *Biosensors & Bioelectronics*.2013, **43**: 336-347.

OUYANG, C.-Y., Y.-K. LIN, et al., Secretion of metal-binding proteins by a newly discovered OsmY homolog in Cupriavidus metallidurans for the biogenic synthesis of metal nanoparticles. *Rsc Advances*.2016, **6**(20): 16798-16801.

PALECEK, E. S., F ; WANG, J (2005). Electrochemistry of Nucleic Acids and Proteins: Towards Electrochemical Sensors for Genomics and Proteomics. Electrochemistry of Nucleic Acids and Proteins: Towards Electrochemical Sensors for Genomics and Proteomics. E. Palecek, F. Scheller and J. Wang. **1:** 1-790.

PARIMELZAGHAN, A., A. ANBARASU, et al., Gene Network Analysis of Metallo Beta Lactamase Family Proteins Indicates the Role of Gene Partners in Antibiotic Resistance and Reveals Important Drug Targets. *Journal of Cellular Biochemistry*.2016, **117**(6): 1330-1339.

PARSY, C. B., C. J. CHAPMAN, et al., Two-step method to isolate target recombinant protein from co-purified bacterial contaminant SlyD after immobilised metal affinity chromatography. *Journal of Chromatography B-Analytical Technologies in the Biomedical and Life Sciences*.2007, **853**(1-2): 314-319.

PASTUSZEWSKI, W., P. DZIEGIEL, et al., Prognostic significance of metallothionein, p53 protein and Ki-67 antigen expression in laryngeal cancer. *Anticancer Research*.2007, **27**(1A): 335-342.

PELLETIER, H. and J. KRAUT, Crystal-structure of a complex between electron-transfer partners, cytochrome-c peroxidase and cytochrome-c. *Science*.1992, **258**(5089): 1748-1755.

PENNISTON, J. T., A. J. CARIDE, et al., Alternative Pathways for Association and Dissociation of the Calmodulin-binding Domain of Plasma Membrane Ca2+-ATPase Isoform 4b (PMCA4b). *Journal of Biological Chemistry*.2012, **287**(35): 29664-29671.

PIN, S., P. VALAT, et al., Ligand-binding processes in hemoglobin - chemical-reactivity of iron studied by xanes spectroscopy. *Biophysical Journal*.1985, **48**(6): 997-1001.

POLANSKI, M. and N. L. ANDERSON, A list of candidate cancer biomarkers for targeted proteomics. *Biomarker insights*.2007, **1**: 1-48.

PORDEA, A., Metal-binding promiscuity in artificial metalloenzyme design. *Current Opinion in Chemical Biology*.2015, **25**: 124-132.

PORTNOY, M. E., L. T. JENSEN, et al., The distinct methods by which manganese and iron regulate the Nramp transporters in yeast. *Biochemical Journal*.2002, **362**: 119-124.

PRICE, R., A. POURSAID, et al., In vivo evaluation of matrix metalloproteinase responsive silk-elastinlike protein polymers for cancer gene therapy. *Journal of Controlled Release*.2015, **213**: 96-102.

PUPKOVA, V. I. and L. M. PRASOLOVA, Pyrogallol red technique is an alternative to routine urinary protein-determining methods. *Klin. Lab. Diagnost*.2007, (6): 17-21.

QIAO, S. P., C. LANG, et al., Metal induced self-assembly of designed V-shape protein into 2D wavy supramolecular nanostructure. *Nanoscale*.2016, **8**(1): 333-341.

RADISKY, D. and J. KAPLAN, Regulation of transition metal transport across the yeast plasma membrane. *Journal of Biological Chemistry*.1999, **274**(8): 4481-4484.

RAFFATELLU, M., M. D. GEORGE, et al., Lipocalin-2 Resistance Confers an Advantage to Salmonella enterica Serotype Typhimurium for Growth and Survival in the Inflamed Intestine. *Cell Host & Microbe*.2009, **5**(5): 476-486.

RALEIGH, J. A., S. C. CHOU, et al., A clinical study of hypoxia and metallothionein protein expression in squamous cell carcinomas. *Clinical Cancer Research*.2000, **6**(3): 855-862.

RAUDENSKA, M., J. GUMULEC, et al., Metallothionein polymorphisms in pathological processes. *Metallomics*.2014, **6**(1): 55-68.

RAUSCH, M. E., L. BEER, et al., A disintegrin and metalloprotease protein-12 as a novel marker for the diagnosis of ectopic pregnancy. *Fertility and Sterility*.2011, **95**(4): 1373-1378.

RIECHERS, A., J. SCHMIDT, et al., Heterogeneous transition metal-based fluorescence polarization (HTFP) assay for probing protein interactions. *Biotechniques*.2009, **47**(4): 837-841.

RIGUEIRA, L. M. B., D. A. P. D. LANA, et al., Identification of metal-binding to proteins in seed samples using RF-HPLC-UV, GFAAS and MALDI-TOF-MS. *Food Chemistry*.2016, **211**: 910-915.

ROBSON, R. M., D. E. GOLL, et al., DETERMINATION OF PROTEINS IN TRIS BUFFER BY BIURET REACTION. *Analytical Biochemistry*.1968, **24**(2): 339-&.

ROESIJADI, G. and J. E. MORRIS (1988). Enzyme-linked immunosorbent assay for metal-binding proteins of mytilus-edulis. Yentsch, C. M., F. C. Mague and P. K. Horan**:** 283-290.

ROHRER, J. S. and N. AVDALOVIC, Separation of human serum transferrin isoforms by high performance pellicular anion-exchange chromatography. *Protein Expression and Purification*.1996, **7**(1): 39-44.

ROCHA, E. R., A. SMITH, et al., Growth inhibition of Bacteroides fragilis by hemopexin: proteolytic degradation of hemopexin to overcome heme limitation. *FEMS Microbiol Lett*.2001, **199**(1): 73-78.

RUOTOLO, R., G. MARCHINI, et al., Membrane transporters and protein traffic networks differentially affecting metal tolerance: a genomic phenotyping study in yeast. *Genome Biology*.2008, **9**(4).

RUTHERFORD, J. C. and A. J. BIRD, Metal-responsive transcription factors that regulate iron, zinc, and copper homeostasis in eukaryotic cells. *Eukaryotic Cell*.2004, **3**(1): 1-13.

RUTTKAY-NEDECKY, B., L. NEJDL, et al., The Role of Metallothionein in Oxidative Stress. *International Journal of Molecular Sciences*.2013, **14**(3): 6044-6066.

SAEBEL, C. E., J. M. NEUREUTHER, et al., A spectrophotometric method for the determination of zinc, copper, and cobalt ions in metalloproteins using Zincon. *Analytical Biochemistry*.2010, **397**(2): 218-226.

SAENSEEHA, S., P. JANWAN, et al., A dot-elisa test using a gnathostoma spinigerum recombinant matrix metalloproteinase protein for the serodiagnosis of human gnathostomiasis. *Southeast Asian Journal of Tropical Medicine and Public Health*.2014, **45**(5): 990-996.

SAFO, M. K. and D. J. ABRAHAM (2003). X-ray crystallography of hemoglobins. Hemoglobin Disorders: Molecular Methods and Protocols. R. L. Nagel. **82:** 1-19.

SAGA, Y., H. HASHIMOTO, et al., Reversal of acquired cisplatin resistance by modulation of metallothionein in transplanted murine tumors. *International Journal of Urology*.2004, **11**(6): 407-415.

SAIER, M. H., JR., V. S. REDDY, et al., The Transporter Classification Database. *Nucleic Acids Research*.2014, **42**(D1): D251-D258.

SALVALAGLIO, M., M. PALONI, et al., A two level hierarchical model of protein retention in ion exchange chromatography. *Journal of Chromatography A*.2015, **1411**: 50-62.

SEBBIO, C., C. CARERE, et al., Interspecies variation in DNA damage induced by pollution. *Current Zoology*.2014, **60**(2): 308-321.

SEEVARATNAM, R., B. P. PATEL, et al., Comparison of Total Protein Concentration in Skeletal Muscle as Measured by the Bradford and Lowry Assays. *J. Biochem*.2009, **145**(6): 791-797.

SELWA, E., E. LAINE, et al., Differential role of calmodulin and calcium ions in the stabilization of the catalytic domain of adenyl cyclase CyaA from Bordetella pertussis. *Proteins-Structure Function and Bioinformatics*.2012, **80**(4): 1028-1040.

SHARGH, V. H., H. HONDERMARCK, et al., Antibody-targeted biodegradable nanoparticles for cancer therapy. *Nanomedicine*.2016, **11**(1): 63-79.

SHEARDOWN, H., R. M. CORNELIUS, et al., Measurement of protein adsorption to metals using radioiodination methods: a caveat. *Colloids and Surfaces B-Biointerfaces*.1997, **10**(1): 29-33.

SHI, K., F. CUI, et al., Metal Ions Guided Self-assembly of Therapeutic Proteins for Controllable Release: From Random to Ordered Aggregation. *Pharmaceutical Research*.2013, **30**(1): 269-279.

SHOVMAN, O., B. GILBURD, et al., The diagnostic utility of anti-cyclic citrullinated peptide antibodies, matrix metalloproteinase-3, rheumatoid factor, erythrocyte sedimentation rate, and C-reactive protein in patients with erosive and non-erosive rheumatoid arthritis. *Clinical & developmental immunology*.2005, **12**(3): 197-202.

SCHMIDT, A. C., B. STORR, et al., Influence of one- and two-dimensional gel electrophoresis procedure on metal-protein bindings examined by electrospray ionization mass spectrometry, inductively coupled plasma mass spectrometry, and ultrafiltration. *Talanta*.2011, **85**(2): 1118-1128.

SCHMIDT, M. H. and J. M. BERG (1992). Predictions of the occurrence and structure of metal-binding domains in gene regulatory proteins. Cold Spring Harbor Monograph Series; Transcriptional regulation. S. L. McKnight and K. R. Yamamoto. **22 PART 1-2:** 599-613.

SCHRODER, H. C., G. DI BELLA, et al., DNA damage and developmental defects after exposure to UV and heavy metals in sea urchin cells and embryos compared to other invertebrates. *Echinodermata*.2005, **39**: 111-137.

SILVA, A. S. and M. FALKENBERG, Analytical interference of quinolone antibiotics and quinine derived drugs on urinary protein determined by reagent strips and the pyrogallol red-molybdate protein assay. *Clin. Biochem*.2011, **44**(12): 1000-1004.

SIMONIAN, M. H. and J. A. SMITH, Spectrophotometric and colorimetric determination of protein concentration. *Current protocols in molecular biology / edited by Frederick M. Ausubel ... [et al.]*.2006, **Chapter 10**: Unit 10.11A-Unit 10.11A.

SKJOT-ARKIL, H., G. SCHETT, et al., Investigation of two novel biochemical markers of inflammation, matrix metalloproteinase and cathepsin generated fragments of C-reactive protein, in patients with ankylosing spondylitis. *Clinical and Experimental Rheumatology*.2012, **30**(3): 371-379.

SMITH, M. C., T. C. FURMAN, et al., CHELATING PEPTIDE-IMMOBILIZED METAL-ION AFFINITY-CHROMATOGRAPHY - A NEW CONCEPT IN AFFINITY-CHROMATOGRAPHY FOR RECOMBINANT PROTEINS. *Journal of Biological Chemistry*.1988, **263**(15): 7211-7215.

SOCHOR, J., M. RYVOLOVA, et al., Fully Automated Spectrometric Protocols for Determination of Antioxidant Activity: Advantages and Disadvantages. *Molecules*.2010, **15**(12): 8618-8640.

SOMMER-KNUDSEN, J. and A. BACIC, A micro-scale method for determining relative metal-binding affinities of proteins. *Molecular Biotechnology*.1997, **8**(3): 215-218.

SONG, Y., H. ZHANG, et al., Proteomic analysis of copper-binding proteins in excess copper-stressed rice roots by immobilized metal affinity chromatography and two-dimensional electrophoresis. *Biometals*.2014, **27**(2): 265-276.

SPAHL, D. U., D. BERENDJI-GRUN, et al., Regulation of zinc homeostasis by inducible NO synthase-derived NO: Nuclear translocation and intranuclear metallothionein Zn2+ release. *Proceedings of the National Academy of Sciences of the United States of America*.2003, **100**(24): 13952-13957.

STAUFFER, C. E., LINEAR STANDARD CURVE FOR FOLIN LOWRY DETERMINATION OF PROTEIN. *Analytical Biochemistry*.1975, **69**(2): 646-648.

SUN, C., H. YANG, et al., Controlling Assembly of Paired Gold Clusters within Apoferritin Nanoreactor for in Vivo Kidney Targeting and Biomedical Imaging. *Journal of the American Chemical Society*.2011, **133**(22): 8617-8624.

SZPUNAR, J., Advances in analytical methodology for bioinorganic speciation analysis: metallomics, metalloproteomics and heteroatom-tagged proteomics and metabolomics. *Analyst*.2005, **130**(4): 442-465.

TAINER, J. A., E. D. GETZOFF, et al., STRUCTURE AND MECHANISM OF COPPER, ZINC SUPEROXIDE-DISMUTASE. *Nature*.1983, **306**(5940): 284-287.

TAKEUCHI, T., T. MORI, et al., Conjugated-protein mimics with molecularly imprinted reconstructible and transformable regions that are assembled using space-

filling prosthetic groups. *Angewandte Chemie (International ed. in English)*.2014, **53**(47): 12765-12770.

THEOCHARIS, S. E., A. P. MARGELI, et al., Metallothionein: A multifunctional protein from toxicity to cancer. *International Journal of Biological Markers*.2003, **18**(3): 162-169.

THOMSON, A. J. and H. B. GRAY, Bio-inorganic chemistry. *Current Opinion in Chemical Biology*.1998, **2**(2): 155-158.

TOYAMA, T., Y. SHINKAI, et al., A convenient method to assess chemical modification of protein thiols by electrophilic metals. *Journal of Toxicological Sciences*.2013, **38**(3): 477-484.

TRUSHINSKAYA, G. V., V. I. SIMONOV, et al., Immune polyclonal anti-hiv serum and anti-hiv-1 gene protein gag monoclonal antibody-based enzyme-immunoassay system for detection of hiv-1 antigens. *Vestnik Rossiiskoi Akademii Meditsinskikh Nauk*.1992, (9-10): 43-47.

TURUNEN, P., H. L. PUHAKKA, et al., Extracellular superoxide dismutase with vaccinia virus anti-inflammatory protein 35K or tissue inhibitor of metalloproteinase-1: Combination gene therapy in the treatment of vein graft stenosis in rabbits. *Human Gene Therapy*.2006, **17**(4): 405-414.

TYTECA, E., J. DE VOS, et al., Applicability of linear and nonlinear retention-time models for reversed-phase liquid chromatography separations of small molecules, peptides, and intact proteins. *Journal of Separation Science*.2016, **39**(7): 1249-1257.

UEDA, E. K. M., P. W. GOUT, et al., Current and prospective applications of metal ion-protein binding. *Journal of chromatography. A*.2003, **988**(1): 1-23.

UEHARA, H. and V. A. RAO, Metal-Mediated Protein Oxidation: Applications of a Modified ELISA-Based Carbonyl Detection Assay for Complex Proteins. *Pharmaceutical Research*.2015, **32**(2): 691-701.

VANDERSLICE, N., A. S. MESSER, et al., Using HPSEC to quantify the effect of gamma-carboxylation on divalent metal-induced compaction of vkd-proteins and biological function. *Journal of Thrombosis and Haemostasis*.2015, **13**: 322-322.

VESSIERES, A., M. SALMAIN, et al., Carbonyl metallo immune assay: a new application for Fourier transform infrared spectroscopy. *Journal of Pharmaceutical and Biomedical Analysis*.1999, **21**(3): 625-633.

VINCENTI, M. P., L. A. WHITE, et al., Regulating expression of the gene for matrix metalloproteinase-1 (collagenase): Mechanisms that control enzyme activity,

transcription, and mRNA stability. *Critical Reviews in Eukaryotic Gene Expression*.1996, **6**(4): 391-411.

VOSS, J., L. SALWINSKI, et al., A method for distance determination in proteins using a designed metal ion binding site and site-directed spin labeling: Evaluation with T4 lysozyme. *Proceedings of the National Academy of Sciences of the United States of America*.1995, **92**(26): 12295-12299.

VUNNUM, S., V. NATARAJAN, et al., Immobilized metal affinity chromatography - Self-sharpening of protein-modulator interfaces in frontal chromatography. *Journal of Chromatography A*.1998, **818**(1): 31-41.

WANG, C., R. VERNON, et al., Prediction of structures of zinc-binding proteins through explicit modeling of metal coordination geometry. *Protein Science*.2010, **19**(3): 494-506.

WANG, Y., H. LI, et al., Identification of copper-binding proteins in soybean seeds by immobilized metal affinity chromatography and mass spectrometry. *Plant Biosystems*.2014, **148**(1): 88-95.

WEI, M.-Y., L.-H. GUO, et al., Electrocatalytic oxidation of tyrosines shows signal enhancement in label-free protein biosensors. *Trac-Trends in Analytical Chemistry*.2012, **39**: 130-148.

WEI, Z., T. NISHIMURA, et al., Characterization of glycans in a lactoferrin isoform, lactoferrin-a. *Journal of Dairy Science*.2001, **84**(12): 2584-2590.

WILLE, H., S. EHSANI, et al., Descent of the Prion Protein Gene Family from the Extracellular Domain of an Ancestral Zip Metal Ion Transporter. *Biophysical Journal*.2010, **98**(3): 708A-708A.

WILLE, H., C. GROVAERTS, et al., Electron crystallography of the scrapie prion protein complexed with heavy metals. *Archives of Biochemistry and Biophysics*.2007, **467**(2): 239-248.

WU, J., Z. FU, et al., Biomedical and clinical applications of immunoassays and immunosensors for tumor markers. *Trac-Trends in Analytical Chemistry*.2007, **26**(7): 679-688.

XU, Q. and J. J. DAVIS, The Diagnostic Utility of Electrochemical Impedance. *Electroanalysis*.2014, **26**(6): 1249-1258.

YAMAMORI, E., M. ASAI, et al., Calcium/calmodulin kinase IV pathway is involved in the transcriptional regulation of the corticotropin-releasing hormone gene promoter in neuronal cells. *Journal of Molecular Endocrinology*.2004, **33**(3): 639-649.

YAMANAKA, R., Y. HIRASAKA, et al., Metallothionein labeling for CLEM method for identification of protein subunits. *Microscopy (Oxford, England)*.2014, **63 Suppl 1**: i32-i32.

YAMAUCHI, O., A. ODANI, et al., Metal-amino acid chemistry. Weak interactions and related functions of side chain groups. *Journal of the Chemical Society-Dalton Transactions*.2002, (18): 3411-3421.

YANG, J. Y., T. I. CHIEN, et al., Heparin interference in the cerebrospinal fluid protein assay measured with a pyrogallol red-molybdate complex. *Clin. Chim. Acta*.2009, **408**(1-2): 75-78.

YANG, Y., R. I. BOYSEN, et al., Analysis of peptides and protein digests by reversed phase high performance liquid chromatography-electrospray ionisation mass spectrometry using neutral pH elution conditions. *Analytica Chimica Acta*.2015, **872**: 84-94.

YU, Z., C. HAN, et al., Fast separation and characterization of water-soluble proteins in wheat grains by reversed-phase ultra performance liquid chromatography (RP-UPLC). *Journal of Cereal Science*.2013, **57**(3): 288-294.

ZHANG, A., C. ZHANG, et al., A modified IMAC method for the capture of target protein from mammalian cell culture harvest containing metal chelating species. *Biotechnology and Bioengineering*.2012, **109**(3): 747-753.

ZHANG, Y.-M., Y.-J. WANG, et al., Effects of heavy metals Cd2+, Pb2+ and Zn2+ on DNA damage of loach Misgurnus anguillicandatus. *Acta Hydrobiologica Sinica*.2006, **30**(4): 399-403.

ZITKA, O., M. RYVOLOVA, et al., From Amino Acids to Proteins as Targets for Metal-based Drugs. *Current Drug Metabolism*.2012, **13**(3): 306-320.

ZOR, T. and Z. SELIGER, Linearization of the bradford protein assay increases its sensitivity: Theoretical and experimental studies. *Anal. Biochem.*1996, **236**(2): 302-308.

ZOR, T. and Z. SELIGER, Linearization of the bradford protein assay increases its sensitivity: Theoretical and experimental studies. *Analytical Biochemistry*.1996, **236**(2): 302-308.

ZOU, Y., Y. SUN, et al., Critical Nucleus Structure and Aggregation Mechanism of the C-terminal Fragment of Copper-Zinc Superoxide Dismutase Protein. *Acs Chemical Neuroscience*.2016, **7**(3): 286-296.

8 SEZNAM ZKRATEK

CaM	Kalmodulin
CAMKIV	Kalmodulin kináza
CREB	Buněčný transkripční faktor
GSH	Redukovaný glutathion
GSSG	Oxidovaný glutathion
HRP	Křenová peroxidáza
IEC	Iontově výměnná kapalinová chromatografie
Ig	Imunoglobuliny
IRE	Železo responzivní element
LF	Laktoferin
MT	Metallothionein
QDs	Kvantové tečky
ROS	Reaktivní částice kyslíku
SFIA	Injekční analýza v zastaveném toku
SOD	Superoxiddismutáza
TMB	3,3',5,5'-Tetramethylbenzidine

9 SEZNAM OBRÁZKŮ

Obrázek 1: Citovanost článků obsahující klíčové slovo "metal binding proteins" **12**

Obrázek 2: Redoxní cyklus metallothioneinu **17**

Obrázek 3: Schéma vnitrobuněčné signální dráhy pro regulaci CRH genu **35**

Obrázek 4: Modelové schéma transkripční regulace železo-responzivního elementu (IRE). **37**

Obrázek 5: Nutriční imunita **39**

Obrázek 6: Schéma biosenzoru pro detekci patogenních bakterií založený na metodě ELISA **46**

Obrázek 7: Elektrochemický biosenzor na čipu pro detekci H_2O_2. ..... **50**